International Conference

Advanced Carbon Nanostructures

Abstracts of Invited Lectures
&
Contributed Papers

June 29 - July 03, 2015
St. Petersburg, Russia

Проект реализован при финансовой поддержке Правительства Санкт-Петербурга

Organizers

- **Ioffe Physical-Technical Institute**, St.Petersburg, Russia
- **National Research Centre "Kurchatov Institute", B.P.Konstantinov Petersburg Nuclear Physics Institute**, Russia
- **National Research Center "Kurchatov Institute",** Moscow, Russia
- **St.Petersburg State Institute of Technology (Technical University),** Russia

Official Partners

- **Russian Foundation for Basic Research**
- **Goverment of Saint-Petersburg**
- **Fund for Infrastructure and Educational Programs**
- **Dmitry Zimin Dynasty Foundation**
- **Chemical Abstracts Service**

International Advisory Committee

F. Banhart	Strasbourg University, France
J. Davidson	Vanderbilt University, USA
M. Dresselhaus	Massachusetts Institute of Technology, USA
L. Echegoyen	University of Texas At El Paso, USA
T. Enoki	Tokyo Institute of Technology, Japan
D. Gruen	Argonne National Laboratory, USA
D. Guldi	University of Erlangen-Nurnberg, Germany
R. Kalish	Israel Institute of Technology, Technion, Israel
W. Kraetschmer	Max-Plank Institute, Germany
H. Kroto	Florida State University, USA
E. Osawa	Nanocarbon Research Institute Ltd., Japan
H. Shinohara	Nagoya University, Japan
F. Wudl	University of California, USA

Organizing Committee

A.Ya. Vul' (Conference Chair) Ioffe Institute, St. Petersburg, Russia

S.V. Kidalov (Chair)	Ioffe Institute, St. Petersburg, Russia
B.B. Chaivanov	National Research Center "Kurchatov Institute", Russia
V.F. Ezhov	St Petersburg Nuclear Physics Institute, Russia
A.V. Kirillin	Russian Foundation for Basic Research, Russia
P.S. Kop'ev	Ioffe Institute, St. Petersburg, Russia
V.V. Kveder	Institute of Solid State Physics, Chernogolovka, Russia
V.T. Lebedev	National Research Centre "Kurchatov Institute", B.P.Konstantinov Petersburg Nuclear Physics Institute, Russia
N.V. Lisitsyn	St. Petersburg State Institute of Technology, Russia
O.M. Nefedov	Branch of Chemistry and Material Sciences of the Russian Academy of Science, Russia
M.Yu. Romanovsky	Department of General Physics, Russian Academy of Science
S.A. Tsyganov	Russian Foundation for Basic Research, Russia
A.G. Zabrodsky	Ioffe Institute, Russia

International Programme Committee

M.V. Baidakova (Co-Chair)	Ioffe Institute, St. Petersburg, Russia
A.T. Dideikin (Co-Chair)	Ioffe Institute, St. Petersburg, Russia
A.E. Aleksensky	Ioffe Institute, St. Petersburg, Russia
A.S. Artjomov	Lebedev Physical Institute, Moscow, Russia
V.Yu. Dolmatov	Federal State Unitary Enterprise "Special Design and Technological Office "Technolog", St. Petersburg, Russia
Yu.S. Grushko	St. Petersburg Nuclear Physics Institute, Russia
A.V. Eletskii	National Research Center "Kurchatov Institute", Russia
M. Korobov	Moscow State University, Russia
S.V. Kozyrev	Center for Advanced Studies of St. Petersburg State Polytechnical University, St. Petersburg, Russia
A.V. Krestinin	Institute of Problems of Chemical Physics, Russia
I.I. Kulakova	Moscow State University, Russia
V.L. Kuznetsov	Boreskov Institute of Catalysis, Novosibirsk, Russia
L.B. Piotrovsky	Institute of Experimental Medicine North-West Branch of RAMS, St. Petersburg, Russia
O.A. Shenderova	International Technology Center, USA
A.M. Shikin	St. Petersburg State University, Russia
V.I. Sokolov	Institute of Organoelement Compounds, Moscow, Russia
V.M. Titov	Institute of Hydrodynamics, Novosibirsk, Russia
A.P. Vozniakovskii	Federal State Unitary Enterprise Scientific Research Institute for Synthetic Rubber, St. Petersburg, Russia
A.Ya. Vul'	Ioffe Institute, St. Petersburg, Russia

Local Organizing Committee

I.V. Vorobyova (Chair)	Ioffe Institute, St. Petersburg, Russia
T.P. Kazantseva	Ioffe Institute, St. Petersburg, Russia
B.M. Silin	Ioffe Institute, St. Petersburg, Russia
L.V. Sharonova	Ioffe Institute, St. Petersburg, Russia

Technical Group

D.B. Shustov	Web-site, Ioffe Institute, St. Petersburg, Russia
A.N. Trofimov	Ioffe Institute, St. Petersburg, Russia
K.N. Guliaeva	Ioffe Institute, St. Petersburg, Russia

in association with Agency for Science and Technology "Intellect"

Invited Lectures

Hydrogenated nanodiamonds: a versatile platform for bio-applications

Arnault J.C. [1]

jean-charles.arnault@cea.fr
[1] CEA, LIST, Diamond Sensors Laboratory, Gif sur Yvette, France

Nanodiamonds (NDs) are promising nanoparticles for biomedicine applications [1, 2]. They are scalable with sizes from 100 nm down to 5 nm. Their potential as negative control in nanotoxicology studies was well demonstrated [3]. The intrinsic surface properties of detonation NDs can be tuned playing with their surface chemistry allowing a control of their surface charge [4]. Detonation NDs were exposed to H_2 microwave plasma using a home-made set-up. A high affinity of H-NDs toward water molecules was demonstrated by BET. Stable H-NDs aqueous suspensions were obtained with a Zeta potential of + 45 mV at pH= 7.4. Its origin was related to a transfer doping occurring onto 5 nm NDs based on the diamond semi-conductive behavior [5].

This talk will focus on the assets of hydrogenated NDs for bio-applications. First, cationic H-NDs exhibit a high affinity for small interfering RNA (siRNA) and are capable of delivering them in cells with limited toxicity [6]. With siRNA/H-NDs complexes, a high inhibition efficacy of EWS/FLI-1 gene expression in Ewing sarcoma cell line was measured. Electron microscopy investigations showed H-NDs in endocytosis compartments. The association of EWS/FLI-1 silencing by the siRNA/H-NDs complex with a vincristine treatment yielded a potentiation of the toxic effect of this chemotherapeutic drug [6].

With H-NDs, a new “one-step” grafting technique of any amino-ended moiety aqueous medium was developed, well adapted for bio-functionalization. Reported on bulk hydrogenated diamond [7], it was successfully transferred onto detonation H-NDs. By contact in buffer solution, the grafting of aminated-modified ferrocene or biotin was carried out through a spontaneous approach. Quality and efficiency of the grafting were characterized (XPS, FTIR, TGA). To assess the bio-activity of the resulting conjugates, biotin modified H-NDs were further locally immobilized on substrate through an avidin/biotin biological model. This new “one-step” grafting route combines cleanliness, rapidity and efficiency.

Moreover, H-NDs can act as an active nanoparticle. Besides enhanced colloidal properties, electron transfer arising from H-NDs was also found to confer therapeutic properties to NDs. Indeed, a radiosensitization effect was evidenced in vitro on radioresistant Caki 1 cancer cells and involved biological mechanisms were investigated [8].

The microwave set-up was adapted for tritium labeling of detonation NDs. Sequential radioactivity measurements at different temperature thresholds during an air oxidation showed that stable radioactive labeling comes not only from surface ^{3}H-C bond but also from the diffusion of ^{3}H deep inside nanodiamonds [9]. These results demonstrate the excellent stability of tritium incorporated into NDs and opens the way to biodistribution studies.

References

1. Mochalin et al, Nat. Nanotech. 7 (2012) 11;
2. Arnault in “Novel Aspects of Diamond” Springer (2015) 85
3. Paget et al., Nanotoxicology 8 (2014) 46
4. Krueger et al., Adv. Funct. Mater. 22 (2012) 890
5. Petit et al., Nanoscale 5 (2013) 8958
6. Bertrand et al., Biomaterials 45 (2015) 93
7. Agnes et al., IOP Proceeding 16 (2010) 012001
8. Petit et al., IEEE International conference on Nanotechnology (2013) 174
9. Girard et al., Chem. Comm. 50 (2014) 2916

Regioselective Bis-Additions to Empty and Endohedral Clusterfullerenes: Tether or Cluster Control?

Echegoyen L [1] *, Ceron M.* [1] *, Izquierdo M.* [2]

echegoyen@utep.edu
[1] Univ. of Texas at El Paso, El Paso, TX, USA
[2] Univ. Complutense de Madrid, Madrid, Spain

Several strategies have been utilized to control the regiochemistry of multiple additions on fullerene cages, most notable being the tether-directed-remote functionalization method, originally introduced by Diederich et al. In this method, two reactive centers, separated by a rationally designed tether (preferably rigid and with the appropriate length to guide the *bis*-addition regioselectively) are attached to the fullerene cages. This strategy works well with C_{60} and to some degree with C_{70}, but surprisingly it fails completely when applied to endohedral clusterfullerenes, such as $Sc_3N@C_{80}$. In these cases only one reactive center leads to a fullerene adduct while the other remains unattached. These observations are interesting because independent *bis*-adducts (non-tethered) are easily formed without difficulty, see structure below. More interestingly, the number of *bis*-adduct regioisomers that form is very limited, indicating that the cluster inside must play an important role in directing the exohedral additions. These results will be presented and discussed in detail.

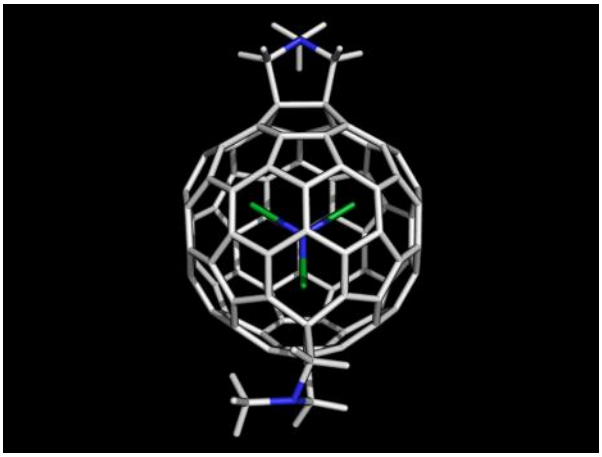

Nanocarbons-inorganic hybrid materials as next-generation nanocomposites for photocatalytic applications

Eder D. [1]

dominik.eder@uni-muenster.de
[1] Institute for Physical Chemistry, University of Munster, Munster, Germany

Hybridising nanocarbon materials, such as CNTs and graphene, with active inorganic nanomaterials constitutes a powerful strategy towards designing new-generation functional materials for environmental and energy applications [1,2]. The close coexistence of the two phases facilitates interfacial charge and heat transfer processes, which in turn enhance exciton separation and increase the lifetime of charge carriers. As a consequence, nanocarbon hybrids have shown increased sensitivities in gas sensors, improved efficiencies in photovoltaics, enhanced capacities in supercapacitors, and superior activities in heterogeneous photocatalysis [3].

In this talk, I will briefly introduce the concept of nanocarbon-inorganic hybrids, discuss various hybridisation strategies and present intriguing examples for the photocatalytic performance of nanocarbon hybrids (i.e. water purification [4] and water splitting [5]). In particular, I will demonstrate how their activity can be remarkably increased by purposefully engineering interfaces and morphology. For example, growing ultra-thin single-crystalline Ta_2O_5 films on the surface of CNTs has increased the activity for hydrogen evolution remarkably compared to hybrids with the typical polycrystalline oxide coatings [6]. This improvement is attributed to fewer grain boundaries, which alleviates electron transport to the interface, and the formation of a Schottky-type junction, which facilitates charge transfer and separation at interfaces. Finally, I will discuss the nature and extent of interfacial charge and energy transfer and elaborate on their impact on the hybrids' properties using electrochemical (i.e. chronoamperometry, EIS) and photoluminescence techniques.

References

1. Eder and A. H. Windle, *Adv. Mater.*, **2008**, 20, 1787-1793.
2. Eder, *Chem. Rev.*, **2010**, 110, 1348.
3. "Nanocarbon-inorganic hybrids: Next generation composites for sustainable energy applications", Eds: D. Eder, R. Schlögl, Publisher: de Gruyter 2014.
4. Shearer, A. Cherevan, D. Eder, *Adv. Mater.*, **2014** 26, (15), 2295-2318.
5. Ren, E. Kim, S. W. Pattinson, K. S. Subrahmanyam, C. N. R. Rao, A. K. Cheetham and D. Eder, *Chem. Sci.*, **2012**, 3, 209-216.
6. Cherevan, P. Gebhardt, C. J. Shearer, M. Matsukawa, K. Domen and D. Eder, *Energy Environ. Sci.*, **2014**, 7, 791-796.

Engineering of Bio-Nano Interfaces on 2D Nanomaterials by Self-Assembled Peptides

Hayamizu Y. [1]

hayamizu.y.aa@m.titech.ac.jp
[1] Tokyo Institute of Technology, Tokyo, Japan

Developing elegant hybrid systems of biological molecules on two-dimensional nanomaterials, such as graphene, is a key in creating novel bio-nanoelectronic devices, where versatile biological functions are integrated with electronics of nanomaterials. Biomolecules self-assembling into organized structures on these nanomaterials offer a novel bottom-up approach, where biomolecular architectures spatially govern the electronics of nanomaterials. Despite the enormous potential in bridging nano- and bio-worlds at the molecular scale, no work has yet realized a way to control electronic and/or optical properties of nanomaterials by the biomolecular structures. Our research target is the control of the interface between biotechnology and nanotechnology. More specifically, we employ solid binding peptides or artificially-designed peptides[1-3], which have specific binding affinities to 2D nanomaterials and an ability to form peptide nanostructures on atomically flat surfaces. These peptides spontaneously organize into coherent monolayer-thick nanostructures on surfaces of graphene and other 2D nanomaterials with a thickness of one layer of atoms. New design of peptide sequences and selections of nanomaterials templating peptide self-assembly can create a complex Bio-Nano system, which has two different features arise from the peptides (self-assembly) and nanomaterials (unique electronic properties).

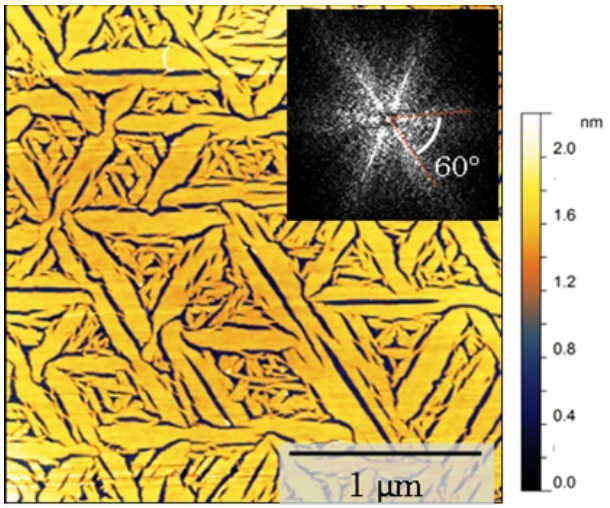

Fig.1.Atomic force microscope (AFM) image of self-assembled peptides on graphite surface. The inset shows the Fast Fourier Transform (FFT) image of the AFM indicating 6-fold symmetry.

References

1. C. R. So, Y. Hayamizu, H. Yazici, C. Gresswell, D. Khatayevich, C. Tamerler, and M. Sarikaya, ACS Nano, **6** (2) (2012) 1648-1656.
2. T. R. Page, Y. Hayamizu, C. R. So, and M. Sarikaya, Biosens. Bioelectron., **33** (1) (2012) 304-308.
3. D. Khatayevich, C. R. So, Y. Hayamizu, Carolyn Gresswell, and Mehmet Sarikaya, Langmuir, **28** (2012) 8589.

Single-walled carbon nanotubes: production in Russia and some perspectives of their technical applications

Krestinin A.V. [1,2]

kresti@icp.ac.ru
[1] Institute of Problems of Chemical Physics RAS, Chernogolovka Moscow Region, Russia
[2] Carbon Chg Ltd, Chernogolovka Moscow Region, Russia

Among all other carbon nanoparticles the single-walled carbon nanotubes (SWCNTs) are most promising for technical application due to their unique properties: extremely high strength and Yung's modulus, thermal conductivity, external specific surface, electrical conductivity and other properties.

However, up to now no technology has been developed for mass production of SWCNTs that restrains their practical application.

Recently, a small company Carbon Chg Ltd. in Chernogolovka started manufacturing SWCNTs – products of research grade by the arc discharge technology. In the last year one new company OCSiAl in Novosibirsk has developed a new technology and brought in work the equipment for mass production of SWCNTs by float catalyst technology using hydrocarbons as carbon source. The market product of OCSiAl named TUBALLÔ is now one of the best products in the world market among as-produced SWCNTs evaluated by nanotube content and price to quality ratio. Detailed characterization of SWCNT-products in Russian market is presented in the report [1].

Large-scale production of SWCNTs in Russia makes appropriate some forecasts on technical application of SWCNTs in the nearest future. It is evident that in many materials where carbon black is used conventionally, it could be replaced partially or entirely by SWCNTs to make better material properties. This is the case of lithium - ion batteries, automotive tires, resins for special purposes, paints and antistatic covers, etc.

The following applications are promising for strengthening polymeric matrices. (1) SWCNTs at concentration of 0.1 – 0.5% induced in partially crystallized polyimide improve tensile strength of nanocomposite nearly twice to ~ 500 MPa and improve stiffness of nanocomposite nearly twice as well to ~6 GPa [2]. (2) SWCNT-based nanomodifier for epoxy binder at concentration of 0.3 – 0.5% can improve tensile strength at yield and stiffness of nanocomposite by 30-40% [3].

Application of SWCNTs in materials for supercapacitors and fuel cells with polymeric membranes is very promising as well [4].

References

1. A.V. Krestinin, N.N. Dremova, E.I. Knerelman, L.N. Blinova, V.G. Zhigalina, and N.A. Kiselev Nanotechnologies in Russia, in press.
2. V.E. Smirnova, I.V. Govman, E.M. Ivan'kova, A.L. Didenko, A.V. Krestinin, G.I. Zvereva, V.M. Svetlichnyi, and V.E. Yudin, Polymer Science, Ser. A, 2013, vol. 55(4), pp. 268-278
3. A.V. Krestinin , G.I. Zvereva. XII Int. Conf. on Nanostructured Materials. Lomonosov Moscow State University, 13-18 July 2014, Abstracts, p. 544.
4. 4. A.A. Mikhaylova, E.K. Tusseeva, N.A. Mayorova, A.Yu. Rychagov, Yu.M. Volfkovich, A.V. Krestinin, O.A. Khazova, Electrochemical Acta, v.56, pp.3656-3665(2011).

Biocompatible water-soluble Endometallofullerenes: peculiarities of self-assembly in aqueous solutions and ordering under magnetic field applied

Lebedev V.T. [1] , *Kulvelis Yu.V.* [1] , *Runov V.V.* [1] , *Szhogina A.A.* [1] , *Suyasova M.V.* [1]

vlebedev@pnpi.spb.ru

[1] Petersburg Nuclear Physics Institute, NRC Kurchatov Institute, Gatchina, Russia

Review of variety of endofullerenes encapsulating rare earth elements (e.g. $Gd@C_{82}$) [1,2] or new substances with 3d-metals such as $Fe@C_{60}$ recently synthesized [3] (Fig.1) is presented to estimate their biomedical potential assuming the advanced applications of these substances as the effective contrasting agents (Magneto-Resonance Imaging, X-ray Tomography) and possible isotopic tracers when metal atoms are activated or transformed into radioactive isotopes by neutron irradiation in nuclear reactor ($Mo@C_{60}(OH)_{30}$, $^{98}Mo \rightarrow {}^{99}Mo \rightarrow {}^{99m}Tc$).

Unique physical and chemical properties of water-soluble forms of paramagnetic endometallofullerenes have to set the conditions of their applications in particular for their hydroxylated derivatives (fullerenols) demonstrated various trends of molecular self-assembly in aqueous solutions when the features of ordering may be altered by chemical additives (pH-factor) and especially by external magnetic field applied. The methods of polarized neutron scattering have been used to search unknown mechanisms of paramagnetic fullerenols organization into multilevel supramolecular structures of non trivial fractal nature influenced by the factor of fullerenols concentration and the dipolar interactions of molecules intensified in magnetic field. The recent achievements [1-3] in synthesis, modification and structural studies of fullerenols' ensembles in aqueous media modeling physiological conditions are discussed.

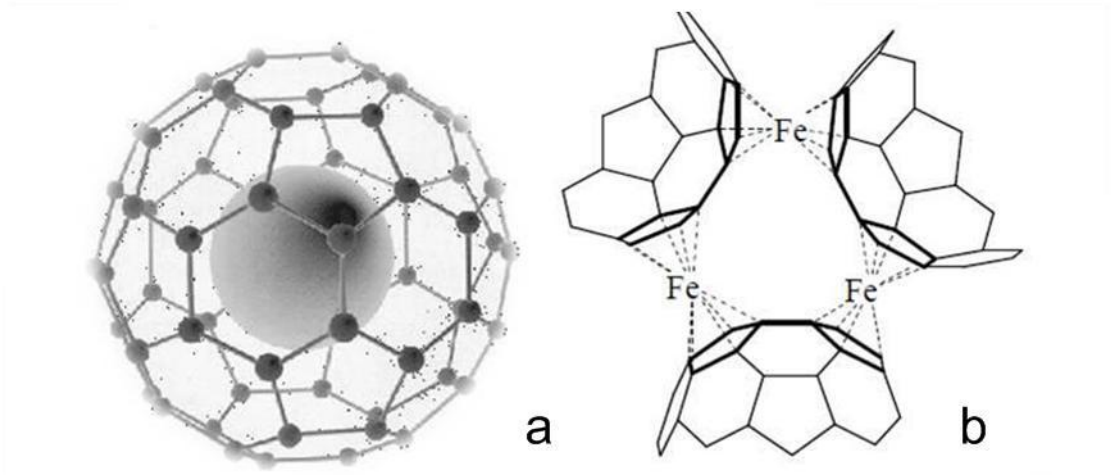

Fig.1. Coordination of iron atom with carbon atoms in endohedral and exohedral complexes with fullerene C_{60} (a,b).

References

1. Lebedev V. T., Kulvelis Yu. V., Runov V. V., Sedov V. P., Szhogina A. A., Journal of Surface Investigation. X_ray, Synchrotron and Neutron Techniques (2014) **8**, 1044.
2. Kozlov V.S., Suyasova M.V., Lebedev V.T., Russian Journal of Applied Chemistry (2014) **87**, 121.
3. Sedov V.P., Szhogina A.A., Lebedev V.T., Chernenkov Yu.P., Aksenov V.L., Kovalchuk M. V. New endohedral metallofullerenes with encapsulated iron atoms. // J. Chem. Phys. Lett. 2015 (in press).

Carbon nanostructures and health

Piotrovskiy L.B. [1]

Levon-piotrovsky@yandex.ru
[1] Institute of Experimental Medicine, Saint Petersburg, Russia

Carbon nanostructures are very aesthetic. Are they really possesing something useful for Life?

Carbon nanostructures can be used in biology and medicine –as drug as such, as vehicles in delivery systems, as containers in depot forms.

As for the role of defects in their structures for biological properties – is it advantageous or not?

ADME (absorbtion, distribution, metabolism and excretion) of carbon nanostructures - can the living systems destroy the carbon nanostructures? Sometimes yes? But…So, if we speak about biocompatibility, can we also speak about lifecompatibility? And this is the main question, the answer to which determines the possibility of using carbon nanostuctures in biology and medicine.

Nano- and microcrystalline diamond films and structures for photonics grown by a microwave plasma chemical vapor deposition

Ralchenko V.G. [1] , *Sovyk D.N.* [1] , *Khomich A.A.* [1] , *Vlasov I.I.* [1] , *Shershulin V.A.* [1] , *Kurdyukov D.A.* [2] , *Golubev V.G.* [2] , *Tukmakov K.N.* [3]

ralchenko@nsc.gpi.ru

[1] General Physics Institute RAS, Moscow, Russia

[2] Ioffe Physical-Technical Institute RAS, Petersburg, Russia

[3] Samara State Aerospace University, Samara, Russia

Diamond films of different structures, from nanocrystalline to epitaxial single crystal layers, can be produced chemical vapor deposition (CVD) technique to fit demands for specific applications. This talk will be focused on template-mediated growth of diamond films with a special reliefs with interesting optical properties, such as 3D photonic crystals, antireflective structures, micro-and nanopillars containing bright color centers [1,2]. The approach, also called “replica technique”, is based on pattering of the substrate rather than the film itself, thus the nucleation side of the free-standing film copies the substrate shape. The realization of the method using CVD process in a microwave plasma is illustrated by a number of examples.

Arrays of bright diamond photoemitters in the form of micro- and nanopillars pillars (400 nm diameter) with silicon-vacancy (SiV) color centers strongly emitting at 738 nm wavelength are produced. The fabrication process includes the CVD diamond homoepitaxial growth through vertical channels formed in Si mask on a diamond substrate, the mask also serving as the Si source for diamond doping. The strong photoluminescence (PL) emission from the SiV centers localized within the pillars and the PL decay time have been measured. The PL emission of nanometer scale Si-doped CVD diamond particles grown on Si substrates will also be considered.

3D periodic opal structures composed of thin-walled (20 nm) diamond spheres (shells) of 260-400 nm diameter, closely packed in a cubic lattice, have been grown using an inverted opal made of silicon as a template. Diamond opal obtained after the template etching demonstrates properties of a photonic crystal with Bragg reflection in the visible spectral range. The porous diamond can be of interest akso for electrochemical and chromatography applications.

Macroscopic diamond structures with intricate shapes, such as antireflective pyramidal surfaces and microchannels were also fabricated using the templating. In order to get high-definition replicas the necessity to achieve high nucleation density by seeding nanodiamonds (ND) is underlined.

References

[1] D. Sovyk, V. Ralchenko, M. Komlenok, A. Khomich, V. Shershulin V. Vorobyov, I. Vlasov, V. Konov, and A. Akimov, Appl. Phys. A. (2015) **118**, 17.

[2] D.N. Sovyk, V.G. Ralchenko, D.A. Kurdyukov, S.A. Grudinkin, V.G. Golubev, A.A. Khomich, and V.I. Konov, Phys. Solid State (2013) **55**, 1120.

Two dimensional strong localization of electrons in antidot graphene

Sheng P. [1]

sheng@ust.hk
[1] Department of Physics and William Mong Institute of Nano Science and Technology, HKUST, Clear Water Bay, Kowloon, Hong Kong

Through exponential sample-size scaling of conductance, we demonstrate strong electron localization in three sets of nanostructured antidot graphene samples with localization lengths of 1.1, 2, and 3.4 μm. The large-scale mesoscopic transport exists as a parallel conduction channel to 2D variable range hopping, with a Coulomb quasigap around the Fermi level. The opening of the correlation quasigap, observable below 25 K through the temperature dependence of conductance, makes possible the exponential suppression of inelastic scatterings and thereby leads to an observed dephasing length of 10 μm.

Work done in collaboration with Haijing Zhang, Jianming Lu, Wu Shi, Zhe Wang, Ting Zhang, Mingyuan Sun, Yuan Zheng, Qihong Chen, Ning Wang, and Juhn-Jong Lin.

References

Phys. Rev. Lett. 110, 066805 (2013).

Endohedral and Exohedral Functionalization of Fullerenes

Yang S. [1]

sfyang@ustc.edu.cn

[1] University of Science and Technology of China, Hefei , China

The most unique structure of fullerene is its hollow interior, which can encapsulate some species such as atom and molecules. Endohedral functionalization of fullerene generates endohedral fullerenes [1,2]. On the other hand, fullerene can be used as a "module" of organic reactions, and numerous fullerene derivatives have been synthesized via exohedral functionalization of fullerenes. Based on the strong electron-accepting ability, fullerene derivatives have been widely applied as acceptors in organic solar cells [3]. In this talk, we present our recent successful isolation of the long-sought small-bandgap $Sc_3N@C_{82}$ [4] and the discoveries of two novel endohedral fullerenes, including the first metal sulfide clusterfullerene $M_2S@C_{82}$ (M = Sc, Y, Dy, Lu) [5] and the first monometallic cyanide clusterfullerene — YCN@Cs(6)-C_{82}[6]. Besides, we synthesized an open-cage endohedral fullerene derivative involving a 13-membered ring [7] and an azide addition derivative via exohedral functionalization of endohedral fullerenes [8]. More recently, a nonclassical fullerene derivative $C_{96}Cl_{20}$ was synthesized via chlorination of C_{100} fullerene [9].

This work was supported by the National Natural Science Foundation of China (nos. 21132007, 21371164), National Basic Research Program of China (no. 2011CB921400).

Keywords: fullerenes, endohedral fullerenes, exohedral fullerenes, chemical functionalization

References

1. Popov, A. A.; Yang, S. F.; Dunsch, L. *Chem. Rev.* **2013**, *113*, 5989.
2. Yang, S. F.; Wang, C. R. *Endohedral Fullerenes: From Fundamentals to Applications*. World Scientific Publishing Co. Pte. Ltd. (2014).
3. Li, Y. F. *Acc. Chem. Res.* **2012**, *45*, 723.
4. Wei, T.; Wang, S.; Liu, F. P.; Tan, Y. Z.; Zhu, X. J.; Xie, S. Y.; Yang, S. F.; *J. Am. Chem. Soc.* **2015**, *137*, 3119.
5. Dunsch, L.; Yang, S. F.; Zhang, L.; Svitova, A.; Oswald, S.; Popov, A. *J. Am. Chem. Soc.* **2010**, *132*, 5413.
6. Yang, S. F.; Chen, C. B.; Liu, F. P.; Xie, Y. P.; Li, F. Y.; Jiao, M. Z.; Suzuki, M.; Wei, T.; Wang, S.; Chen, Z. F.; Lu, X.; Akasaka, T. *Sci. Rep.* **2013**, *3*, 1487.
7. Wang, G.-W.; Liu, T.-X.; Jiao, M.; Wang, N.; Zhu, S.-E.; Chen, C.; Yang, S. F.; Bowles, F.; Beavers, C. M.; Olmstead, M. M.; Mercado, B. Q.; Balch, A. L. *Angew. Chem. Int. Ed.* **2011**, *50*, 4658.
8. Liu, T.-X.; Wei, T.; Zhu, S.-E.; Wang, G.-W.; Jiao, M.; Yang, S. F.; Bowles, F.; Olmstead, M. M.; Balch, A. L. *J. Am. Chem. Soc.* **2012**, *134*, 11956.
9. Yang S. F.; Wang, S.; Kemnitz, E.; Troyanov, S. I. *Angew. Chem. Int. Ed.* **2014**, *53*, 2460.

Oral Contributions

Graphene Quantum dots in fluorographene matrix: properties and possible applications

Antonova I.V. [1] , *Nebogatikova N.A.* [1] , *Prinz V.Ya.* [1]

antonova@isp.nsc.ru
[1] Institute of Semiconductor Physics, Novosibirsk, Russia

Arrays of graphene quantum dots (GQDs) imbedded in a dielectric matrix are one of the promising materials for such applications as optoelectronic devices, sensors, memory elements, biological areas, bioimaging systems, and medicine. Chemical functionalization of graphene is a powerful approach when the physical properties can be engineered to fit a specific requirement for both fundamental science and future applications. Combination of graphene with the most stable its derivative fluorographene created by means of local chemical functionalization is the most interesting and promising way to fabricate these quantum structures. Arrays of quantum dots is also the most interesting system to study effects associated with a quantization of energy, an interaction between GQDs and processes of charge transfer between the QDs within the array.

In this report we have demonstrated formation regularities and results of study properties of the QD arrays embedded in a dielectric matrix of fluorographene. The method to create GQDs is based on the effects of self-organization during the chemical functionalization of graphene or few layer graphene in aqueous solution of hydrofluoric acid. We have discussed the formation of GQD arrays, their structural and electronic properties, and perspectives of their applications. The simplicity of the functionalization process, the lack of aggressive environments and high temperatures, as well as the opportunity to manage with their parameters and properties distinguish this method of creating the GQD arrays. Moreover, the stability of the fluorographene matrix provides stability properties films with GQD arrays.

The structural changes and stages of GQD evolution are analyzed. To study the changes in the graphene films during fluorination we have used simultaneously scan in surface topography and lateral forces AFM measurement modes. This allowed us to visualize of GQDs and to estimate GQD size and density. The GQD size were assessed as 400 - 10 nm and their density as $6x10^{8}$ – $6x10^{10}$ cm^{2}.

The process of relaxation of nonequilibrium charge trapped in the GQDs with size of 70 nm or less in the fluorographene matrix without and under illumination (daylight, 10^{17} - 10^{18} photons / cm^{2}s). Without illumination by the charge spectroscopy (Q-DLTS) up to three dimensional quantization levels in GQDs (0.14, 0.21 and 0.30 eV) were observed. It was found that the relaxation time of nonequilibrium charge depends exponentially on the temperature and the thickness of the films with GQDs. The decrease in the charge relaxation time with increasing film thickness has been shown to be due to the change in the potential barriers of flourographene. In the case of the daylight Q-DLTS measurements revealed a system of shallow levels with activation energy from 0 to 0.16 eV. The relaxation time of the charge in this case falls from milliseconds to microseconds, and does not depend on the layer thickness. We have suggested that, inhomogeneous in fluorination barriers separating GQDs have a complex structure with potential fluctuations. The values of activation barriers in the layer with quantum dots were also extracted from transport and Q-DLTS measurements for layers with small GQDs and large fluorographene matrix.

Among the possible applications of the layers with GQDs in the fluorographene matrix promising them for use in the elements of the flash and resistive memory.

Adhesion behavior of detonation nanodiamonds monolayers in various applicative environments

Couty M. [1] , *Girard H.A.* [1] , *Saada S.* [1]

magdalena.couty@cea.fr
[1] CEA, LIST, Diamond Sensors Lab., Gif-sur-Yvette, France

Further than seeding for film growth by Chemical Vapor Deposition (CVD), diamond nanoparticles (ND) monolayers are used for an increasing number of applications including sensitive coatings for surface acoustic wave sensors [1], tissue scaffold engineering, platforms for proteins immobilization on biosensors and protection against corrosion [2]. Therefore, it is essential to know the adhesion behavior of these layers in their applicative environment i.e. the effects of temperature, humidity, chemical environment, etc. However, this point remains poorly documented in literature until now. Only few studies led by Atomic Force Microscopy on single particles in air or nitrogen have been reported [3, 4].

We present here a statistic approach assessing the whole layer adhesion behavior in soft or harsh conditions by mimicking several applicative environments: (i) saturated KCl for biological buffers, (ii) polystyrene microbeads for cells (similar in size and Young's modulus), (iii) acetone for lift-off and cleaning processes, (iv) HCl for corrosion and (v) water microdroplets for drying and sample ageing during storage. ND monolayers were deposited from detonation particles exhibiting either positive or negative zeta potential, using spin-coating, electrostatic or layer-by-layer assembly. It allowed us to prepare a wide range of homogeneous layers with densities ranging from 10^{+10} to 10^{+11}/cm^2 and various size distributions between clusters and single particles. The layers were then submitted to sonication in the previously mentioned liquids and exposed to condensation/evaporation of water microdroplets. Both adhesion and mobility were evaluated, respectively through particle density and layer homogeneity.

Surprising results were obtained. For instance, sonication in a saline solution or polar organic solvent was more critical for a layer adhering through electrostatic interactions than for one adhering only through Van der Waals forces. Just half of the used deposition methods led to layers enough resistant to undergo shocks against a soft material mimicking cells. We also evidenced ND mobility driven by air/water interfaces. Therefore, several post-treatments including short CVD exposure and annealing were developed. Some of them successfully improved adhesion and suppressed mobility.

ND layer adhesion behavior goes further than simple particle detachment from the surface. There is also particle motion and reorganization into clusters. In conclusion, the deposition method has to be carefully chosen in accordance with the targeted application and in some cases post-treatments are necessary. We provide here a guidebook of suitable methods ensuring ND adhesion in different environments. Furthermore, the investigation method and the highlighted phenomena could serve as a reference study and be extended to any other kind of nanoparticle.

References

1. E. Chevallier, E. Scorsone, P. Bergonzo, Sensor Actuat B (2011) **154**, 238.
2. J. Opitz, J. Michael, B. Bendjus, I. Hannstein, N. Schreiber, S. Abud, A.K. Adler, V. Lapina, M. Meyendorf, J. Schreiber, 18th World Conf. on Nondestructive Testing, 16-20 April 2012, Durban, South Africa.
3. H. Lu, J. Goldman, F. Ding, Y. Sun, M. X. Pulikkathara, V. N. Khabashesku, B. I. Yakobson, J. Lou, Carbon (2008) **46**, 1294.
4. R. Aravind, L. Lutkus, B. Legum, APS Meeting, March 2013, Baltimore, MD, USA.

Structure control at the nanoscale in fluorinated graphitized carbon blacks through the fluorination route

Dubois M. [1] , *Ahmad Y.* [1] , *Disa E.* [1] , *Guerin K.* [1] , *Petit E.* [1] , *Thomas P.* [2] , *Mansot J.-L.* [2]

marc.dubois@univ-bpclermont.fr

[1] Clermont University, ICCF UMR CNRS 6296, Aubiere, France

[2] Groupe de Technologie des Surfaces et Interfaces (GTSI), Universite des Antilles et de la Guyane, Pointe a Pitre, France

Graphitized carbon blacks appear an interesting for starting material of fluorination. Two synthesis ways were applied to fluorination of a novel nano-sized graphitized carbon black: (i) direct fluorination (under a flux of pure molecular fluorine) and (ii) controlled fluorination by TbF_4 thermal decomposition. The thermal, electrochemical and tribologic properties of the various fluorinated nanocarbons obtained have been investigated. Fluorinated compounds produced by means of controlled fluorination present higher thermal stability and better tribologic properties than those obtained using direct fluorination. On the other hand, the study of the electrochemical performances as electrode material in primary lithium battery underlines that the direct fluorination is more efficient than the controlled way taking into account the energy and power densities. Each fluorination way leads to specific mechanisms of covalent grafting of fluorine atoms onto nanocarbons. These mechanisms have been studied by deep physical–chemical characterizations by X-ray diffraction (XRD), transmission electronic microscopy (TEM) and solid state nuclear magnetic resonance (NMR) with ^{13}C and ^{19}F nuclei in order to determine the C-F bond nature, the structure and textural properties of the fluorocarbon compounds. Graphitized carbon blacks appear as intermediate between a closed structure (such as carbon nanofibers) and an opened one (such as carbon nanodiscs) (Figure 1) and that changes during fluorination. The electrochemical and tribologic properties of fluorinated graphitized carbon blacks seem to be directly related to the different repartition of fluorinated and unfluorinated regions in the carbonaceous lattice.

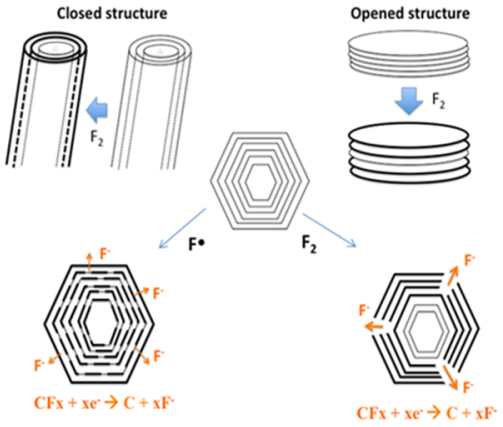

Fig.1. Fluorination of GCBs results in closed structure using TbF_4 and opened one with F_2. The damages in this latter case favor the diffusion of fluorine during electrochemical discharge.

Alkali-cluster intercalated fullerides for hydrogen storage

Gaboardi M. [1] , *Magnani G.* [1] , *Aramini M.* [1] , *Pontiroli D.* [1] , *Ricco' M.* [1] , *Milanese C.* [2] , *Cavallari C.* [3] , *Mauron P.* [4]

mattiagianandrea.gaboardi@fis.unipr.it
[1] Department of Physics and Earth Sciences, University of Parma, Parma, Italy
[2] H2-Lab., University of Pavia, Pavia, Italy
[3] Institut Laue-Langevin, Grenoble, France
[4] EMPA, division Hydrogen and Energy, Dubendorf, Switzerland

Alkali-cluster intercalated fullerides have been recently investigated with renewed interest, appearing as a novel class of materials for hydrogen storage applications, thanks to their proved capability to reversibly uptake high amounts of hydrogen via a complex chemisorption mechanism. In this work the synthesis, the structural investigation and the hydrogen storage properties of Li_xC_{60} and Na_xC_{60} will be presented, for *x* varying between 6 and 12. The structural properties were investigated by means of in-situ neutron diffraction and the analysis of the Pair Distribution Function (PDF) obtained from high-energy synchrotron diffraction. The mechanism of hydrogenation was unveiled by means of the Muon Spin Relaxation spectroscopy (μSR). These crystals were proved to reversibly absorb up to 5 wt% H_2 at moderate temperature and pressure [1,2] through the catalytic effect of intercalated clusters [3,4]. Recently, we also identified some strategies to further improve the absorption in this class of materials. On the one hand, we succeeded to add Pt and Pd nanoparticles to Li fullerides, whose known catalytic activity towards hydrogen dissociation allows to increase up to 5.9 wt% H_2 the absorption performances [5]. On the other hand, we also studied the H_2 absorption/desorption properties of the mixed intercalated phases $Na_xLi_{(6-x)}C_{60}$, succeeding in increase the absorption kinetics of about 67% and lowering the desorption enthalpy from 60 to 50 kJ/mol [6].

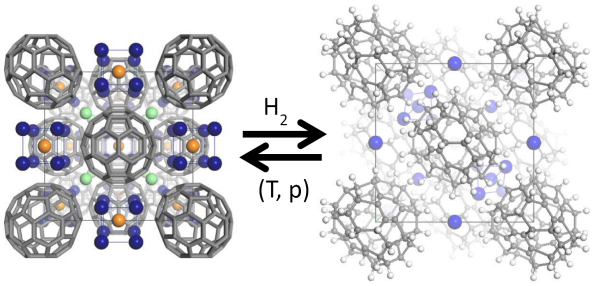

hydrogen absorption/desorption of $Na_{10}C_{60}$

References

1. P. Mauron, A. Remhof, A. Bliersbach, et al., Int. J. Hydrogen Energy (2012) 37, 14307.
2. P. Mauron, M. Gaboardi, A. Remhof, et al., J. Phys. Chem. C (2013) 117, 22598.
3. M. Aramini, M. Gaboardi, G. Vlahopoulou, et al., Carbon N. Y. (2014) 67, 92.
4. M. Gaboardi, C. Cavallari, G. Magnani, D. Pontiroli, S. Rols, and M. Riccò, Carbon N. Y. (2015) accepted manuscript.
5. M. Aramini, C. Milanese, D. Pontiroli, et al., Int. J. Hydrogen Energy (2013) 9, 1.
6. M. Gaboardi, C. Milanese, G. Magnani, A. Girella, P. Galinetto, D. Pontiroli, M. Riccò, manuscript in preparation (2015).

Investigation of the response of asymmetric carbon nanodevices to sub-THz and THz radiation

Gayduchenko I.A. [1,2] , *Fedorov G.E.* [1,2,3] , *Kardakova A.I.* [2] , *Voronov B.M.* [2] , *Finkel M.I.* [2] , *Klapwijk T. M.* [2,4] , *Goltsman G.N.* [2]

igorandg@gmail.com

[1] National Research Center Kurchatov Institute, Moscow, Russia

[2] Moscow State Pedagogical University, Moscow, Russia

[3] Moscow Institute of Physics and Technology (State University), Dolgoprudny, Russia

[4] Kavli Institute of Nanoscience, Delft University of Technology, Delft, Netherlands

Terahertz radiation has uses in applications ranging from security to medicine. However, sensitive room-temperature detection of terahertz radiation is notoriously difficult. The use of nano-scale objects is very attractive to invent and discover cost-effective solutions for new THz detectors. One particular route is the use of carbon nanomaterials: single-wall carbon nanotubes (SWCNTs) and graphene and it already braught very encouraging results even at room temperature [1,2]. Here we report on the DC voltage response of asymmetric carbon nanodevices to terahertz (THz) and sub-THz radiation in the frequency range of 130 GHz to 2.5 THz. While it is not clear if the observed effects can be used to develop efficient THz detectors we note that at room temperature the responsivity of our devices goes up to 15 V/W– far above the values reported previously for carbon nanodevices in microwave or THz range.

Three main types of asymmetric carbon nanodevices, depending on sensing element material, are considered: graphene devices and devices based on semiconducting or quasi-metal CNTs. We use the FET configuration with channel length from 1 to 4 microns. The devices are coupled to the radiation with a logarithmic spiral antenna which also serves for DC contacts. The source and drain electrodes are made of metals with different work function.

Response of such devices is analyzed in terms of thermal and diode effects. Sign of the DC signal, its power, temperature and gate voltage dependence observed are consistent with this scenario. Photovoltaic effects at low temperatures are also discussed.

Finally the thermoelectric power (TEP) of a ballistic 1D conductor is calculated as a function of the gate voltage accounting for the Schottky barriers at the CNT/metal interface. The simulations results are compared to the response of our devices in order to highlight the thermal origin of some of its features.

This work was supported by the Ministry of Education and Science of the Russian Federation under Contract No. 14.586.21.0003 (project ID RFMEFI58614X0003), Contract No. 14.B25.31.0007 and Russian Foundation for Basic Research under Grant № 14-02-31533.

References

1. Fedorov, A. Kardakova, I. Gayduchenko, I. Charayev, B. M. Voronov, M. Finkel, T. M. Klapwijk, S. Morozov, M. Presniakov, I. Bobrinetskiy, R. Ibragimov and G. Goltsman, Appl. Phys. Lett. (2013), **103**, 181121
2. Xinghan Cai, Andrei B. Sushkov, Ryan J. Suess, Mohammad M. Jadidi, Gregory S. Jenkins, Luke O. Nyakiti, Rachael L. Myers-Ward, Shanshan Li, Jun Yan, D. Kurt Gaskill, Thomas E. Murphy, H. Dennis Drew & Michael S. Fuhrer, Nature Nanotechnology (2014), **9**, 814

Energy transfer in quantum dots/multi layer graphene nanostructures

Gromova Yu.A. [1] , *Reznik I.A.* [1] , *Vovk I.A.* [1] , *Rackauskas S.* [2] , *Alaferdov A.V.* [2,3] , *Moshkalev S.A.* [2] , *Orlova A.O.* [1] , *Baranov A.V.* [1] , *Fedorov A.V.* [1]

Yulia.a.gromova@gmail.com
[1] ITMO University, Saint Petersburg, Russia
[2] Center for Semiconductor Components, UNICAMP, Campinas, Brazil
[3] Lobachevsky State University of Nizhni Novgorod, Nizhni Novgorod, Russia

Investigation of hybrid structures based on nanocarbons and semiconductor quantum dots is very attractive in course of development of photovoltaic, optoelectronic and sensor devices [1, 2]. There are few reports about photoinduced enhancement of graphene conductivity in structures with quantum dots [1, 3]. In this works amplification mechanism is attributed to the charge transfer from quantum dots to graphene under light illumination. However, theory [4] predicts very efficient energy transfer between fluorophore and graphene mediated by nonradiative coupling between the fluorophore dipole and electron−hole pair excitations in graphene. Our experimental data suggest influence of energy transfer from quantum dots to graphene on photoinduced conductivity changes as well.

We have formed graphene/quantum dots nanostructures on Pt microelectrodes by sequential deposition of multilayer graphene flakes and quantum dot layers. The exterior view of nanostructure is shown on Fig.1. For nanostructure formation were used multi layer graphene nanobelts from Nacional de Grafite (Brazil) and CdSe/ZnS quantum dots of different core size synthesized by high-temperature organometallic synthesis. We used quenching of quantum dots by ammonia vapor[5] for formation of new nonradiative channel for quantum dots deactivation that allow us to estimate rate of graphene conductivity enhancement in 10^9 s^{-1}. This quite slow process more likely attributed to energy transfer than to charge transfer. We have demonstrated dependence of electrical photoresponse in present nanostructures on quantum dots energy structure also.

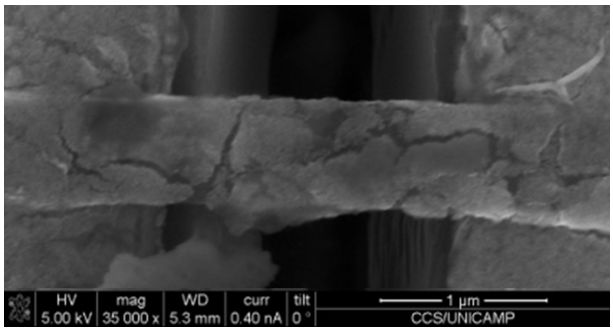

Fig.1. SEM images of a multi layer nanobelt connecting a pair of Pt electrodes after and 3 sequential depositions of QDs by modified Langmuir-Blodgett technique

References

1. Konstantatos, M. Badioli, L. Gaudreau, J. Osmond, M. Bernechea, F.P.G. de Arquer , F. Gatti and Frank H. L. Koppens, Nature nanotechnology (2012) **7**, 365.
2. T. Yin, T.-H. Kim, J.-W. Choi and K.-B. Lee, Phys. Chem. Chem. Phys. (2013) **15**, 12785
3. Sun , Z. Liu , Jinhua Li , G. Tai , S.-P. Lau and F. Yan, Adv. Mater. (2012) **24**, 5878
4. S. Swathi and K. L. Sebastian, J. Chem. Phys.(2009) **130**, 086101
5. A O Orlova, Yu A Gromova, V G Maslov, O V Andreeva,A V Baranov, A V Fedorov, A V Prudnikau, M V Artemyev and K Berwick, Nanotechnology (2013) **24**,335701

Reinforcement of epoxy resin composites with fluorinated carbon nanotubes

Kharitonov A.P. [1,2] , *Simbirtseva G.V.* [1] , *Kharitonova L.N.* [1] , *Tkachev A.G.* [2] , *Blohin A.N.* [2] , *Dyachkova T.P.* [2] , *Maksimkin A.V.* [3] , *Chusov D.I.* [3] , *Cherdyntsev V.V.* [3]

khariton@binep.ac.ru

[1] Branch of the Talrose Institute for Energy Problems of Chemical Physics of the Russian Academy of Sciences, P.B.56, Chernogolovka, Moscow region, 142432, Russia.

[2] Tambov State Technical University, Sovetskaya street, 106, Tambov, 392000, Russia

[3] MISIS, Leninskii prospect, 6, Moscow, Russia

A short review of polymer composites reinforcement by fluorinated carbon nanomaterials will be presented. In the current research fluorinated carbon nanotubes (CNTs) were applied to reinforce the polymer composite. CNTs “Taunit-M” were produced by “Nanotechcenter Ltd” (city Tambov, Russia). Epoxy resin type bisphenol-A was used. CNTs were treated by the direct fluorination method at temperatures 150 and 250^{o}C. Concentration of fluorinated and Fluorination did not influence thermal stability of CNTs below 300^{o}C. Insertion of fluorinated CNTs into epoxy resin did not worsen thermal stability of filled composites. Fluorinated CNTs were more efficient in reinforcement (both tensile strength and flexural strength) as compared with virgin (untreated) CNTs. Fluorinated at 250^{o}C CNTs did not result in composite reinforcement. The best reinforcement was obtained when CNTs were fluorinated at 150^{o}C. The insertion of 0.1 weight % of fluorinated at 150^{o}C CNTs into polymer matrix resulted in increase of the composite tensile strength up to 89.6 MPa (35% increase as compared to unfilled composites). Such reinforcement exceeded all the literature reinforcement data for epoxy composites based on epoxy resins similar to used in the current study. Module was increased up to 1644±76 MPa (30% increase as compared to unfilled composites). Decrease of concentration of fluorinated CNTs to 0.05 weight % or its increase to 0.5 weight % resulted in a tensile strength decrease as compared with unfilled epoxy resin. Flexural strength was also improved when fluorinated CNTs were used as fillers. The best results were obtained when 0.2 weight % of fluorinated at 150^{o}C CNTs was added to epoxy resin. In that case flexural strength was equal to 199.7±4.8 MPa. Flexural strength was improved by 58% as compared to unfilled epoxy and exceeded maximum found in available literature value by 43% for the bisphenol-A type epoxy resin composites. Flexural module for the composite with 0.2 weight % of fluorinated CNTs was equal to 3603±86 MPa. Insertion of fluorinated CNTs into a polymer matrix resulted in glassy temperature increase by 2 to 14^{o}C and did not influence the composites thermal stability. Fractography of filled and unfilled composites fracture surface was studied by electron microscopy technique. Results of the research may permit the articles weight decrease without strength loss or the strength increase accompanied with no weight increase. Reinforced composites can be applied for several industries: aviation, automotive, wind turbine propeller blades, for producing yachts and boats etc..

The research has been supported by the grant of the Russian Foundation of Basic Research 13-03-12086-OFI-M and State Contract #16.711.2014/K from the Ministry of Education and Sciences of Russian Federation.

Monomeric, dimeric and polymeric coordination complexes of fullerenes with transition metals

Konarev D.V. [1] , *Troyanov S.I.* [2] , *Khasanov S.S.* [3] , *Lyubovskaya R.N.* [1]

konarev3@yandex.ru

[1] Institute of Problems of Chemical Physics RAS, Chernogolovka, Russia

[2] Moscow State University, Leninskie Gory, Moscow, Russia

[3] Institute of Solid State Physics RAS, Chernogolovka, Russia

Fullerene C_{60} forms a variety of transition metal complexes with palladium, rhodium, ruthenium and others [1]. Such complexes can show promising magnetic and conducting properties when paramagnetic transition metals are used or the charge is partially transferred from metal to fullerene. We developed new approach to synthesize coordination fullerene complexes in which nickel(II) and cobalt(II) halides coordinated by phosphine or diphosphine ligands are reduced together with fullerenes.

It was shown that nickel in zero oxidation state forms monomeric $Ni(L)(\eta^2\text{-}C_{60})$ species. Nickel atoms can also bridge fullerenes into the $\{Ni(Ph_3P)\}_2(\mu_2\text{-}\ \eta^2\text{:}\ \eta^2\text{-}C_{60})_2$ dimers and even the $[\{Ni(Me_3P)_2\}(\mu_2\text{-}\eta^2\text{:}\ \eta^2\text{-}C_{60})]_\infty$ polymers (Fig. 1) [2, 3].

Cobalt in zero oxidation state also forms monomeric and dimeric complexes with C_{60}. In the dimers, cobalt with paramagnetic $S = 1/2$ spin state shows effective magnetic coupling of spins. The formation of cobalt bridged dimers is accompanied by the decrease of interfullerene distances and, in one case, the coordination of bridged cobalt atoms triggers dimerization of fullerenes and doubly-bonded $[(C_{60})_2]$ dimer are formed.

It was shown that the $(Cp^*IrI_2)_2$ and $\{Cp^*Mo(CO)_2\}_2$ dimers interact with the $C_{60}^{\cdot-}$ radical anions to form anionic complexes $(TBA^+)\{(Cp^*IrCl)(\eta^2\text{-}C_{60})\}^-$ [4] and $(PPN^+)\{(Cp^*Mo(CO)_2)\ (\eta^2\text{-}C_{60})\}^-$ (PPN^+ is bis(triphenylphosphoranylidene)ammonium). The $Cp^*Ir^{II}I$ and $Cp^*Mo^{I}(CO)_2$ units are η^2-coordinated to the 6-6 bonds of the C_{60}^- anions in these complexes.

All presented coordination fullerene complexes were obtained as single crystals allowing one the determination of their molecular structure. We present their optical and magnetic properties

The work was supported by the Russian Science Foundation (project 14-13-00028)**.**

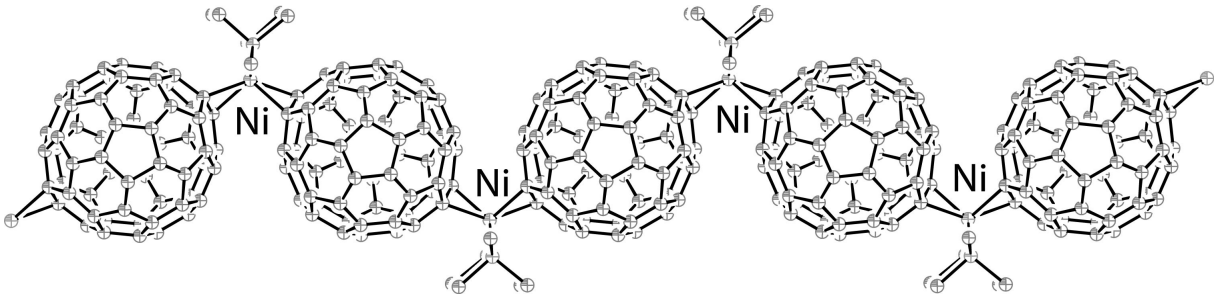

Fig.1. View on coordination $[\{Ni(Me_3P)_2\}(\mu_2\text{-}\eta^2\text{:}\eta^2\text{-}C_{60})]_\infty$ polymer formed by C_{60} and Ni as bridges.

References

1. A. L. Balch and M. M. Olmstead, Chem. Rev., 1998, **98**, 2123.
2. D.V. Konarev, S.I. Troyanov, Y. Nakano, et al., Dalton Trans., 2014, **43**, 17920.
3. D.V. Konarev, S.S. Khasanov, Y. Nakano, et al., Inorg. Chem., 2014, **53**, 11960.
4. D.V. Konarev, S.I. Troyanov, A.V. Kuzmin, Y. Nakano, S.S. Khasanov, A. Otsuka, H. Yamochi, G. Saito and R.N. Lyubovskaya, Organometallics, 2015, in press

Hall effect sensors on the basis of carbon material composed of carbon nanotubes and graphene like nanostructures

Matveev V.N. [1] *, Levashov V.I.* [1] *, Kononenko O.V.* [1] *, Matveev D.V.* [2] *, Kasumov Yu.A.* [1] *, Khodos I.I.* [1] *, Volkov V.T.* [1]

oleg@iptm.ru

[1] Institute of Microelectronics Technology and High Purity Materials, Chernogolovka, Russia

[2] Institute of Solid State Physics, Chernogolovka, Russia

Hall effect sensors with an active area of micron and submicron sizes are fabricated from various metals, alloys, semimetals, semiconductors, on the basis of two-dimensional electron gas (2DEG) and graphene [1-3]. These sensors are widely used in different fields of science, technology and medicine. Application of nanoparticles in medical diagnostics as well as some other applications requires considerable miniaturization of Hall sensors without loss in magnetic field sensitivity which is defined as $S=\Delta R_h(B)/\Delta B$, were ΔR_h is the Hall resistivity and B is the magnetic induction. S ordinarily drops as the sensor active area decreases. In this work we present the results on the fabrication and miniaturization of Hall Effect sensors from carbon material which consists of carbon nanotubes and graphene like nanostructures.

Carbon films were grown by the CVD method with a short-time acetylene inflow. The catalyst used for carbon film growth consist of a 10 nm Al/1 nm Fe or Ni bilayer which was deposited on oxidized silicon substrate. Aluminum film was deposited by electron-beam deposition. Laser ablation was used for Fe deposition and Ni was deposited by the self ion assisted deposition technique. The substrate with catalyst bilayer was annealed in air for two minutes at 800°C in order to form catalyst nanoparticles. The synthesis was performed in the temperature range from 850° to 950°C. The carbon film synthesis was described in details in Ref [4].

It was found from TEM investigations that the carbon films consisted of carbon nanotubes and bundles of them, and graphene like carbon nanostructures. Films grown on Ni catalyst contained very low concentration of CNT's.

Unusually high magnetic field sensitivity obtained from Hall measurements, was observed in the films (1500 and 3000 Ω/T for Fe and Ni catalyst, respectively). The effect of scaling the size of the Hall sensor from carbon films on its magnetic field sensitivity has been investigated. The sensitivity of the Hall sensor with an active area size of 0.13×0.13 μm^2 was found to be 1140 Ω/T, which is much higher than reported in literature. This carbon material is promising for the fabrication of Hall effect sensors of submicron size.

References

1. V. Panchal, O. Iglesias-Freire, A. Lartsev, R. Yakimova, A. Asenjo, and O. Kazakova, IEEE Trans. Magn. (2013) **49**, 3520.
2. V. Panchal, K. Cedergren, R. Yakimova, A. Tzalenchuk, S. Kubatkin, O. Kazakova, J. Appl. Phys. (2012) **111**, 07E509.
3. R. K. Rajkumar, A. Manzin, D. C. Cox, S. R. P. Silva, A. Tzalenchuk, O. Kazakova, IEEE Trans. Magn. (2013) **49**, 3445.
4. V.N. Matveev, V.I. Levashov, O.V. Kononenko, D.V. Matveev, V.T. Volkov, Ya.B. Volkova, and I.I. Khodos, Bull. Russ. Acad. Sci. Phys. (2014) **78**, 854.

Thermodynamic model to account for sorption/swelling properties of graphite oxide.

Korobov M.V. [1] , *Rebrikova A.T.* [1] , *Avramenko N.V.* [1] , *Shiliaeva E.A.* [1] , *Talyzin A.V.* [2]

mkorobov49@gmail.com

[1] Chemistry Department, Moscow State University, Moscow, Russia

[2] Umea University, Department of Physics, S-90187 Umea

Graphite oxide (GO), a long – known non-stoichiometric derivative of graphite, has attracted wide attention recently as a precursor for preparation of various graphene based materials. Contrary to graphite, GO is hydrophilic, dispersible in water and easily sorbs polar solvents into inter-layer space. Simple sonication in polar solvents leads to exfoliation of GO with formation of graphene oxide which can be then reduced to graphene or to chemically modified graphene. Very strong interest was recently attracted to multilayered GO materials obtained by deposition of graphene oxide (G-*ne*O) sheets from water solution: thin films, papers, membranes. In particular, G-*ne*O membranes were suggested for nanofiltration, separation of vapor and liquid mixtures. The properties of the membranes can be controlled using variations of humidity.

In the present study sorption properties and swelling of GO and G-*ne*O were studied using isopiestic method, dynamic sorption, differential scanning calorimetry (DSC) and temperature programmed X-ray diffraction.

Sorption of solvents (S) (S = H_2O, CH_3OH, DMF, THF, NMP, DMSO and etc.) by Hummers and Brodie graphite oxides (H-GO and B-GO) and corresponding swelling were considered in terms of equilibrium phase diagrams. Swelled H-GO was treated as a bulk homogeneous solid solution of H-GO and S, while more uniformly oxidized B-GO was thought to form weak-bonded solid solvates (B-GO – S) with the temperature independent composition. First order phase transitions (incongruent melting of solvates) were experimentally observed in a number of B-GO – S systems. The thermodynamic model proposed accounts for non monotonous temperature and pressure dependencies of H-GO swelling. Temperature (pressures) maximums of swelling/sorption observed in the experiment are singular points appearing in the binary systems GO-S at melting points of S. At such points enthalpies of sorption change sign from positive to negative. Above the melting points sorption/swelling goes down. This indicates that exfoliation of GO at temperatures above the ambient is not a result of increasing swelling.

The concepts of crystalline and osmotic swelling typically used to describe layered swelled structures were critically examined and then employed for GO-S systems. XRD and sorption data were combined to calculate the density of different S within the solvent layers in the inter-plane space of GO. Possible structures of such layers were discussed. Poor correlation was found between sorption/swelling data and dispersibility of GO in the same solvent S.

Experimental sorption data for H-G-*ne*O – H_2O system were used to simulate the permeation of water through the H-G-*ne*O membrane. Assuming linear dependence of permeation rate over sorption the experimental permeation rate vs. humidity curve was reproduced.

This work was supported by the RFBR grant 15-03-02168.

Auger analysis of the graphite oxide chemical and elemental composition

Mikoushkin V.M. [1] , *Kriukov A.S.* [1] , *Shnitov V.V.* [1] , *Solonitsyna A.P.* [1] , *Fedorov V.Yu.* [1] , *Dideikin A.T.* [1] , *Sakseev D.A.* [1] , *Vilkov O.Yu.* [2] , *Lavchiev V.M.* [3]

Emreu30@gmail.com

[1] Ioffe Institute, St.Petersburg, Russia

[2] St. Petersburg State University, St. Petersburg, Russia

[3] Institute for Microelectronics and Microsensors, Johannes Kepler University, Linz, Austria

Graphite oxide (GO) is of great interest due to its important applications (e.g., flexible displays) and the opportunity to obtain graphene by its reduction [1]. Therefore developing GO diagnostics is a topical problem. In this work, an Auger-technique has been developed for the chemical and elemental composition analysis of GO films. The technique is based on the Auger transition energies C*KVV* and O*KVV* of the GO main functional groups obtained in the experiment with using synchrotron radiation [2]. It involves the iteration procedure for the experimental spectrum decomposition into elementary contributions corresponding to the main functional groups without using usually unknown spectra of these groups. Fig.1 shows an example of the Auger O*KVV* spectrum decomposition into contributions corresponding to the hydroxyl (C-OH) and epoxide (C-O-C) functional groups. The decomposition gives the chemical composition ratio [C-OH] : [C-O-C] = 63 : 37. Taking into account the known stoichiometry of the functional groups, the film elemental composition can be obtained with essentially higher accuracy compared to the ordinary elemental coefficient method: [C] : [O] : [H] = 46 : 33 : 21. Hence the O/C ratio usually used for GO characterization is 0.49 : 0.51. This ratio confirms the extremely high oxidation extent of the GO films studied earlier by the well known and widely used X-ray photoelectron spectroscopy method [3]. The advantages of the technique are not only relative simplicity and high accuracy but also the possibility to combine it in one vacuum chamber with other methods, e.g., with scanning electron microscopy (SEM). This technique enables solving the task under the condition of intense electron-beam-induced static charging of dielectric GO films. Another advantage of the technique is the opportunity to determine the content of chemically bound hydrogen atoms which cannot be revealed by Auger and XPS methods directly.

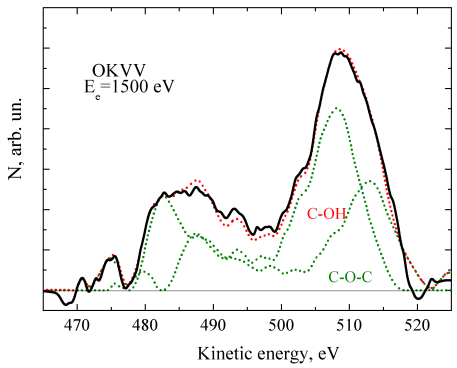

Fig. 1. OKVV Auger spectrum of the GO film decomposed into contributions from the main functional groups.

References

1. Y. H. Wu, T. Yu, Z.X. Shen. J. Appl. Phys. 108 (2010) 071301.
2. V.M. Mikoushkin, A.S. Kriukov, V.V. Shnitov, et al., J. Electron. Spectrosc. Relat. Phenom. (2015) 199, 51.
3. V.M. Mikoushkin, V.V. Shnitov, S.Yu. Nikonov, et al., Technical Physics Letters 37 (2011) 942.

Radiation-induced nucleation of diamond from amorphous carbon

Kvashnin A.G. [1,2] , *Sorokin P.B.* [2,1,3] , *Billups W.E.* [4]

aleksandr.kvashnin@phystech.edu

[1] Moscow Institute of Physics and Technology (State University), Dolgoprudny, Russia
[2] Technological Institute for Superhard and Novel Carbon Materials, Troitsk, Moscow, Russia
[3] Emanuel Institute of Biochemical Physics RAS, Moscow, Russia
[4] Department of Chemistry and The Richard E. Smalley Institute for Nanoscale Science and Technology, Rice University, Houston, USA

Chemical vapor deposition (CVD) of diamond has been developed so that diamond growth on diamond at sub-atmospheric pressure is efficient and well understood.[1] In contrast, diamond growth on non-diamond surfaces requires a nucleation step that has only recently been addressed.[2] Biased enhanced nucleation (BEN) has been shown to provide the most controlled pathway for nucleation onto non-diamond surfaces.[3,4] This process allows nucleation to be achieved either by direct ion beam bombardment[5] or by exposing a negatively biased substrate to a CVD plasma.[3,4] Nucleation sites that have been identified include formation of randomly oriented diamond on graphite edges[6 -8] and for heteroepitaxial oriented growth on silicon.[9]

Electron irradiation of anthracite functionalized by dodecyl groups leads to recrystallization of the carbon network into diamonds. A bulk process consistent with bias enhanced nucleation is proposed in which the dodecyl group provides hydrogen during electron irradiation. Recrystallization into diamond occurs in the hydrogenated graphitic subsurface layers. Unfunctionalized anthracite could not be converted into diamond during electron irradiation. The dependence of the phase transition pressure on cluster size was estimated, and it was found that diamond particles with a radius up to 20 nm could be formed.

We find that the graphene cluster with hydrogen bound to the surface has a binding energy that is less than the binding energy of the corresponding diamond cluster. Since this difference is negative, the formation of diamond will occur without an activation barrier. These results can be critically important in the synthesis of ultrasmall diamond particles and can stimulate further investigations of sp3 hybridized carbon particles.

References

1. Bundy F.P., Hall H.T., Strong H.M., Wentorf jun. R.H. // Nature. 1955. V. 176. N. 4471. P. 51-55
2. Lifshitz Y., Kohler T., Frauenheim T., Guzmann I., Hoffman A., Zhang R.Q., Zhou X.T., Lee S.T. // Science. 2002. V. 297. N. 5586. P. 1531-1533
3. Yugo S., Kanai T., Kimura T., Muto T. // Applied Physics Letters. 1991. V. 58. N. 10. P. 1036-1038
4. Jiang X., Klages C., Zachai R., Hartweg M., Füsser H. // Applied Physics Letters. 1993. V. 62. N. 26. P. 3438-3440
5. Zhang W.J., Sun X.S., Peng H.Y., Wang N., Lee C.S., Bello I., Lee S.T. // Phys. Rev. B. 2000. V. 61. N. 8. P. 5579-5586
6. García M.M., Jiménez I., Vázquez L., Gómez-Aleixandre C., Albella J.M., Sánchez O., Terminello L.J., Himpsel F.J. // Applied Physics Letters. 1998. V. 72. N. 17. P. 2105-2107
7. Hoffman A., Heiman A., Christiansen S.H. // J. Appl. Phys. 2001. V. 89. N. 10. P. 5769-5774
8. Lambrecht W.R.L., Lee C.H., Segall B., Angus J.C., LI. Z., Sunkara M. // Nature. 1993. V. 364. N. 6438. P. 607-610
9. Lee S.T., Peng H.Y., Zhou X.T., Wang N., Lee C.S., Bello I., Lifshitz Y. // Science. 2000. V. 287. N. 5450. P. 104-106

On the influence of the nC60, nC70 aggregate structure on the toxicity of aqueous fullerene solutions

Kyzyma O.A. [1,2] , *Tomchuk A.A.* [1] , *Mikheev I.V.* [3] , *Koshlan I.V.* [1] , *Koshlan N.A.* [1] , *Blaha P.* [1,4] , *Korolovych V.F.* [2,5] , *Korobov M.V.* [3] , *Almasy L.* [6] , *Bulavin L.A.* [2] , *Avdeev M.V.* [1] , *Aksenov V.L.* [7,1]

kizima@nf.jinr.ru

[1] Joint Institute for Nuclear Research, Dubna, Moscow Reg., Russia

[2] Taras Shevchenko Kyiv National University, Kyiv, Ukraine

[3] Faculty of Chemistry, Moscow State University, Moscow, Russia

[4] Faculty of Nuclear Sciences and Physical Engineering, Czech Technical University in Prague, Prague,Czech Republic

[5] Saratov State University, Saratov, Russia

[6] Wigner Research Centre for Physics, Budapest, Hungary

[7] National Research Center "Kurchatov Institute", Moscow, Russia

Applications of fullerene water solutions (FWS) in medicine and cosmetics [1,2] are of current interest due to their antioxidant, antitumor and antibacterial properties. However, up to now there is no absolute answer to the question about the side effects of these systems in living organisms. In the literature both positive and negative health influences have been reported depending on the type of primary organic solvents used in the synthesis and the cluster size distribution in the final solutions, as well as on the chemical modification of fullerenes resulting in a wide class of biologically active derivatives. In particular, there are indications [3] that cytotoxicity and antibacterial properties of FWS correlate with the aggregate formation. The latter also has an impact on the environment, since after utilization the FWS interacting with natural salts coagulate, which significantly complicates their removal.

The aim of this work was to clarify whether the size characteristics and structure of nC60 and nC70 aggregates in FWS prepared by two different methods affect the cytotoxicity of these solutions, which has been analyzed in *in vitro* tests on mammalian fibroblasts of Chinese hamsters, line V-79 [4]. The complex structural characterization of FWS has included a wide range of various methods (small-angle X-ray and neutron scattering, dynamic light scattering, atomic force microscopy, transmission electron microscopy, UV-Vis spectroscopy) and has not shown any significant correlation between the aggregate organization in the initial FWS and the survival rate of the cells incubated during two weeks in physiological solutions with different FWS additions. All of the systems studied have shown rather low cytotoxicity (cell survival rate of 90% and higher).

References

1. *Oberdorster E. Environ. Health Perspect. 2004, 112 (10), 1058–1062.*
2. *Moussa F. Nano Letters. 2005, 5 (12), 2578–2585.*
3. *Lyon D.Y., Adams L.K., Falkner J.C., Alvarez P.J. Environ. Sci. Technol. 2006, 40, 4360-4366.*
4. *Kyzyma E. A., Tomchuk A. A., Bulavin L. A. J. Surf. Inv., 2015, 9(1) 1-5.*

Hydrogen bonds influence on fluorescence of detonation nanodiamond

Laptinskiy K.A. [1] , *Burikov S.A.* [1] , *Khusainova E.N.* [1] , *Rosenholm J.M.* [2] , *Shenderova O.* [3] , *Vlasov I.I.* [4] , *Dolenko T.A.* [1]

laptinskij@physics.msu.ru

[1] Lomonosov Moscow State University, Moscow, Russian Federation

[2] Pharmaceutical Sciences Laboratory, Faculty of Science and Engineering, Abo Akademi University, 20500 Turku, Finland

[3] Adamas Nanotechnologies, Inc., 8100 Brownleigh Dr, Suit 120, Raleigh, NC, 27617 US

[4] General Physics Institute, Russian Academy of Sciences, Moscow, 119991 Russia

Despite the many hypotheses, at present there is no single theory to explain the nature of the fluorescence of detonation nanodiamonds (NDs). This work is devoted to study of the effect of hydrogen bonding on the fluorescent properties of detonation NDs.

Suspensions of detonation NDs modified by hydroxyl groups in various solvents: water, methanol, DMSO - were studied. Various properties of the solvents, as well as change of the temperature provided change of hydrogen bonds strength in the suspensions around the nanoparticles. The studies were carried out by optical and correlation spectroscopy.

With the help of Raman and fluorescence spectroscopy, substantial influence of the interactions of detonation ND-COOH with different solvent molecules in suspensions on the properties of each other was found. As a result of comparative analysis of Raman and fluorescence spectra of suspensions of ND-COOH in water, methanol and DMSO, it was found that more intense fluorescence of nanoparticles in suspensions corresponds to weaker hydrogen bonding between NDs and solvent molecules. The authors explain the revealed effects by different shift of energy levels of electron-excited states of surface groups of nanoparticles under the influence of hydrogen bonds.

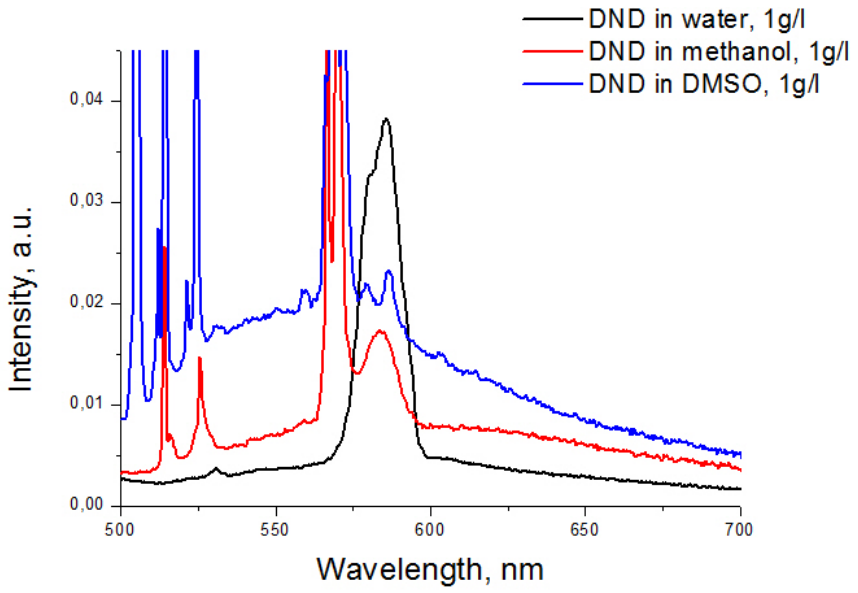

Fig.1 Raman and fluorescence spectra of NDs suspensions with the same concentration in different solvents.

Nanodiamonds and nanodiamonds-reinforced composites for functional applications: bulk coating fabrication, microstructure characterization and property evaluation

Li H. [1] , *Peng Y.* [2] , *Chen X.* [1] , *Liu Y.* [1] , *Lu S.* [1] , *Huang J.* [1]

lihua@nimte.ac.cn

[1] Ningbo Institute of Materials Technology and Engineering, Chinese Academy of Sciences, Ningbo, China

[2] Peng Tan Technology Company Ltd., Shanghai, China

Nanodiamonds (NDs) have attracted extensive attentions due to their unique structural features and exceptional properties discovered in recent years. However, regardless of the exciting research progresses made on NDs in a variety of areas, difficulties in technology transfer still remain as a major hurdle limiting their potential applications. Use of ND particles in the form of coatings/films might open a new window for the ease of accomplishing their versatile applications. Yet cost-efficient large-scale fabrication of bulk coatings using the nano particles is a persistent challenge. Here we report a novel suspension thermal spray approach for depositing NDs and their composites. Both flame spray and plasma spray processes were employed for the coating deposition using pure NDs (5-8 nm) and typically selected composites, nano-titania/NDs and nano-hydroxyapatite/NDs, as the starting feedstock. The coatings with tunable thickness ranging from microns to hundreds of microns have been successfully fabricated. Transmission electron microscopy characterization together with Raman spectroscopy detection evidenced that the characteristics of NDs can be very well retained or tuned during the coating processing. Our results show that the structure transformation of NDs to nano onion-like fullerenes (OLF, 6-8 layers) enhanced the photocatalytic performances and the biocompatibility of the titania/NDs coating and the hydroxyapatite/NDs coating respectively. The unique presence of OLFs instead of NDs in the titania-based coatings promoted significantly photocatalytic degradation of methylene blue and extinguishment of Escherichia coli bacteria. Use of NDs as additives in the hydroxyapatite coatings showed great promises for enhancing the mechanical strength of and promoting adsorption of serum proteins and subsequent attachment and proliferation of osteoblast cells on the coatings. The results will shed some light on coating fabrication and applications of the NDs-containing composites.

Surface modifications of detonation nanodiamonds probed by multi-wavelength Raman spectroscopy

Mermoux M. [1] , *Crisci A.* [2] , *Petit T.* [3] , *Girard H.A.* [4] , *Arnault J.C.* [4]

michel.mermoux@lepmi.grenoble-inp.fr
[1] CNRS - LEPMI
[2] CNRS - SIMAP
[3] Institute of Methods for Materials Development - Helmholtz Zentrum Berlin
[4] CEA/LIST

Diamond nanoparticles or nanodiamonds (NDs) produced by detonation synthesis have attracted a lot of attention over the last years. Because its potential applications are numerous, studies of this material aim to understand, control and tailor its physical and chemical properties which are given by the combination of an inert diamond core with a surface rich in functional groups [1]. Indeed ND crystallites are composed of diamond cores of a few nanometers in diameter, partially or completely covered by a thin layer of graphitic and / or amorphous carbon, and bearing carboxyl-, hydroxyl and carbonyl functionalities on the surface.

Raman spectroscopy is commonly used for the characterization of those detonation nanodiamonds. When observable, the Raman spectrum of those nanoparticles is usually composed by a broadened and downshifted first-order Raman mode of the cubic lattice and a broad peak at about 1600 – 1650 cm^{-1}. Previous studies have shown that this broad peak seems to be sensitive to the NDs surface chemistry. However, the assignment of this peak is still unclear [1,2 and references herein]. In this study, different chemical and thermal treatments were carried out in order to selectively modify their surface chemistry and track the resulting changes in the Raman spectrum.

Detonation NDs (provided by NanoCarbon Research Institute Ltd and PlasmaChem) were either hydrogenated using a microwave plasma [4] or annealed under air or vacuum to induce surface carboxylation or graphitisation [5]. Various visible as well as UV excitation lines were used for Raman analysis. Using excitation in the deep UV range, analysis conditions (atmosphere and incident power) must be chosen carefully. Even moderate laser powers can lead to strong and irreversible modifications in the observed spectra. To date, no clear correlation between the line shape of the spectra and the H and/or O content of the particle shells have been obtained. Only a clear signature of a “graphitized” surface has been observed. Heating in H_2 atmosphere may promote sp^2 bonding [6].

References

1. N Mochalin, O Shenderova, D. Ho and Y Gogotsi, Nat. Nanotechnol. (2012) **7**, 11
2. V. Mochalin, S. Osswald and Y Gogotsi, Chem. Mater. (2009) **21**, 273
3. S. Osswald, G. Yushin,.V. Mochalin, S.O. Kucheyev and Y. Gogotsi, J. Am. Chem. Soc. (2006) **128**, 11635
4. A. Girard, T. Petit, S. Perruchas, T. Gacoin, C. Gesset, J.C. Arnault and P. Bergonzo, Phys. Chem. Chem. Phys. (2011) 13, 11517
5. T. Petit, J.C. Arnault, H.A.Girard, M. Sennour; T.Y. Kang,; C.L.Cheng and P.Bergonzo, Nanoscale, (2012) 4, 6792
6. M. Mermoux, A. Crisci, T. Petit, H.A. Girard and J.C. Arnault, J. Phys. Chem C, (2014) 118, 2341

Approaches to the analysis of aqueous dispersions of fullerenes C_{60} and C_{70} and their related materials

Mikheev I.V. [1,2] , *Volkov D.S.* [1,2] , *Korobov M.V.* [1] , *Proskurnin M.A.* [1,2]

mikheev.ivan@gmail.com

[1] Chemistry Department, Lomonosov Moscow State University, Moscow, Russia

[2] Analytical Centre of Lomonosov Moscow State University / Agilent Technologies Authorized Partner Laboratory

Unique properties of carbon nanomaterials, especially fullerenes and their dispersions find increasingly wide acceptance in basic science and applied technologies. During the last decade, they are in demand in up-to-date energy systems and fine-chemical and drug synthesis. Recently, much attention has been paid to their use in medicine e.g. for drug delivery into cells or for attaching various substances to cell membrane surface. Here, one of the difficulties is the synthesis of non-toxic water-soluble fullerene compounds that can be introduced into human body. In this regard, aqueous dispersions of unmodified fullerenes (AFD) are of importance. Nonetheless, AFDs show certain difficulties and often call for a chemical modification or the use of the toxic organic solvents. In addition to it, the aggregation properties of AFDs have not been studied in full. Thus, this hinders their use in medicine. Solid materials based on AFDs also catalyzed much interest nowadays. However, the characterization and control of such new ADF-based materials are not well developed. Towards this goal, the preparation and physicochemical studies of new materials—and based not only on the fullerene C_{60} but on the other fullerenes as well—seem rather topical. The aim of this study is to develop approaches to the analysis of the fullerene aqueous dispersions and related materials.

AFDs of C_{60} and C_{70}, and of a technical mixture of C_{60} and C_{70} were prepared according to the procedure of solvent-exchange protocol. Total organic carbon analyzer was used for developing the procedure for determination of carbon concentrations in AFDs. The content of fullerenes in their aqueous dispersions at a very low level (ppm) makes the use of classical methods of chemical analysis almost impossible. Thus, to solve this problem, low concentrations of fullerenes were determined using thermal-lens spectrometry. To prove the state of the unmodified fullerene in AFDs, their UV-visible absorption spectra as well as spectra of the toluene extracts were recorded; the data show that the majority of fullerene in AFDs is not chemically modified. Furthermore, MALDI confirmed the unmodified state of fullerenes in their AFD. An important parameter (as the cell membrane is able to pass a very limited size of the molecule clusters or aggregates into the cell) is the distribution of fullerene cluster size, which was implemented by DLS and HRTEM. The ultrasonic-assisted extraction of fullerenes from AFDs to organic phase was observed and studied to estimate the physicochemical parameters of this process.

The preparation of the fullerene materials for fullerene C_{70} consisted of two steps: preparation and ultracentrifugation of C_{70} AFD. As well, the material preparation called for carrying out the physicochemical analysis of the material and corresponding AFD for the sake of a comparison with existing data for C_{60} AFD. Likewise, it is a challenging and high priority task to work out methodology for the analysis and the progress in analysis procedure applied to fullerene materials. First, for this purpose we used differential scanning calorimetry (DSC) and HRTEM to estimate the state of the material.

Acknowledgments. The work is supported by The Russian Scientific Foundation, grant no. 14-23-00012. We are grateful to Agilent Technologies — Russia and its CEO, Dr. Konstantin Evdokimov, for providing the equipment used in this study.

Fullerenes as effective modifiers of carbon nanotubes and carbon fibers

Mordkovich V.Z. [1,2] , *Zhukova E.A.* [1] , *Karaeva A.R.* [1,2] , *Urvanov S.A.* [1]

mordkovich@tisnum.ru

[1] Technological Institute for Superhard and Novel Carbon Materials, Moscow, Russia

[2] INFRA Technology LLC, Moscow, Russia

Fullerenes are usually considered apart from their relatives of fibrous nature such as carbon fibers or nanotubes. Indeed, the properties of fullerenes are very different, especially spectroscopic and chemical features. However, the very difference may become a source of new properties born from combination of molecular fullerene C_{60} and fibrous carbons. The possible use of C_{60} as a fibrous carbon modifier has been extensively studied in our lab for recent years.

This work represents both conceptual and experimental study of modification of various fibrous carbons (PAN-derived carbon fiber, CVD-produced carbon nanotubes) with fullerenes. It has been established that the new properties maybe reached through at least two steps of interaction, i.e. adsorption and immobilization. Adsorption was experimentally realized through impregnation of fibrous carbons with fullerene solution in toluene or in CS_2. It was found out that the most efficient technique for immobilization is intensive irradiation by continuous-wave green laser (wavelength 514 nm, power 10.3 W/cm^2. The modified fibrous carbons were investigated by scanning and transmission electron microscopy (SEM and TEM), XPS, AES, Raman spectroscopy thus establishing structure, morphology, surface coverage, etc. An example of 100 %-covered carbon nanotube is shown in electron micrograph in Fig. 1.

The results of instrumental studies showed that fullerene molecules are immobilized with covalent bonds effectively decreasing the surface concentration C-O bonds, the oxygen concentration in general and healing some of the surface defects. The thickness of this C_{60} film is 2-3 nm only. The C_{60} content in such nano-composites may reach 37 % in case of nanotubes, while in case of fibers the C_{60} content is much lower. It was shown also that the combination of fullerenes with fibrous carbons in one immobilized cmposites leads to drastic alteration of mechanical properties as well as of chemical durability.

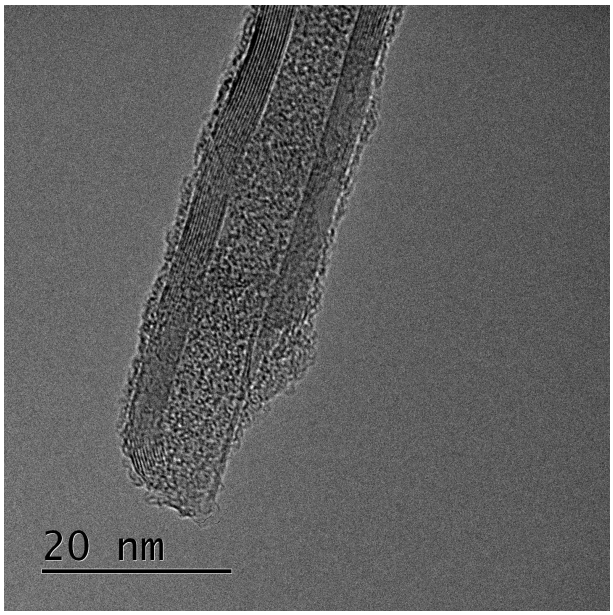

Fig. 1. TEM of multiwalled carbon nanotubes with C_{60} immobilized at the surface.

Ultrafast cooling dynamics of photoexcited carriers in monolayer graphene on SiO_2

Nakamura A. [1] , *Koyama T.* [2] , *Kishida H.* [2] , *Ito Y.* [3] , *Yoshida K.* [3] , *Tsuji M.* [3] , *Ago H.* [3]

a.nakamura@nagoya-u.jp

[1] Toyota Physical and Chemical Research Institute, Nagakute, Aichi 480-1192, Japan

[2] Department of Applied Physics, Graduate School of Engineering, Nagoya University, Chikusa, Nagoya 464-8603, Japan

[3] Graduate School of Engineering Sciences, Kyushu University, Kasuga, Fukuoka 816-8580, Japan

Graphene has unique conduction and valence bands with linear dispersion which contact each other at the K and K′ points of the Brillouin zone. Owing to its linear dispersion bands, graphene shows extremely intriguing electronic and optical properties [1]. Recent experiments [2,3] and theoretical studies [4] of carrier relaxation have shown that photoexcitation by a short laser pulse initially creates non-equilibrium carriers, which experience ultrafast thermalization *via* carrier-carrier and carrier-phonon scattering followed by cooling with emission of phonons. The key to the application of graphene materials to optoelectronic devices is a fundamental understanding of the ultrafast dynamics of carrier relaxation in graphene at low photoexcitation densities in ambient environments.

In this paper, we report the carrier dynamics in single monolayer graphene on an SiO_2 substrate at room temperature investigated by means of femtosecond time-resolved luminescence spectroscopy [5]. The luminescence kinetics in the near-infrared region of 0.7–1.4 eV upon excitation at 1.55 eV show an increase in the decay time with decreasing photon energy; the fast and slow time constants of the double-exponential decay are 60 and 360 fs for 0.9 eV, 60 and 530 fs for 0.8 eV and 90 and 1100 fs for 0.7 eV, respectively. The photon-energy-dependent decay suggests cooling of the photoexcited carriers. The observed luminescence kinetics are analyzed based on the two-temperature model of thermalized carriers, taking into account the carrier-phonon interactions and the Fermi energy shift by carrier doping from the substrate. The observed luminescence in the range of 0.7–0.9 eV is well-reproduced by the model, while the luminescence decaying in 300 fs in the range 1.0–1.4 eV cannot be reproduced by this model.

The results indicate that the carrier system is in nearly thermal equilibrium, but there exist nonthermal carrriers at the early stages at times shorter than ~300 fs. Our analysis also showed that carrier-optical phonon coupling is predominant over carrier-acoustic phonon coupling in the carrier cooling process at a carrier temperature of ~400 K. Furthermore, we find the importance of the carrier-doping effect induced by the substrate on the carrier cooling dynamics; the carrier doping suppresses a rise in carrier temperature by optical excitations due to the larger heat capacity of carriers.

References

1. A. K. Geim and K. S. Novoselov, Nat. Mater. (2007) **6**, 183.
2. J. M. Dawlaty, S. Shivaraman, M. Chandrashekhar, F. Rana, M. G. Spencer, Appl. Phys. Lett. (2008) **92**, 042116.
3. D. Sun, Z.-K. Wu, C. Divin, X. Li, C. Berger, W. A. de Heer, P. N. First, T. B. Norris, Phys. Rev. Lett. (2008) **101**, 157402.
4. S. Butscher, F. Milde, M. Hirtschulz, E. Malic, A. Knorr, Appl. Phys. Lett. (2007) **91**, 203103.
5. T. Koyama, Y. Ito, K. Yoshida, M. Tsuji, H. Ago, H. Kishida, A. Nakamura, ACS Nano (2013) **7**, 2335.

Photoluminescence of matrix-isolated carbon quantum dots

Nelson D.K. [1] , *Razbirin B.S.* [1] , *Starukhin A.N.* [1] , *Kravets V.A.* [1] , *Eurov D.A.* [1] , *Kurdyukov D.A.* [1] , *Stovpiaga E.Yu.* [1] , *Golubev V.G.* [1]

a.starukhin@mail.ioffe.ru
[1] Ioffe Institute, St.Petersburg, Russia

The photoluminescence properties of matrix-isolated carbon quantum dots (CD) have been investigated under different excitation conditions and over a wide temperature region. The dots were initially formed by pyrolysis of (3-aminopropyl)triethoxysilane (APTES) in mesoporous matrices of silicon dioxide. Dissolving the matrix in a hydrofluoric acid yielded the CD colloidal solution. Thus the properties of the CD in these quite different matrices have been studied.

A room-temperature photoluminescence spectrum of the CD excited by UV or the 405 nm violet laser was found to consist of a broad asymmetrical band with its maximum position slightly dependent on the matrix composition. A resonant excitation of the emission by a radiation with longer wavelengths is shown to cause narrowing the emission band and shifting the band maximum to the longer wavelength side with increasing excitation wavelength. Lowering the sample's temperature to 77 K under conditions of resonant monochromatic excitation with $\lambda_{exc} \geq 532$ nm was established to result in splitting the CD emission band into a doublet. Kinetics of the low-temperature emission exposes two components (fast and slow), whose decay times differ by many orders of magnitude. The long-lived component is especially intensive in the frozen CD colloidal solution while it is very weak in case of the CD in the silicon dioxide matrix. The time-resolved spectroscopy revealed an essential difference in the emission band positions in the spectra of the fast and slow components.

The photoluminescence spectra were interpreted in terms of the emission of carbon quantum dots with their nonuniform size distribution. The origin of electronic states responsible for the fast and slow components of the CD luminescence is discussed.

Preparation and characterisation of trimodal porous graphitic carbon monolithic composites containing detonation nanodiamonds and thermally induced nano-carbons

Nesterenko P.N. [1] , *Duffy E.* [1] , *Paull B.* [1]

Pavel.Nesterenko@utas.edu.au
[1] Australian Centre for Research on Separation Science (ACROSS), University of Tasmania, Hobart, Australia

In the last decade preparation of carbon-on-carbon monolithic porous composites having a hierarchical pore structure, and inter-connected channels in their pore network gained strong interest in various research areas [1,2]. This work presents new results on preparation of continuous carbon rods with trimodal porous structure. The preparation includes the polymerisation of resorcinol-formaldehyde mixture containing microspherical silica particles as template for the formation of macroporous inter-connected structure, detonation nanodiamonds (DND) as regulators of micro- and mesoporous structure and $FeCl_3$ as a graphitization catalyst of pyrolysis. The carbonaceous materials composed of amorphous carbon, DND and thermally annealed carbon onions were obtained by pyrolysis at 900°C or 1250°C of the precursor resin following by etching of silica particles by HF.

It was found that the content of DND in precursor resin can effectively control the porous structure of the prepared materials, and temperature of pyrolysis defines type of nano-carbons present in the final composite. Materials were characterised by high-resolution electron microscopy, revealing a trimodal porous structure, and confirming the graphitization of nanodiamond resulting in quasi-spherical carbon onions and buckydiamonds. Raman spectroscopy demonstrated the enhanced graphitization effect resulting from the thermal conductivity of DND. The pore structure and surface area were characterised through the nitrogen adsorption technique with BET surface areas ranging from 214 m^2/g up to 449 m^2/g depending on the nano-carbon content and temperature of pyrolysis. The adsorption behaviour of two organic dyes was investigated. This work was supported by grants from the Australian Research Council to ACROSS (DP110102046 and DP150101518).

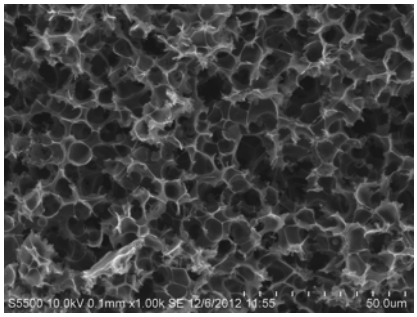

Fig.1. Electronic microscopy image of carbon-nanocarbon composites containing 5% of detonation nanodiamonds in polymerisation mixture and grafitised at 1250°C.

References

1. He, K.B. Male, P.N. Nesterenko, D. Brabazon, B. Paull, J.H.T. Luong, ACS Appl. Mater. Interfac. (2013) **5**, 8796.
2. Duffy, X. He, E. Nesterenko, D. Brabazon, A. Dey, S. Krishnamurthy, P. Nesterenko, B. Paull, RSC Adv. (2015) **5**, 22906.

Studying of microsecond lifetime charge separated states in substituted porphyrin-fullerene dyads

Pyshniak M.G. [1] , *Povolotskiy A.V.* [1] , *Mereshchenko A.S.* [1] , *Tveryanovich Y.S.* [1] , *Konev A.S.* [1] , *Khlebnikov A.F.* [1] , *Prolubnikov P.I.* [1] , *Levin O.V.* [1]

mari-maya@bk.ru
[1] Saint Petersburg State University, Saint Petersburg, Russia

At the moment donor-spacer-acceptor molecular systems become one of the most popular objects of modern nanoscience, nanotechnology and organic optoelectronics [1, 2]. One of the main effect in these areas is the intermolecular photoinduced electron transfer. The electron transfer from a donating moiety to an accepting moiety upon consumption of an electromagnetic energy quant by the molecule leads to the formation of the donor radical cation and the acceptor radical anion (charge separated state) and represents the key process in conversion of solar energy [3, 4].

In the present work the photochemistry of series of covalently linked axially symmetric porphyrin-fullerene dyads with a rigid pyrrolo[3,4-*c*]pyrrolic linker was studied by means of time-resolved photoluminescence and transient absorption spectroscopy. From the data obtained it might be concluded that the major relaxation pathways of the singlet electronic excited state are fluorescence into the ground state and intersystem crossing into the porphyrin-localized triplet excited state. Also, the relatively long-lived charge separated state, which is probably originated from the porphyrin-localized triplet excited state, was revealed. Moreover, it was demonstrated that the choice of the substituents in the porphyrin fragment is essential to achieve long lifetime of the CS state in a dyads. Therefore, the introduction of *p*-Br substituent prevents the formation of the CS state or reduces its lifetime beyond nanosecond range, while introduction of *p*-MeO group to *meso*-phenyl ring increases the lifetime of the CS state, being up to 4 μs for a species with *meso*-(*p*-$MeOC_6H_4$) substituents.

We gratefully acknowledge the financial support of the Russian Foundation for Basic Research (Grant No. 14-03-00187) and Saint Petersburg State University (Grant No. 12.38.78.2012). A.S.M. acknowledges Saint Petersburg State University for the financial support (postdoctoral fellowship #12.50.1562.2013). Flash photolysis, luminescence and UV/VIS absorption spectra were measured at Center for Optical and Laser Materials Research, Saint Petersburg State University.

References

1. Sh. Fukuzumi, K. Ohkubo, Dalton Trans. (2013) 42, 15846.
2. H. Imahori, T. Umeyama, K. Kurotobi, Y. Takano, Chem. Comm. (2012) 48, 4032.
3. D. Wróbel, A. Graja, Coord. Chem. Rev. (2011) 255, 2555.
4. H. Imahori, Org. Biomol. Chem. (2004) 2, 1425.

The electronic and spin structure of Graphene/Au/Ni, Graphene/Pt and its applications in spintronics

Rybkina A.A. [1] , *Rybkin A.G.* [1] , *Klimovskikh I.I.* [1] , *Filianina M.V.* [1] , *Skirdkov P.N.* [2,3,4] , *Zvezdin K.A.* [2,3,4] , *Zvezdin A.K.* [2,3,4] , *Shikin A.M.* [1]

rybkina-anna@bk.ru

[1] Saint Petersburg State University, Saint Petersburg 198504, Russia

[2] A. M. Prokhorov General Physics Institute, Russian Academy of Sciences, Vavilova st. 38, Moscow 119991, Russia

[3] Moscow Institute of Physics and Technology, Institutskiy per. 9, Dolgoprudny 141700, Russia

[4] Russian Quantum Center, Skolkovo, Moscow Region 143025, Russia

The unique properties of graphene originating from the linear dispersion of π states near the Fermi level make it truly irreplaceable material for use in nanoelectronics and spintronics. Graphene exhibits a very small spin–orbit splitting of π states (less than 1 meV) because of small atomic number of carbon. Combined with the high mobility of charge carriers, this accounts for the large spin relaxation length in graphene, which makes graphene very promising for application in spintronics as a material for efficient transport of spin currents.

The electronic structure of graphene formed on top of Ni(111) substrate has distorted dispersion of π states near the Fermi level in the region of K point of the graphene Brillouin zone (BZ) due to the hybridization of π states of graphene with d states of Ni. So, the direct contact of graphene and Ni(111) can be difficult use for spintronics applications. However, intercalation of Au underneath of graphene/Ni(111) restores the electronic structure of quasi-freestanding graphene with linear dispersion of π states near the Fermi level in the region of K point of the BZ. Moreover the intercalation of Au leads to hybridization of Au 5d and π states of graphene and the creation of a large spin–orbit splitting of the π band. The resulting modification of the spin structure of π states can be explained in terms of a spin-dependent avoided crossing effect between Au d states and π states of graphene. In the region where the π band dispersion is linear, the spin splitting of the π states is constant with a magnitude of ~100 meV. In that way we offer the model of graphene spin filter [1] which use the contact of MG/Au/Ni(111) instead of ferromagnetic contact as reported in literature.

The electronic and spin structure of the Graphene/Pt(111) was investigated. A large spin-orbit splitting of graphene π states (~80 meV) induced by substrate with formation of non-degenerated Dirac-cone spin states at the K point of the BZ crossed with spin-polarized Pt 5d states at the Fermi level was found [2]. We show that this spin structure can be used as a spin current source in spintronic device. By theoretical estimations and micromagnetic modeling based on the experimentally observed spin-orbit splitting, we demonstrate that the induced intrinsic magnetic field in such structure might be effectively used for induced remagnetization of the (Ni-Fe)-nanodots arranged atop the interface [3].

References

1. A. Rybkina, A. G. Rybkin, V. K. Adamchuk, D. Marchenko, A. Varykhalov, J. S´anchez - Barriga and A M Shikin, Nanotechnology (2013) **24**, 295201
2. M. Shikin, I. I. Klimovskikh, S. V. Eremeev, A. A. Rybkina, M. V. Rusinova, A. G. Rybkin, E. V. Zhizhin, J. Sánchez-Barriga, A. Varykhalov, I. P. Rusinov, E. V. Chulkov, K. A. Kokh, V. A. Golyashov, V. Kamyshlov, and O. E. Tereshchenko, Phys. Rev. B(2014) **89**, 125416
3. M. Shikin, A. A. Rybkina, A. G. Rybkin, I. I. Klimovskikh, P. N. Skirdkov, K. A. Zvezdin, and A. K. Zvezdin, Applied Physics Letters (2014) **105**, 042407

Electrochemical and EPR studies of some $M_2@C_{82}$ Endohedral Fullerenes.

Samoylova N. [1] , *Svitova A.* [1] , *Krylov D.* [1] , *Stevenson S.* [2] , *Popov A.* [1]

natalivrn@gmail.com
[1] Leibniz Institut for Solid State and Materials Research, Dresden
[2] Indiana-Purdue University, Fort Wayne

Fascinating electronic properties of endohedral metallofullerenes (EMFs) and especially their behavior in charge transfer processes have been in focus of many scientists since the middle of 1990s, when sufficient amounts of EMFs became available.

Nevertheless, the electrochemical behavior of $M_2@C_{82}$ EMFs family practically has not been studied to date.

Here we report the electrochemical properties of $Lu_2@C_{82}$ (2 isomers: with C_{3v} and C_s symmetry) $Er_2@C_{82}$ (also 2 isomers: with C_{3v} and C_s symmetry) and $Sc_2@C_{82}$-C_{3v}.

Uv-vis and NIR absorbtion spectroscopy data and theoretical calculations demonstrate the unique structure of $M_2@C_{82}$ EMFs with two M^{2+} ions inside the cage, connected with metal-metal bond (despite the fact that in majority of EMFs metal is in oxidation state 3^+).

Cyclic voltammetry experiments has revealed the cathodic shiftnof the first oxidation potential for Sc_2- and Er_2-EMFs in comparison with coincident isomers of $Lu_2@C_{82}$, caused by the significant difference in position of the HOMO metal-metal bonding orbital.

Monocation of $Sc_2@C_{82}$-C_{3v}, generated by chemical oxidation, has also been studied with EPR spectroscopy. Due to the high spin density at $4s^1$ -Sc^{2+} nuclei the coupling constant is extremely big (199.2 Gauss), that provides the second order effects in line position and variations of the signal line width.

Nanocrystalline diamond films and nanoparticles with controlled bright photoluminescence of silicon-vacancy color centers produced by in situ doping from silane

Sedov V.S. [1,2] , *Khomich A.A.* [1,2] , *Vlasov I.I.* [1,2] , *Vul A.Ya.* [3] , *Ralchenko V.G.* [1,2]

sedovvadim@yandex.ru

[1] A.M. Prokhorov General Physics Institute of Russian Academy of Sciences, Moscow, Russia

[2] National Research Nuclear University MEPhI, Moscow, Russia

[3] Ioffe Physical-Technical Institute, St. Petersburg, Russia

Silicon-vacancy (SiV) color centers in diamond attract an increasing interest for applications in single-photon emitters in quantum information technologies and biocompatible fluorescent biomarkers based on diamond nanoparticles [1]. The SiV defect shows a strong photoluminescence (PL) with narrow zero phonon line at 738 nm and weak vibronic sidebands that is an advantage in comparison with the better studied NV center in diamond. Having a choice between Si^+ ion implantation and *in situ* doping in course of diamond chemical vapor deposition [2], the latter approach seems to be preferable as it allows avoiding the residual damage inherent to the implantation process. Here we used monosilane SiH_4 addition to CH_4-H_2 mixtures to grow Si-doped nanocrystalline diamond (NCD) films and isolated nanoparticles in a controllable way by microwave plasma CVD.

The diamond films and particles were deposited on AlN substrates by MPCVD in CH_4/H_2 gas mixtures. The NCD films with grain size d ≈70 nm were produced by adding silane in gas in content up to SiH_4/CH_4=0.8%. The Si-doped films revealed a strong SiV PL emission at 738 nm excited at wavelength of 473 nm, which, however, shows a nonmonotonic behavior with amount of SiH_4 added. The highest PL intensities, integrated and normalized to Raman diamond peak, are measured at SiH_4/CH_4 ratio of 0.2% for NCD films, the PL revealing a quenching at higher doping. The PL changes for NCD films after oxidation at temperatures of up to 700 °C will also be touched. The present results on the Si doping in a wide range of silane concentrations can be useful for choice of optimal growth and doping conditions for diverse applications, in particular, for production of luminescent diamond nanoparticles via milling techniques [3].

This work was supported by the RFBR grant No. 14-02-31772 and grant of the President of the Russian Federation No. 2575.2015.5.

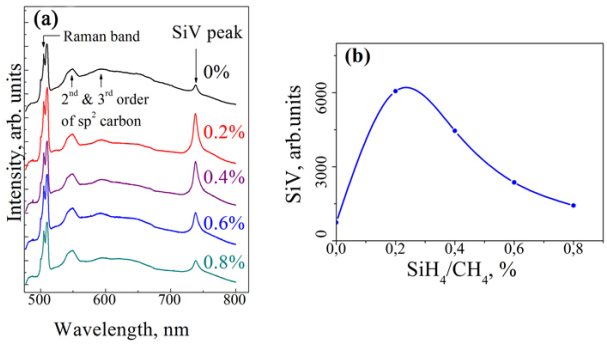

PL spectra (a) and dependence of 738 nm PL line intensity on silane content (b) for NCD films.

References

1. I. Aharonovich and E.Neu, Adv. Opt. Mater. (2014) **2**, 911.
2. Grudinkin, N. Feoktistov, et al. J. Phys. D: Appl. Phys. (2012) **45**, 062001.
3. E. Neu, C. Arend, E. Gross, et al. Appl. Phys. Lett. (2011) **98**, 243107.

Optical biosensing using graphene oxide

Stebunov Yu.V. [1] , *Aftenieva O.A.* [1] , *Arsenin A.V.* [1]

ystebunov@gmail.com
[1] Laboratory of Nanooptics and Plasmonics, Moscow Institute of Physics and Technology, Dolgoprudny, Russian Federation

Graphene oxide is an oxidized counterpart of graphene and possesses sp2 and sp3 hybridized carbon atoms, and different functional groups such as epoxy, carboxyl, hydroxyl, and others. These unique chemical properties and a high chemical affinity of graphene oxide to biological molecules provide an opportunity for biosensing applications [1]. Last years, several publications were devoted to the usage of graphene oxide in optical biosensors based on surface plasmon resonance (SPR). SPR biosensors exploit the phenomenon of surface plasmon, which is an electromagnetic wave excited at the interface of metal and dielectric and excitation conditions depend on the refractive index of the dielectric media above the metal layer [2]. Therefore, biomolecules adsorbing on the metal surface change resonant conditions making possible to investigate properties of biochemical processes.

In present work, sensor chips based on the thin films of graphene oxide were considered (Fig. 1) [3]. Graphene oxide was deposited from an aqueous solution on the surface of gold film using airbrushing technique. Optical and structural properties of obtained GO films were investigated by atomic force microscopy and spectroscopic ellipsometry and then used for the simulations of multilayered structures comprising graphene oxide. According to the simulations, thin layers of graphene oxide with thickness up to 20 nm can improve biosensor sensitivity by 25%. Using obtained graphene oxide sensor chips the biosensing assay was performed for investigation of DNA-DNA interactions. Comparing to commercial sensor chips based on dendrimeric structures of carboxymethylated dextran it was obtained 2.5 times higher adsorption of biomolecules on the surface of sensor chip that enhances its limit of detection. In addition, obtained sensor chips possesses a property of bioselectivity to investigated biomolecules and can be used multiply times with simple procedure of surface regeneration.

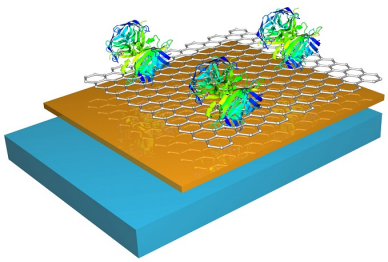

Fig.1. A general view of graphene oxide sensor chip comprising a glass substrate, a gold film with thickness of 32 nm, a graphene oxide film, and a layer of biomolecules deposited on the surface of graphene oxide.

References

1. E. Morales-Narváez and A. Merkoçi, Adv. Mater. (2012) 24, 3298.
2. B.M. Schasfoort and A. J. Tudos, Handbook of Surface Plasmon Resonance, The Royal Society of Chemistry, Cambridge, 2008.
3. A.V. Arsenin and Yu.V. Stebunov, RU Patent Application No. 2527699 (Feb 2013); WO/2014/129933 International Application No. PCT/RU2013/001100 (Aug 2014).

Inorganic Synthesis in Carbon Nanoreactors: Stepwise Formation of Low-dimensional Nanomaterials

Stoppiello C.T. [1] , *Chamberlain T.W.* [1] , *Fay M.W.* [2] , *Biskupek J.* [3] , *Kaiser U.* [3] , *Khlobystov A.N.* [1,2]

pcxcts@nottingham.ac.uk

[1] School of Chemistry, University of Nottingham, Nottingham, UK

[2] Nottingham Nanotechnology and Nanoscience Centre, Nottingham, UK

[3] Central Facility for Electron Microscopy, University of Ulm, Ulm, Germany

Carbon nanotubes (CNTs) – atomically thin cylinders of sp^2 hybridized carbon – are relatively chemically inert, have extremely high mechanical stability and are available in different diameters from sub-nanometre to hundreds of nanometres. Due to the hollow nature of CNTs, it is possible to insert a wide variety of atoms, molecules and ionic salts into the internal cavity resulting in the formation of 1D molecular arrays and crystals.[1]

We report a new universal approach for the formation of quasi one dimensional inorganic materials inside CNTs via the sequential encapsulation of molecular precursors which contain the appropriate elemental building blocks and subsequent reaction (figure 1a). The chemically inert nature of such nanosized containers makes CNTs ideal candidates for use as both reaction vessels, in which the precursors can be combined, and 1D templates which can direct the formation of products which are unfavoured or impossible to synthesise in the bulk phase.[2] Our methodology enables the formation of inorganic materials inside nanotubes previously unachievable through traditional sublimation or molten phase filling techniques.

Low-voltage, aberration-corrected high-resolution transmission electron microscopy (AC-HRTEM) can be used to visualize transformations and reactions within the nanotube in real time.[3,4] Details of the atomic structure of the nanomaterial and the effects that 1D confinement imposes on the nanomaterial are probed by AC-HRTEM revealing distortion of the quasi 1D crystal structure and unique dynamic behaviour within the CNT (figure 1b). The discovery of methodology to form new, and exciting inorganic nanomaterials with potentially remarkable functional properties, in a bespoke fashion from simple precursors with atomic precision is an important advance in the field of nanomaterials.

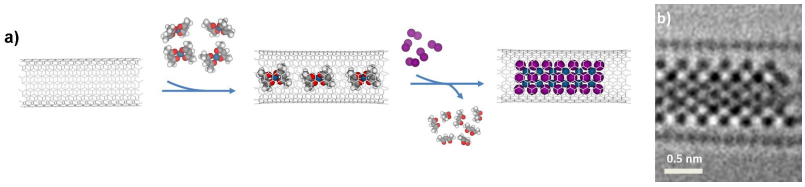

Figure 1 a) Schematic illustration depicting how an inorganic material can be formed utilising the nanotube as both reaction vessel and 1D template via the addition of elemental precursors and subsequent reaction. b) AC-HRTEM provides atomic resolution structural information for the resultant inorganic material encapsulated within the CNT.

References

[1] D.A. Britz, A.N. Khlobystov, Chem. Soc. Rev. (2006) **35**, 637.

[2] D.A. Britz, A.N. Khlobystov, K. Porfyrakis, A. Ardavan, G.A.D. Briggs, Chem. Commun. (2005) 37.

[3] T.W. Chamberlain, N.R. Champness, M. Schroder, A.N. Khlobystov, Chem. Eur. J. (2011) **17**, 668.

[4] A. Chuvilin, A.N. Khlobystov, D. Obergfell, M. Haluska, S. Yang, S. Roth, U. Kaiser Ang. Chem. Int. Ed. (2010) **49**, 193.

Chlorination-promoted shrinkage of fullerene cages by multiple C_2 losses

Troyanov S.I. [1] , *Ioffe I.N.* [1] , *Yang S.* [2]

stroyano@thermo.chem.msu.ru

[1] Chemistry Department, Moscow State University, Moscow, Russia

[2] Department of Materials Science and Engineering, University of Science and Technology of China, Hefei, China

It is known that pristine Isolated Pentagon Rule fullerenes are thermally rather stable showing thermally induced transformations only above 1000 °C [1]. The fullerene carbon cages retain their connectivities at chemical treatments so that almost the whole of the fullerene chemistry concerns exohedral derivatization without changing the cage connectivity. In the last few years, several examples were reported about halogenation-promoted cage transformations [2-5]. While the first report revealed the cage shrinkage of C_{60} upon fluorination at rather harsh conditions [2], in the following examples, C_2 losses in higher fullerenes were promoted by chlorination at significantly milder conditions [3-5]. Every removal of a 5:6 C–C bond from a classical [5,6]fullerene creates a cage heptagon at the abstraction place thus producing a non-classical cage. Another type of cage transformations in fullerenes is a Stone-Wales rearrangement, a rotation of a C–C bond by 90°, thus transforming an IPR cage to another IPR or, alternatively, non-IPR cage, i.e., that containing pentagon-pentagon fusion(s). In some cases, a combination of C_2 losses and Stone-Wales transformations can also occur that results in chlorides of non-classical fullerenes with very unusual cage structures and shapes.

In this report, several cases of cage shrinkage will be presented which proceed with the formation and even elimination of cage heptagons. Up to three successive C_2 losses have been found to occur upon chlorination of C_{86}, C_{88}, and C_{100} fullerenes with VCl_4 at ca. 350°C.

Chlorination of C_{86} fullerene resulted in the isolation and structure elucidation of chlorides with non-classical C_{84} and C_{82} cages containing respectively one and two heptagons in the carbon cage. The structures of two intermediates ($C_{84}Cl_n$) and one final ($C_{82}Cl_{30}$) products have been determined.

Chlorination of C_{88} fullerene revealed a branched skeletal transformation with the formation of chlorides with non-classical C_{86} and C_{84} cages containing respectively one and two heptagons in the carbon cage. The structures of two intermediate ($C_{86}Cl_n$) and three final ($C_{84}Cl_{26}$) products have been revealed.

Chlorination of C_{100} fullerene demonstrated that a cage shrinkage can proceed with the formation and as well as elimination of cage heptagons. Two final products, $C_{96}Cl_{20}$ and $C_{94}Cl_{22}$, have been isolated as a result of a branched skeletal transformation which includes C_2 losses and a Stone-Wales rearrangement.

The work is supported by the Russian Foundation for Basic Research (grants 15-03-04464 and 15-03-05083).

References

1. J. Cross and M. Saunders, J. Am. Chem. Soc. (2005) **127**, 3044.
2. A. Troshin, A.G. Avent, A.D. Darwish, N. Martsinovich, A.K. Abdul-Sada, J.M. Street, and R. Taylor, Science (2005) **309**, 278.
3. Wei, S. Yang. E. Kemnitz, and S.I. Troyanov, Chem. Asian J. (2015) **10**, 559.
4. I.N. Ioffe, S. Yang, S. Wang, E. Kemnitz, L.N. Sidorov, and S.I. Troyanov, Chem. Eur. J. (2015) **21**, DOI: 10.1002/chem.201406487.
5. Yang, S. Wang, E. Kemnitz, and S.I. Troyanov, Angew. Chem. Int. Ed. (2014) **53**, 2460.

The unique spin structure in Graphene/Au/Re(0001) near the Fermi level

Voroshnin V.Y. [1] , *Klimovskikh I.I.* [1] , *Filianina M.V.* [1] , *Rybkin A.G.* [1] , *Shikin A.M.* [1]

Vl.Voroshnin@yandex.ru
[1] Saint-Petersburg State University, Saint-Petersburg, Russia

A rapid development of nanoelectronics implies graphene as a very promising material. Graphene has a lineal dispersion of pi-band near the Fermi level which allows us to consider charge-carries as massless Dirac fermions. However Graphene is a 2D crystal then it's interaction with substrate and ad atoms are important. Using these effects we can form the unique electronic structure in graphene.

Graphene doesn't have a large spin-orbit interaction (only 5 meV), but by hybridisation with another spin-split band it might be obtained [1]. Moreover due to increased spin-orbit interaction we expect to observe the topological gap in pi-states of graphene near the Fermi level in the region of the K point. Authors of the article [2] predicted the existence of topological states in there.

In our experiment we used the sample of monocrystal Re(0001), which has spin-orbit spitting d-states near the Fermi level, to synthesize graphene by cracking propylene [3]. Then we intercalated Au atoms underneath graphite monolayer and formed a quasi-free graphene [3]. Using methods of angle resolved photoemission spectroscopy (ARPES) and spin-resolved photoemission spectroscopy (SRPES) we investigated electronic states of core-levels and valence band. For analysis of the sample's surface geometry we used the method of Low-Energy Electron Diffraction (LEED). The most interesting feature in this system is the hybridisation of Re states with pi-states of graphene near the Fermi level though Au monolayer and also the effect of crossing Re-Au hybridised stated with pi-states of graphene.

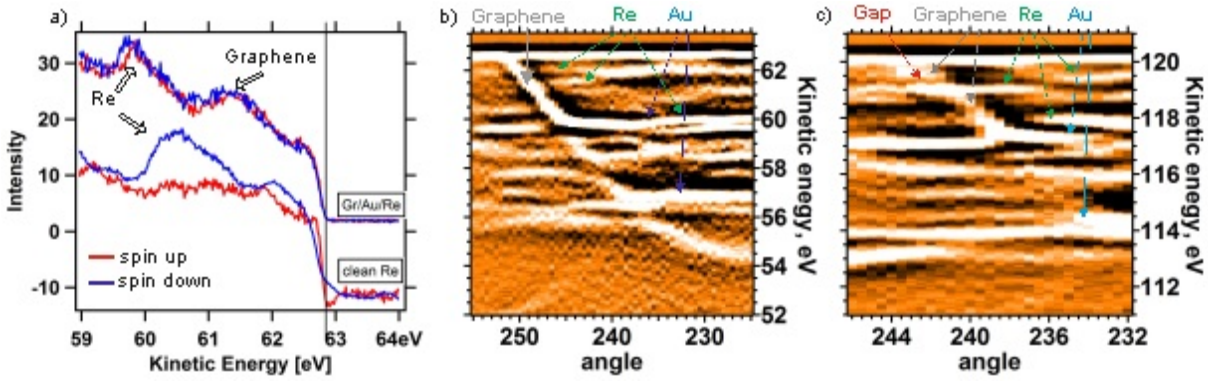

References

1. D. Marchenko, A. Varykhalov, Applied Physics Letters 98, 122111 (2011)
2. Yuanchang Li, Peizhe Tang, Physical Review B 87, 245127 (2013)
3. Shikin, A.M., Prudnikova G.V., Physical Review B 62, 13202 (2000)

Round Table 1: Theory and modelling

When simulation helps experiment. Several examples of study of novel 2D materials with specific properties

Sorokin P.B. [1,2,3]

PBSorokin@gmail.com
[1] Emanuel Institute of Biochemical Physics of RAS, Moscow, Russian Federation
[2] Technological Institute of Superhard and Novel Carbon Materials, Moscow, Russian Federation
[3] National University of Science and Technology MISiS, Moscow, Russian Federation

The simulation methods plays significant role in the modern material science. They are especially important in the study of new materials which properties still didn't properly investigated in experiment. Here I will present our results in the field of theoretical analysis of the already experimentally obtained materials and our predictions of perspective structures which can display specific properties.

In the first part of my talk I will focus on the predictions of new effects in nanoworld and will show their confirmations by available experimental data. I will show that formation of diamond films [1] facilitated by chemical adsorption of adatoms on the multilayer graphene surface, and explain how the pressure of phase transition is reduced and formally turns negative [2]. In such "chemically induced" phase transition both chemistry and compression concurrently serve as the driving factors for diamond film formation. I will continued to discuss this effect through the films with hexagonal diamond (lonsdaleite) type structure and further show that under the particular external conditions and using particular adsorbate atoms films with the specific structure can be formed [3]. Developed theory successfully described experimental results of formation of diamond nanoclusters in the amorphous carbon. We estimated dependence of phase transition pressure upon the cluster size, it was found that diamond particles with the radius up to 20 nm can be formed only by hydrogenation [4].

I will show the results of investigation of general graphitization tendency in ultrathin slabs of the ionic compound [5,6] which can be used as a part of 2D heterostructures. We determine the critical slab thickness for a range of systems, below which a spontaneous conversion from a cubic to a layered graphitic structure occurs, driven by surface energy reduction in surface-dominated structures.

Finally I will present results of joint theoretical-experimental studies of investigation of properties of graphene on the different substrates. I will show that computational approach can effectively describe such experimental situation and allows to explain the changing of electronic properties of graphene by substrate [7].

This work was supported by the Russian Science Foundation project 14-12-01217.

References

1. L.A. Chernozatonskii, P.B. Sorokin, A.A. Kuzubov, B.P. Sorokin, A.G. Kvashnin, D.G. Kvashnin, P.V. Avramov and B.I. Yakobson, J. Phys. Chem. C (2011) **115**, 132
2. A.G. Kvashnin, L.A. Chernozatonskii, B.I. Yakobson, P.B. Sorokin, Nano Letters (2014) **14**, 676
3. A.G. Kvashnin, P.B. Sorokin, J. Phys. Chem. Lett. (2014) **5**, 541
4. L.Yu. Antipina, P.B. Sorokin, J. Phys. Chem. C (2015) **119**, 2828
5. P.B. Sorokin, A.G. Kvashnin, Z. Zhu, D. Tománek, Nano Letters (2014) **14**, 7126
6. A.G. Kvashnin, P.B. Sorokin, D. Tománek, J. Phys. Chem. Lett. (2014) **5**, 4014
7. S. Entani, L.Yu. Antipina, P.V. Avramov, M. Ohtomo, Y. Matsumoto, N. Hirao, I. Shimoyama, H. Naramoto, Y. Baba, P.B. Sorokin and S. Sakai, Nano Research (2015)

On the orientational disorder of molecules in the low-temperature phase of the fullerene-C_{60}

Dzyabchenko A.V. [1]

adz@cc.nifhi.ac.ru

[1] L.Ya. Karpov Physico-Chemical Institute, Moscow, Russian Federation

Fullerene-C_{60}, the first member of the fullerene family demonstrates the phenomenon of orientation disorder caused by its quasi-spherical molecular shape. The extent of such a disorder varies from almost isotropic distribution of molecular orientations in the room temperature cubic *Fm*3*m* phase to the partial disorder in the cubic *Pa*3 phase which arises below the 1st order phase transition at 250K. The neutron diffraction studies of the *Pa*3 phase (David, *et* al., 1992) indicate the presence of two orientational states: state P (double bond close to pentagon) and the state H (double bond close to hexagon). Both states are in equilibrium with each other: thus, the content of component P changes steadily from 84% at 90 K (below which the *Pa*3 phase turns out to be completely frozen) to 63% at T_c 250 K. A popular point of view on the nature of this P/H disorder assumes that the molecule undergo uniaxial rotation jumps about its threefold symmetry axis coinciding with the body diagonal of the cubic cell. However, theoretical considerations show that such a transition path, spanning angular distance of ~60°, is associated with a high potential barrier. Moreover, this path is not the shortest one, for other transition paths with down to 30° rotation amplitude, coupled with smaller potential barriers, there exist [1].

Remarkably, both states, if considered separately, as perfect crystals of *Pa*3, *Z*=4 symmetry, demonstrate their stability as local energy minima, provided a proper intermolecular potential is used for energy calculation; the essential feature of such an empirical potential, LLM, is the contribution of electrostatic energy (up to ~10% for the P state) from the Coulomb interaction of positive q = 0.25 and negative q = -0.50 point charges placed on the 60 single and 30 double bonds, respectively. The key feature of the two models is that state P is 0.7 kcal/mol more stable than H, but at the same time its equilibrium unit-cell volume is greater. Consequently, the model is found capable to explain the experimental evidences on of the P/H equilibrium, including their behavior at elevated pressure.

Still, the question persists until at present on how particularly the P and H packins coexist in the same crystal. On this matter we report here on our model of the P/H crystal disorder based on minimization of the energy function $E_{P/H} = xE_P + (1\text{-}x)E_H$. Here E_P and E_H are lattice energy functions of purely P and purely H configurations, depending on the six cell dimensions and two sets of rigid body parameters: u, v, w, φ, q, ψ, of which one set acts exclusively on state P, whereas second on state H. The two states thus influence each other via their common unit cell parameters a, b, c, a, β, g only. With such a model we assume that both states occur in the same monocrystalline sample as extended domains, whose overall dimensions are large enough to make the influence of domain walls onto the energetics of the composed system neglidgible.

One principal result of a series of numerical calculations performed on the present model is that the composed system demonstrates energetic stability in the full range of relative P to H contents. Moreover, there is a kind of synergy effect, for with any composition, the optimized P/H system is found lower in energy than the quantity $E' = xE_{min(P)} + (1\text{-}x)E_{min(H)}$, where $E_{min(P)}$ and $E_{min(H)}$ are minimized energies of pure components.

References

1. Dzyabchenko A. V., Agafonov V.N. Chem. Phys. Reports (1999), **18**, 227.

Modelling electrical properties of CNTs/epoxy nanocomposites

Eletskii A.V. [1] , *Knizhnik A.A.* [2,3] , *Popov P.V.* [2] , *Potapkin B.V.* [2,3] , *Kenny J. M.* [4,5]

eletskii@mail.ru

[1] National Research University "Power Engineering Institute", Moscow, Russia
[2] National Research Centre "Kurchatov Institute", Moscow, Russia
[3] Kintech Lab Ltd, Moscow, Russia
[4] Institute of Polymer Science and Technology, ICTP-CSIC, Madrid, Spain
[5] Institute of Macromolecular Compounds of the Russian Academy of Sciences S. Petersburg, Russia

Addition of carbon nanotubes (CNTs) into a polymer matrix imparts new properties to the material which is caused by unique characteristics of CNTs. One of the advantages of the usage of CNTs as a conductive addition to composite materials relates to a high aspect ratio (ratio of the length to the diameter) of these objects. Due to this feature the addition of about 0.1% CNTs to a polymer matrix results in the enhancement of the composite conductivity by 8 – 10 order of magnitude which transforms an insulating material into a conductor. Electrical properties of CNT doped polymer composites demonstrate the percolation behavior, in accordance with which at excess of threshold filler loading the charge transport is provided by few conducting paths formed by contacting nanotubes. In this research the results of computer simulation of the percolation behaviour of such composites are presented. The dependences of the percolation threshold position and the absolute magnitude of the conductivity near the threshold from the aspect ratio of CNTs, the degree of CNT alignment, the degree of homogeneity of the CNT distribution over the material have been calculated and discussed. A special attention is paid to the electrical contact between neighbouring nanotubes that usually limits the electric conduction of CNT doped composites.

Theoretical investigation of ultrahigh stiffness in nanopolycrystalline diamond.

Erohin S. V. [1] , *Sorokin P.B.* [1]

sverohin@tisnum.ru
[1] Technological Institute For Superhard And Novel Carbon Materials, Troitsk, Moscow, Russia

Superhard materials (diamond, c-BN etc.) attract a special interest in the modern material science. The possible fabrication of material harder than diamond (ultrahard materials) can create the new branch in science and technology due to high potential to extend the boundaries of applicability of devices and tools based on them and allow effective processing of superhard materials. The investigations of such kind materials are generally separated on two branches: amorphous carbon materials which superior hardness and stiffness is not yet completely understood and polycrystallites which hardness is dependent on the grain size. Most likely, the hardness higher than that of diamond can display only nanopolycrystalline diamond (NPD) with grain size ~10^1 nm; this conclusion is supported by available experimental data of successful fabrication of ultrahard NPD [1,2].

Here we theoretically investigated in details the elastic properties of nanopolycrystalline diamond with crystallite sizes up to 10 nm. By analyzing the contributions from grains of single crystal structure and amorphous interface we obtained the dependence of bulk modulus of NPD on the crystallites average size which was fully supported by atomistic simulation of number of NPD models. Despite of very good correspondence between analytical and computational data several structures with ultrahigh stiffness were found which are not fitted to the predicted trend. We investigated the nature of such specific behavior and proposed new mechanism of ultrahigh stiffening which can explain reference experimental results.

Fig. 1. The example of NPD structure used in the simulation. The presented supercell contained 3 grains with average sizes 30 Å. The grains and interface are colored by orange and red color, respectively.

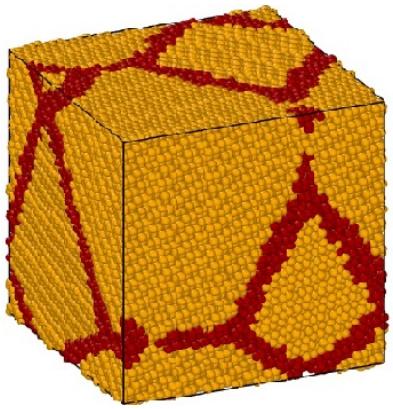

References

1. Q. Huang, D. Yu, B. Xu, W. Hu, Y. Ma, Y. Wang, Z. Zhao, B. Wen, J. He, Z. Liu, Nature (2014) **7504,** p. 250.
2. T. Irifune, A. Kurio, S. Sakamoto, T. Inoue, H. Sumiya, Nature (2003) **6923,** p. 599.

Is graphane the most stable carbon monohydride?

Kondrin M.V. [1] , *Brazhkin V.V.* [1]

mkondrin@hppi.troitsk.ru

[1] Institute for High Pressure Physics RAS, 142190 Troitsk, Moscow, Russia

Until the discovery of graphene the organic structures with dimensionality higher than 1 were proposed only occasionally [1]. However the successful synthesis of graphane [2] (that is 2-dimensional hydrocarbon film where hydrogen atoms are bound to graphene plane and so induces sp^3-hybridization accompanied with corresponding corrugation of the carbon plane) instigates interest in synthesis of hydrocarbon polymers in higher dimensions. The first move in this direction was the proposition of van-der-Waals bonded graphane sheets [3] stacked in the direction normal to planes and it was shown that this structure is more energetically favourable than benzene.

However almost simultaneously the efforts of invention of hydrocarbon structures comletely covalently bounded in 3D took place. Up to now there were proposed at least four 3D hydrocarbons [4]. Although they are more energetically favourable than cubane but all of them significantly loose in energy (more than 0.3 eV per CH group) to molecular benzene and stacked graphane sheets. Such a difference in energy are due to significant deviation of bond angles in 3D structures from the tetrahedral one.

In our report we propose completely covalently bonded 3D hydrocarbons whose cohesive energies according to DFT calculations are not worse than that of benzene and graphanes. These structures can be regarded as sublattices of known carbon structures so the strain exerted on the crystal lattice is minimal and mostly caused by steric interactions of hydrogen atoms. We suppose that these structures could be obtained through high pressure/high temperature treatment. Due to their porous structure they may turn out to be useful as mechanical, optoelectronic or biological materials.

The authors acknowledge financial support from the RSF (Grant No. 14-22-00093).

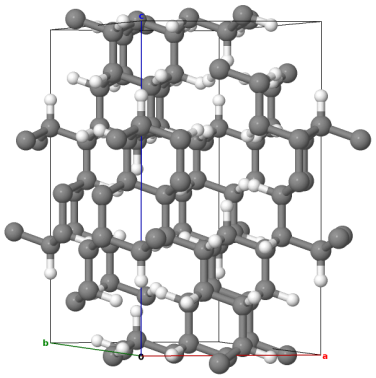

Diamond monohydride -- hypothetical completely covalently bonded hydrocarbon

References

1. M. H. F. Sluiter, Y. Kawazoe, Phys. Rev. B (2003) **68**, 085410
2. D. C. Elias, R. R. Nair, T. M. G. Mohiuddin, S. V. Morozov, P. Blake, M. P. Halsall, A. C. Ferrari, D. W. Boukhvalov, M. I. Katznelson, A. K. Geim, K. S. Novoselov, Science (2009) **323,** 610
3. X.-D. Wen, L. Hand, V. Labet, T. Yang, R. Hoffman, N. W. Ashcroft, A. R. Oganov, A. O. Lyakhov, PNAS (2011) **108**, 6833
4. C.-S. Lian, H.-D. Li, J.-T. Wang, Sci. Rep. (2015) **5**, 07723

Electromagnetic radiation by electrons in corrugated graphene

Ktitorov S.A. [1,2] , *Mukhamadiarov R.I.* [1]

ktitorov@mail.ioffe.ru

[1] Ioffe Institute, St.Petersburg, Russia

[2] St. Petersburg Electrotechnical University LETI, St. Petersburg, Russia

The recent experimental study has shown that a flat geometry of graphene is unstable that leads to forming of corrugations: topological defects and ripples [1]. Electrons motion through the rippled graphene sheet induces an electromagnetic radiation. The mechanism of formation of the bremsstrahlung radiation in graphene is similar to one in the undulator or wiggler [2]. While the electron trajectory in an undulator and wiggler deviates from the direct line due to the periodic system of the dipole magnets, electron trajectory in graphene is getting curved due to the ripples.

Our aim is to study the electromagnetic radiation of electrons in the corrugated graphene in the presence of the transport electric current [3] in the ballistic regime. A spatial period of ripples in graphene could reach several hundreds of nanometers [1]. This makes the semiclassical approach feasible. Despite of the "quasirelativistic" character of the spectrum, the ratio of Fermi velocity to the speed of light is much smaller, than unity and we can neglect a retardation of the electromagnetic radiation. All these points give us a reason to consider a motion of electrons in graphene within the classical approach. The most important mechanisms are bremsstrahlung, cyclotron, and undulator radiation [2]. The emission mechanism under the consideration resembles one in the undulator but practically without retardation.

We analyzed radiation using a few distinct models. At first model we consider geometric mechanism, directly connected with the presence of undulations, at the second – the pseudo gauge field effect making trajectory to get curved in the base plane. Both regular and random ripple structures are considered. Our results can be useful in experimental observation of graphene inhomogeneities and in making electromagnetic radiation generators of infrared and terahertz bands on graphene. We considered here an impact of the ripples in the monolayer graphene on its electromagnetic properties. The electromagnetic radiation was actually calculated with a use of the standard electromagnetic theory. Two cases, of regular and random structures are analyzed. Nonlinear relation between the random height function $h(x,y)$ and the gauge field $\mathbf{A}$ is shown to create the radiation frequency distribution central peak.

References

1. M. A. H. Vozmediano, M. I. Katsnelson, and F. Guinea, Phys. Rep. (2010) **496**, 1.
2. D. F. Alferov, Yu. A. Bashmakov and E. G. Bessonov, Sov. Phys. Tech. Phys. (1974) **18**, 1336.
3. K. Tantiwanichapan, J. DiMaria, S. N. Melo and R. Paiella, Nanotechnology (2013) **24**, 375205.

Graphene oxide and reduced graphene oxide in light of computationally supported neutron scattering study

Sheka E.F. [1] , *Natkaniec I.* [2] , *Rozhkova N.N.* [3] , *Buslaeva E.Yu.* [4] , *Tkachev S.V.* [4] , *Gubin S.P.* [4] , *Mel'nikov V.P.* [5] , *Druzbicki K.* [2,6]

sheka@icp.ac.ru

[1] Peoples Friendship University of Russia,

[2] Adam Mickiewicz University, Poznan, Poland

[3] Institute of Geology, Karelian Research Centre RAS, Petrozavodsk, Russia

[4] Institute of General and Inorganic Chemistry, RAS, Moscow, Russia

[5] Semenov Institute of Chemical Physics RAS, Moscow, Russia

[6] Frank Laboratory of Neutron Physics, Joint Institute for Nuclear Research, Dubna, Russia

The current paper presents results of an extended neutron scattering study of a set of graphene oxide (GO) and reduced graphene oxide (rGO) products of different origin. The first part concerned the rGO of natural origin presented by shungite carbon [1], the second was related to synthetic GO and rGO with the latter produced in the course of chemical treatment [2], and the third part was devoted to another pair of synthetic GO/rGO products with the latter produced via thermo exfoliation of the parent GO [3]. The study involved both the neutron diffraction (ND) and inelastic neutron scattering (INS).

The neutron diffraction patterns confirmed stacking structures of all the species consisting of a number of layers of nanosize (natural products) and microsize (synthetic products) lateral dimension and the interlayer distances of 7.0-7.2Å and 3.4-3.5Å for GO and rGO, respectively. The one-phonon amplitude-weighted density of vibrational states represents the inelastic incoherent neutron scattering spectra of the products. Calculations of spectra were performed in the framework of semi-local density functional theory. The computational models were adjusted to the atom mass content of both GO and rGO species.

The performed study has convincingly shown that neutron scattering clearly distinguishes GO and rGO species and well exhibits both common features and differences related to the members of both communities. If retained water in GOs and graphene-hydride nature of rGOs provide the commonality of dynamic properties within each of the community, the difference in the relevant sheet topology is responsible for a noticeable variability of the latter. The study has convincingly shown the topochemical nature of a large polyvariance of both GO and rGO products evidencing its topochemical nature.

References

1. F. Sheka, N.N. Rozhkova, K. Hołderna-Natkaniec, I. Natkaniec, Nanosystems: Phys. Chem. Math. (2014) **5**, 659.
2. Natkaniec, E.F. Sheka, K. Drużbicki, K. Hołderna-Natkaniec, S.P.Gubin, E.Yu. Buslaeva, S.V. Tkachev, J. Phys. Chem. C (2015) (submitted).
3. F. Sheka, I. Natkaniec, V.P. Mel'nikov, K.Druzbicki, Nanosystems: Phys. Chem. Math (2015) (submitted).

Round Table 2: Technical applications of nanocarbons

Controlled synthesis of high-performance CNT-fiber by CVD for multifunctional nanocomposites fabrication

Aleman B. [1] , *Reguero V.* [1] , *Mas B.* [1] , *Vilatela J.J.* [1]

belen.aleman@imdea.org
[1] IMDEA Materials Institute, Madrid, Spain

CNT-fiber was produced by direct spinning of long CNTs from the gas phase *(Figure 1a)* as they grow by floating catalyst chemical vapor deposition (CVD)[1].

On one hand, through the addition of sulfur it is possible to control the type of CNTs that make up the fiber from SWCNTs to MWCNTs[2], which is mainly manifested in Raman spectra by the upshift in the 2D-peak position *(Figure 1b)*. The increase in sulfur promoter also results in a higher reaction yield from 0.7% to 9%. Combining multiscale characterization techniques we establish the composition of the catalyst particles and position in the isothermal section of the C−Fe−S ternary diagram at 1400 °C.

On the other hand, we have also analyzed how controlling parameters as precursor feed rate, hydrogen atmosphere and winding rate, favors the CNT-bundles alignment along the fiber axis leading to an improvement of the mechanical properties with moduli ranging from 5-20 GPa/SG to 40 GPa/SG for non-oriented and oriented fibers respectively *(Figure 1c)*. The orientation degree is confirmed by SEM images and SAXS/WAXS diffraction patters *(Figure 1d)*.

In summary, the fine control of the building blocks at a molecular scale of a high surface area material (~ 170 m^2/g) as CNT-fiber, will lead to tailor the structure of hierarchical materials through its combination with polymers and semiconductors for structural[3] and energy storing applications[4].

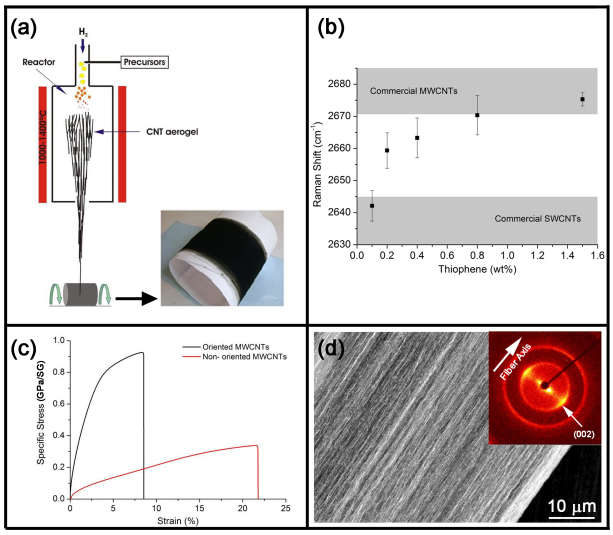

(a) Direct spinning CVD process scheme and as-spun CNT-fiber photograph. (b) Upshift in the Raman 2D-peak position with increasing thiophene. (c) Strain-stress curves for oriented and non-oriented CNT-fibers. (d) SEM image of an oriented fiber and its SAXS/WAXS pattern.

References

[1] Li Y-L, Kinloch IA, Windle AH. Science 2004;304:276–8.
[2] Reguero V, Alemán B, Mas B, Vilatela JJ. Chem Mater 2014;26:3550–7.
[3] Vilatela JJ, Khare R, Windle AH. Carbon 2012;50:1227–34.
[4] Su F, Miao M. Nanotechnology 2014;25:135401.

Laser-induced carbon structures with controlled functional properties – new perspectives for applications

Abramov D.V. [1] , *Arakelian S.V.* [1] , *Kutrovskaya S.* [1] , *Kucherik A.* [1] , *Prokoshev V.G.* [1]

arak@vlsu.ru
[1] Vladimir State Univeristy

1. Synthesis of new carbon materials by laser irradiation of carbon target is an actual branch of laser physics. Laser sources with different pulse duration allow to change the heating rate of carbon with realization of different transition scenarios such as solids-liquid-vapor.

The obtaining of different allotropic forms of carbon depends on the conditions (pulse duration, energy, repetition rate, etc.) of laser action.

Last years, methods of laser irradiation on the carbon target in a liquid medium are actively developed. In this case the formation of a cavitation bubble, which can provide additional pressure on the target surface, the value of which can reach values of 10 GPa depends on laser irradiation conditions. Also, using laser setups with femtosecond pulse duration near the target surface, leads to a transition of the liquids into the «liquid plasma», which ensures both high temperature and high pressure in the area of influence

2. Experiments of laser action on carbon target in the air and in water are presented in this paper.

For the realization of different regimes of laser surface modification of the target and the formation of micro- nanoparticles in a liquid the YAG: Nd laser with a pulse duration from 0.5 ms up to 20 ms (pulse energy up to 50J) and the Ti: Sp femtosecond laser with 50 fs pulse duration (pulse energy up to 0.01 J) were applied.

Melting processes were observed (in a real time scale) during the laser irradiation of samples in air by millisecond laser.

The dependence on the laser beam, pulse duration, focusing conditions leads to a formation of domains and centers of melting with dimensions which are defined by the conditions of the experiment

During the process of laser irradiation of the target in the water, the surface layer explosion of the target due to local boiling supercritical fluid, «cold» ablation, solid-phase modification of the sample surface were observed. During the colloidal droplets deposition the structures like carbon foam were observed.

3. The results of comparative experiments on laser effects on carbon targets, placed in water and liquid nitrogen, are presented as well. The possibility of obtaining carbon nanoparticles with small deviation from the mean size, when the laser impact is of moderate intensity on the target placed in the water. Demonstrated change of the Raman spectra depending on the conditions of laser irradiation and the target material. When ablation of carbon targets in liquid nitrogen occurs, the graphene like multilayer structures are induced. Studies of surface carbon target after laser exposure, which allow us to talk about the development of various laser-induced processes, depending on the duration of the laser pulse and the target material

4. The obtained results can be used in the future to obtain new nanostructured carbon materials with different/varied properties. These methods of direct laser deposition with additional geometric and/or physical structuring management is promising for the formation of thin carbon films with controlled geometry/topology for different applications in modern photonics.

Diamond-tungsten carbide nanocomposites as working elements for fine turning and drilling tools

Bochechka O.O. [1] , *Nazarchuk S.M.* [1] , *Lutsak E.M.* [1] , *Gavrilova V.S.* [1] , *Stahniv M.E.* [1] , *Zabolotnyj S.D.* [1] , *Shpadkivska T.O.* [1]

bochechka@ism.kiev.ua
[1] V. Bakul Institute for Superhard Materials of NASU, Kyiv, Ukraine

The diamond-tungsten carbide nanocomposite was produced by HP-HT sintering of diamond nanopowder with nanoparticles of a tungsten-containing substance. The mixtures were prepared by chemical method [1]. We have used ASM5 0.1/0 statically synthesized diamond nanopowder, and a tungsten trioxide nanopowder as components of the mixtures. Before sintering the mixture was heat-treated in a hydrogen atmosphere.

According to X-ray analysis, the sintered samples include WC tungsten carbide and WO_3 tungsten oxide. Tungsten carbide was formed as results of both the direct interaction of diamond with tungsten and reactions in the W–C–O system [2]. Nanoparticles of tungsten carbide formed in voids between the diamond nanoparticles are chemically bonded with them. This improves physico-mechanical properties of the composite. The composite combines high hardness (HV = 25 GPa), fracture toughness (K_{IC} = 6.6 MPa·m$^{1/2}$), and thermal stability (at 1370 K K_{ts} = 0.86).

Fine turning of aluminum alloy A6 sample of diameter of 60–65 mm was made. Round cutting insert of nanocomposite of diameter of 7±0.025 mm served as the working element of the tool. Fixation was carried out mechanically. Cutter had a rake angle g of 0°; flang angle a of 10. Feed was 0.25 mm/rev and cutting speed was 4.5 m/s. The formed surface has a surface roughness Ra of 0.4 μm and waviness Raw of 0.7 μm.

Working elements for drilling tools were manufactured by machining samples of the diamond polycrystalline composite material (DPCM). DPCM samples were obtained by HP-HN reaction sintering of mixture of diamond and tungsten powders. Diamond powder mixture consisted of two levels of dispersivity. The mixture composition was determined on the basis of the data, obtained in the study of crushing diamond powders with different particles under the high pressure influence on them. Sintering parameters were determined by sintering of diamond - tungsten carbide composite based on nanopowder UDD. DPCM Knoop hardness at a load of 10 N on the indenter is 47 ± 7 GPa. At the same time under high pressure and temperature one of the frontal surfaces of the DPCM samples was metalized by Cu-Ti alloy. Cutting tools for rotary drilling of bore holes with a diameter of 33 mm for sling anchorage of underground working, equipped with the specified work items were developed and manufactured. The laboratory tests showed the usefulness of the developed tools for drilling anchor drill holes in rocks up to 168 MPa strength and abrasion up to 45 mg.

References

1. V. Novikov, O.O. Bochechka, S.M. Nazarchuk, V.S. Gavrilova, G.S. Oleinik, L.O. Romanko, I.A. Sveshnikov, S.D. Zabolotnyi. Patent of Ukraine 50931 // Byull. 2010, **12**.
2. N. Nazarchuk, A.A. Bochechka, V.S. Gavrilova, L.A. Romanko, N.N. Beljavina, L.I. Aleksandrova, V.N. Tkach, E.F. Kuzmenko, S.D. Zabolotnyi, J. Superhard Materials (2011) **33**, N. 1, 1.

Graphene nanobelts films for highly sensitive, semi-transparent and flexible pressure and strain resistive sensors

Alaferdov A.V. [1] *, Rackauskas S.* [1] *, Savu R.* [1] *, Vaz A.* [1] *, Rackauskas T.* [1] *, Moshkalev S.A.* [1]

stanisla@ccs.unicamp.br
[1] UNICAMP, Campinas, Brazil

A simple low-cost approach to fabricate new type of resistive sensors based on multi-layer graphene nanobelts (lengths up to 20-50 um, widths 1-5 um, thickness 2-20 nm) has been developed. The nanobelts are obtained from natural graphite and can be done flexible or rigid, depending in the process conditions. The sensor operates at low voltage (0.1-1 V), has low power consumption (less than 1 mW) and can be used for both strain and pressure measurements. The sensor has a sensitive film consisting of randomly oriented graphene nanobelts forming a continuous conductive layer by percolation, with the average film thickness in the range of 20-50 nm. The film is deposited over flexible substrates like PDMS using modified Langmuir-Blodgett method. The strain and pressure sensing mechanisms in so produced devices are due to deformation-dependent resistance of contacts between individual nanobelts. Extremely high sensitivity to strain (gauge factor >25) and dynamic range (strain up to 40%) have been demonstrated. The sensor can be used in a wearable form for monitoring of blood pressure with high sensitivity. Possible applications of the sensor include detection of strain, touch, vibrations, acoustic signals.

Other emerging applications of this new nanomaterial (e.g., in photonics) will be also discussed.

Fluorinated graphene suspension and films for different applications

Nebogatikova N.A. [1] , *Antonova I.V.* [1,2] , *Prinz V.Ya.* [1]

nadonebo@gmail.com

[1] Institute of Semiconductors Physics SB RAS, Novosibirsk, Russia

[2] Novosibirsk State University, Novosibirsk, Russia

We have suggested an easy and technologically simple method for graphene suspension fluorination. We have examined the interaction between a suspension of graphene in dimethylformamide and an aqueous solution of hydrofluoric acid. The functionalizing treatment took place at room temperature. The experimental evidences proving the fluorination of suspension flakes during the functionalizing treatment are based on the evolution of Raman spectra, XPS and FTIR data, emergence of insulating film properties. A set of thin, thermally and chemically stable films with different fluorination degree was created on the silicon substrate.

The obtained films demonstrate the evolution of structural and electrical properties with increasing of chemically modification treatment duration. By means of scanning electron and atomic force microscopy, we showed that the characteristic particle sizes in the formed films and the thicknesses of the films themselves depended on the time during which the suspension was treated in the aqueous solution of HF. The decreased thickness and a roughness reduction on the surface of the films were shown with increasing the treatment duration. This effect was found to be accompanied with simultaneous transition of the flakes from conducting to insulating state. Surprisingly an additional splitting off for initial flakes and their fractionation in finer flakes that occurred during the treatment of the suspension was observed (as a result of the interaction, the suspension particles undergo an additional splitting).

The film dielectric constant ε of the films was determined to be equal to 3.2 down to 1.1 depending on the fluorination degree of the material. It was shown that films prepared from a fluorinated suspension exhibit high breakdown fields (> $1x10^6$ V/cm), and they contain low charge densities in the film and at the interface with silicon in metal-dielectric-semiconductor structures, the fixed charge density in the film and the density of interface states being ~$(1-5)x10^{10}$ cm^{-2}. Such excellent characteristics of the dielectric film (high breakdown electrical field and low densities of charges) make them promising layers for the use as insulating elements in thin-film device structures.

Obtained dielectric films exhibit good structural and electrical properties. Owing to the simple preparation procedure of such films and easiness of their application onto substrates, and also owing to the possibility of obtaining very thin layers, fluorinated graphene films offer promise in application as dielectric layers in thin-film device structures. Moreover, the films from the fluorinated suspension are cheap, practically feasible and easy to produce.

Graphene-based shungite nanocarbon as a catalyst supporter

Rozhkova N.N. [1] , *Trenikhin M.V.* [2] , *Gorlenko L.E.* [3] , *Yemelyanova G.I.* [3] , *Lunin V.V.* [3]

rozhkova@krc.karelia.ru

[1] Institute of Geology, Karelian Research Centre RAS, Petrozavodsk, Russia

[2] Institute of Hydrocarbons Processing, Siberian Branch RAS, Omsk, Russia

[3] Department of Chemistry, Moscow State University, Moscow, Russia

Shungite carbon from different deposits Shun'ga (Sh) and Nigozero (N), formed under different conditions, were found to be similar in the structure and properties of nanocarbon, such as a multi-level structural pattern and physico-chemical properties, attributed to distinctive interaction between the nanostructural elements of carbon and water. The size distribution of pores for all shungites is characterized by the dominance of micro- and submesopores, less than 0.7 –5.0 nm in size, and correlates with the sizes of basic structural elements (graphene fragments ~ 1 nm) and with the sizes of primary shungite carbon (ShC) aggregates [1].

The hydrothermal effect on ShC from N deposit in nature has led to the release of graphene fragments and their primary aggregates and to a reduction in the amount of metal impurities. A similar process was carried out in a laboratory on ShC from Sh deposit. Nanoparticles, produced from water dispersion, coincide practically in adsorption parameters with ShC from N deposit [2].

The catalytic activity of platinum on shungite nanocarbon in a hydrogen peroxide decomposition reaction is one order of magnitude higher than that of activated carbons and several times higher than that on the oxide carriers, namely Al_2O_3 and SiO_2.

Changes in the packing of the structural units of graphene in ShC aggregates are responsible for a difference in its activity even when condensed from aqueous dispersion at ambient conditions. As a result of such activation, the specific surface of ShC increases by two orders of magnitude. The main contribution to the increase in total porosity is made by micro- and meso-porosity.

Pt nanoparticles on ShC were characterized by Raman spectroscopy, TEM, X-ray and electron diffraction to corroborate a substantial change in the structural parameters of ShC and the sizes of the metal catalyst for the samples from Sh and N deposits.

The catalytic effect of Pt on ShC observed is due to the distinctive structural pattern of ShC, primarily the graphene nature of the basic structural element [3]. The graphene has a dipole moment of ~5.6 D, as estimated from experimental data [4]. The characteristics, which manifest themselves in the electronic properties of ShC comparable with the oxide catalyst supporters, are discussed.

The work of N.N.R. was supported by Basic Research Program, RAS, Earth Sciences Section-5 and grant RFBI 13-03-00422.

References

1. N.N. Rozhkova, G.I. Yemel'yanova, L.E. Gorlenko, A.V Gribanov, V.V. Lunin, Glass Physics and Chemistry (2011) **37**(6), 613.
2. N.N. Rozhkova, *Russian Journal of General Chemistry* (2013) **4**, 240.
3. E. F. Sheka, N.N. Rozhkova, Int Journ Smart Nano Mat. (2014) **5,** 1.
4. A.R. Hairullin, T.P. Stepanova, N.N. Rozhkova, S.V.Gladchenko, St.Petersburg State Polytechnical University Journal. Physics and Mathematics (2012) **4** (153), 111.

Development of novel flexible composites reinforced based on carbon fibers coated with carbon nanotubes

Urvanov S.A. [1]

urvanov@tisnum.ru
[1] Technological Institute for Superhard and Novel Carbon Materials, Troitsk, Moscow, Russia.

Carbon fibers (CFs) have always been very attractive filler for manufacturing of highly strong composite materials. And at the same time polymers such as most of silicones and polyurethanes are widely used primarily owing to their mechanical characteristics and chemical and biological inertness. In this context we tried to combine properties of these materials. But there is a very considerable challenge for development such composites: namely low adhesion between CFs and most of polymer matrices. In a number of studies to solve this problem CFs surface was covered with carbon nanotubes (CNTs) by catalytic chemical vapor deposition (CVD) where nanotubes act as “anchors” and prevent the slipping out of CFs from polymer matrices [1-4]. The only significant disadvantage of this method is the deterioration of the mechanical properties of the fiber during the modification process, which is caused by the interaction between CFs surface and catalyst particles needed for CNTs growth [1, 4].

In the current study we report the novel flexible and strong composite materials based on nanotube-coated CFs and elastic matrices. CNTs were obtained by CVD method on CFs surface. For introduction of catalyst particles the impregnation method was used. It included the coating of CFs surface with protective layer of aluminum oxide for preventing the destruction process of CFs during CNTs synthesis. Influence of the CNTs on CFs tensile strength and interfacial shearing strength was estimated by single fiber tests.

It was found the effective load transfer between the fiber and the matrix is influenced by the CNTs which results into improved mechanical performance of the composites. Also rigidity of composites increased approximately 20% and at the same time the samples were flexible. Thus samples of produced composite combine properties of components and have a high resistance to delamination.

In conclusion the development of such composites is a perspective way for producing flexible, strong and cheap materials with advanced functionality.

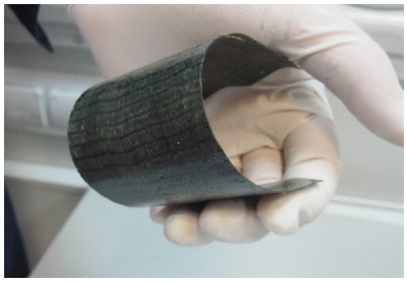

Fig.1. Photograph of a sample of flexible composite based on modified carbon fiber.

References

1. D. Greef, A. Magrez, E. Couteau, J.-P. Locquet, L. Forro, J. W. Seo, Physica Status Solidi B (2012) v. 249, p.2420.
2. H. Qian, A. Bismarck, E. S. Greenhalgh, G. Kalinka, M. S. P. Shaffer, Chem. Mater. (2008) v.20, p.1862.
3. Q. Zhang, J. Liu, R. Sager, L. Dai, and J. Baur, Comp. Sci. and Tech. (2009), v.69, p.594.
4. K. J. Kim, J. Kim, W.-R. Yu, J. H. Youk, J. Lee, Carbon (2013) v. 54, p. 258.

Poster session 1:
Fullerenes.
Nanodiamond particles.

Regioselective protonation of cis-2-$C_{60}(CF_2)_2$ dianion

Bogdanov V.P. [1] , *Romanova N.A.* [1] , *Belov N.M.* [1] , *Goryunkov A.A.* [1]

vb@thermo.chem.msu.ru

[1] Chemistry Department, Lomonosov Moscow State University, Moscow, Russia

Fine tuning of an electronic structure of a fullerene cage can be performed via structural modification of the cage as well as a exahedral attachment of various groups to sp^2-carbon atoms. Insertion of difluorocarbene :CF_2 is prospective way for cage modification yielding homofullerenes with preserving of an conjugated p-electron system and enhanced electron affinity. Among those compounds [6,6]-opened $C_{60}(CF_2)$ and isomers of $C_{70}(CF_2)$ in neutral and anionic forms are the most fully studied [1–3]. In particular, it was shown, that the excess charge density in dianions $C_{60}(CF_2)^{2-}$ and $C_{70}(CF_2)^{2-}$ is localized on carbon atoms bearing bridging CF_2 group [2, 3]. This made it possible to develop a strategy of regioselective synthesis of dihydride $C_{60}(CF_2)H_2$ [3].

Difluoromethylenated fullerenes with two or more groups are virtually unstudied. The only isomer *cis-2*-$C_{60}(CF_2)_2$, where CF_2 groups are inserted into [6,6]-bonds of adjacent hexagons, is structural characterized [1].

Here we report the first results of *cis*-2-$C_{60}(CF_2)_2$ hydrogenation via protonation of in situ generated fulleroid dianions. It was shown, that hydrogenation proceeds successively with formation of dihydride $C_{60}(CF_2)_2H_2$ and tetrahydride $C_{60}(CF_2)_2H_4$. The hydrogenated products were chromatographically isolated and characterized by means of MALDI mass spectrometry, UV/Vis and NMR spectroscopy. The compound structures were elucidated by spectral data and with quantum chemical calculation at the DFT level of the theory. DFT calculations of relative energies and charge distribution of anionic and hydrogenated intermediates makes it possible to suppose mechanism of hydrogenation of *cis-2*-$C_{60}(CF_2)_2$.

References

1. S. Pimenova, A.A. Kozlov, A.A. Goryunkov, V.Yu. Markov, P.A. Khavrel, S.M. Avdoshenko, I.N. Ioffe, S.G. Sakharov, S.I. Troyanov, L.N. Sidorov. *Chem. Commun*. (2007), p. 374.
2. A. Samoylova, N. M. Belov, V. A. Brotsman, I. N. Ioffe, N. S. Lukonina, V. Yu. Markov, A. Ruff, A. V. Rybalchenko, P. Schuler, O. O. Semivrazhskaya, B. Speiser, S. I. Troyanov, T. V. Magdesieva. A. A. Goryunkov. *Chem. Eur. J.* (2013) **19**, p. 17969
3. A. A. Goryunkov, E. S. Kornienko, T. V. Magdesieva, A. A. Kozlov, V. A. Vorobiev, S. M. Avdoshenko, I. N. Ioffe, O. M. Nikitin, V. Yu. Markov, P. A. Khavrel, A. Kh. Vorobiev, L. N. Sidorov. *Dalton Trans*. (2008) **48**, p. 6886

Synthesis, identification and physical-chemical properties of trismalonates of light fullerenes $C_{60}[=C(COOH)_2]_3$ and $C_{70}[=C(COOH)_2]_3$

Charykov N.A. [1,2] , *Semenov K.N.* [1,3] , *Manyakina O.S.* [2] , *Ivanova K.A.* [3] , *Keskinov V.A.* [2,1] , *Letenko D.G.* [4] , *Nikitin V.A.* [5] , *Klepikov V.V.* [2] , *Cherepkova I.A.* [2] , *Matuzenko M.Yu.* [2] , *Tyurin D.P.* [2] , *Shestopalova A.A.* [2] , *Ivanova K.V.* [6]

ncharykov@yandex.ru

[1] Public Joint Stock Company "Scientific andProduction Association "TECHNOLOGIES", Saint-Petersburg, Russia

[2] Saint-Petersburg State Technological Institute (Technical University), Saint-Petersburg, Russia

[3] Saint-Petersburg State University, Saint-Petersburg, Russia

[4] Saint-Petersburg State University of Architecture and Civil Engineering, Saint-Petersburg, Russia

[5] Saint-Petersburg State Polytechnical University, Saint-Petersburg, Russia

[6] Saint-Petersburg State Electro-Technical University (LETI), Saint-Petersburg, Russia

The synthesis of water soluble tris-malonates of light fullerene $C_{60}[= C(COOH)_2]_3$ and $C_{70}[= C(COOH)_2]_3$ was provided by the method [1]. Yield of formed fullerenes trismalonatesis ≈ 65 - 70 mass % from theoretical. Identification of both trismalonates was provided by the methods of: element analysis, infrared and electronic spectroscopy, complex thermal analysis.

In $C_{60}[= C(COOH)_2]_3$-water and $C_{60}[= C(COOH)_2]_3$-water binary systems at 25°C concentration dependencies of density, average and partial molar volumes of water and both trismalonates, refraction indexes were measured. Molar and specific fullerenes trismalonates refractions was determined and calculated according to additive refraction rule.

In $C_{60}[= C(COOH)_2]_3$-water and $C_{60}[= C(COOH)_2]_3$-water binary systems at 25°C concentration dependencies of electrical conductivity, hydrogen indicator, seeming dissociation degrees and concentration dissociation constants of $C_{60}[= C(COOH)_2]_3$and $C_{70}[= C(COOH)_2]_3$ in water solutions were investigated.

Solubility of $C_{60}[= C(COOH)_2]_3$ and $C_{70}[= C(COOH)_2]_3$ in water in temperature range 20-80°C was determined. Both diagrams consist of two branches of the crystallization: first one - of crystal hydrate of fullerenes trismalonate, second – of non-hydrated fullerenes trismalonate and have one invariant point, corresponds to saturation by two mentioned solid phases. Thermal gravimetrical analysis of crystal hydrate of $C_{70}[= C(COOH)_2]_3$ was provided.

The investigation of concentration dependence of the dimension of the associates of $C_{60}[= C(COOH)_2]_3$and $C_{70}[(=C(COOH)_2]_3$ in water solutions at 25°C we have provided by the method of the dynamic light scattering in visible wavelength region. Different types associates (monomers form I-type, I-type form II-type, II-type form III-Type…) were discovered. For the description association processes in these systems the model of consequent hierarchical association model was used.

Concentration dependencies of temperature of the crystallization of H2O (ice), i.e. cryometrical investigations of $C_{60}[= C(COOH)_2]_3$and $C_{70}[(=C(COOH)_2]_3$ water solutions were provided. Excess functions (activity coefficients of fullerene trismalonates and water activity) were calculated.

Investigations were supported by Russian Found of Fundamental Investigations – RFFI (Project N 15-08-08438) and with the help of the equipment of Resource Center of S-Petersburg State University GEOMODEL.

References

1. Lamparth I., Hirsch A. J. Chem. Soc. Chem. Commun. 1994. P. 1727–1728.

Comparative characteristics of metallofullerenes, clusterfullerenes with carbide and nitride synthesized under high and low pressure

Churilov G.N. [1] , *Dudnik A.I.* [1] , *Vnukova N.G.* [1] , *Dubinina I.A.* [2]

churilov@iph.krasn.ru

[1] Kirensky Institute of Physics SB RAS, Krasnoyarsk, Russia

[2] Siberian Federal University, Krasnoyarsk, Russia

Fullerene may be considering the one of the most beautiful molecule particular endohedral molecular. Fullerene may be referring to the most perspective substances of 21 century in the context of applied investigations [1]. The capabilities of that fullerenes are identified for theorists, who predict the on the base of quantum chemical calculations because that substances are approachable only in unperceivable amount. At this paper we present the results of our investigations in the area of search of advance synthesis. The synthesis of carbon condensate contained endohedral fullerenes was carried by us in the range of high and low pressure (0.02-0.4 MPa). The setup contained two pairs of electrodes which lay at the perpendicular planes and are directed at the angle (57°) to vertical axial of symmetry. This set up is modified variant of the set up described earlier [2]. The investigation results shown that the quantity of endohedral fullerene contained at the carbon condensate mainly depend on pressure and current intensity. Their specific value and used solvents are necessary for each class.

The work was partially supported by the Ministry of Education and Science of Russian Federation № 14.613.21.0010; Russian Foundation for Basic Research № 15-03-06786.

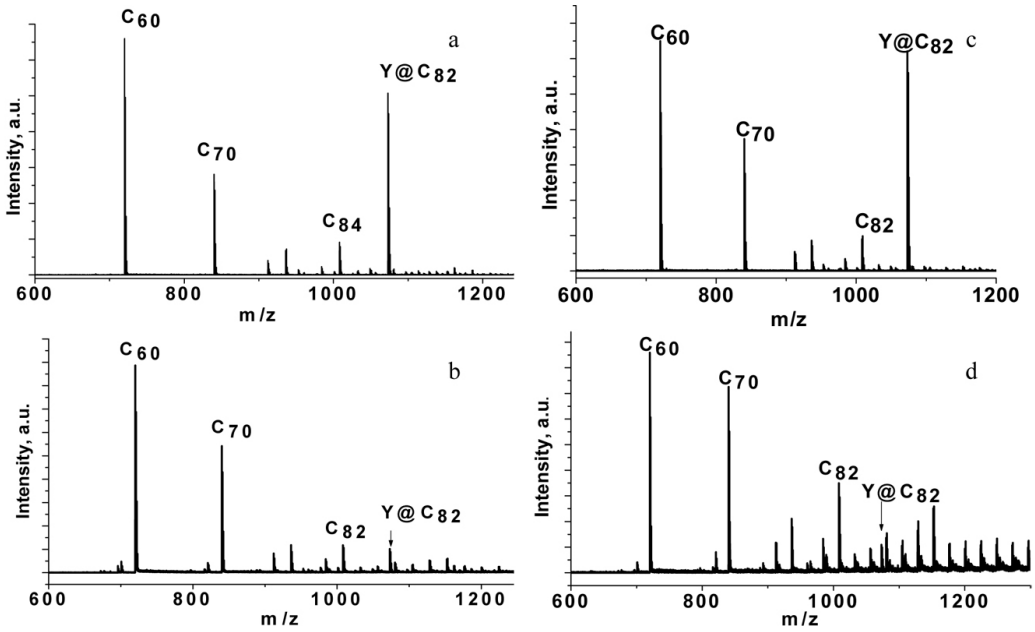

Fig.1. Mass spectra of fullerene extract from $Y@C_{82}$ containing soot (positive ion): a- pyridine extract, b- CS_2 extract from the soot synthesized under 0,1 MPa; c - pyridine extract, d- CS_2 extract from the soot synthesized under 0,4 MPa (Bruker BIFLEXTM III Time-of-Flight mass spectrometer with laser desorption).

References

1. A.A. Popov, S. Yang, and L. Dunsch, Chem. Rev. (2013) Volume 113, 5989.

2. G.N. Churilov, W. Kratschmer, I.V. Osipova, G.A. Glushenko, N.G. Vnukova, A.L. Kolonenko, A.I. Dudnik, Carbon (2013) Volume 62, 389.

Comparative study of antioxidant activity of fullerenols including higher and endohedral fullerenols by inhibition of adrenaline autoxidation

Dubinina I.A. [1] , *Dudnik A.I.* [2] , *Vnukova N.G.* [2] , *Churilov G.N.* [2]

churilov@iph.krasn.ru

[1] Siberian Federal University, Krasnoyarsk, Russia

[2] Kirensky Institute of Physics SB RAS, Krasnoyarsk, Russia

Fullerenes have antioxidant activity but extremely poor biocompatibility so they must be chemically functionalized before being practically used. C_{60} and C_{70} fullerenols have good water-solubility and found to have outstanding antioxidant activity, thus they have potentials in medical applications.

We synthesized the fullerene mixture and purified individual C_{60} and C_{70} fullerenes by HPLC [1]. Hydroxylated fullerenes was synthesized in acidic conditions by treatment with nitric acid. Antioxidant activity of fullerenols was measured according to Hasanova et. al [2] by the inhibition of adrenalin autoxidation. The reaction mixture contained 0.1 cm^3 of 0.1% adrenalin hydrochloride, 2 cm^3 carbonate buffer, pH 10.2, and 0.03 cm^3 of fullerenole solution. The increase in absorbance due to adrenalin autoxidation was monitored at 347 nm and the percentage inhibition of the maximal rate of increase in absorbance was determined. According to [2], more than 10% inhibition rate shows the antioxidant activity of investigated solution. This method has been developed for measuring antioxidant activity of vegetative gathering and for the first time applied for fullerenols. Experiment demonstrated both C_{60} and C_{70} fullerenols to possess antioxidant potential – 19.8% and 24.1% accordingly. Thus, we expect higher fullerenols to have even higher antioxidant activity. Endohedral fullerenols encapsulating a metal atom within the fullerene cage are of our current interest as pharmaceuticals for therapy and diagnosis.

The work was partially supported by the Ministry of Education and Science of Russian Federation № 14.613.21.0010; Russian Foundation for Basic Research № 15-03-06786.

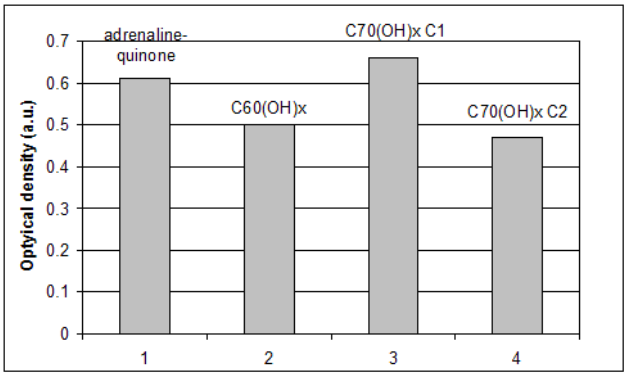

Fig. 1. Increase in absorbance of adrenaline solution: 1 – pure adrenaline, 2 – in addition of $C_{60}(OH)_x$, 3 - in addition of $C_{70}(OH)_x$ with C1 concentration, 4 - in addition of $C_{70}(OH)_x$ with C2 = 0,5 C1 concentration.

References

1. G.N. Churilov, W. Kratschmer, I.V. Osipova, G.A. Glushenko, N.G. Vnukova, A.L. Kolonenko, A.I. Dudnik, Carbon (2013) Volume 62, 389.
2. Hasanova S.R., Plehanova T.I.,Gashimova D.T.,Galiahmetova E.H., Klysh E.A. (2007) Proc. of Voronezh State University. Series: Chemistry. Biology. Pharmacy. 1, 163.

Optical properties investigation of X-ray irradiated composite C_{60}-CdTe thin films

Elistratova M.A. [1] , *Zakharova I.B.* [1] , *Romanov N.M.* [1,2] , *Kvyatkovskii O.E.* [2]

elistratovamari@yandex.ru
[1] St. Petersburg State Polytechnic University, St. Petersburg, Russia
[2] Ioffe Institute, St.Petersburg, Russia

Fullerene C_{60} appears to be a good acceptor material for making bulk heterojunction with A_2B_6 donors. CdTe-C_{60} materials are of a great interest in molecular electronics and optoelectronics, but investigation of semiconductor impurities intercalation in fullerite crystals are not enough at research view [1,2]. In this work we report about nanocomposite fullerene films doped by CdTe with concentrations from 10 to 50 mol. %. Thin films were obtained by means of vacuum co-evaporation in a Knudsen cell on Si, KBr, ITO-glass substrate. Surface morphology and phase constitution of prepared films were measured by secondary electron microscopy and energy-dispersive X-ray spectroscopy.[3]

The samples were subjected to X-ray irradiation in REIS-D equipment with a rhenium anode. X-ray energy flux was $5 \cdot 10^{-3}$J/s during 6 hour. Transmittance in UV-VIS region, photoluminescence at 77 K and IR Fourier spectra are measured. The additional peaks in photoluminescence spectra at 1.99 eV were detected. It is found that intensive X-ray irradiation of the films gives rise to considerable enhancement of intensity of the additional peak in pure C60 samples. In the case of composite films this peak becomes prevalent in spectra of irradiated films. The possible reason is that X-ray irradiation brings to dimerization and of the C60 matrix and formation a new electronic structure.

DFT/B3LYP quantum-chemical calculations for $[C_{60}]_n$CdTe molecular complexes, $(C_{60})_2$ and $C_{120}O$ dimers were performed to elucidate some experimental results. The calculations give the optimized geometry, formation energy for molecular complexes and excitation electron spectrum in satisfactory agreement with optical experiments.

References

1. Klesper, R. 1. Baumann, J. Bargon, J. Hormes H. Zumaqu´e-d´ıaz, G.A. Kohring. Investigationson the behaviour of C60 as a resist in X-ray lithography. Applied Physics A (2005) 80, p. 1469-1479
2. S. Shibu, A. Sonoda, Z. Tao, Q. Feng, A. Furube, S. Masuo, L. Wang, N. Tamai, M. Ishikawa, V. Biju. Photofabrication of Fullerene-Shelled Quantum Dots Supramolecular Nanoparticles for Solar Energy Harvesting, ACS Nano, (2012) 6, p. 1601–1608
3. B. Zakharova, V.M. Ziminov, N.M. Romanov, O.E. Kvyatkovskii, T.L. Makarova. Optical and structural roperties of fullerene films doped with cadmium telluride. Physics of the Solid State (2014) 56, p. 1064-1070

Development of method for prediction of fullerenes and endohedral metallofurrenenes relative stability

Fedorov A. [1,2] , *Irle S.* [3] , *Yoshifumi N.* [4] , *Visotin M.* [5] , *Kuzubov A.* [5] , *Popov Z.* [1]

alex99@iph.krasn.ru

[1] L. V. Kirensky Institute of Physics SB RAS, Krasnoyarsk, Russia

[2] Krasnoyarsk Institute of RailwayTransport, Krasnoyarsk, Russia

[3] Department of Chemistry, Graduate School of Science, Nagoya University, Nagoya, Japan

[4] Nakai research group, Waseda university, Tokyo, JAPAN

[5] Siberian Federal University, Krasnoyarsk, Russia

A new method for estimation of nanostructures relative yields at high temperature synthesis is developed. The method is based on calculation of probabilities of nanostructure or molecule breakdown due to breach of one of its surficial chemical bonds. This probability is calculated as a sum of one-bond-breach probabilities, i.e. the probability of one chemical bond to stretch over some critical distance, while molecule goes through thermal vibrations. Applying the Central Limit Theorem and assuming that all vibrations are independent, one can obtain the probability of one bond break through calculating vibration eigen frequencies and eigenvectors. Thus, summing over all the bonds, the probability of the whole molecule breakdown can be found.

This method was used for calculation of relative stability for all possible IPR (isolated pentagon rule) and some non IPR isomers of fullerenes, beginning with C20 and up to C100. Expecting the yield of some fullerene to be proportional to the stability of this fullerene or to the inverse of the fullerene breakdown probability, the relative yields of different fullerenes were obtained. The results can qualitative explain the experimental yields of different fullerenes. The method has been also applied for calculation of some endohedral metallofurrenenes yields, which allowed to explain the difference in yields of fullerenes and endohedral furrenenes.

Since the method is based on universal propositions, one can expect that this method can provide an explanation of other nanostructures yields at high temperatures.

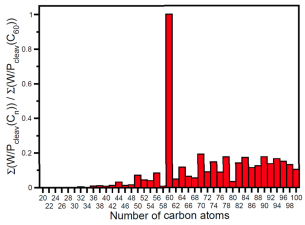

Calculated relative yield for all IPR and some non IPR fullerenes from C_{20} to C_{100} at temperature 3000 K

References

[1] A. S. Fedorov, D. A. Fedorov, A. A. Kuzubov, et al., PRL 107, 175506 (2011)
[2] H.W. Kroto and K. McKay, Nature (London) 331, 328 (1988).
[3] R. F. Curl, M.-K. Lee, and G. E. Scuseria, J. Phys. Chem. A 112, 11 951 (2008).
[4] S. C. O'Brien, J. R. Heath, R. F. Curl, and R. E. Smalley, J. Chem. Phys. 88, 220 (1988).
[5] G. Zheng, S. Irle, and K. Morokuma, J. Chem. Phys. 122, 014708 (2005).
[6] S. Irle, G. Zheng, Z. Wang, and K. Morokuma, J. Phys. Chem. 110, 14 531 (2006).
[7] G. Ulmer, E. E.B. Campbell, R. Kuhnle, et al., Chem. Phys. Lett. 182, 114 (1991).
[8] C. Piskoti, J. Yargen, and A. Zettl, Nature (London) 393, 771 (1998).

Novel highly soluble double-caged fullerene derivatives for energy conversation

Brotsman V.A. [1] *, Ioutsi V.A.* [1] *, Trukhanov V.A.* [2] *, Belov N.M.* [1] *, Paraschuk D.Yu.* [2] *, Goryunkov A.A.* [1]

aag@thermo.chem.msu.ru

[1] Lomonosov Moscow State University, Chemistry Department

[2] Lomonosov Moscow State University, Physical Department, 119991, Moscow, Russia

Among the variety of fullerene derivatives, the compounds comprising two or more fullerene cages are of particular interest as prospective materials for fabrication of photoactive layers in organic electronic devices.

A new family of fullerene based compounds, namely, soluble double-caged [60]-, [70]- and [60/70]fullerene derivatives linked through pyrrolizidine and cyclobutan bridges, has been synthesized by simple procedures and in high yield. The crude mixtures of double-caged fullerene derivatives were subjected to multistep separation using column chromatography and HPLC. As a result 5 isomers of double-caged [70]fullerene ester and two isomers of [60/70]fullerene ester were isolated and characterized by means of high resolution MALDI mass spectrometry, ^{1}H, ^{13}C and two-dimensional correlation NMR spectroscopy, IR and UV/Vis spectroscopy. Their optical properties in solution and in the solid state were studied. A significantly stronger absorption in [70]fullerene-containing derivatives relative to [60]fullerene esters in solution in the visible range was observed. Synthesized compounds demonstrate good solubility in the common hydrocarbon solvents due to the presence of long alkyl chain. Thus, the solubility of the double-caged compound in *ortho*-dichlorobenzene exceeds 30 mg/ml. High solubility and extended 56π- or 66π-electron systems make these double-caged compounds applicable for testing in organic photovoltaic. Here we report the study of the double-caged fullerene esters as possible materials for photovoltaic applications. Bulk-heterojunction solar cells based on these novel double-caged [60]- and [70]fullerene derivatives blended with P3HT and other polymers were fabricated and discussed. The optimal fabrication conditions were found. The mobility of charge carriers in films of the double-caged fullerene derivatives was measured and discussed. Experimental solar cells demonstrated the power conversion efficiencies up to 3.5% which exceeds other known double-caged fullerene derivatives. The photoelectric characteristics of the solar cells will be presented and discussed.

This work was partially supported by the Russian Foundation for Basic Research (grant no. 14-03-31815 mol_a).

Hypothetic phase diagram of fullerene solution

Rozhkov S.P. [1] , *Goryunov A.S.* [1]

goryunov@krc.karelia.ru
[1] Institute of Biology, Karelian Research Centre RAS, Petrozavodsk, Russia

The best-known examples of molecules with short-range pair interaction are fullerenes and globular proteins remarkable for the cluster organization of condensed phases [1]. They are characterized with similar thermodynamic characteristics. Phase diagrams (PDs) have been constructed for the solutions of globular proteins [2], while no PDs for fullerenes have been proposed [3]. There are models of C_{60} cluster formation in solutions used to interpret the anomalous dependence of C_{60} solubility on temperature [3]. The ability to form crystallosolvates could be related to phase transition (PT) at 260K induced by variation in the parameters of the crystalline lattice of fullerite from simple cubic (sc) to face-centered (fcc). Deformed body-centered (bcc) or body-centered tetragonal (bct) crystalline lattices of nanoparticles may be formed as a result of interaction with solvent [4]. These crystalline polymorphs could be due to the various electron states of a C_{60} because of the thermally induced restructuring of the double bonds in the C_{60} frame [5].

Hypothetic PD of C_{60} solutions may be presented in temperature - packing density coordinates by analogy with protein solution PD, containing spinodal and binodal regions [3] as well as the lower density region of crystalline phase with sc-lattice formed by C_{60} with a packing density of 0.52. Type one PT occurs at 260K, and C_{60} form the densest (0.74) fcc-phase (the higher density part of PD). However, as temperature rises, molecules with varying electron structures may appear in dispersion. The appearance of metastable phases with C_{60} forming a distorted lattice, e.g. (bcc) with a packing density of 0.68 (hpc) or (bcc+hpc), induced by interaction with solvent (crystallosolvates), would be more optimum for such molecules. If packing density reaches the binodal with increasing concentration of carbon, then PT of L-L type occurs leading to metastable dense phase formation. As temperature rises above the critical point, dynamic clusters remain as phantoms of low-temperature metastable phases (the supercritical region is expected to be single-phase), and their "solubility" declines because crystallosolvates lose stability and solid-phase embryos with dense fcc lattice are formed.

If the concentration (packing density) of nanoparticles reaches the spinodal boundary, then the stability of the metastable phase pattern of the solution is disturbed, triggering the formation of gel-like nonequilibrium nanostructures by aggregation. Caused by evaporation or salting-out, a solid phase may arise in the supercritical region as a multi-level structural pattern which consists of nanosized lattices and mesoscopic liquid-crystalline fractal-structured carbon nanoparticle clusters.

This work is supported by RFBI grant №13-03-00422.

References

1. C. Gripon, L. Legrand, I. Rozenmann, F. Boue, and C. Regnau, J. Cryst. Growth (1998), **183,** 258.
2. P.G. Vekilov, J. Phys.: Condens. Matter. (2012), **24**, 193101.
3. M.V. Avdeev, V.L. Aksenov, and T.V. Tropin, Rus. J. Phys. Chem. A (2010), **84**(8), 1273.
4. B.W. Goodfellow, and B.A. Korgel, ACS Nano (2011), **5**(4), 2419.
5. D.V. Schur, S.Yu. Zaginaichenko, A.D. Zolotarenko, and T.N. Veziroglu, In: B. Baranovski et al. (eds.). Carbon nanomaterials in clean energy hydrogen system (Springer Sci.+ Bisiness Media B.V., 2008), p.85.

Method of the quantitative express analysis of endohedral fullerenes

Koravanets V.S. [1] *, Vnukova N.G.* [2] *, Kolonenko A.L.* [2] *, Dubinina I.A.* [1] *, Churilov G.N.* [2] *, Guliaeva U.E.* [1]

churilov@iph.krasn.ru

[1] Siberian Federal University, Krasnoyarsk, Russia

[2] Kirensky Institute of Physic SB RAS, Krasnoyarsk, Russia

The endohedral fullerenes, in spite of unique properties and applications for electronics, medicine and etc. are not widely investigated. In order to easing of this situation a grate number of investigators develop the effective synthesis methods of endohedral fullerenes [1]. Also it is necessary to develop the methods of quickly contained diagnostic of metallofullerene at extracts. One of the methods for their fast determination at the fullerenes extracts is presented by us at this paper. On the fist stage, fullerene extract identified by mass spectroscopy. If endohedral fullerenes only one type are presented at mass spectra: estimated the weigh of atom-guest in the fullerene molecules (for example, with the help of optical emission spectroscopy) and known the weight of analyzed sample, we can determinate the endohedral fullerene content at the extract, for example, pyridine fullerene extract contained Y@C82 (fig.1).

If endohedral fullerenes more than one types are presented at mass spectrum, it is necessary to use HPLC. In that case it is necessary to determinate the content of fractions which corresponded to each types of endohedral fullerenes. The synthesis effectiveness will be determinate if we know this information and atom-guest content. With the help of this method using mass spectrometer (Bruker BIFLEXTM III Time-of-Flight mass spectrometer with laser desorption) and spectrograph (type PGS-2, dispersion of 7,4 Å/mm) the content of endohedral fullerene $Y@C_{82}$ was estimated. The content of YC_{82} was 1,2 wt.%. That result was confirmed by weight method and by HPLC (Agilent Technologies 1200 Series HPLC system equipped with a Cosmosil Buckyprep (10mm×250 mm) column).

The work was partially supported by the Ministry of Education and Science of Russian Federation № 14.613.21.0010; Russian Foundation for Basic Research № 15-03-06786.

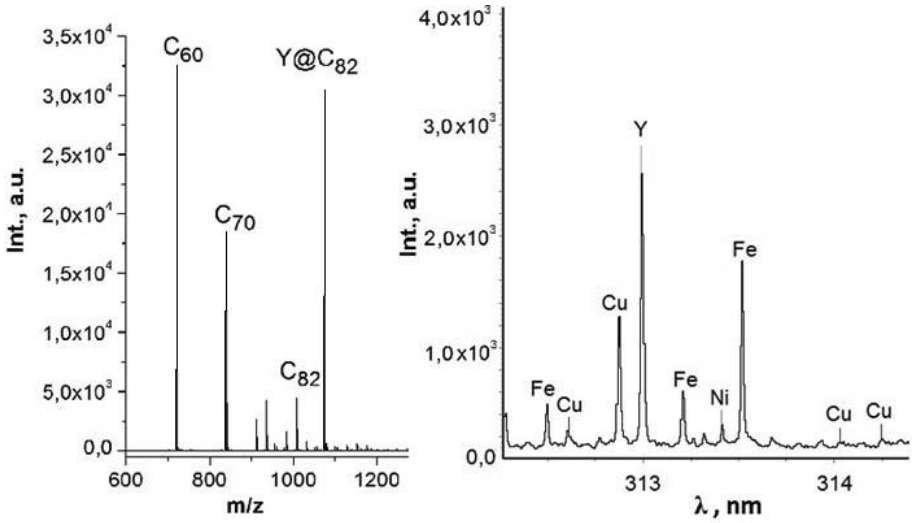

Fig.1. Mass spectrum (positive ion) and optical emission spectrum of pyridine fullerene extract contained $Y@C_{82}$.

References

1. N. Bezmelnitsin. J. Am. Chem. Soc. (2006) Volume 128, 15793.
2. N. Churilov, etc. Carbon (2013) Volume 62, 389.

INVESTIGATION AND MODELING OF EVOLUTION OF UV-VIS SPECTRA OF C_{60}/NMP SOLUTION

Jargalan N. [1,2] *, Tropin T.V.* [1] *, Avdeev M.V.* [1] *, Aksenov V.L.* [1,3]

narmandah@jinr.ru

[1] Joint Institute for Nuclear Research, Dubna, Russia

[2] Institute of Physics and Technology, Mongolian Academy of Sciences, Ulaanbaatar, Mongolia

[3] Petersburg Nuclear Physics Institute, National Research Centre "Kurchatov Institute", Gatchina, Russia

Various properties of fullerene solutions continuously attract the interest of scientists throughout the world, with a lot of research works being published on the subject [1-5]. The kinetics of dissolution and concomitant processes (including complex formation and cluster growth) are also intriguing and were investigated on different occasions [3-4, 6].

In our previous work [6], the kinetics of dissolution were investigated for fullerene solvents such as benzene, toluene and N-methyl-2-pyrrolidone (NMP) by UV-Vis spectrometry. As it is well known, the stable characteristic absorption peaks (e.g. at ~330 nm) disappear for C_{60}/NMP solutions, owing to the formation of fullerene-solvent complexes. This fact does not allow one to directly measure the kinetics of dissolution in C_{60}/NMP via spectrophotometry.

In the present work, we report more results of investigation of the kinetics of evolution of the UV-Vis spectra of C_{60}/NMP solution (concentration 0.3 mg/ml) during dissolution process. The samples were prepared at different external conditions – the stirring speed and temperature were varied in a wide range (25-100 ˚C, 0-400 rot/min). We model the kinetics of simultaneously occurring processes in the solution via a system of simple kinetic equations and obtain the corresponding parameters dependence on preparation conditions. The obtained results will allow one in the future to take account of these effects while modeling the kinetics of slow growth of large clusters in C_{60}/NMP solutions.

References

1. Beck M.T., Mandi, G., Fullerene Sci. and Technol., (1997), **5(2)**, 291-310.
2. Avdeev, M.V., Khokhryakov, A.A., Tropin, T.V., Andrievsky G.V., et al., Langmuir, (2004), **20**, 4363–4368.
3. Tropin, T. V., Jargalan, N., Avdeev, M. V., Kyzyma, O. A., Sangaa, D., Aksenov, V. L., Physics of the Solid State, (2014), **56**, 148-151.
4. Andrievsky, G.V., Klochkov, V.K., Karyakina, E.L., Mchedlov-Petrossyan, N.O., Chem. Phys. Lett., (1999), **300**, 392-396.
5. Kyzyma, O.A., Korobov, M.V., Avdeev, M.V., Garamus, V.M., Petrenko, V.I., Aksenov, V.L., Bulavin, L.A., Fullerenes, Nanotubes and Carbon Nanostructures, (2010), **18**, 458-461.
6. Jargalan, N., Tropin, T. V., Avdeev, M. V., Aksenov, V. L., Journal of Surface Investigation: X-ray, Synchrotron and Neutron Techniques, (2015), **1**, 16-20.

Technology of Separation and Purification of Fullerenes and the Synthesis of High Purity Individual Fullerenes

Keskinov V.A. [1,2] , *Blochin A.A.* [2] , *Murashkin Yu.V.* [2] , *Postnov V.N.* [3,1] , *Gruzinskaya E.G.* [1]

keskinov@mail.ru

[1] Public Joint Stock Company "Scientific andProduction Association "TECHNOLOGIES", Saint-Petersburg, Russia

[2] Saint-Petersburg State Technological Institute (Technical University), Saint-Petersburg, Russia

[3] Saint-Petersburg State University, Saint-Petersburg, Russia

Semi-industrial technology of separation and purification of individual light fullerenes – C_{60} and C_{70} and also heavy fullerenes mixture (C_{76} + C_{78} + C_{84}) from fullerenes mixtures with the different composition was elaborated and tested (Patient [1]). Fullereneseparationis carried out by the method of column chromatography with the use of the original mixed mineral-carbon nano-modified sorbent, also produced with the help of the original technology (Patient [2]). Mixedfullerenes solutions for chromatographic separation were prepared on the base of the solid fullerenes concentrates with the different composition by the solution in the aromatic solvents. Concentrates, enriched by the heavy fullerenes were produced by the method of pre-chromatography crude separation, elaborated by the authors [3]. Initial fullerene soot was produced by the method of the graphite erosion in helium-carbon plasmain the electric arc (see, for example [4]). Mixed fullerenes solutions were given to the chromatographic columns with the working volume from 8 to 50 liters, fulfilled by mixed mineral-carbon nano-modified sorbent for fullerenes separation. The separation of the different fullerenes concentrates consisted of 80 – 90 mass % of light fullerene C_{70}, on one hand, and consisted of 30 - 80 mass % of the sum of heavy fullerenes, on the other hand, was investigated. In all cases output chromatographic columns authors got separate fullerenes fractions with the following purity: fullerene C_{60} – not less than 99.9 mass %, fullerene C_{70} – not less than 99.5 mass %, sum of fullerenes C_{76} + C_{78} + C_{84} - not less than 98 mass %. In the case of the separation of the solutions, enriched by fullerene C_{70}, yield of fullerene C_{70} into pure fractionswas 75 – 90 mass % (nearly 3 - 5 g for 8 liters column and 23 – 27 g for 50 liters column). Yield was depending on the fullerene composition and the load on the volume unit of the column. In the case of the separation of the solutions, enriched by heavy fullerenes, yield of heavy fullerenes into pure fractionswas 50 – 85 mass %. Yield was also depending on the fullerene composition, the load on the volume unit of the column and the type of aromatic solvent (toluene, o-xylene, o-dichlorbenzene).

Investigations were supported by Russian Found of Fundamental Investigations – RFFI (Project N 15-08-08438) and with the help of the equipment of Resource Center of Saint-Petersburg State University GEOMODEL.

References

1. Konstantin N. Semenov, Teresa Regueira, Josefa Fernández, Nikolay A. Charykov , Igor V. Murin. J. of Molecular Liquids. 2015. V.209. P.71-76.
2. Keskinov V.A., Charykov N.A., Blokhin A.A., Murashkin Yu.V. Metod of Fullerene separation. Rus. Patient. Application N20134135540/05. Positive Deceision 19.03.2015.
3. V.A. Keskinov, N.A. Charykov, M.V. Keskinova, Yu.V. Murashkin, A.A. Blokhin, K.N. Semenov. Pre-chromatography crude separation of light fullerenes by poly-thermal re(crystallization) method. Nanosystems: Physics, Chemistry, Mathematics. 2013. N3. P.344.
4. E.G.Gruzinskaya, V.A. Keskinov, M.V.Keskinova, K.N.Semenov, N.A. Charykov. Fullerene Soot of Electric Arc Synthesis. Nanosystems: Physics, Chemistry, Mathematics. 2012. N3. P.83.

Quasi-fulleranes, fulleranes as main products of organics fullerenization

Kharlamov A. I. [1] , *Bondarenko M. E.* [1] , *Kharlamova G. A.* [2]

dep73@ipms.kiev.ua

[1] Frantsevich Institute for Problems of Materials Science of NASU, Krzhyzhanovsky St. 3, 03680 Kiev, Ukraine

[2] Taras Shevchenko National University of Kiev, Volodymyrs'ka St. 64, 01601 Kiev, Ukraine

Author method of pyrolysis (AMP) as process of fullerenization of organics molecules (benzene, toluene, xylenes, ethanol, pyridine) for forming of closed spheroidal homo- and heteroatomic molecules and structures of carbon will be considered. Basic products of fullerenization – quasi-fulleranes (C_nH_{n-6}–C_nH_{n-2} (n=20–54)) [1] and fulleranes ($C_{60}H_4$–$C_{60}H_{60}$, $C_{70}H_8$–$C_{70}H_{44}$) [2] containing up to 5.7 mass% hydrogen. The first time have been detected by a mass spectrometric method the cluster with m/z 780, the thin structure of that spectrum completely corresponds to fullerane of equiatomic composition, $C_{60}H_{60}$. Powdery samples of hydrogenated carbon molecules in gram quantities have been obtained. Dehydrogenation of fulleranes and quasi-fulleranes as the products of fullerenization at ~ 50°C starts, while dehydrogenation of fulleranes synthesized at fullerene hydrogenation at temperatures above 400°C observes. Synthesized products fullerenization of n-hexane are a source of hydrogen in a wide temperature interval (50-750°C). In products of fullerenization the quasi-fullerenes (C_{40}, C_{42}, C_{48}) and small carbon molecules (C_3-C_{18}) [3] are detected also. At fullerenization of pyridine molecules exohedral polyazafullerenes and nitrogen-doped carbon onions is formed also. Main peculiarity of AMP – the products of fullerenization are formed into vapour-gas phase but are condensed and deposited away from high-temperature zone of reaction where is realized only the grown of carbon nanostructures due to heterophase reactions.

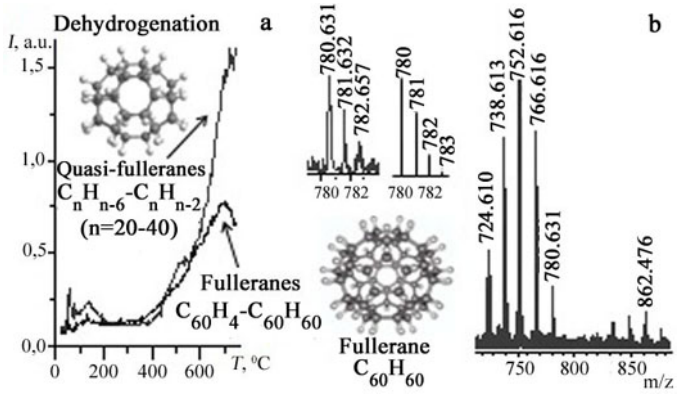

Fig.1. Thermograms of quasi-fulleranes and fulleranes dehydrogenation (a); anions mass spectrum of the fulleranes with expansion around m/z 780 peak and the calculated isotope mass ratio for $C_{60}H_{60}$ molecule (b).

References

1. A. I. Kharlamov, M.E. Bondarenko, and G. A. Kharlamova, Russ. J. Appl. Chem. (2015) **88**, 48.
2. A. I. Kharlamov, M.E. Bondarenko, and N.V.Kirillova, Russ. J. Appl. Chem. (2012) **85**, 233.
3. A. I. Kharlamov, G. A. Kharlamova, and M.E. Bondarenko, Russ. J. Appl. Chem. (2013) **86**, 1174.

Electronic properties of highly trifluoromethylated C_{70} fullerenes

Kosaya M.P. [1] , *Romanova N.A.* [1] , *Rybalchenko A.V.* [1] , *Tamm N.B.* [1] , *Goryunkov A.A.* [1]

maria.cosaya@yandex.ru

[1] Department of Chemistry, Lomonosov Moscow State University, Moscow, 119991, Russia

Fullerenes are known to be good electron acceptors with high electron affinity values. Derivatization of fullerenes via addition reactions results in sp^3-hybridization of carbon atoms that usually leads to decrease the electron affinity of molecule. Addition of two and more groups can result in the formation of rather different conjugated fragments; therefore isomeric molecules vary in the electron affinity and may be even more acceptable than the initial fullerene [1], and hence isomeric compounds are distinguished in absorption and fluorescence spectra, electron affinity, and reduction potentials.

Presently, electrochemical properties of low trifluoromethylated fullerenes $C_{70}(CF_3)_n$ with n=2–12 are well known [1] while no data are available on electrochemical and photochemical properties of the structurally characterized highly trifluoromethylated fullerenes $C_{70}(CF_3)_n$ with n=14–20. He we reported first results of investigation of electrochemical and spectroscopic properties of highly trifluoromethylated derivatives of fullerene C_{70}.

The crude mixture of $C_{70}(CF_3)_n$ with n=12–20 was synthesized in heterogeneous reaction of solid C_{70} with gaseous CF_3I in ampoule, according to previously reported protocol [2]. The sealed ampoule with loaded reagents was heated in furnace with hot zone temperature of 380–420 °C and cold zone temperature of 25 °C. Isomeric pure derivatives were isolated by means of HPLC and were characterized by means of MALDI mass spectrometry and spectral techniques. The electrochemical behavior of isomeric pure $C_{70}(CF_3)_n$ with n=10–16 was studied by using of cyclic voltammetry. It was found, that in contrast to C_{70} derivatives with 2–8 CF_3 groups, which are characterized by reversible electron transfers up to di- and trianions, the reduction of highly trifluoromethylated fullerene C_{70} derivatives is accompanied by chemical transformations. The possible pathways of such transformations are reviewed. It was shown, that experimentally determined first reduction potentials of the compound under study are in good agrees with DFT predicted electron affinity values. The relationships between electron affinities values of $C_{70}(CF_3)_n$ derivatives and CF_3 group addition patterns are discussed.

The work is supported by the Russian Foundation for Basic Research (grant 15-03-07665).

References

1. O.V. Boltalina, A.A. Popov, I.V. Kuvychko, N.B. Shustova, S.H. Strauss, Chem. Rev., (2015) **115**, 1051.

2. D.V. Ignat'eva, A.A. Goryunkov, N.B. Tamm, I.N. Ioffe, S.M. Avdoshenko, L.N. Sidorov, A. Dimitrov, E. Kemnitz, S.I. Troyanov, Chem. Commun., (2006), 1778.

Hydrogenation of S_6-symmetrical $C_{60}(CF_3)_{12}$

Lavrent'eva O.N. [1] , *Romanova N.A.* [1]

lavrolja@mail.ru

[1] Department of Chemistry, Lomonosov Moscow State University, Moscow, 119991, Russia

The compound S_6-$C_{60}(CF_3)_{12}$ is the most synthetic available poly(trifluoromethyl)fullerene. However further synthetic applicability of the compound is restricted by its very low solubility in most organic solvents [1]. The only example of successful functionalization is chlorination of S_6-$C_{60}(CF_3)_{12}$ in $SbCl_5$ media yielding mixed chloro- and trifluoromethylderivative S_6-$C_{60}(CF_3)_{12}Cl_{12}$ [2].

Here, we report the first results of hydrogenation of S_6-$C_{60}(CF_3)_{12}$ via reaction with either 9,10-dihydroantracene or $NaBH_4$. The crystalline S_6-$C_{60}(CF_3)_{12}$ was prepared by the known method using an ampoule reaction of C_{60} with CF_3I [1] and recrystallizated from hot *o*-dichlorobenzene. Purified sample of S_6-$C_{60}(CF_3)_{12}$ was characterized by IR, NMR ^{19}F spectroscopy and MALDI mass spectrometry.

Hydrogenation of S_6-$C_{60}(CF_3)_{12}$ with melted 9,10-dihydroantracene was performed in sealed tube at heating under argon atmosphere. Unlikely starting material, prepared product is soluble in toluene/hexane mixtures. According to MALDI mass spectral and HPLC analyses, the high temperature hydrogenation of S_6-$C_{60}(CF_3)_{12}$ leads to complex mixture of hydrogenated trifluoromethylfullerenes with partial loss of CF_3 groups characterized by composition of $C_{60}(CF_3)_nH_m$, where n=8–12 and m=8–18.

Treatment of S_6-$C_{60}(CF_3)_{12}$ by $NaBH_4$ at moderate temperature results in selective formation of dodecahydrodenated derivative $C_{60}(CF_3)_{12}H_{12}$ according to MALDI MS data. The synthesized product was HPLC purified and characterized by means of MS MALDI, IR, UV/Vis, NMR spectroscopes. Possible attachment moieties of hydrogen atoms within $C_{60}(CF_3)_{12}H_{12}$ were proposed on basis of NMR data and quantum chemical calculations at the DFT level of theory.

References

1. S.I. Troyanov, A. Dimitrov, E. Kemnitz, Angew. Chem. Int. Ed. (2006) **45**, 1971.
2. S.I. Troyanov, E. Kemnitz, Mendeleev Commun. (2008) **18**, 27.

C_{60}-CuTPP optical and magnetic properties investigation

Elistratova M.A. [1,2] , *Zakharova I.B.* [1] , *Kvyatkovskii O.E.* [3] , *Lahderanta E.* [2] , *Zakharchuk I.* [2] , *Makarova T.L.* [2]

elistratovamari@yandex.ru

[1] St. Petersburg State Polytechnical University, St. Petersburg, Russia

[2] Lappeenranta University of Technology, Lappeenranta, Finland

[3] Ioffe Institute, St.Petersburg, Russia

Fullerene based molecular complexes are the subject of intensive study due to the technological interest the carbon electronics and devices based on it [1, 2]. Recent studies of metal-porphyrin (*M*(II)TPP) compounds have demonstrated the possibility of using a porphyrin as a material for artificial systems for photosynthesis and chemical sensors. *M*(II)TPP compounds and corresponding C_{60}*M*(II)TPP compounds are of a great interest as promising materials for optoelectronics, due to the donor-acceptor pairs formation with fullerene [3]. C_{60}CuTPP thin films were produced by vacuum deposition in quasi-closed volume on Si, KBr and glass substrates. SEM data gives that self-organization of molecules CuTPP under the conditions vapor deposition in vacuum lead to formation of nanorods with a diameter of about 20-50 nm. Bulk sample for magnetic measurements were prepared by evaporation from C_{60}CuTPP (1:1 molar concentration) solution in toluen.

Photoluminescence (PL) spectra of pure materials and molecular complexes were measured. The reduction in emission intensity in the presence of C_{60} is due to fluorescence quenching due to the photoindused charge transfer between C_{60} and CuTPP molecules. Quantum-chemical calculations of optimized geometry and electronic structure of CuTPP-C_{60} complexes were performed. It was done in frame of density functional theory (DFT) with the hybrid functional B3LYP using MOLCAO-SCF method at 6-31G(d) level. DFT calculations have shown that a pair C_{60} and CuTPP forms a stable molecular complex of C_{2v} symmetry, with formation energy $E(C_{60})+E(\text{CuTPP})-E(C_{60}\text{CuTPP})=0.08$ eV and HOMO-LUMO gap equal to 1.88 eV. Charge transfer between the components of the complex in the ground state is small, of the order of 0.02 q_e.

The temperature dependence of magnetization M(T) data measured under an applied field of 1 kG and 70 G for a powder samples of CuTPP and C_{60}CuTPP give us the temperature dependence of magnetic susceptibility in a weak magnetic field. The field cooling (FC) and zero-field cooling (ZFC) curves are basically paramagnetic throughout the whole temperature range 3-300K.

References

1. Forrest R. 2000. Active optoelectronics using thin-film organic semiconductors. IEEE J. Sel. Top. Quantum Electron., **6**, No. 6, 1072–1083.
2. Reid I. *et al.* 2009 Electronic structure of the organic semiconductor copper tetraphenylporphyrin (CuTPP) *Applied Surface Science* **256**, 720-725.
3. V. Konarev *et al*. 2001. New Molecular Complexes of Fullerenes C60 and C70 with Tetraphenylporphyrins [M(TPP)], in which M -H2 , Mn, Co, Cu, Zn, and FeCl. Chem. Eur. J., **7**, No. 12, 2625-2636.
4. Danilovic, C. L. Lin, and T. Yuena, 2007. Magnetic properties of an FeII*meso*-tetra4-pyridylporphyrin network. J. of Appl.Phys. **101**, 09E103

The molar heat capacity and thermodynamic characteristics of C_{60} and C_{70} fullerenols

Markin A.V. [1] , *Koryukina T.I.* [1] , *Smirnova N.N.* [1] , *Semenov K.N.* [2] , *Sologubov S.S.* [1]

markin79@mail.ru

[1] Nizhny Novgorod State University, Nizhny Novgorod, Russian Federation

[2] Saint Petersburg State University, Saint Petersburg, Russian Federation

The unique properties of light fullerenes (C_{60} and C_{70}) have determined the large number of studies which are mainly devoted to describe synthesis and study physical and chemical properties of fullerenes and their numerous functional derivatives [1]. Fullerene derivatives containing various numbers of hydroxyl groups attached per fullerene are called fullerenols. The fullerenols obtained retain the biological and chemical properties of the C_{60} fullerene; that allows using such derivatives in water-soluble oils, as additives to spirit production, in pharmacology, and in medicine.

Firstly, the temperature dependences of heat capacities $C_p = f(T)$ of C_{60} and C_{70} fullerenols in the range from 6 to 360 K by adiabatic vacuum calorimetry and in the rage from 350 to 670 K by differential scanning calorimetry were measured. The thermal stability of the fullerenols was studied by thermogravimetry (TG209F1 Netzsch Geratebau, Germany).

It was revealed that in the studied temperature range fullerenols undergoes no phase changes: heat is gradually changing with increasing temperature. In the temperature range between 350 and 570 K the irreversible transformation caused by the keto-enol isomerization in fullerenols was detected and its thermodynamics characteristics were determined and discussed. Also keto-enol isomerization was confirmed by ^{13}C NMR spectra. It should be noted that for tested compounds the phase transitions typical for C_{60} and C_{70} didn't take place on heat capacity curves.

The experimental data was used to calculate the thermodynamic functions, namely heat capacity, enthalpy, entropy and Gibbs function in the range from 0 to 350 K. The value of standard entropy of formation of the complexes from simple substances at T = 298.15 K has been determined.

The low-temperature heat capacity (T < 50 K) was analyzed on based of the multifractal model of the heat capacity solids and as results the conclusions about the structure for under study complexes were estimated. The temperature dependence of heat capacity in the low-temperature region (T < 20 K) is well described by the limiting Deby's law for the tested compounds as well as for fullerites C_{60} and C_{70}.

The standard thermodynamic properties of the studied C_{60} and C_{70} fullerenols and C_{60} and C_{70} fullerites were compared and discussed.

This work was performed with the financial support of the Ministry of Education and Science of the Russian Federation (Contract No. 4.1275.2014/K)

References

1. *Semenov K.N., Charykov N.A., Keskinov V.N.* Fullerenol Synthesis and Identification. Properties of the Fullerenol Water Solutions // *Chem. Eng. Data* **2011,** *56,* 230–239

Quantum Chemical Study of the Oxidative Elimination of the C_2 Fragments from Fullerenes

Mazaleva O.N. [1] , *Ioffe I.N.* [1] , *Troyanov S.I.* [1] , *Granovsky A.A.* [2]

ioffe@thermo.chem.msu.ru
[1] Moscow State University, Moscow, Russia
[2] Firefly Project, Moscow, Russia

In the recent years, a novel class of fullerene reactions has been discovered – the skeletal transformations. Accessible in pristine fullerenes only beyond 1000°C, they were found to proceed at as low as 300-400 °C when being assisted by chlorination with VCl_4 and/or $SbCl_5$. Of particular interest are cage shrinkage transformations that consist in abstraction of the C_2 units from the carbon cage, up to three consecutive C_2 losses having been observed so far [1]. These processes typically result in formation of seven-membered rings within the fullerene cages thus giving rise to a new family of non-classical fullerene structures.

The possible pathways of the chlorination-assisted C_2 elimination were addressed theoretically in some recent works [1-3]. However, it has been found out that two distinct subtypes of C_2 elimination can be distinguished, of which only one can be satisfactorily explained without invoking additional assumptions about the reactive admixtures in the system. Chlorination of higher fullerenes usually produces molecules with polycyclic aromatic substructures isolated from each other by chlorinated belts. When a C_2 unit is being eliminated from such belt, chlorination and chlorine migration through exchange with the medium contribute to a considerable reduction in the activation barriers of C-C bond cleavage and rearrangement. On the contrary, C_2 elimination from an intact aromatic substructure observed, e.g., in C_{86} [2,4] cannot be readily rationalized, since chlorination of the carbon sites involved is largely unfavorable, which would increase the effective activation energy.

In the present work, we investigate a hypothesis that C_2 abstraction can also be promoted by minor oxygen admixtures in the reaction medium. On the basis of the DFT calculations, an oxidative pathway is proposed that ultimately leads to elimination of a C_2 unit in the form of two CO molecules. It is demonstrated that the oxidative C_2 loss will be specific only to a limited family of fullerene substrates where the ensuing cage transformation would sufficiently contribute to the thermodynamic favorability of the process. We also present a comparative performance study of a range of exchange-correlation functionals, including some recent double hybrid functionals, in application to reaction and activation energy calculations in the complex fullerene systems in question.

The present work was supported by the RFBR grant 15-03-05083. We thank the Supercomputer Center of the Moscow State University for computational support.

References

1. I.N. Ioffe, S. Yang, S. Wang, L.N. Sidorov, E. Kemnitz, and S.I. Troyanov, Chem. Eur. J. (2015) **21,** 4904.
2. I.N. Ioffe, C. Chen, S. Yang, L.N. Sidorov, E. Kemnitz, and S.I. Troyanov, Angew. Chem. Int. Ed.(2010) **49**, 4784.
3. I.N. Ioffe, O.N. Mazaleva, L.N. Sidorov, S. Yang, T. Wei, E. Kemnitz, and S.I. Troyanov, Inorg. Chem. (2013) **52**, 13821.
4. T. Wei, S. Yang, E. Kemnitz, and S.I. Troyanov., Chem. Asian J. (2015) **10**, 559.

Pressure-assisted photopolymerization in the molecular donor-acceptor fullerene complex $\{Cd(dedtc_2)\}_2 \bullet C_{60}$

Meletov K. P. [1] , *Arvanitidis Y.* [2] , *Cristofilos D.* [2] , *Kourouklis G.* [2]

mele@issp.ac.ru

[1] Institute of Solid State Physics RAS, Chernogolovka, Moscow region 142432, Russia

[2] Aristotle University of Thessaloniki, GR-54 124 Thessaloniki, Greece

The pressure-assisted photopolymerization in the molecular donor-acceptor fullerene complex $\{Cd(dedtc_2)\}_2 \bullet C_{60}$ was observed in the pressure region 2÷6 GPa. After the phase transition near ~2 GPa, confirmed by Raman and X-ray studies [1], the Raman spectra exhibit time-dependent changes under laser illumination characterized by the appearance of additional peaks in the frequency region of the $A_g(2)$ pentagon-pinch (PP) mode of C_{60} monomer. The new peaks at lower energies are related to the photo-induced oligomers with different number of sp^3-like coordinated carbon atoms per molecular cage. The polymer content depends on the laser power density and sample temperature, while at constant laser power remains almost constant up to 6 GPa. At higher pressure the photopolymerization is suppressed abruptly (Fig.1).

The support by the Russian Foundation for Fundamental Research, grant № 15-02-01495, and to the RAS Presidium Program “Matter under high compression” is greatly acknowledged. The authors are grateful to Dr. D. Konarev for providing the fullerene complexes.

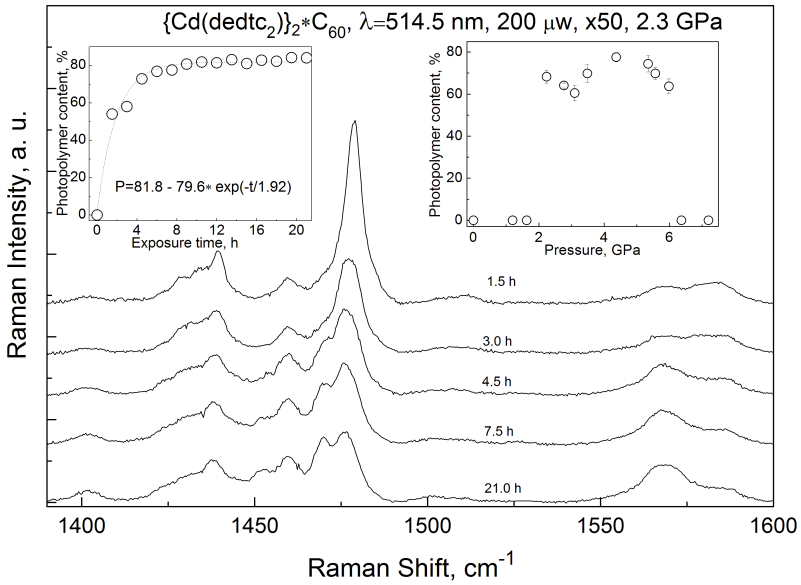

Fig.1. Time evolution of the Raman spectra of the $\{Cd(dedtc_2)\}_2 \bullet C_{60}$ complex in the region of the PP-mode. Left inset: polymer content, as ratio of the polymer $A_g(2)$ peak intensities to the total Raman intensity, as a function of the illumination time (circles) fitted by an exponential growth function (line). Right inset: pressure dependence of the polymer content.

References

1. K.P. Meletov, D. V. Konarev, A. O. Tolstikova, JETP (2015), **147**, in press.

Comparative Raman study of the photo-oligomers stability in the donor-acceptor fullerene complex {Pt(dbdtc$_2$)}•C$_{60}$ and pristine C$_{60}$

Meletov K. P. [1] , *Arvanitidis Y.* [2] , *Cristofilos D.* [2] , *Kourouklis G.* [2]

mele@issp.ac.ru

[1] Institute of Solid State Physics RAS, Chernogolovka, Moscow region 142432, Russia

[2] Aristotle University of Thessaloniki, GR-54 124 Thessaloniki, Greece

We have studied the photopolymerization process and stability at elevated temperature of the fullerene oligomers in the molecular donor-acceptor fullerene complex {Pt(dbdtc$_2$)}•C$_{60}$ and pristine C$_{60}$. These materials show fast polymerization under the 514.5 nm laser illumination used for Raman excitation. The polymerization is manifested by the appearance of additional peaks at the frequency region of the non-degenerate A$_g$(2) pentagon-pinch (PP) mode of the C$_{60}$ monomer. The new peaks are shifted to lower energies in accordance with the empirical dependence of the A$_g$(2) mode frequency on the number of the sp^3-like coordinated carbon atoms per molecular cage. The polymer content as a function of temperature under constant laser power density indicates that the photo-induced oligomers in the fullerene complex {Pt(dbdtc$_2$)}•C$_{60}$ are stable up to ~80 °C, while in the case of the pristine C$_{60}$ they decompose to monomer at ~140 °C. These values are considerably smaller than the decomposition temperature of 260 °C for the HPHT polymers of C$_{60}$.

The support by the Russian Foundation for Fundamental Research, grant № 15-02-01495, and to the RAS Presidium Program “Physics of compressed matter” is greatly acknowledged. The authors are grateful to Dr. D. Konarev for providing the fullerene complexes.

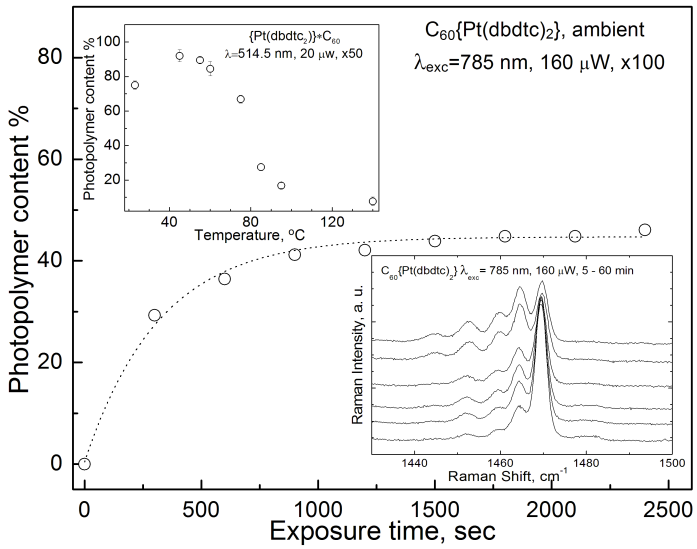

Fig.1. Polymer content, as ratio of the polymer A$_g$(2) peak intensities to the total Raman intensity, as a function of the illumination time (circles) fitted by an exponential growth function (dotted line). Bottom inset: Time evolution of the Raman spectra of the {Pt(dbdtc$_2$)}•C$_{60}$ complex in the region of the PP-mode. Top inset: Temperature dependence of the polymer content in the {Pt(dbdtc$_2$)}•C$_{60}$ complex.

Influence of Carbon Form (Fullerite, Graphite) on Structural Condition of Mehanocomposites Cu-25at.%C

Nikonova R.M. [1] , *Larionova N.S.* [1] , *Lad'yanov V.I.* [1]

rozamuz@ya.ru

[1] Physical-Technical Institute of th e Ural Branch of Russian Academy of Sciences Izhevsk, Russia

Nanocarbon modification of metals and alloys appears to have considerable promise in developing materials of the new generation. An effective technique for preparation various non-equilibrium nanocrystalline Me-C composites is mechanochemical synthesis (MS). Nanocomposites Cu-25at.%C (fullerites $C_{60/70}$ and graphite C_g) have been produced by mechanical synthesis in AGO-2S ball mill. The structural and morphological changes of samples after alloying were examined by X-ray diffraction, thermal analysis (TGA/DSC), scanning electron and optic microscopy, Raman spectroscopy. Depending on the carbon forms a different kinetics of deformation of Cu-C composites is observed.

It has manifested about significant differences in the shape of the particles, their dispersity. In both systems the formation of a supersaturated solid solution of carbon in copper Cu (C) due to high deformation effects has been established. But the depending of crystal structure parameters $a_{Cu}(t_{MS})$ and $L(t_{MS})$ from time of MS for Cu-$C_{60/70}$ and Cu-C_g composites is different (Fig.). Higher values $a_{Cu}(t_{MS})$ for Cu-$C_{60/70}$ system at initial times MS (1-2 hours) compared with Cu-C_g caused due to the additional dissolving in the copper matrix adsorbed oxygen with Cu (C, O) solid solution formation.

Raman spectroscopy showed that the observed differences in the studied Cu-$C_{60/70}$ and Cu-C_g are due to higher deformation stability of fullerite compared with graphite. When occurs complete destruction fullerite/fullerenes (more than 4 hours MS) the Cu-$C_{60/70}$ systems behaves similarly to Cu-C_g.

The work has been carried out under financial support of the program the Presidium of Ural Brunch, RAS (grant 15-20-2-22 «Elaboration and synthesis of new hydrogen-storage nanocomposites based Mg-C using various forms of carbon (fullerenes, graphite, nanotubes)»).

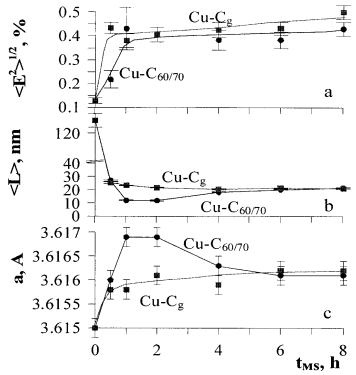

Fig. Dependence of microstress (a), the crystallite sizes (b), and the lattice parameter (c) of the copper of composites Cu-$C_{60/70}$ and Cu-C_g on time MS

Evolution of the structure of fullerenes C_{60} in the ball-milling process

Rud A.D. [1] *, Kirian I.M.* [1] *, Nikonova R.M.* [2] *, Biliy N.M.* [3] *, Lad'yanov V.I.* [2] *, Lakhnik A.M.* [1]

rud@imp.kiev.ua

[1] G.V. Kurdyumov Institute for Metal Physics of NASU, Kiev, Ukraine

[2] Physical-Technical Institute of the UrB of the RAS, Izhevsk, Russia

[3] Taras Shevchenko National University of Kiev, Kiev, Ukraine

The structural changes occurring in the crystalline samples of fullerenes C_{60} after ball-milling in a planetary mill Pulverisette 6 with different processing time were investigated. To study an evolution of the fullerenes structure X-ray diffraction, Raman spectroscopy and electron microscopy investigations were performed. The structural changes that occur in fullerenes C_{60} at mechanical activation processing are studied in [1]. Based on model atomic configurations obtained by reverse Monte Carlo method, the quantitative characteristics describing the structure of fullerite C_{60} in the initial state and after ball-milling are established.

The bond angles distributions for the reconstructed atomic configurations in fullerenes C_{60} in the initial state and ball-milled ones were calculated. It was shown that it is characterized for the pristine fullerenes C_{60} by a broad maximum, which decomposes into two components with the positions of ~ 110 and ~ 117°. It stays in place after ball-milling treatment for 1 hour, but a low intensive broad asymmetric maximum with position of ~60° appears, what indicates displacements of carbon atoms from equilibrium positions in the structure of molecules C_{60}. Further increase of milling time results in disappearance of maxima characteristic of structure of the molecule. The distribution takes the form typical for carbon materials in the amorphous state [2,3].

Statistical analysis of atomic rings in the structure of ball-milled fullerenes was performed using S. King criterion. The pristine molecule of C_{60} is characterized by 5- and 6-fold rings. At the initial stage of ball-milling treatment (1-3 hours) the molecules partially decomposes into individual atoms, what results in appear of essential amount of 3-fold rings with simultaneous decrease of the percentage of 5- and 6-fold ones. After 14 hours of the processing, 3-fold rings are dominated in the carbon material produced, what indicates full amorphization of fullerenes C_{60}. Using the method of radial distribution function, it is found that amorphous carbon possesses graphite-like type of short-range order.

The Raman spectra (λ = 514 nm) of the samples in initial state are typical for fullerenes. However in the process of mechanical activation, intensity of the bands of fullerenes is gradually reduced until extinction. After 14 hours of grinding, the Raman spectrum contains two broad bands with maxima at ~ 1362 cm^{-1} and 1580 cm^{-1}, what corresponds to the position of D- and G-bands of disordered graphite structure.

Thus it is established that at fullerenes C_{60} ball-milling two processes take place: an amorphization of the initial crystalline fullerenes on the early stages of mechanical activation and their graphitization after 14 hours of grinding.

References

1. V. I. Lad'yanov, R. M. Nikonova, N. S. Larionova, V. V. Aksenova, V. V. Mukhgalin, A. D. Rud', Physics of the Solid State (2013), Vol. 55, P.1319.
2. A. D. Rud, I. M. Kiryan, Journal of Non-Crystalline Solids (2014), Vol. 386, P. 1.
3. http://arxiv.org/pdf/1412.1982v1.pdf

Phase transformations in amorphous fullerite C_{60} under high pressure and high temperature

Borisova P.A. [1] , *Blanter M.S.* [2] , *Brazhkin V.V.* [3] , *Somenkov V.A.* [1] , *Filonenko V.P.* [3]

borisovapa@mail.ru

[1] National Research Centre Kurchatov Institute, Moscow, Russia

[2] Moscow State University of Instrumental Engineering and Information Science, Moscow, Russia

[3] Institute for High Pressure Physics, Troitsk, Moscow region, Russia

First phase transformations of amorphous fullerite at high temperature (up to 1800 K) and high pressure (up to 8 GPa) have been investigated and compared with the known studies in the crystalline fullerite. The study was conducted by neutron diffraction and Raman spectroscopy. The amorphous fullerite was obtained by ball-milling. It was shown that under thermobaric treatment crystallization of amorphous fullerite into C_{60} molecular modification is not observed, and it transforms into amorphous-like or crystalline graphite. A kinetic diagram of phase transformation of amorphous fullerite in temperature-pressure coordinates was constructed for the first time. Unlike crystalline fullerite, crystalline polymerized phases were not formed under thermobaric treatment on amorphous fullerite. Amorphous fullerite turned out to be less resistant to thermobaric treatment, and amorphous-like or crystalline graphite were formed at lower temperatures than in crystalline fullerite. The phases produced from amorphous fullerite have microhardness substantially lower than the phase produced from the crystalline fullerene.

From the gathered data it follows that amorphous fullerite in all cases of thermic and baric impact undergoes transformations from molecular phase into atomic, and these transformations can go doubly: amorphous fullerite → amorphous graphite → crystalline graphite under higher pressure; or amorphous fullerite → intermediate amorphous phase → amorphous graphite → crystalline (turbostratic type) graphite under ambient pressure. At the same time in crystalline fullerite transformation from molecular phases to atomic (graphite, diamond) goes under higher pressure through a series of molecular polymerized phases. This shows that amorphization decreases stability of a molecule and causes its collapse, while high pressures eventually contribute to formation of denser atomic phases.

This study was supported by the Russian Foundation for Basic Research (project nos. 13-02-00208a).

Fullerene C_{60} containing polymer stars in mixed matrix membranes

Vinogradova L.V. [1] *, Pulyalina A.Yu.* [2] *, Toikka A.M.* [2] *, Polotskaya G.A.* [1,2]

polotskaya@hq.macro.ru

[1] Institute of Macromolecular Compounds RAS, St. Petersburg, Russia

[2] Saint Petersburg State University, Institute of Chemistry, St. Petersburg, Russia

The development of membrane technologies promotes the search of novel effective membranes to solve ecologically important problems of industry. The most modern type is mixed matrix membranes (MMMs) generally obtained by an inclusion of nanoparticles into a polymer matrix. However, the agglomeration of small nanoparticles (fullerenes, nanotubes, etc) may create the selective delamination on the interface between the polymer matrix and the agglomerated nanoparticle phase which results in defects of membrane structure.

To prevent the agglomeration, different methods of nanoparticle modification could be applied. In the present work, fullerene C_{60} molecule was modified by anionic polymerization and turned to branching centre of polymer stars with six or twelve arms. Polystyrene (PS), poly(2-vinylpyridine), and poly-*tert*-butylmetacrylate were used as arms . The novel MMMs were obtained by inclusion of fullerene C_{60} containing polymer stars as filler into the matrix of polyphenylene oxide [1].

The MMMs were researched for the separation of methanol - ethylene glycol mixture; this problem has arisen from the joint involvement of these alcohols in a number of syntheses or technological processes. Mass transfer of methanol and ethylene glycol through the MMMs was studied by sorption and pervaporation tests. The inclusion of C_{60} containing polymer stars into the matrix resulted in increasing the sorption and diffusion parameters of both alcohols in membranes. The degree of sorption for methanol is more than twice larger and the effective diffusion coefficient is more than 3 orders of magnitude higher than those for ethylene glycol. In pervaporation of methanol-ethylene glycol mixture the total flux through MMMs and the value of separation factor increase with a growth of the filler concentration up to 5 wt%. The enhancement effect is connected with both the architecture of C_{60} containing polymer stars and structural peculiarity of C_{60} branching centers, which contain added arms of different chemical nature capable to form different types of self organization.

Acknowledgment. The authors acknowledge the Russian Foundation for Basic Research (project 15-03-02131). The work was also supported by Fellowship of President of Russian Federation.

References

1. G.A.Polotskaya, L.V.Vinogradova, E.L.Krasnopeeva. RF Patent № 138018// BI 2014. № 6.

On the structure of nanoparticles in aqueous dispersion of fullerene C_{60} and their hydroxylation

Purgina D.D. [1] , *Andreev S.M.* [1] , *Bashkatova E.N.* [1] , *Khaitov M.R.* [1]

purgina_d@mail.ru
[1] NRC Institute of Immunology FMBA of Russia, Moscow, Russia

The aqueous dispersion of fullerene C_{60} (nC_{60}) is a promising drug for biomedical applications. Earlier, we have described a simple method for preparing a dispersion nC_{60} based on mixing a solution of crystalline fullerene in N-methylpyrrolidone (NMP) with water and followed by exhaustive dialysis. Some indirect evidence obtained suggest that fullerene in the nC_{60} is partially hydroxylated [1]. To clarify the role of organic solvent, NMP, in the formation of the nC_{60}, we have replaced NMP by pyridine. It was found that absorption spectrum of pyridine/nC_{60} was very similar to that described for the NMP/nC_{60}. FTIR spectrum of dried sample showed an intense absorption band at 1000-1150 cm^{-1} characteristic for C-O vibrations, and its mass spectrum displayed minor peaks, which also could be interpreted as products of C_{60} partial hydroxylation, $C_{60}(OH)_2$, $C_{60}(OH)_{11}$ and $C_{60}(OH)_{12}$. Thus, a suitable solvent should be amphiphilic, with good affinity to both fullerene and water.

Strong evidence of the presence of hydroxyl groups in nC_{60} could be the reaction of acylation to form an ester. To this purpose, we have treated a sample of nC_{60} (obtained via NMP) with trifluoroacetic anhydride. FTIR spectrum of the obtained product showed the appearance of a small peak at 1780-1790 cm^{-1}, which apparently indicates the presence of the ester group. It should be noted that currently spectra fullerenol esters are not described in the literature.

Next, we tried to introduce hydroxyl groups into fullerene using strong bases, such as tetraethyl ammonium hydroxide/sodium hydroxide, in NMP/water medium followed by dialysis. As a result, we have obtained the solution with characteristic for fullerenol spectral parameters: sloping smooth curve in UV-Vis spectrum and strong absorption bands at 3400-3200, 1600, 1390 and 1060 cm^{-1} in FTIR spectrum. Freeze-dried samples were readily soluble in water. Mass spectrometry showed the presence fullerene molecules with 11, 12 and 21 hydroxyl groups. Trifluoroacetylation of dried sample afforded to product with characteristic ester peaks; the samples were soluble in dimethylformamide and insoluble in toluene.

We consider the process underlying the C_{60} solubilization can involve a complexation of C_{60} with NMP followed by partial hydroxylation of nanoparticle surface stabilizing the nC_{60} aggregates in water. This method is potentially suitable for preparation of aqueous solutions of higher fullerenes and endofullerenes.

References

1. Andreev S., Purgina D., Bashkatova E. et al. // Fullerenes, Nanotubes and Carbon Nanostructures, 2015, DOI:10.1080/1536383X.2014.998758.

Thermodynamic functions of poly(trifluoromethyl)fullerenes $C_{60}(CF_3)_n$, n=2-18, by isodesmic reaction's method

Romanova N.A. [1] , *Druzhinina A.I.* [1] , *Papina T.S.* [1] , *Varuschenko R.M.* [1] , *Luk'yanova V.A.* [1] , *Goryunkov A.A.* [1] , *Sidorov L.N.* [1]

rna@thermo.chem.msu.ru

[1] Department of Chemistry, Lomonosov Moscow State University, Moscow, Russia

Experimental investigations of thermodynamic properties of trifluoromethylfullerenes were significantly hampered by the fact that preparation of pure compounds in amounts required for thermodynamic studying is a rather difficult task [1]. Nevertheless, the large-scale synthetic availability of S_6-symmetrical $C_{60}(CF_3)_{12}$ [2] opens up possibility of its thermochemical studies and determination of thermodynamic functions of broad range of poly(trifluoromethyl)fullerenes by isodesmic reaction's method. Previously, we synthesized gramme-scale amount of S_6-$C_{60}(CF_3)_{12}$ and determined its thermodynamic functions ($\Delta_f H_m^o$(g) = –5923 ±148 kJ/mol, S_m^o(g) = 1582 ±14 J/mol K and $\Delta_f G_m^o$(g) = –5184 ±148 kJ/mol) at 298.15 K [3].

Here we reported the enthalpy of formation and C–CF_3 bond dissociation enthalpies , for the broad range of structurally characterized poly(trifluoromethyl)fullerenes $C_{60}(CF_3)_n$, n=2–18, by method of isodesmic reactions (Table 1). The enthalpy of formation of $C_{60}(CF_3)_n$, n = 2–18 were estimated according to equation:

$\Delta_f H_m(C_{60}(CF_3)_n) = [n/12 \cdot \Delta_f H_m^{exp}(C_{60}(CF_3)_{12}) + (1–n/12) \cdot \Delta_f H_m^{exp}(C_{60})] – \Delta_{r1} H^{Th}$, (1)

where $\Delta_{r1} H^{Th}$ value is DFT calculated enthalpy of reaction of disproportionation:

$C_{60}(CF_3)_n = n/12 \cdot (S_6\text{-}C_{60}(CF_3)_{12}) + (1–n/12) \cdot C_{60}$. (2)

Table 1. The enthalpies of formation and C–CF_3 bond dissociations of structurally characterized $C_{60}(CF_3)_n$ compounds.

Compound	The locant indexation according to IUPAC recommendation	$\Delta_f H_m^o$(g)/ (kJ·mol^{-1})	$\Delta_r H$/ (kJ·mol^{-1})[a]	
			k=n	k=2 k=1
$C_{60}(CF_3)_2$	1,7	1111	235	235 279
$C_{60}(CF_3)_4$	1,6,11,18	–303	236	237 273
$C_{60}(CF_3)_6$	1,6,11,18,24,27	–1720	237	238 264
$C_{60}(CF_3)_{10}$	1,6,11,16,18,24,27,36,54,60	–4520	234	225 260
$C_{60}(CF_3)_{12}$	1,6,11,16,18,26,36,44, 46,49,54,60	–5923	233	231 279
$C_{60}(CF_3)_{12}$	1,6,8,11,16,18,23,28, 31,36,41,57	–5905	232	222 255
$C_{60}(CF_3)_{14}$	1,3,6,8,11,13,18,23,33,41,46,49,51,57	–7266	229	202 251
$C_{60}(CF_3)_{16}$	1,3,6,11,13,18,22,24,27,32,33,41,43,46,51,59	–8624	227	210 238
$C_{60}(CF_3)_{18}$	1,3,6,11,13,18,22,24,27,32,35,37,41,43,46, 49,52,54	–9999	225	215 280

[a] calculated according equation: $1/k \cdot C_{60}(CF_3)_n = 1/k \cdot C_{60}(CF_3)_{n-k} + CF_3$

References

1. O.V. Boltalina, A.A. Popov, I.V. Kuvychko, N.B. Shustova, S.H. Strauss, *Chem. Rev.*, (2015) **115**, 1051.
2. S.I. Troyanov, A. Dimitrov, E. Kemnitz, Angew. Chem. Int. Ed. (2006) **45**, 1971.
3. N.A. Romanova, T.S. Papina, V.A. Luk'yanova, A.G. Buyanovskaya, R.M. Varuschenko, A.I. Druzhinina, A.A. Goryunkov, V.Yu. Markov, R.A. Panin, L.N. Sidorov, J. Chem. Thermodyn. (2013) **66**, 59.

What fullerene, C_{60} or C_{70}, is more reactive towards peroxy radicals? A DFT study

Sabirov D.Sh. [1] , *Garipova R.R.* [1] , *Bulgakov R.G.* [1]

diozno@mail.ru
[1] Institute of Petrochemistry and Catalysis of RAS, Ufa, Russia

Radical reactions of fullerenes find wide applications varying from synthetic chemistry to inhibition of biochemical processes [1]. Reaction of C_{60} with peroxy radicals $ROO^{\bullet}$ takes special place in fullerene radical chemistry. It provides promising synthetic route to oxygen-rich fullerene derivatives (*e.g.*, $C_{60}(OO^tBu)_n$ and $C_{60}O(OO^tBu)_n$), which are perfect precursors for further regioselective transformations [2, 3]. Additionally, interaction with peroxy radicals underlies fullerene antioxidant activity in diverse oxidation processes [3].

Currently, the reactivity of the other fullerenes towards radicals is discussed. There are some unexplained experimental results on the comparative reactivity of C_{60} and C_{70} towards peroxyl radicals. As experimentally found, C_{60} is the more reactive towards $^tBuOO^{\bullet}$ [2] whereas C_{70} is more reactive towards cumylperoxy radicals $CumOO^{\bullet}$ [3]. That is why these reactions became an objective of the present theoretical work.

We have found the structures and energies of transition states of $ROO^{\bullet}$ addition to C_{60} and different reactive sites of C_{70} fullerene by density functional theory method PBE/3ζ, which was previously successfully applied to computational thermochemistry of radical reactions of fullerenes [4]. According to the calculations performed for *tert*-buthylperoxy and cumylperoxy radicals, activation barriers do not vary significantly from one fullerene to the other (See the Table below; $\Delta H^{\neq}$ and rate constants k in parentheses are given in kJ mol^{-1} and L mol^{-1} s^{-1}, respectively). However, the corresponding rate constants calculated in terms of Eyring equation differ.

Fullerene reaction site	$C_{60/70} + {}^tBuOO^{\bullet} \rightarrow {}^tBuOOC_{60/70}^{\bullet}$	$C_{60/70} + CumOO^{\bullet} \rightarrow CumOOC_{60/70}^{\bullet}$
C_{60}	25.6 (100)	21.6 (14.5)
C_{70}, atoms of:		
type ***a***	28.6 (16.40)	28.1 (4.56)
type ***b***	28.2 (45.60)	23.9 (8.56)
type ***c***	25.4 (8.70)	28.6 (50.00)
type ***d***	28.0 (3.60)	28.0 (5.47)
type ***e***	49.6 (0.1×10^{-5})	47.4 (2.1×10^{-4})

As follows from the k values for reaction of unequivalent C_{70} atoms, atoms **b** and ***c*** of C_{70} are most reactive towards $^tBuOO^{\bullet}$ and $CumOO^{\bullet}$ radicals, respectively. It is noteworthy that rate constants of $^tBuOO^{\bullet}$ addition to C_{70} are less than the respective value for C_{60}, and *vice versa* – it is higher than $k(C_{60})$ in the case of cumylperoxy radical addition. The reasons of the different reactivity of C_{60} *versus* C_{70} towards $ROO^{\bullet}$ are discussed.

The work is supported by RFBR (project 14-03-97050 r_povolzh'e_a).

References

1. M. D. Tzirakis, M. Orfanopoulos, *Chem. Rev.* **113** (2013) 5262.
2. Z. Xiao, F. Wang, Sh. Huang, et al., *Org. Chem.* **70** (2005) 2060.
3. R. G. Bulgakov, D. I. Galimov, U. M. Dzhemilev, *Russ. Chem. Rev.* **88** (2014) 677.
4. D. Sh. Sabirov, R. G. Bulgakov, *Comput. Theor. Chem.* **963** (2011) 185.

Anisotropy of polarizability of fullerene bisadducts perspective as electron acceptor materials

Sabirov D.Sh. [1] , *Terentyev A.O.* [1] , *Bulgakov R.G.* [1]

diozno@mail.ru

[1] Institute of Petrochemistry and Catalysis of Russian Academy of Sciences, Ufa, Russia

As synthetic strategies in fullerene organic chemistry are developed, bis- and multiadducts come into wide use and applications. For example, bisPCBM, bisdihydronaphtho-C_{60} and other bisadducts are considered as perspective electron-acceptor materials [1]. Developing structure–property relationships may facilitate the screening of appropriate compounds for this purpose. The description of bisadducts' diversity may be performed by their physicochemical properties (measured or calculated).

We have calculated anisotropies of polarizabilities a^2 of various C_{60} and C_{70} bisadducts by accurate DFT methods. General regularities in structure–property relations for bis[60]PCBM and bis[70]PCBM are discussed as well as their use for searching effective electron-acceptor fullerene-based materials for organic solar cells.

We have found a correlation between a^2 of dihydronaphthyl-C_{60} bisadducts $C_{60}dhn_2$ and the key output parameters of organic solar cells, based on them [2]. The bisadducts with the lowest a^2 values (*e-*, *trans-4-*, and *trans-2*-$C_{60}dhn_2$) demonstrate in organic solar cells the highest power conversion efficiencies PCE and open-circuit voltages V_{OC}. On the contrary, the devices, utilizing highly anisotropic adducts, show the lowest one. The physical origins of the found correlation are discussed [3]. These may be understood in terms of (1) the dependence of dielectric permittivity on the polarizability (according Clausius–Mossotti equation), (2) the changes in polarizability under formation of fullerene charge-transfer complexes, (3) influence of polarizability on wetting processes (according to de Gennes equation), which are important when organic solar cells are produced via mixing polymer and fullerene derivative.

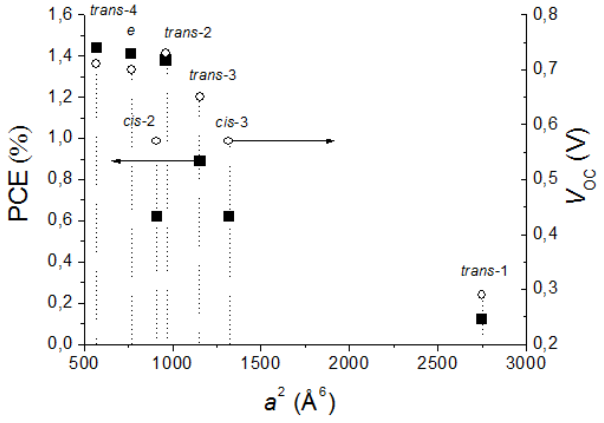

Correlation between the output parameters of organic solar cells, based on bis(dihydronaphtho)fullerene derivatives, and anisotropies of regioisomeric $C_{60}dhn_2$. Output parameters PCE and V_{OC} are taken from the experimental work [1].

References

1. S. Kitaura, K. Kurotobi, M. Sato, Y. Takano, T. Umeyama and H. Imahori, *Chem. Commun.* **48** **(**2012) 8550.
2. D. Sh. Sabirov, *J. Phys. Chem. C* **117** (2013) 9148.
3. D. Sh. Sabirov, *RSC Adv.* **4** (2014) 44996.

Regioselective nucleophilic cyclopropanation and alkilation of C_2-$C_{70}(CF_3)_8$

Semivrazhskaya O.O. [1] , *Apenova M.G.* [1] , *Lukonina N.S.* [1] , *Belov N.M.* [1] , *Troyanov S.I.* [1] , *Goryunkov A.A.* [1]

semivrazhskaya@gmail.com
[1] Department of Chemistry, Lomonosov Moscow State University, Moscow, Russia

Trifluoromethylated derivatives of fullerenes C_{60} and C_{70} are of the particular interest as promising materials for construction of organoelectronic devices due to their enhanced electron affinity, chemical stability and ability to undergo multiple reversible electrochemical reductions. It was found, that specific arrangement of CF_3 addends governs electronic affinities of the isomeric molecules in range of 0.5 eV [1]. Furthermore, it has been shown recently, that near-equatorial arrangement of eight CF_3 groups in C_s-symmetrical $C_{70}(CF_3)_8$ provides regioselectivity to a number of reactions of its further functionalization. The sterical unhindered chlorination [2] and cyanation [1] of C_s-$C_{70}(CF_3)_8$ proceeds selectively at its near-equatorial [5,6]-double bond while nucleophilic addition of the bulky diethyl bromomalonate carbanion results in cyclopropanation at more sterically accessible [6,6]-bonds at the poles of the fullerene cage [3]. Thus, functionalization of trifluoromethylated fullerenes is promising approach to achieve predetermined regiochemistry and, consequently, required chemical and electronic properties.

Here we reports the results of the nucleophilic cyclopropanation of C_2-symmetrical $C_{70}(CF_3)_8$ by the Bingel reaction and its modification due to Hirsch (aka Bingle-Hirsch reaction). The Bingel reaction regioselectively occurs at near-polar regions yielding isomeric-pure $C_{70}(CF_3)_8[C(CO_2Et)_2]$ monoadduct and C_2-$C_{70}(CF_3)[C(CO_2Et)_2]_2$ bisadduct. Unexpectedly, the Bingle-Hirsch reaction, apart from compounds mentioned above, affords alkylation at near-equatorial site resulting in $C_{70}(CF_3)_8[CH(CO_2Et)_2]H$. The structures of compounds obtained were unequivocally determined by means of ^1H and ^{19}F NMR spectroscopy and X-Ray single crystal data. The unexpected influence of the addition pattern in C_2-$C_{70}(CF_3)_8$ to such regioselectivity of the studied reactions are interpreted by means of quantum chemical calculation performed at the DFT level of the theory.

References

1. O.V. Boltalina, A.A. Popov, I.V. Kuvychko, N.B. Shustova, S.H. Strauss, *Chem. Rev.*, (2015) **115**, pp 1051–1105.
2. A.A. Goryunkov, N.A. Samokhvalova, P.A. Khavrel, N.M. Belov, V.Yu. Markov, L.N. Sidorov and S.I. Troyanov, *New J Chem*. (2011) **35**, pp. 32–35.
3. N.S. Ovchinnikova, A.A. Goryunkov, P.A. Khavrel, N.M. Belov, M.G. Apenova, I.N. Ioffe, M.A. Yurovskaya, S.I. Troyanov, L.N. Sidorov and E.Kemnitz, *Dalton Trans*. (2011) **40**, p. 959.

Formation of fullerenes at the transformation of amorphous carbon inside carbon nanotube

Sinitsa A.S. [1] , *Lebedeva I.V.* [1] , *Popov A.M.* [2] , *Knizhnik A.A.* [1]

alexsinitsa91@gmail.com
[1] NRC Kurchatov Institute, Moscow, Russian Federation
[2] Institute of Spectroscopy of Russian Academy of Sciences, Troitsk, Russian Federation

Despite the fact that fullerene molecules have been known for almost 30 years the mechanism of fullerene formation still remains a debated topic (see [1,2] for reviews). Since fullerene is the ground state for carbon system of about 100 atoms spontaneously self-assembled formation of fullerenes occurs for various initial systems which range from a chaotic mixture of carbon atoms and small molecules to a graphene flake. Here we consider amorphous carbon as new possible initial system for fullerene formation. Carbon nanotubes are found to act as nanoreactors which allows to study *in situ* structure transformation by heat treatment or under electron irradiation by high-resolution electron microscopy [3]. Here we study the process of transformation of amorphous carbon to fullerene at high temperature and/or under electron irradiation inside carbon nanotube by molecular dynamics simulations. As the result of simulations a fullerene-like structures were obtained (see Figure). The structural characteristics during the transformation are studied.

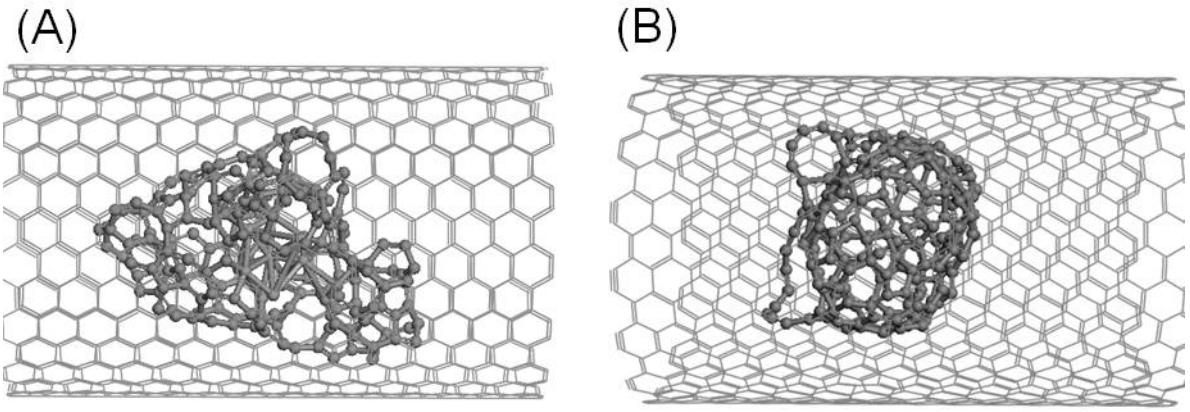

Figure. One of the MD-trajectories: from initial amorphous carbon structure (A) to fullerene-like structure B) at MD-simulation temperature of 2500 K.

References

1. E. Lozovik, A.M. Popov, Formation and growth of carbon nanostructures: fullerenes, nanoparticles, nanotubes and cones, Physics Uspekhi, 1997, 40, 717.
2. Irle, G.S. Zheng, Z. Wang, K. Morokuma, The C-60 formation puzzle "solved": QM/MD simulations reveal the shrinking hot giant road of the dynamic fullerene self-assembly mechanism, J. Phys. Chem. B, 2012, 110, 14531
3. W. Chamberlain, J. Biskupek, G. A. Rance, A. Chuvilin, T. J. Alexander, E. Bichoutskaia, U. Kaiser and A. N. Khlobystov, Size, Structure, and Helical Twist of Graphene Nanoribbons Controlled by Confinement in Carbon Nanotubes, ACS Nano, 2012, 6, 3943.

Multitip field emitters with fullerene protecting coatings.

Sominski G.G. [1] , *Taradaev E.P.* [1] , *Tumareva T.A.* [1] , *Mishin M.V.* [1]

sominski@rphf.spbstu.ru

[1] St. Petersburg State Polytechnical University, Russia

Cold field emitters are attractive for use in many electron devices. However, their application is limited by a low durability of such emitters at high currents in technical vacuum. The main reasons for field emitters failure in the electron devices operating at technical vacuum conditions are connected with a sputtering of their surface under the influence of the bombardment by residual gas ions, and also with the emitters destruction due to overheating at high emission currents and/or under the action of the ponderomotive forces.

At present, methods for creating multitip semiconductor structures are well developed. However, in order to successfully use such structures in electron devices, it is necessary to ensure their high conductivity, as well as to protect semiconductor structures from the destructive action of ion bombardment and ponderomotive forces. In the works [1,2], performed by the authors, the layer of molybdenum with thickness 20-30 nm was deposited on the surface of silicon multitip structure to provide high their conductivity and strength. To protect emitter against the destructive action of ion bombardment, thin (2 monolayer) coating of C_{60} fullerene molecules activated by potassium ions flow was used, because as it had been shown previously [3], such coating is stable and self-reproducing in conditions of intensive ion bombardment. The fullerene coating was deposited over the molybdenum one. In performed earlier [1,2] experiments, the silicon structures of small area (~ $2 \cdot 10^{-3}$ cm^2) with about 300 tips on the surface were used as a base of the cathode. The cathodes with double-layer metal-fullerene coatings durably operated in technical vacuum (~ 10^{-7} Torr) at the emission currents that did not exceed the value of 1 - 2 mA.

In the present work, the silicon cathode with double-layer coating having the surface area of about 0.2 cm^2 and 4500-4800 tips of the same shape as the tips of the previously studied systems [1,2] was created and studied. It follows from these measurements that an increase in the maximum achievable emission currents with such a cathode is approximately equal to the rise of the tips quantity on the surface as compared to the previously studied [1,2] cathodes. From our point of view, the obtained data indicate that a further growth of the emission current from the multitip systems with two-layer protective coatings is possible if the quantity of the tips on the structure is increased. Such increase can be achieved by increasing of the cathode area or by increasing of the amount of the tips on the cathode surface at a constant area.

To select possible ways to increase field emission current, numerical calculations of the characteristics of multitip systems were carried out at different surface morphology. The calculations showed that the emission current of cathodes used in this work could be increased about 4 times without change of their area if optimal morphology was selected.

References

1. G. Sominski, E.P. Taradaev, T.A. Tumareva, M.V. Mishin, and A.N. Stepanova, Proc. of 39th Int. Conf. Infrared, Millimeter, and THz Waves, September 14-19, 2014), Tucson, USA, W5-P25.7.
2. G. Sominskii, T.A. Tumareva, E.P.Taradaev, M.V. Mishin, A.N. Stepanova, Technical Physics (2015) **60**, No1, p.133.
3. A. Tumareva, G. G. Sominskii, Technical Physics (2013) **58**, No7, p.1048

Theoretical study of ultrahard carbon nanocomposite based on polymerized fullerenes

Kvashnina Yu.A. [1,2] *, Kvashnin A.G.* [1,2,3] *, Chernozatonskii L.A.* [3] *, Sorokin P.B.* [1,2,3]

PBSorokin@gmail.com

[1] Technological Institute for Superhard and Novel Carbon Materials, Moscow, Russian Federation

[2] Moscow Institute of Physics and Technology, Dolgoprudny, Russian Federation

[3] Emanuel Institute of Biochemical Physics, Moscow, Russian Federation

The successful synthesis of superhard and ultrahard material based on polymerized fullerenes for the first time was reported in a series of experimental papers by Blank et al. [1] where the fabrication of an amorphous carbon material called “tisnumit” consisting of polymerized fullerenes C_{60} with hardness and bulk modulus significantly exceeding the corresponding characteristics of diamond was carried out. However, identification of the atomic structure of fabricated ultrahard materials based on fullerenes has not been performed yet.

The theoretical analysis made earlier by Chernozatonskii et al. [2] showed that the model of a new three-dimensional polymerized fullerite well corresponded with the experimental data by X-ray diffraction [1] and should have had lower lattice parameter than the relaxed structure. Nevertheless, this data allows one to conclude that the increasing rigidity of a polymerized fullerite is originated from the mechanical strain induced by the surrounding carbon material.

In the present theoretical work [3], the effect of stiffening of polymerized fullerenes by considering the model of two different polymerized fullerites grains embedded in a single-crystal diamond matrix was investigated. The X-ray diffraction patterns for proposed nanocomposite with different grain sizes were calculated and in a good agreement with corresponding experimental data [1]. Thus, the proposed theoretical model is consistent with the experimentally obtained ultrahard “tisnumit”. The atomic structure of such complicated systems was investigated in details. The bulk modulus of the nanocomposites depending on the thickness of a diamond matrix between the fullerite grains and on the grain sizes was determined. The great augmentation of the bulk modulus from 590 GPa to 1712 GPa which is in a good agreement with experimental data was obtained. Nature of ultrahigh stiffness of this unique material was explained by analyzing of its atomic structure and map distribution of atom-projected bulk moduli. The calculated map shows that the key to ultrahigh stiffness lies in the compressed fullerite grain displaying an enhanced bulk modulus with respect to bulk diamond.

References

1. Popov, B. Kulnitskiy, V. Blank, Comprehensive Hard Mater. (2014) **3**, 515
2. Chernozatonskii, N. Serebryanaya, B. Mavrin, Chem. Phys. Lett. (1999) **316**, 199
3. A. Kvashnina, A.G. Kvashnin, M.Yu. Popov, B.A. Kulnitskiy, I.A. Perezhogin, E.V. Tyukalova, L.A. Chernozatonskii, P.B. Sorokin, V.D. Blank, J. Phys. Chem. Lett. (2015)

Fullerenes and fullerenols survival under irradiation: isotopic metallofullerenes for biomedicine

Suyasova M.V. [1] , *Szhogina A.A.* [1] , *Shilin V.A.* [1] , *Sedov V.P.* [1] , *Kozlov V.S.* [1] , *Lebedev V.T.* [1]

marinasuyasova@pnpi.spb.ru

[1] Petersburg Nuclear Physics Institute, NRC Kurchatov Institute, Gatchina, Russia

Recent results review in the study of endofullerenes and their water-soluble derivatives survival having been irradiated by fast and thermal neutrons in the reactor WWR-M (PNPI) are presented. The synthesis methods findings have allowed preparing the new unique radio isotopes based on Mo, Gd, Fe atoms encapsulated in C_{60} cages with grafted hydroxyl groups to fullerenes. Thus, finally obtained metallofullerenols $Me@C_{2n}(OH)_{38-40}$ demonstrated a good stability when they are accumulated the total fluences up to 10^{16} cm^{-2} while a substantial damage of fullerenols in solid phase was observed for the fluences ~ 10^{17}-10^{18} cm^{-2}.

The non phonon excitation mechanisms were proposed for understanding the fullerenols interaction nature with fast neutrons. In particular, fast electron shaking is suggested as the most probable process [1,2]. The studies seems to be very actual for advanced medical applications of metallofullerenes and their isotopic forms for the diagnostics (MRI) and tumors therapy. The active component (heavy metal, isotope) in such molecules is screened from surrounding tissues and the intoxication risks have been minimized.

Individually isolated fullerenes and fullerenols were prepared by composite electrodes arc evaporation and following fullerene soot extraction[3], chromatographic separation by the HPLC and hydroxylation. Irradiation was carried out in the zone of the WWR-M reactor for 0.5 - 32 hours for the samples: C_{60}, C_{70}, C_{84}, $Gd@C_{82}$ and $Gd@C_{2n}$ mixtures; $C_{60}(OH)_{30}$, $C_{70}(OH)_{30}$, $M@C_{2n}(OH)_{38-40}$ (M=Tb, Sc, Gd, Fe, Pr, Mo) and $M@C_{2n}(OH)_{38-40}$ with $C_{60}(OH)_{30}$ mixtures [4,5].The clusters radiation resistance/survival study included several stages when metallofullerenes and fullerenol had been demonstrated chemical activity under aerobic conditions. Several factors were analyzed: fast neutrons contribution to empty cages destruction, Szilard-Chalmers reaction, cluster size effects et al. Finally, for carbon structures the survival during fast and thermal neutrons irradiation (fluence up to 10^{19} cm^{-2}) was defined at the scale where empty carbon clusters owned higher stability than endohedral fullerenes. The hydroxylated derivatives radiation resistance are compared to metallofullerens and empty fullerrenes, as shown at Fig.1.

The work was supported by the RFBR (grant 14-23-01015 ofi_m).

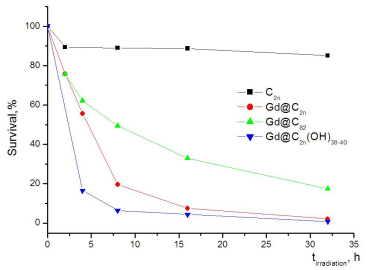

Fig. 1 - Fullerenes and fullerenols survival.

References : [1] Yu.S. Grushko, M. A. Khodorkovski, V. S. Kozlov, et al. // Fullerenes, Nanotubes, Carbon Nanostructures. 2006. № 14. P. 249. [2] V. Averbukh , L.S. Cederbaum // Phys. Rev. Lett. 2006. V. 96. P. 401. [3] Yu.S. Grushko, V.P. Sedov, V.A. Shilin // Journal of App. Chem. 2007. V. 80 (3). P. 450. [4] V. T. Lebedev , Yu. S. Grushko, V. P. Sedov, V. A. Shilin, V. S. Kozlov, S. P. Orlov,P. A. Sushkov, S. G. Kolesnik, A. A. Szhogina, and V. V. Shabalin // Physics of the Solid State. 2014. V. 56, № 1. P. 178. [5] A. A. Szhogina., V.A. Shilin, V.P. Sedov, V. T. Lebedev // Crystallography (in print).

Trifluoromethyl derivatives of fullerene C_{78}

Tamm N.B. [1] , *Kosaya M.P.* [1] , *Fritz M.A.* [1] , *Troyanov S.I.* [1]

tamm@thermo.chem.msu.ru

[1] Chemistry Department, Moscow State University, 119991, Moscow, Russia

In addition to the main components, C_{60} and C_{70}, many higher fullerenes, though with a very low abundance, are also present in the fullerene soot. Among them, fullerene C_{78} has a high relative abundance, just after the most abundant C_{84}. C_{78} can exist in five topologically different isomers [1], four of which have been confirmed experimentally [2,3]. Nonetheless, the data on the chemistry of C_{78} isomers are known by a few examples only [4-8].

In the present work, we isolated the C_{78} fraction from the fullerene mixture (an extract of fullerene soot) by high performance liquid chromatography (HPLC) using toluene as the eluent. The C_{78} fraction which contained all extractable C_{78} isomers was trifluoromethylated in ampules with gaseous CF_3I at 450 °C for 2 h. The obtained mixture of CF_3 derivatives was then subjected to HPLC separation with the use of hexane or a hexane/toluene mixture as the eluents. Slow evaporation of the solvent from HPLC fractions or recrystallization from other organic solvents afforded small crystals which were investigated by single-crystal X-ray diffraction with the use of synchrotron radiation.

Structural data were obtained for CF_3 derivatives of two similar isomers, $C_{78}(2)$ and $C_{78}(3)$, both possessing the same C_{2v} symmetry. The cages of C_{2v}-$C_{78}(2)$ and C_{2v}-$C_{78}(3)$ differ by the position only one C–C bond. Molecular structures were determined for $C_{78}(2)(CF_3)_{10}$, $C_{78}(2)(CF_3)_{12}$, $C_{78}(3)(CF_3)_{12}$, and $C_{78}(3)(CF_3)_{14}$. The addition patterns of 10-14 CF_3 groups on C_{78} fullerene cages are discussed and compared with each other and with the data from the literature [5,6].

It was established that the addition of two CF_3 groups to $C_{78}(2)(CF_3)_{10}$ proceeds without changing the positions of ten groups already attached. The addition is accompanied by the formation of an isolated C–C double bond on the fullerene $C_{78}(2)$ cage, whereas two of 12 cage pentagons remain unoccupied.

In contrast, in the molecular structure of $C_{78}(3)(CF_3)_{12}$, each of 12 pentagons is occupied by one CF_3 group. The addition of two more CF_3 groups to $C_{78}(3)(CF_3)_{12}$ is accompanied by changing the positions of several groups and the formation of an isolated C–C double bond on the fullerene cage in $C_{78}(3)(CF_3)_{14}$.

The work is supported by the Russin Foundation for Basic Research (grant 15-03-04464).

References

1. P.W. Fowler and D.E. Manolopoulos, An Atlas of Fullerenes, Clarendon, Oxford, 1995.
2. F. Diederich, R.L. Whetten, C. Thilgen, R. Ettl, L. Chao and M.M. Alvarez, Science 1991, **254**, 1768.
3. N.B. Shustova, B.S. Newell, S.M. Miller, O.P. Anderson, R.D. Bolskar, K. Seppelt, A.A. Popov, O.V. Boltalina and S. H. Strauss, Angew. Chem. Int. Ed., 2007, **46**, 4111.
4. A. Herrmann and F. Diederich, J. Chem. Soc., Perkin Trans. 2, 1997, 1679.
5. I.E. Kareev, A.A. Popov, I.V. Kuvychko, N.B. Shustova, S.F. Lebedkin, V.P. Bubnov, O.P. Anderson, K. Seppelt, S.H. Strauss and O.V. Boltalina, J. Am. Chem. Soc. 2008, **130**, 13471.
6. N.B. Tamm and S.I. Troyanov, Mendeleev Commun. 2009, **19**, 198.
7. K.S. Simeonov, K.Yu. Amsharov and M. Jansen, Chem.–Eur. J., 2008, **14**, 9585.
8. S.I. Troyanov, N.B. Tamm, C. Chen, S. Yang and E. Kemnitz, Z. Anorg. Allg. Chem. 2009, **635**, 1783.

A new method for functionalization of fullerenes under Kulinkivich reaction conditions

Tuktarov A.R. [1] , *Shakirova Z.R.* [1] , *Khuzin A.A.* [1] , *Dzhemilev U.M.* [1]

TuktarovAR@gmail.com
[1] Institute of Petrochemistry and Catalysis of RAS, Ufa, Russia

In this report we present the results of original research associated with the development of a new methodology for the directed and selective functionalization of carbon clusters via the reaction of C_{60} with nitriles or cyanoacetate in combination with EtMgX under the action of titanium based complex catalysts.

Thus, the interaction between C_{60} fullerene, EtMgBr and diverse nitriles in toluene at 80 °C in the presence of Ti(O*i*-Pr)$_4$ as the catalyst in argon atmosphere using the mole ratio of initial reactants C_{60} : RCN : [Mg] : [Ti] = 1 : 15 : 30 : 10 led to fullerotetrahydropyridines in 15−60 % yield after hydrolysis of the reaction mixture with dilute hydrochloric acid [5% HCl (aq)].

In order to extend the scope of application of our method to functionalize carbon clusters using nitriles under Kulinkovich-Szimonyak reaction conditions, the interaction between C_{60} fullerene and ethyl cyanoacetates has been also studied under selected reaction conditions. In contrast to nitriles, this reaction with ethyl cyanoacetates in the presence of Ti(O*i*-Pr)$_4$ as the catalyst and EtMgBr (Ti(O*i*-Pr)$_4$/EtMgBr reagent) gave previously hard- accessible aminomethanofullerenes in 40−90 % yield.

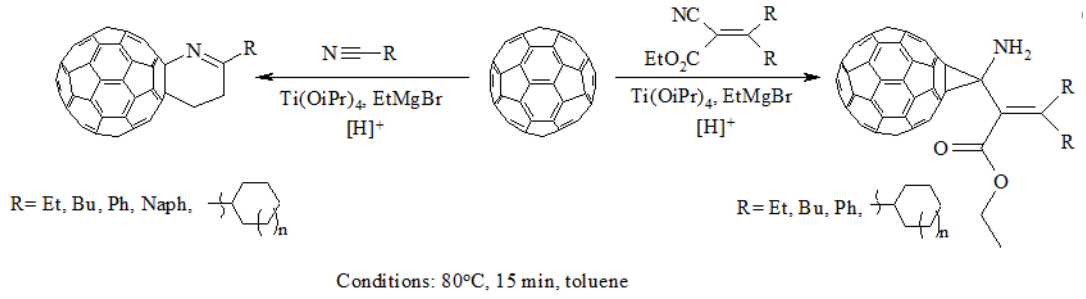

This work was performed under financial support of Russian Foundation for Basic research (Project No. 15-03-01042).

Synthesis and electronic properties of functionally substituted fullerenes – nanoscale optical molecular switches.

Tuktarov A.R. [1] , *Khuzin A.A.* [1] , *Shakirova Z.R.* [1] , *Akhmetov A.R.* [1] , *Khalilov L.M.* [1] , *Tulyabaev A.R.* [1] , *Yanybin V.M.* [1] , *Dzhemilev U.M.* [1]

TuktarovAR@gmail.com

[1] Institute of Petrochemistry and Catalysis of RAS, Ufa, Russia

As is well known, the major limiting factor in supercomputer design is a critical size of silicon transistors, responsible for achieving high performance. One possible way to solve the problem is to replace the conventional silicon transistors by single molecules useful as a organic molecular switches, which, as researchers believe, several orders of magnitude smaller than the most miniature device. This will eventually lead to a multi-billion-fold increase in the efficiency of the new computer systems as compared to modern computers, in which the silicon cells are used.

To solve the above problem, while selecting promising materials, we focused on fulleropyrrolidines, which were synthesized under Prato reaction conditions. Having hetaryl ethylene fragments they can easily undergo electron recombination (breaking and restoration of carbon-carbon bonds) under UV irradiation.

Our studies revealed that the synthesized fulleropyrrolidines A have photochromic properties, and under ultraviolet light (λ = 330 nm) converted to a thermally stable closed form B, which, when irradiated with visible light (λ = 530 nm), transitioned back to the original open form A. This feature of fulleropyrrolidines opens up prospects for designing a high-performance computer.

This work was financially supported by Grant of Russian science foundation (№ 14-13-00296)

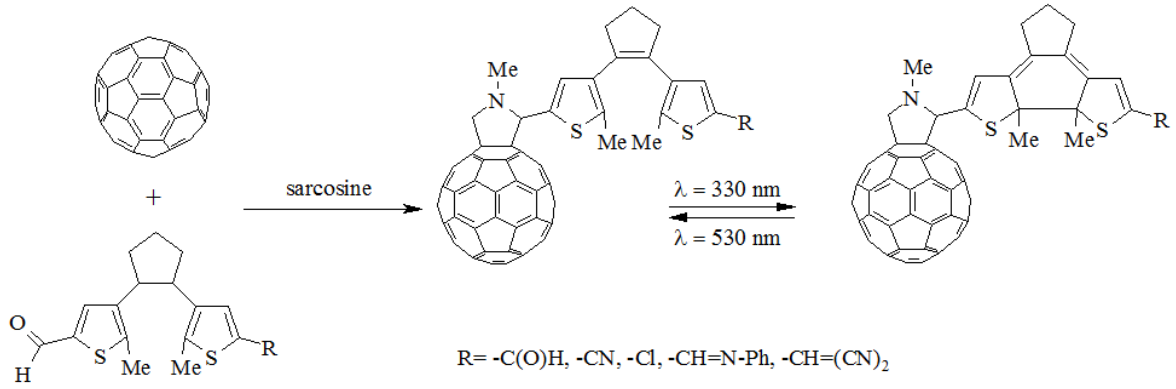

Electrical contact properties of the composite material reinforced by superelastic hard carbon particles obtained from fullerenes under pressure

Ushakova I.N. [1] , *Izmaylov V.V.* [2] , *Chernogorova O.P.* [1] , *Drozdova E.I.* [1] , *Ekimov E.A.* [3]

Ush.in@yandex.ru

[1] Baikov Institute of Metallurgy and Materials Sciences RAS, Moscow, Russia

[2] Tver State Technical University, Tver, Russia

[3] Vereshchagin Institute for High Pressure Physics RAS, Troitsk, Moscow Region, Russia

Modern electrical contact devices undergo increasing electrical and mechanical loads and the action of corrosive environments. This requires the development of new electrical-contact materials combining good electrical conductivity, wear resistance, antifriction properties, corrosion resistance, etc. Such combination of the service properties of electric contact materials can be provided by composite materials, e.g., by the new metal-based composite materials reinforced by superelastic hard carbon particles obtained from fullerenes under pressure [1].

The samples of copper-based composite materials reinforced by carbon particles were synthesized from a mixture of copper powder and 10 wt. % fullerenes (C_{60+70}) at a pressure of 8 GPa at 800°C. The microhardness of the carbon particles was measured with a UMT-3MO multifunctional tester recording the load-unloading curve at a load of 0.5 N. The electrical-contact properties of the samples were tested according to the procedure recommended in [2]. The electroerosive wear of the composite materials was tested by the method described in [3].

The copper-based composite materials reinforced by the carbon particles having a unique combination of mechanical properties such as a microhardness of 30 - 35 GPa, a Young's modulus of 180-200 GPa, and a high ratio of hardness to elastic modulus ($H/E > 0.15$), demonstrate good electrical contact characteristics. The minimum contact resistance of the composite materials is comparable to that of a gold reference sample. In electroerosive wear, the composite material substantially (by a factor of >3) surpasses the BrKh07 bronze, which is widely used for high-current electrical contacts. This shows that the composite materials reinforced by superelastic hard carbon particles are advantageous for the application as electrical contact material.

References

1. Chernogorova, E. Drozdova, I. Ovchinnikova, A. Soldatov, E. Ekimov, Journal of Applied Physics (2012) **111**, 112601.
2. ASTM B667 – 97: Standard Practice for Construction and Use of a Probe for Measuring Electrical Contact Resistance, 2014.
3. V.V.Izmaylov and M.V.Novoselova, RF Patent No. 2265862, Byull. Izobret., 2005, no. 34.

Effect of the structure of fullerites on the properties of their high-pressure high-temperature transformation product

Chernogorova O.P. [1] *, Drozdova E.I.* [1] *, Ushakova I.N.* [1] *, Sirotinkin V.P.* [1] *, Ekimov E.A.* [2] *, Benavides V.* [3] *, Soldatov A.V.* [3,4] *, Agafonov S.S.* [5]

ush.in@yandex.ru

[1] Baikov Institute of Metallurgy and Materials Science (IMET), 119991 Moscow, Russia

[2] Vereshchagin Institute for High Pressure Physics RAS, Troitsk, Moscow Region, Russia

[3] Engineering Sciences Mathematics, Lulea University of Technology, SE - 97187, Lulea, Sweden

[4] Department of Physics, Harvard University, Cambridge, MA 02138, USA

[5] National Research Center Kurchatov Institute, Kurchatov sq. 1, Moscow, 123182 Russia

The properties of the composite materials (CM) reinforced by superelastic hard carbon particles derived from fullerenes under high-pressure high-temperature (HPHT) treatment are determined by the particle mechanical properties, which in turn depend on the structure of the initial C_{60} fullerites. For the structure modification, the C_{60} fullerite crystals were subjected to mechanical activation (MA) in a ball mill for up to 90 hours. According to the XRD data, a significant refinement of coherent domains (to ~ 20 nm) occurs already after MA for one hour. With increasing ball milling time, the X-ray peaks of C_{60} fullerites undergo broadening up to a wide halo after treatment for 90 hours. The MA treatment of the C_{60} fullerites changes the scheme of their polymerization upon subsequent HPHT processing (600°C, 8 GPa): the fractions of two-dimensional rhombohedral and tetragonal phases significantly decrease, while the fractions of one-dimensional orthorhombic polymers and dimers increase. In general, the scheme of polymerization approaches that observed for unresolved $C_{60/70}$ mixture. The amorphization of C_{60} upon MA suppresses the formation of regularly oriented nanoclusters of graphene planes after the collapse of fullerene molecules upon heating under pressure [1]. The structure of the carbon phase obtained from mechanoactivated fullerites at a relatively low synthesis temperature (800°C, 8 GPa) consists of randomly arranged short packets of 2-3 graphene layers. The Fourier transform of the HRTEM image of such structure is represented by a broadened circle typical of amorphous structure, and the fracture surfaces of the broken carbon particles exhibit typical amorphous conchoidal fracture. Mechanoactivation of C_{60} for 48 hours results in a significant increase in hardness (from 18 to 32 GPa) and Young's modulus (from 104 to 256 GPa) of the products of the fullerene molecule collapse upon the above synthesis conditions and in some decrease in the elastic recovery upon indentation (from 94 to 80%). The increased hardness of the reinforcing particles produced from mechanoactivated C_{60} fullerites and the retention of a high elastic recovery increases the wear resistance of the composite material by a factor of 4-10 and decreases the friction coefficient by a factor of two. Due to the reinforcement by 10 wt % superelastic hard carbon particles, the wear resistance of the Co-based CM surpasses that of the matrix metal more than by two orders of magnitude, and the friction coefficient of the CM is decreased by a factor of 3.5-4.

References

1. O. Chernogorova, I. Potapova, E. Drozdova, V. Sirotinkin, A. Soldatov, A. Vasiliev, E.Ekimov, Applied Physics Letters (2014) **104**, 043110-1.

Influence of dimers rows formation effect on growing diamond crystal surface morphology

Averchuk G.Y. [1] *, Kurkina E.S.* [2] *, Koltsova E. M.* [1]

altermn@gmail.com
[1] IT department, Mendeleyev University of Chemical Technology of Russia, Moscow, Russia
[2] CMC faculty, Lomonosov Moscow State University, Moscow, Russia

The investigation of obtaining specific diamond crystal configuration is an important task today, since synthetic diamonds can be a basis for a new generation of semiconductors and templates of future quantum computers [1, 2].
Chemical vapor deposition method is one of the most advanced methods for producing diamond crystals. At the same time, it is necessary to highlight key factors of crystal surface formation at adjusted parameters of deposition environment. The software package that simplifies construction of a microscopic model of crystal growth process was developed by our work group. The set of elementary reactions that occur with atoms of crystal surface could be described by software system. The system evolution with given events stream is modeled using kinetic Monte Carlo method. An important feature of software system is the ability to describe influence of local environment on the rate of elementary processes, which called lateral interactions [3]. That lateral interactions allows us to observe effects of dimers rows formation on surface of growing crystal in process simulation.
A simple rule for dimers lateral interactions: the presence of neighboring dimers in a row reduces energy barrier of new dimer formation and increases barrier to break one. Dimers rows forms along the {100} plane of a diamond crystal. Long rows of dimers contribute to increasing of average migration length of adatoms on surface. Dimers rows prevent adatom etching from surface and have beneficial effect to filling new atomic layers of crystal. The particles can migrate along dimers row and interacts with other migrating particles. After particles interaction the new dimer at next atomic layer could be formed immediately. This dimer is the minimum critical nucleus of the next layer of crystal. The influence on each other dimers decreases and mean length of dimers row too at lower temperatures. Therefore, the crystal grows slowly and the surface roughness becomes significant. Conversely, higher temperatures promote formation of long dimers rows and hence smooth crystal surface. Thus, the effect of dimers rows formation appears as growth rate increasing and can facilitate multilayer crystal growth. This work was supported by RFBR grant 14-07-00960

References

1. J.E. Butler, M.W. Geis, K.E. Krohn, J. Lawless Jr, S. Deneault, T.M. Lyszczarz, D. Flechtner, and R. Wright, Semicond. Sci. Technol (2003) 18, S67.
2. A.P. Nizovtsev, S. Ya, Kilin, F. Jelezko, T. Gaebal, I. Popa, A. Gruber, and J. Wrachtrup, Opt. Spectrosc. (2005) 99, 233.
3. E.S. Kurkina, G.Y. Averchuk, Comput. Math. Model. (2013), 526

Novel hybrid magnetoactive nanomaterial based on Fe containing DNDs

Zharikova E.F. [1] *, Neumolotov N.K.* [1] *, Efimov N.N.* [1] *, Minin V.V.* [1] *, Baranchikov A.E.* [1] *, Imshennik V.K.* [2] *, Maksimov Yu.V.* [2] *, Ochertyanova L.I.* [1] *, Zhilov V.I.* [1] *, Fomina I.G.* [1] *, Eremenko I.L.* [1]

evgeniyazharikova@yandex.ru

[1] N.S. Kurnakov Institute of General and Inorganic Chemistry RAS, Moscow, Russian Federation

[2] N.N. Semenov Institute of Chemical Physics RAS, Moscow, Russian Federation

Ultrananocrystalline particles produced by detonation of carbon explosive materials (detonation nanodiamonds, DNDs, characteristic size of particles ~ 3-6 nm) have unique physical and chemical properties and very attractive for the nearest future nanotechnological applications The researchers all around the world pay increasing attention to the development of new approaches and methods of design such class of hybrid nanomaterials and to detailed investigation of their chemical and physical properties. In the present work, we use the solution chemistry methods for doping disaggregated and carboxylated DNDs by Fe^{3+} ions generated from inorganic salt $FeCl_3 \cdot 6H_2O$. Study of the microstructure of the samples was carried out by Scanning electron microscopy (SEM) with a local X-ray analysis, as well as the samples were studied by Inductively coupled plasma mass-spectrometry, Atomic absorption spectroscopy, Fourier Transform Infrared Spectroscopy, Electron spin resonance spectroscopy, and Mössbauer spectroscopy. Surprisingly, the new compounds Mössbauer spectra Fe-DND-CO_2 contain signals from both the Fe^{3+} and Fe^{2+} ions. The temperature dependence of magnetic susceptibility and the field dependence of the magnetization for samples of Fe-DND-CO_2 were performed.

The field dependence is well described by the Langevin function with the value of the effective magnetic moment $\mu = 1.07\ (\pm\ 0.04)\ \mu_B$. Such a low value of the effective magnetic moment can be explained by the presence of antiferromagnetic interactions in the sample.

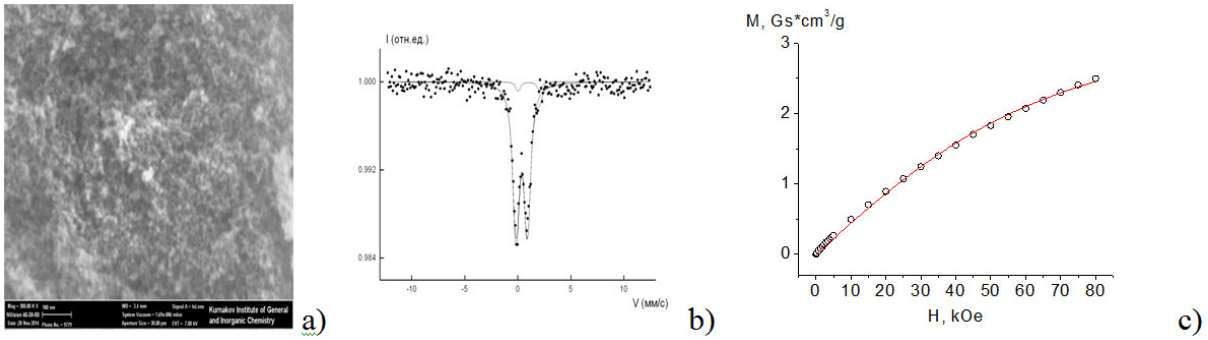

Fig 1. Microphotographs, SEM (a), Mössbauer spectrum Fe (b), and M(H) at 2 K (c) for the sample of Fe-NDs-CO_2.

References

Zharikova E.F., Efimov N.N. and Fomina I.G. thank the Russian Science Foundation (project No. 14-13-00795) and other coauthors are grateful the Federal Agency for Scientific Organizations for financial support of this research. Stable suspension and powder of 4-5 nm particles of detonation nanodiamonds for surface modification with Fe was made at Ioffe Physical-Technical Institute (St.Petersburg).

Control of Si-V color centers photoluminescence in nanodiamond particles embedded in a planar microcavity

Grudinkin S.A. [1] , *Feoktistov N.A.* [1] , *Medvedev A.V.* [1] , *Dukin A.A.* [1] , *Golubev V.G.* [1]

grudink@gvg.ioffe.ru
[1] Ioffe Institute, St. Petersburg, Russia

In recent years, the upsurge of interest in diamond and its optical properties is largely due to the presence of optically active centers, color centers (CCs), in this material. To the CCs family belong, e.g., point defects of the nitrogen–vacancy and silicon–vacancy types. These centers exhibit bright and stable photoluminescence with a short lifetime. The unique luminescent properties of CCs in diamond open up wide prospects for application of the given material in solid state emitters, quantum informatics, photonics, and biomedicine. To control spontaneous emission rate, external quantum efficiency of emission, luminescent band the CCs can be embedded in an optical microcavity (MC) in which conditions are created for the effective coupling of CCs with the electromagnetic eigenmodes of microcavity.

We suggest an approach to the development of a planar hybrid MC for controlling the photoluminescent from an array of isolated nanodiamond particles with embedded CCs. A planar MC is a structure constituted by two distributed Bragg reflectors (DBRs) and an active layer in between. To obtain a high Q factor of a MC at a small number of layers in the DBRs, we used alternating pairs of quarter wave layers of amorphous hydrogenated silicon carbide (a-$Si_{1-x}C_x$:H) and amorphous silicon dioxide (a-SiO_2) with a large ratio of their refractive indices (2.7/1.4). The a-$Si_{1-x}C_x$:H and a-SiO_2 layers were produced by plasma enhanced chemical vapor deposition in a single technological cycle. The active layer constituted by separate luminescent nanodiamond particles embedded in an a-$Si_{1-x}C_x$:H layer. The role of the emitter is played by a point defect Si–V constituted by a Si substitution atom and two nearby lattice vacancies in diamond. This CC is characterized by a small width of the zero phonon photoluminescent line at a wavelength of 738 nm (line width ~8 nm at room temperature), weak intensity of the phonon replica lines, and a short lifetime of ~ 1 ns. Controlled doping with Si was performed by the addition of silane to the working gas mixture during the course of microwave chemical vapor deposition growth of nanodiamond particles. Before depositing the top distributed Bragg reflector on active layer, we carried out a procedure in which a plane parallel, optically homogeneous, and smooth active layer was created. For this purpose, the bottom DBR with nanodiamond particles synthesized on it was covered with an a-$Si_{1-x}C_x$:H layer with a refractive index close to that of diamond (~2.3). Precision mechanical polishing of the a-$Si_{1-x}C_x$:H layer deposited on the diamond particles was performed with a detonation synthesis nanodiamond powder having an average grain size of ~4 nm. Because the nanodiamond powder was used for polishing, the root mean square deviation of the surface roughness of the active layer was ~2 nm.

As a result, narrowing to 5 nm of the zero phonon line at a wavelength of 738 nm and suppression of the phonon wing in the photoluminescence spectrum of the Si–V color centers were achieved in the fabricated planar hybrid microcavity.

Single-digit diamond and aggregates of diamond nanoparticles in motor oil lubrication on steel–steel high load contact

Ivanov M. [1] , *Smirnov S.* [2] , *Ivanov D.* [1] , *Shenderova O.* [3] , *Pavlyshko S.* [2] , *Osawa E.* [4] , *Vanchugova O.* [1]

m.g.ivanov@urfu.ru

[1] Ural Federal University, Yekaterinburg, Russian Federation

[2] Institute of Engineering Science Ural Branch RAS, Yekaterinburg, Russian Federation

[3] International Technology Center, Raleigh, USA

[4] NanoCarbon Research Institute, Tokita, Japan

Development of new lubricants and lubricant additives are critical from both energy conservation and environmental impact viewpoints. For example, total frictional losses in a typical diesel engine can be greater than 10% of the total fuel energy. Current oil-based technologies, which were developed with a focus on wear elimination, rely heavily on sulfur, phosphorous and/or chlorine based additives that have a propensity for bioaccumulation and environmental toxicity. Disposal and inadvertent discharge of oil-based lubricants is another major world-wide environmental concern. Recent studies have shown that lubricant formulations containing nanoparticles are capable of reducing friction and wear at sliding interfaces [1].

This paper presents results of ring-on-disk experiments to test the tribological properties of commercial motor oil Ravenol HCS 5W40 and the oil containing small amounts of single digit (5nm) Nanodiamond particles (NanoAmando) or aggregates of 10nm particles, as well as their combinations with molybdenum dialkyldithiophosphate (MoDDP) and perfluoropolyether (PFPE) to compare the efficacy of different nanodiamond in the engine oil under different sliding conditions. Analysis of coefficient of friction, wear and surface roughness was performed. It was observed that 10 nm nanodiamond particles in combination with MoDDP formed synergistic composition and demonstrated reduced friction coefficient and reduced wear in both ring and disk as compared to pure Ravenol. Based on roughness studies, the most probable mechanism is polishing of surface asperities in combination with the protective action of MoDDP. It was observed, however, that NanoAmando combined with MoDDP demonstrated increased friction and wear as compared to pure Ravenol. NanoAmando@PFPE demonstrate more efficient lubrication engine oils suspensions compared to NanoAmando in combination with MoDDP. Results from related experiments that are examining the influence of different textures and roughness on tribological performance will also be discussed.

References

1. M. G. Ivanov, S. V. Pavlyshko, D. M. Ivanov, I. Petrov, O. Shenderova, *JVST B*, 28, 4, 869-876 (2010)

Size-dependent photoluminescent properties and photon statistics of NV centers in HPHT nanodiamonds

Khomich A.A. [1] , *Vlasov I.I.* [1] , *Nunn N.* [2] , *Shenderova O.* [2] , *Kudryavtsev O.S.* [3]

antares-610@yandex.ru

[1] General Physics Institute RAS, Moscow, Russia

[2] Adamas Nanotechnologies Inc., 8100 Brownleigh Dr., Raleigh, NC 27617

[3] National Research University of Electronic Technology, Moscow, Russia

Size-dependent luminescent properties of nitrogen-vacancy centers were studied by photoluminescence (PL) spectroscopy in a set of high preassure- high temperature (HPHT) nanodiamonds (NDs) of varied size (10-200 nm) before and after electron irradiation and high temperature annealing. The samples were irradiated with 2 MeV electron, dose of 2.5-5.0x10^{18} cm^{-2}, followed by annealing of the samples in vacuum at T=800 °C for 1 hour. Finally all samples were annealed in air at 550 °C for 15 min to form O-terminated ND surface. In the samples with a large size of diamond nanoparticles, ≥ 100 nm, the PL enhancement was about 100, as compared to the original sample. For smaller NDs the PL enhancement decreases with particle size. A partial transfer of negatively charged NV (NV^-) to neutral NV (NV^o) is observed in 30-nm NDs. A broad-band PL dominates in 10-nm NDs before and after electron irradiation of this sample. The reduction of PL enhancement with ND size is explained by interaction of near-surface NV centers with the surface defects. Photon correlation spectroscopy measurements (photon antibunching) was used to determine number of NV centers in single ND particles of different sizes.

This work was supported by RSF grant no. 14-12-01329. The authors (O.S. and N.N.) wish to acknowledge support from the National Institute of Health under SBIR Contract HHSN268201300030C, NHLBI COAC Services Branch, RFP No. PHS 2013-1, Topic 80, "Fluorescent Nanodiamonds for In Vitro and In Vivo Biological Imaging".

Is DLS applicable for investigation of nanodiamonds smaller than 4 nm?

Koniakhin S.V. [1] *, Eliseev I.E.* [2] *, Terterov I.N.* [2]

kon@mail.ioffe.ru

[1] Ioffe Institute, St.Petersburg, Russia

[2] St Petersburg Academic University - Nanotechnology Research and Education Centre of the Russian Academy of Sciences, St.Petersburg, Russia

The determination of particle size by dynamic light scattering uses the Stokes-Einstein relation, which connects the diffusion coefficient of nanoparticle and its size. The Stokes-Einstein relation can break down for nanoscale objects [1]. Here we employ a molecular dynamics simulation of fully solvated 1-5 nm carbon nanoparticles for the refinement of the experimental data obtained for nanodiamonds in water by using dynamic light scattering.

The diffusion coefficients of nanoparticles were calculated using molecular dynamics (MD) in an explicit solvent (TIP4P/2005 water model) in the Gromacs 4.5.4 package [2]. The nanoparticles were modeled [3] as carbon nanocrystals with a diamond-type lattice (sp3 hybridization) of an approximately spherical shape with diameters of 1 nm, 1.5 nm, 2 nm, 3 nm, 4 nm, and 5 nm.

The analysis of the obtained dependence of the diffusion coefficient on particle's size allows concluding that for particles larger than 3 nm the Stokes-Einstein relation describes the diffusion coefficient with high accuracy. For 2 nm and smaller nanoparticles, the Stokes-Einstein relation shows the tendency to underestimate the diffusion coefficient obtained in simulations. The main result of the study is that the accuracy of the Stokes-Einstein relation is acceptable for the accurate size measurements by dynamic light scattering of most part of nanodiamond types.

S.K. acknowledges the Dynasty foundation and Zhores I. Alferov foundation.

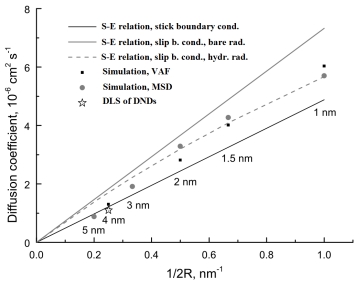

Diffusion coefficients for particles of various sizes 2R. The solid lines represent the predictions of Stokes-Einstein with bare radius used relation for stick (black) and slip (grey) boundary conditions. The dashed curve shows the Stokes-Einstein relation modified by the the hydrodynamic radius substitution. Black squares show the results of the VAF simulations and grey circles show the results of the MSD simulations. The star shows the value obtained from the DLS experiment for 4nm nanodiamonds.

References

[1] J. R. Schmidt and J. L. Skinner. Hydrodynamic boundary conditions, the Stokes-Einstein law, and long-time tails in the brownian limit. The Journal of Chemical Physics, **119** (15) 8062 (2003).

[2] B. Hess, C. Kutzner, D. van der Spoel, and E. Lindahl. Gromacs 4: Algorithms for highly efficient, load-balanced, and scalable molecular simulation. Journal of Chemical Theory and computation, **4**(3) 435–447 (2008).

[3] S.V. Koniakhin · I.E. Eliseev · I.N. Terterov · A.V. Shvidchenko · E.D. Eidelman · M.V. Dubina, Molecular dynamics-based refinement of nanodiamond size measurements obtained with dynamic light scattering, Microfluidics and Nanofluidics, in press (2015).

The divacancy V–C=C–V configurations on the diamond surface: quantum-chemical simulation

Lvova N.A. [1] , *Ananina O.Yu.* [2] , *Severina E.V.* [2]

nlvova@tisnum.ru

[1] Technological Institute for Superhard and Novel Carbon Materials, Troitsk, Moscow, Russia

[2] Zaporizhzhya National University, Physical Faculty, Zaporizhzhya, Ukraine

Diamond properties are largely determined by the defects, both biographical and encountered during the processing, namely ion implantation [1]. Experimental and theoretical works [2] are mainly devoted to the study of stability and influence of vacancy and divacancy defects on the bulk properties of diamonds. However, the structure and properties of defects on a clean diamond surface remain insufficiently studied. Such a situation promotes the use of quantum-chemical modeling [3,4]. This paper presents the results of calculations of the geometric, electronic, and adsorption properties of divacancy defects on the C(100) and C(111) diamond surfaces. Defective conditions on a clean, reconstructed surface are considered; stable configurations of divacancy defects differing in geometries, electronic properties, and formation energy are determined. We also evaluate the energy barriers between the V–C–C–V; V–C=C–V, and divacancy V_2 states.

The presence of defects leads to a change in surface adsorption activity and significantly affects the energy of adsorption and desorption of the particles. As adsorbate particles, we selected the H_2 hydrogen molecules, O_2 oxygen and H_2O water molecules. Potential adsorption sites on the reconstructed surface are surface chain atoms in the vacancy area with unsaturated bonds (involved in the formation of delocalized electron clouds) and atoms with double bonds. In this paper, we evaluated the energy characteristics of adsorption, such as adsorption activation energy $\boldsymbol{E_{act}}$ and binding energy (heat of adsorption, $\boldsymbol{q}$), and proposed the mechanisms of adsorption and desorption of molecules.

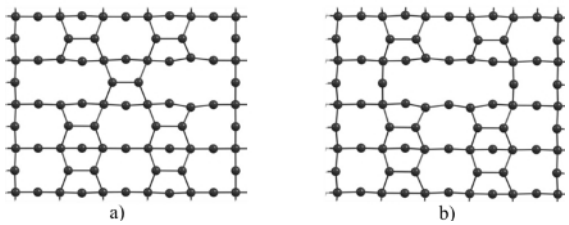

The divacancy on the diamond (100)-2×1 surface: a) V–C=C–V; b) V2 configurations.

References

1. Hyde-Volpe, B. Slepetz, M. Kerteszthe, J. Phys. Chem. C (2010) **114**, 9563.
2. A. Khmelnitsky, V.A. Dravin, A.A. Tal, M.I. Latushko, A.A. Khomich, A.V. Khomich, A.S. Trushin, A.A. Alekseev, S.A. Terentiev, Nuclear Instruments and Methods in Physics Research B (2013) **304,** 5.
3. A. Lvova, O.Yu. Ananina, Russian Journal of Physical Chemistry A (2013) **87**, 1515.
4. A. Filicheva, N.A. Lvova, and O. Yu. Ananina, Fullerenes, Nanotubes, Carbon Nanostruct. (2012) **20**, 616.

Boundary thermal resistance and heat conductance of nanodiamond based composites

Meilakhs A.P. [1] , *Eidelman E.D.* [1,2] , *Shakhov F.M.* [1]

mejlaxs@mail.ioffe.ru
[1] Ioffe Institute, St. Petersburg, Russia
[2] St. Petersburg State Chemical-Pharmaceutical Academy, St. Petersburg, Russia

As it was first found by Kapitza, a heat flow from one material to another is accompanied by a temperature jump at the interface. The proportionality coefficient relating the temperature jump to the heat flux is known as thermal boundary resistance or the Kapitza resistance. Thermal resistance in nanodiamond based composite materials is determined by thermal resistance at the phase boundaries. We investigate Kapitza resistance in three ranges of phonon transmission coefficient: small, medium and high.

In the case of medium transmission coefficient of phonons, we introduced a new method for calculating the Kapitza resistance [1]. The main idea of this method is the generalization of Chapman-Enskog method [2] for the case of the interface between two media.

In the case of small transmission coefficient we proposed a new mechanism for heat transport. We take into account oscillations inherent in the insulator but having frequencies higher than maximum possible frequencies of oscillations in metal [3]. This means that such oscillations should decay far from the boundary on the metal side. Such oscillations interact with electron gas in metal, thus, the energy is transferred from the insulator to the metal. This model explains high thermal conductivity of diamond-copper composite prepared from tungsten coated diamond particles [4,5].

In the case of high transmission coefficient we found that Kapitza resistance is independent from the type of insulator [6]. Electrons are involved in the heat transfer only at a certain distance from interface. Consequently, the heat transfer near the interface is less efficient, resulting in additional contribution to the boundary thermal resistance. Relaxation resistance can be expressed as:

$r_{rel} = (\kappa_{ph}\theta)^{-1/2}$.

Here κ_{ph} is a phonon heat conductivity, θ characterizes the efficiency of heat transfer between electrons and phonons.

We apply our theory in the study of properties of high-pressure sintered detonation nanodiamonds. We experimentally observed that nanodiamond composites have different heat transfer mechanism than micro diamond composites. E.g. thermal conductivity of sintered nanodiamonds decreases with increasing sound velocity. It shows that the partial graphitization of nanodiamonds starts at smaller temperatures than the graphitization of bulk diamond and microdiamond.

This research was supported by the Russian Scientific Foundation (grant \# 14-13-00795).

References

1) A.P. Meilakhs, PSS (2015), **57,** 148
2)L. D. Landau and E. M. Lifshitz, *Course of Theoretical Physics*, Vol. 10: *Physical Kinetics* (Nauka, Moscow,1979; Butterworth–Heinemann, Oxford, 1981)
3) A.P. Meilakhs, E.D. Eidelman, JETP Letters (2013), **97**, 38-40
4)A.M. Abyzov, S.V. Kidalov, F.M. Shakhov, Appl. Therm. Engineering (2012), **48**, 72-80
5)C. Zhang, R. Wang, Zh. Cai, Ch. Peng, N. Wang, J. Material Science (2014)
6)A.P. Meilakhs, E.D. Eidelman, JETP Letters (2014), **100**, 81

Characterization of Aqueous Dispersions of Nanodiamonds and Fullerenes by Photothermal Spectroscopy

Proskurnin M.A. [1,2] *, Mikheev I.V.* [1,2] *, Volkov D.S.* [1,2] *, Korobov M.V.* [1] *, Ivshukov D.A.* [1] *, Pustovalov M.V.* [1]

mikheev.ivan@gmail.com

[1] Chemistry Department, Lomonosov Moscow State University, Moscow, Russia

[2] Analytical Centre of Lomonosov Moscow State University / Agilent Technologies Authorized Partner Laboratory Moscow, Russia

Multiwavelength, scanning, and transient photothermal (PT, thermal lens and optoacoustic, OA) spectroscopy is used for the investigation and analysis (chemical analysis and the estimation of thermophysical properties and size) of nanodiamonds and fullerenes C_{60} and C_{70} and their organic solutions and aqueous dispersions as promising ultra-dispersed materials having various applications.

We used several approaches—thermal-lens and optoacoustic, transient (time-resolved) and stationary (thermal equilibrium) signals, spatial and time scanning—for estimating the size of clusters in aqueous fullerene and nanodiamonds solutions. The details of the experimental techniques will be provided. The data obtained have been compared to the results from other methods like dynamic laser scattering (DLS), differential scanning calorimetry (DSC) and electron microscopy. All the variants provide complementary information, and PT/OA spectroscopy can be used, along with the data from other methods, to characterize and monitor carbon nanomaterials and their aqueous dispersions. The estimation of the cluster size from two techniques—transient and imaging—giving concordant values and agreeing with DLS data is very invigorating. Although both techniques are currently unable to provide the information with enough precision due to undeveloped mathematical models, this direction of the unraveling photothermal spectroscopy shows very good outlooks.

These data are supplemented by the estimation and determination of photothermal parameters (thermal conductivity, thermal expansion coefficient, heat capacity, thermal diffusivity, thermal effusivity, and density) for aqueous dispersions of nanodiamonds of various brands and fullerenes C_{60} and C_{70} of various concentrations by DSC, densitometry and other techniques. The possibilities to elucidate these parameters from photothermal experiments are discussed.

The possibilities of PT/OA spectroscopy to determine submicrogram concentrations of nanodiamonds and fullerenes are shown. The advantages of these techniques over conventional spectroscopies due to much lower effect of light scattering and the signal enhancement in disperse solutions as well current limitations are discussed. The comparison of photothermal and fluorescence data is made. The necessity to develop robust models for transient and imaging photothermal techniques is outlined.

The possibility of multiwavelength (multispectral) OPO-based PT/OA spectroscopy to complement the conventional spectrophotometric data on the nature of extinction spectra of aqueous nano-sized carbon dispersions is shown. The data are compared with conventional UV-visible spectroscopy. The proposed approach can be used (for nanodiamonds and fullerenes as well as dispersions of various nature) to distinguish between light absorption of these materials, light-scattering contribution, and photothermal effect to the overall picture of their properties.

Acknowledgments. The work is supported by The Russian Scientific Foundation, grant no. 14-23-00012. We are grateful to Agilent Technologies — Russia and its CEO, Dr. Konstantin Evdokimov, for providing the equipment used in this study.

Evaluation of acute toxicity of modified nanodiamond

Isakova A.A. [1] *, Krysanov E.Yu.* [2] *, Demidova T.B.* [2] *, Ivanova M.V.* [3] *, Saphonov A.V* [1] *, Omelchenko O.D.* [1]

isakova_aleks@list.ru

[1] A.N. Frumkin Institute of Physical Chemistry and Electrochemistry RAS, Moscow, Russia

[2] Severtsov Institute of Ecology and Evolution RAS, Moscow, Russia

[3] N. F. Gamaleya FRCEM, Moscow, Russia

Nanodiamonds synthesized by detonation(DND) are promising materials for application in biology. We have already shown that modified nanodiamonds can effectively absorb influenza viruses and cDNA of influenza viruses as well[1]. For their use as a sorbent in devices and filters, it is necessary to determine the influence of modified nanodiamond on the living organisms activities and evaluate the nanodiamond toxic properties. For this purpose, we performed the evaluation of the toxicity of several kinds of nanodiamonds: commercial UDA-GO-VK ("Sinta", Minsk, Belorus), graphitized DNA, chlorinated DNA and aminated DNA. Model organotrophic facultative bacterium *Pseudomonas putida k12*, *zebrafish* caviar, white lab rats were used as a test object for the evaluation of the acute toxicity. The DNA suspensions in appropriate media with a concentration of 10-1000 mg/L were used for the experiments. No DNA acute toxicity was detected in whole studied concentration range. It was found that when adding a DNA suspension into the medium with zebrafish caviar the embryo survival was higher compared with the control group, however, the number of malformation increased. The addition of nanodiamonds into the medium with caviar seems to promote the adsorption of various toxic substances on its surface and suppress the growth of fungi [2]. It was established that the introduction of 2-3 mg of the DNA suspension complexed with influenza virus (H3N2) to white rats leads to the slight increase of monocytes in blood. Other blood parameters remained within the mark. The monocytes increase in blood may be a result of changes in the external environmental factors, including nutrition, stress, etc.

References

1. Ivanova M.V., Burtseva E. I., Ivanova V. T., Trushakova S.V., Isaeva E.I., Shevchenko E.S., Isakova A.A., Manykin A.A., Spitsyn B.V. Adsorption of influenza A and B viruses on detonation nanodiamond materials // MRS Proceedings.- 2012..-V.1452. - mrss12-1452-ff04-06.

2. Shilova O.A., Hamova T.V., Vlasov, D.Yu. et al. The Using Suspensions of Detonation Nanodiamond in Solgel Processing Formation of Biostable Protective Coatings // 3rd International Symposium Detonation Nanodiamonds: Technology, Properties and Applications. 2008.

Nanodiamonds modified polymer membranes for gas separation

Polotskaya G.A. [1,2] , *Avagimova N.V.* [2] , *Toikka A.M.* [2] , *Pientka Z.* [3]

polotskaya@hq.macro.ru

[1] Institute of Macromolecular Compounds RAS, St. Petersburg, Russia

[2] Saint Petersburg State University, Institute of Chemistry, St. Petersburg, Russia

[3] Institute of Macromolecular Chemistry AS CR, Prague, Czech Republic

Modification of existing membrane materials is extensively employed to create suitable membranes with enhanced performance. Among various modification approaches, creation of nanocomposite materials with polymer matrix containing carbon nanoparticles is one of the most cost- and time- saving trends. In the present work membranes was developed on the base of composites prepared by solid phase dispersing nanodiamonds (ND) and polyphenylene oxide (PPO) powders. The aim of the work was estimation of the effect of ND inclusion into polymer matrix, study on structure and gas separation properties of PPO/ND nanocomposite dense film membranes. The character of structural changes was determined by density measurement and free volume parameters calculation. The rise of ND concentration up to 5 wt% in the PPO matrix leads to the increase of the membrane density together with the fractional free volume increase. This fact is not usual and it can influences on diffusion properties of membranes.

Gas transport properties of membranes based on PPO and its composites containing 1, 3, and 5 wt% ND were measured for the series of penetrants H_2, N_2, O_2, CO_2, and CH_4 in a wide temperature range 30÷100°C. The data on coefficients of permeability, diffusion, and solubility were analyzed and used for calculating activation energies and heat of sorption.

It was established that the permeability coefficients for all gases decrease slightly but the ideal selectivity in separation of H_2/N_2, O_2/N_2, and CO_2/CH_4 gas pairs increases with rise of the ND content in membranes. Study on the temperature dependence of H_2, CO_2, O_2, N_2, and CH_4 permeation in membranes of different ND content showed that the permeability coefficients increase with rise of temperature from 30 to 100°C. Data on gas permeation were used to estimate effective activation energies of permeation and diffusion in polymer nanocomposites, such as the heat of sorption. The increase of ND content in polymer leads to decreasing activation energies of diffusion for all gases.

Comparison of the PPO/ND membranes with literature data on gas separation performance was made with Robeson diagram for O_2/N_2 gas pair. The position of PPO membranes in Robeson diagram is improved due to inclusion of ND particles.

Aknowlegments. Authors acknowledge St. Petersburg State University for a research grant (12.38.257.2014). The authors are gratefully acknowledged SCTB "Technolog" Saint-Petersburg for the ND samples.

Oxides formation on surface of mechanically alloyed granules from metal matrix composites with high volume fraction of nanodiamond reinforcements

Popov V.A. [1] , *Prosviryakov A.S.* [1] , *Skryleva E.A.* [1] , *Sagalova T.B.* [1] , *Senatulin B.R.* [1]

popov58@inbox.ru

[1] National University of Science and Technology "MISIS", Moscow, Russia

Metal matrix composites were produced by mechanical alloying of the components to obtain composite granules, followed by consolidation of the granules into a compact material. Commercially, pure copper and zinc were used for the matrix. The content of the ND fraction was varied from 5 up to 30 vol.%. A characteristic feature was revealed, namely, increased air oxidation of composite materials with increased concentration of nanodiamond reinforcing particles. This effect was found for all matrix materials studied, i.e., for copper (Fig.1) and zinc (Fig.2). Presence of oxides in composite structure can lead to limitation of service thermal conditions of composite, because oxides can react with nanodiamonds or other components (Fig.3).

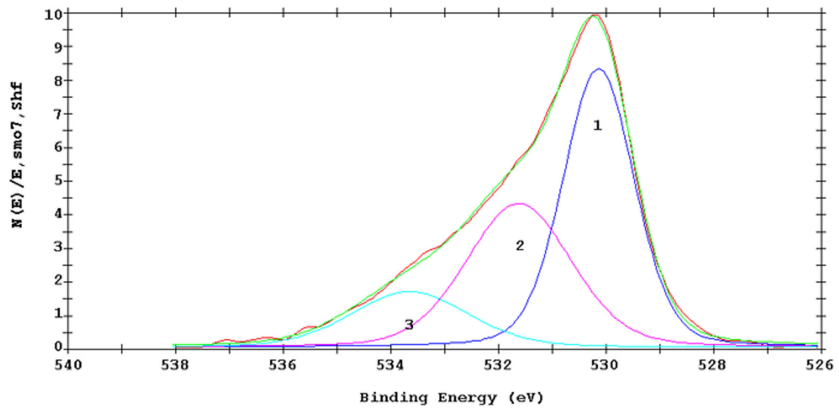

Fig.1. XPS spectra from composite "Cu+20%(vol)ND" specimen: curve 1 (530,3 eV)– Cu2O

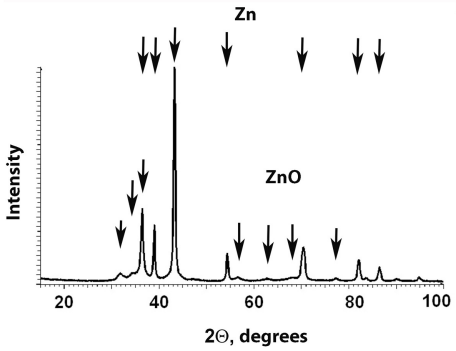

Fig.2. X-ray diffraction patterns from composite "Zn+25%(vol)ND" specimen

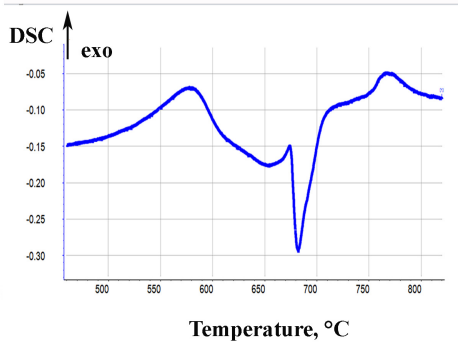

Fig.3. DSC curve from composite "Cu+25%(vol)ND" specimen

The impact of non-agglomerated nanodiamond reinforcing particles on stability of structure of metal matrix composites

Popov V.A. [1] , *Vershinina E.V.* [2]

popov58@inbox.ru

[1] National University of Science and Technology MISIS, Moscow, Russia

[2] Lomonosov Moscow State University of Fine Chemical Technology, Moscow, Russia

According to the “mechanical alloying (MA) – compression” process design [1-5], the samples of composites with aluminum matrix and non-agglomerated nanodiamond reinforcing particles with volume content of 0.5%; 1%; 2.5%; 5%; 10% were produced. Moreover, originally the composite granules with 10% of nanodiamonds were obtained in the planetary mill. Then some granules were removed from mill shells, and aluminum powder was added to get nanodiamond volume concentration of 5%. After 2 hours of processing, the similar procedure was performed to get nanodiamond volume concentration of 2.5%, and so on. The obtained samples were annealed in vacuum under the temperatures of 300°C, 400°C, 450°C, 500°C, and 550°C during 0.5-1.5 hours. Before and after annealing, the regions of coherent scattering were defined in the matrix material of samples, i.e. aluminum. The corresponding results (coherently scattering domains and microdeformation level as function of nanodiamond volume fraction in aluminum matrix and annealing temperature) are represented in Table 1. "Data for specimens after mechanical alloying and cold pressing" and Table 2. "Data for composite “Al+10%ND” specimens after mechanival alloying, cold pressing, hot extrusion and annealing".

The Tables show that non-agglomerated nanodiamonds cause structure stability: in the composite matrix reinforced by nanodiamonds, regions of coherent scattering decrease upon increase of nanodiamond volume concentration, and annealing does not lead to their significant increase.

Table 1

Material, temperature of annealing during 1 h	Domain size D, Å	Micro-deformation e,%
Al+2,5%ND, no anneling	1618	0,00061
Al+2,5%ND, 550 °C	1600	0,00058
Al+5%ND, no annealing	1169	0,00104
Al+5%ND, 500 °C	1321	0,00095
Al+10%ND, no annealing	872	0,0012
Al+10%ND, 550 °C	979	0,318

Table 2

Annealing temperature, °C	Annealing period, h	Domain size D, Å
Initial	0	1430
350	0,5	1600
450	0,5	1475
450	1,5	1580
550	0,5	950

References

1. V.Popov, B.Chernov, A.Prosviryakov, V.Cheverikin, I.Khodos, J.Biskupek, U.Kaiser, J.Alloys Compd. (2014) 615, S433.
2. V.Popov, D.Többens, A.Prosviryakov, Phys. Status Solidi A (2014) 211, 2353.
3. V.Popov, in: Xiaoying Wang (Ed.) Nanocomposites: Synthesis, Characterization and Applications, Nova Science Publishers, Inc., NY, 2013, 369.
4. V.A.Popov, B.B.Chernov, A.M.Nugmanov, G.P.Schetinina. Fullerenes, Nanotubes and Carbon Nanostructures (2012) 20,455.
5. D.Nunes, M.Vilarigues, J.B.Correia, and P.A.Carvalho, Acta Mater. (2012) 60, 737.

High resolution TEM and infrared absorption studies of commercial polycrystalline nanodiamonds with twinning boundaries

Romanov N.M. [1,2] , *Osipov V.Yu* [1] , *Boudou J.-P.* [3] , *Hayashi T.* [4] , *Takai K.* [5]

nikromanov.90@gmail.com

[1] Ioffe Institute, St. Petersburg, Russia

[2] St. Petersburg State Polytechnic University, St. Petersburg, Russia

[3] Laboratoire Aime Cotton - CNRS, University Center Orsay, Orsay Cedex, France

[4] Faculty of Engineering, Shinshu University, Wakasato, Nagano, Japan

[5] Department of Chemical Science and Technology, Hosei University, Koganei, Tokyo, Japan

Nanodiamonds with mean size ranging from ~25 nm to ~1000 nm obtained by dynamic (DyND) syntheses are enough interesting objects among other nanomaterials. The reason for such an interest originates from their unique properties related with the presence of small, but detectable amount of NV^- and other Si- based fluorescent centers inside the diamond crystallites. DyND may be very promising for applications somewhere as specific markers.

DyND samples (Super Syndia SSX) of different mean size were manufactured by L.M. Van Moppes & Sons SA (Switzerland) by means of patented *DuPont* technology, i.e. with the use of shock-wave compression of graphite/copper mixture pressed into pellets from dry water slurry containing some additives (2 wt.%). The product after synthesis was comprehensively treated in hot acids for the removal of non-diamond sp^2-phase, milled by stainless steel beads and then separated on more than ten fractions of different mean size. Trace analysis of commercial SSX products shows about 25 ppm of Si, 320 ppm of Cr, 270 ppm of Fe, 18 ppm of Ti, 80 ppm of Mn and 13 ppm of Cu in the most part of as fabricated samples. Further removal of ferromagnetic impurities and probable remaining metaloxides was carried out by sample treatment in strong acids (or in NaOH) in autoclave at T ~ 160 ^oC and the obtained samples were investigated.

HRTEM of the finest fraction SSX 0-0.05 (median size 25 nm, FWHM – 25 nm) shows that particles have a polycrystalline character with a lot of grain boundaries and twins and mainly consist of countless cubic diamond crystallites with sizes varying from ~5 nm to ~20 nm. Neighboring close twinning boundaries between the crystallites can be considered as a stacking faults of restricted extension (up to 3 nm in the direction perpendicular to the boundaries) in the diamond lattice.

The surface of acid treated SSX particles (polycrystals) is terminated by a set of oxygen containing functional groups that are covalently bound to the surface and appeared there due to oxidizing chemical treatment. Among them are carboxyl, carbonyl, hydroxyl and anhydride ones, as well as the surface C-H groups. The essential infrared (IR) absorption in the range 1050-1200 cm^{-1} is related with C-O and C-O-C groups that exist on the particle surface. The intensity of absorption band at ~1100-1130 cm^{-1} found in the spectra of SSX polycrystals depends upon the particle volume, and not upon its surface, as it is the case for absorption bands of hydroxyl (~1630 cm^{-1}) and carbonyl groups (~1810 cm^{-1}). It probably means that the band at ~1100-1130 cm^{-1} is a specific signature of C-O and C-O-C bonds hardly cemented the diamond grains in the large SSX particles of median size ranging from ~25 nm to ~100 nm. We also discuss the contribution and the role of C-N and Si-O bonds in IR absorption band centered at 1130 cm^{-1}. The presence of interior nitrogen is well confirmed by observation of NV^- centers. Thus, the ratio of intensities of absorption bands at ~1100-1130 cm^{-1} and ~1730-1810 cm^{-1} in diamond polycrystals passed through the oxidizing treatment may be good criterium for evaluation the percentage of inter-grain boundaries with C-O-C, C-O bonds covalently cemented the diamond nano-crystallites in hard aggregates.

Viscosity and gelation in the nanodiamond hydrosols

Shchankin N.V [1] , *Vul A.Ya.* [1] , *Aleksenskii A.E.* [1]

Shchankin.nv@ya.ru
[1] Ioffe Institute, Saint-Petersburg, Russia

The subject of the presented work is the properties of nanodiamond, produced by detonation synthesis (Detonation Nanodiamonds, DND).

The typical size of nanodiamond crystals is approximately 3-5 nm, this estimation confirmed by X-ray and transmission electron microscopy [1]. But the real size of particles of DND that measured by optical microscopy or light scattering are 100-500 nm. [2] The structure and properties of complicated particles of nanodiamond were the field of researches for the long time.

The hydrosols containing the single particles of detonation nanodiamond were produced recently [3] and their properties were not well understood. In Ioffe institute the structure and properties of single-digit hydrosols are studied now.

Applying acoustic method we investigated viscosity dependence on concentration of hydrosols with positive zeta-potential .

The nanodiamonds hydrosols with low concentrations (less than 4.1%) demonstrate the properties of usual liquids with constant viscosity. In the nanodiamonds hydrosols with higher concentration (4.35%) we observed long time increasing of viscosity (thixotropy). This fact may be interpreted as aging of true nanodiamonds gel. We observed the formation of nanodiamond gel after long-time exposure in working cell of the viscosimeter directly. We made the samples of nanodiamonds gels by aging of concentrated nanodiamonds hydrosols.

The data of dynamic light scattering for investigated hydrosols confirmed sol-gel transformation also.

This work was supported by Russian Scientific Foundation (Grant 14-12-00795).

References

1. A.E. Aleksenskii, M.A. Yagovkina, A.Y. Vul', Phys. Solid State (2004), **V.46**, 685.
2. A.I. Shames, A.M. Panich, V.Yu. Osipov, A. E. Aleksenskiy, A.Ya. Vul’, T. Enoki, K. Takai, J. Appl. Phys. (2010), **V.107**, 014318.
3. A.E. Aleksenskii, E.D. Eydelman, A.Ya. Vul', Nanoscience Nanotechnology Lett. (2011), **V.3**, 68.

Chemical composition and early stages of graphitization of de-aggregated particles of detonation nanodiamond

Aleksenskii A.E. [1] *, Baidakova M.V.* [1] *, Dideikin A.T.* [1] *, Shestakov M.S.* [1] *, Shvidchenko A.V.* [1] *, Shnitov V.V.* [1] *, Kidalov S.V.* [1] *, Vul A.Ya.* [1]

mikhail.shestakov@gmail.com
[1] Ioffe Institute, St.Petersburg, Russia

Recently it was shown that effective deaggregation of detonation nanodiamonds (DND) could be performed after low temperature annealing in air [1] or in atmosphere of molecular hydrogen [2]. The hydrosols are promising substances for medical and biotechnological systems due to small size, non-toxity and ability of de-aggregated DND particles attach and carry various molecules and functional groups [3].

We have applied XPS, NEXAFS and FTIR techniques to perform the comprehensive study of structure and chemical composition of nanodiamonds de-aggregated after hydrogen or oxygen annealing. Moreover, both nanodiamonds were annealed at high vacuum at increasing temperatures. Despite of chemical composition differences both types of DND particles demonstrate traces of sp^2-phase forming at substantially low temperatures (over 420 C). This temperature of vacuum annealing is much lower than that was reported in [4]. This low value could be the possible reason underlying both existing processes of thermal de-arrgregation (at hydrogen and oxygen atmospheres) of DND.

Subsequently, vacuum annealing at different conditions were performed with both nanodiamonds and intial purified DND. The impact of the process to DND surface properties was studied with FTIR and DLS techniques.

We believe the data on chemical composition of de-aggregated nanodiamonds will help opening a new way for application of this unique material.

The study was partly supported by the Russian Scientific Foundation (project 14-12-00795).

References

1. Aleksenskii A., Eydelman E., Vul', A. Deagglomeration of detonation nanodiamonds, Nanosci. Nanotechnol. Lett., 3, 68 (2011).
2. Williams O., Hees A., Dieker C., Jager W., Kirste L. Nebel C. Size-dependent reactivity of diamond nanoparticles, ACS Nano, 4, 4824 (2010).
3. Vul' A.Ya., Dideikin A. T., Aleksenskiy A.E., Baidakova M. V. Detonation Nanodiamonds. Synthesis, Properties and Applications. In: "Nanodiamond" Ed. Oliver A Williams, RSC Press pp. 27 - 48 (2014).
4. Petit, T., Arnault, J. C., Girard, H. A., Sennour, M., & Bergonzo, P. Early stages of surface graphitization on nanodiamond probed by X-ray photoelectron spectroscopy. Physical Review B, 84(23), 233407 (2011).

The sol-gel transition in aqueous colloidal solutions of deagglomerated particles of detonation nanodiamond

Aleksenskii A.E. [1] , *Dideikin A.T.* [1] , *Eidelman E.D.* [1,2] , *Kirilenko D.A.* [1] , *Shvidchenko A.V.* [1] , *Vul A.Ya.* [1] , *Zhukov A.N.* [3]

AlexShvidchenko@mail.ru

[1] Ioffe Physical-Technical Institute, Saint-Petersburg, Russia

[2] Saint-Petersburg State Chemical Pharmaceutical Academy, Saint-Petersburg, Russia

[3] Saint-Petersburg State University, Saint-Petersburg, Russia

In recent time nanodiamonds produced by detonation synthesis from carbon of explosives attract increasing attention as a commercially available carbon nanostructures representing of interest to the various applications, including biomedical applications. However, a problem that the resulting particles of detonation nanodiamond are aggregates consisting of primary monodisperse nanoparticles with a size of 4 nm blocked widespread using of these particles for a long time. Only recently, methods of destruction detonation nanodiamond aggregates allowing to obtain substantially monodispersed hydrosols containing diamond particles with a size of about 4 nm have been developed [1-3].

It was found that increasing of the diamond particles concentration to 5 wt. % results in a reversible sol-gel transition titled thixotropy. Experimental evidence of such transition is given in the work. The mechanism of gel formation based on a model of formation of chains from diamond nanoparticles coupled by electrostatic interaction is suggested and the reasons for inability to obtain hydrogels of aggregates of nanodiamond particles are explained. The theoretical arguments and experimental data in favor of this mechanism are given. Electrical properties of these systems are studied.

The study was partly supported by the Russian Scientific Foundation (project 14-12-00795).

References

1. Kruger, F. Kataoka, M. Ozawa, T. Fujino, Y. Suzuki, A.E. Aleksenskii, A.Ya. Vul', E. Osawa, *Carbon* 43, 1722 (2005)
2. A. Williams, J. Hees, C. Dieker, W. Jager, L. Kirste, C.E. Nebel, *ACS Nano* 4(8), 4824 (2010)
3. E. Aleksenskiy, E.D. Eydelman, A.Ya. Vul', *Nanotech. Lett.* 3(1), 68 (2011)

Electrorheological and rheological properties hydrosols of detonation nanodiamonds.

Stolyarova D.Yu. [1] *, Belousov S.I.* [2,3] *, Chvalun S.N.* [2,3] *, Aleksenskii A.E.* [4] *, Shvidchenko A.V.* [4] *, Vul A.Ya.* [4]

stolyarova.d@gmail.com

[1] Enikolopov Institute of Synthetic Polymeric Materials, Moscow, Russia

[2] Karpov Institute of Physical Chemistry,Moscow, Russia

[3] National Research Center Kurchatov Institute, Moscow, Russia

[4] Ioffe Institute, St.Petersburg, Russia

Recently the attention of researchers is drawn to the physical rheological and electrorheological properties of hydrosols detonation nanodiamonds (DND), which industrial production increases from year to year due to the expansion of areas of their practical application. As a result of the detonation of explosives carbonaceous mixture in closed volume and non-oxidizing atmosphere nanoporous agglomerates with a very narrow size distribution in the range of 3 - 7 nm are formed. Electrosurface properties of DND particles in aqueous solutions, such as specific surface charge and zeta potential, largely determine the aggregate stability, rheological and electrorheological characteristics of DND hydrosols.

DND hydrosols are suspensions that are stable in water. The subjects of the research were DND hydrosols samples derived (recovery method) from the original industrial nanodiamonds with the following parameters: dispersion medium - deionized water; the range of concentrations of the dispersed phase from 0.74 to 4.0 weight %; zeta potential of +42 mV (and -42 mV). As a research method rotational viscometer Physica MSR 501 Anton Paar with an electrorheological unit of high voltage and measuring cell "cylinder - cylinder" CC-27E is used.

Series of experiments were carried out in steady shear mode with a rotor speed variation. When the target rotation speed of the inner cylinder is measured torque on the outer cylinder. Flow curves were plotted and viscosity versus shear rate with a superimposed electric field and without. All liquids had a low yield point and at high shear rates of 20 c-1 they conduct as Newton’s ones. In general, the flow curves were approximated by the equation Herschel-Bulkley.

Due to the electrical double layer and the presence of zeta potential on the DND particles hydrosol must be electrorheological system and it should depend on the applied electric field. In this regard, a series of sample tests was carried out under the influence of an external electric field. The range of the electric field strength was from 0 to 10500 V/mm, 20 ° C - measurement temperature.

In this work the results of a series of experiments of the dependence identification of viscosity DND hydrosols for different concentrations and with a positive or negative zeta potential are discussed. The dependences of changes of rheological behavior from increasing the concentration of the dispersed phase in the system are obtained.

The work was supported by RFBR (grant 15-03-01121 A) and the Russian Scientific Fond (grant 14-12-00795)

Nanodiamonds in retained explosion products

Ten K. [1] , *Titov V.* [1] , *Pruuel E.* [1] , *Kashkarov A.* [1]

ten@hydro.nsc.ru

[1] Lavrentiev Institute of Hydrodynamics, Novosibirsk, Russia

A lot of experiments have been done on the analysis of retained products of detonation of condensed oxygen-deficient explosives. Most of the works are devoted to the problems of synthesis of detonation nanodiamonds [1,2]. In the early 2000s, a new method was developed for research on the synthesis of nanodiamonds using synchrotron radiation from high-energy accelerators [3,4]. This technique enabled recording of the diffraction distributions (small-angle X-ray scattering) near the detonation front with an exposure of 1 ns. Paper [4] reports on the measurement of the dynamics of the size of condensed carbon in detonation of TNT/RDX 50/50, TATB, and BTF charges of 20 mm diameter.

This paper presents an analysis of the retained detonation products of exactly the same explosive charges. The charges were exploded in an ice shell in a sealed explosion chamber made of stainless steel. The charge mass was ~ 20; its diameter and length were 20 mm and 30 mm, respectively. The ice mass was 2000 g; its diameter was 100 mm. The detonation products were subjected to microscopic and diffraction analysis. Nanodiamonds were extracted from the soot via the conventional treatment in acid, as well as by blowing with hot-gas (mixture of oxygen and high purity nitrogen) of a predetermined temperature. At the outlet, the gas was checked with the XRD spectrograph for the presence of products of carbon combustion. After completion of the detection of CO and CO_2, the mixture was analyzed using the microscope and the diffractometer, and then the gas temperature was increased by another 50° C. After the heating to 520° C, only nanodiamonds were left in the mixture. The maximum size of nanodiamonds was ~ 5 nm, ~ 4 nm, <2 nm and ~ 100 nm in the products of detonation of TNT, TH 50/50, TATB (at the limit of resolution) and BTF, correspondingly.

The resulting size distributions of nanodiamonds in the studied high explosives coincide with the distributions obtained in dynamic experiments (by SAXS measurements).

References

1. Titov V.M., Anisichkin V.F. and Mal'kov I.Yu. **Synthesis of ultradispersed diamond in detonation waves.** Combustion, Explosion, and Shock Waves, **25, issue 3, pp. 372-379**
2. Danilenko V.V. **Synthesizing and sintering of diamond by explosion.** // Moscow, Energoatomizdat. 2003. 272 p.
3. M. Titov, E. R. Pruuel, K. A. Ten, L. A. Luk'yanchikov, L. A. Merzhievskii, B. P. Tolochko, V. V. Zhulanov, and L. I. Shekhtman. **Experience of Using Synchrotron Radiation for Studying Detonation Processes**.// Combustion, Explosion, and Shock Waves, Vol. 47, No. 6, pp. 1-13, 2011
4. R. Pruuel, K. A. Ten, B. P. Tolochko, L. A. Merzhievskii, L. A. Lukyanchikov, V. M. Aulchenko, V. V. Zhulanov, L. I. Shekhtman, V. M. Titov. **Implementation of the capability of synchrotron radiation in a study of detonation processes**. // Doklady Physics. January 2013, Volume 58, Issue 1, pp 24-28.

Experimental investigations of N and Si dopped cavitational nanodiamonds

Voropaev S.A. [1] , *Galimov E.M.* [1] , *Dushenko N.V.* [1] , *Ponomareva E.A.* [1] , *Shkinev V.M.* [1]

voropaev@geokhi.ru
[1] GEOKHI RAN, Moscow, Russia

Recently, defective structures in nanodiamonds with captured impurity atoms, such as nitrogen, silicon, boron, etc., have drawn great interest from investigators. One promising method of its synthesis developed at the GEOKHI RAN, is the approach using hydrodynamic cavitation in hydro carbonic liquids [1]. The physical and chemical processes occurring in a cavitation bubble at the last stage of its compression are quite similar to the processes occurring in the explosive chamber. Under fast motion of chemically pure ethanol (C_2H_5OH) with the addition 3% of aniline ($C_6H_5NH_2$) on the profiled channel in the form of the Venturi nozzle, cavitation cavities are formed in liquid, which are then compressed in the working chamber, where a sharp pressure jump is formed. The pressure in the shock wave reaching the values of 80–90 MPa provides for the cavitation bubble collapse, which is close to adiabatic compression. As a result of a number of high speed physical and chemical processes of evaporation, heating, and thermal dissociation of ethanol and aniline vapors, the solid carbon phase is synthesized in the cavity, which is then subjected to special chemical treatment [2].

Aniline was added with the purpose of studying the possibility of doping the nanodiamonds with nitrogen and obtaining photoluminescence centers. The original technique of chemical purification of nanodiamonds was developed making it possible to separate a chemically pure product with the fewest expenses. The particles of nanodiamonds were obtained from the mixture of ethanol and aniline of about 2–5 nm in the size with (NV) and N–V–N centers. The photoluminescence spectra testify that the formation of N–V centers is possible together with the diamond phase during cavitation synthesis as individual photoemitters. Possible approaches to synthesize Si-dopped nanodiamonds are discussed, too.

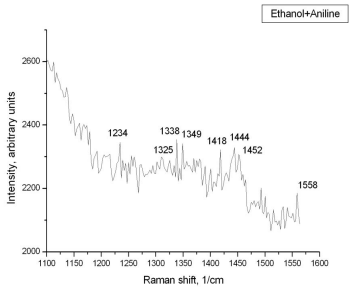

Raman analysis of the produced nanoparticles

References

1. E. M. Galimov. Nature (1973), **243**, 389.
2. S. A.Voropaev, A.Yu. Dnestrivskii, V.N. Skorobogatskii, A.S. Aronin, V.M. Shkinev, O.L. Bondarev, V.V. Strazdovskii, A.A. Eliseev, E.A. Ponomareva, N.V. Dushenko, E.M. Galimov. Doklady Physics (2014), **59**, 503.

Basic-acid properties of particulate detonation nanodiamond

Isakova A.A. [1] *, Skorik N.A.* [2] *, Vostretsova E.N.* [2] *, Indenbom A.V.* [1] *, Abchalimov E.V.* [1]

isakova_aleks@list.ru

[1] A.N. Frumkin Institute of Physical Chemistry and Electrochemistry RAS, Moscow, Russia

[2] Tomsk State University,Tomsk, Russia

Detonation nanodiamond (DND) surface state influence in great extend for its physical-chemical properties. Adsorption of electrolytes and non-electrolytes depends on adsorbent surface charge, and it in turn connected with acid-base properties of the surface. The aim of this work was the study of surface state in the chemical elaboration dependence. Several types of samples: initial DND supplied by Sinta Co, Belarus, and also after high temperature vapor phase treatment partially graphitized $DND_{gr.}$and aminated one, $DND_{am.}$. After the treatment the surface functional termination have been change.Therefore at the DND surface different functional groups, e.g. carboxylic, amine-, amido-, hydroxyl- etc. presented. We investigate acid-basic surface properties. According to proton desorption from the diamond nanoparticles (whan pH go down) the surface centers *pK* by potentiometric titration was estimated. It remarkable, that DND have acid surface and its pK_1 situated in 1 to 4 range. A satisfactory correspondence of determination p*K* results received by two methods was observed. Ionization constants (pK_1) acid groups in the assumption of their basicity equal to one-at the studied types nanodiamonds lay at about 2 [1, 2]. Superficial groups with p*K*=2 can be correspond to carboxyl groups, and with p*K* 5–7 can belong to a second dissociation stage of carboxyl groups or to the lactone groups (i.e. to hydroxyacid esters). The surface characteristic dependence of zeta-potential of aqueous slurries UND-GO-VK, DND_{gr}, DND_{am}, DND_{Cl} from pH has been studied also. At low pH in 0.15 M NaCl water solution positive dzeta potential values was observed. Also remarkable that at different media treatment leading to different surface group content the isoelectric point shift was observed. Practically for UND-GO-VK, DND_{gr}. and DND_{Cl}, dzeta potential value at pH in 2-3 range is equal to 0 мВ and for $DND_{am.}$ isoelectric point at pH 4.5 situated. If to conclude the wide range of different kind of the DND surface acidity with different techniques was studied.

References

1. Spitsyn B.V., Denisov S.A., Skorik N.A., et. al. Relat. Mater. 2010. V. 19. № 2-3. P. 123.
2. Skorik N.A.et al,. Physical Chemistry of Surfaces and Materials Protection. 2011. 47. № 1.PP. 51–55.

Surface functionalization of detonation nanodiamonds as the first step on the way to their applications

Voznyakovskii A.P. [1] , *Kalinin A.V.* [1] , *Sivtsov E.V.* [2] , *Gostev A.I.* [2] , *Chechuha M.R.* [2] , *Pozdnyakov A.O.* [3]

voznap@mail.ru

[1] Lebedev Research Institute for Synthetic Rubber, Saint-Petersburg, Russia

[2] Saint-Petersburg State Institute of Technology, Saint-Petersburg, Russia

[3] A.F. Ioffe Physico-Technical Institute, Saint-Petersburg, Russia

Filling of a polymeric matrix by nanodispersed substances for obtaining of nanocomposites is a modern trend of polymeric materials producing with the wide range of improved properties. From the point of view of the polymer materials science the most promising way of achievement of the purpose is using of nanocarbons. Nowadays the various kinds of nanocarbons are known having a real possibility to be successfully used in practice of the materials science These are fullerenes/fullerene soot, multiwall carbon nanotubes (MWNT), detonation nanodiamonds (DND)/ diamond blend (DB). It should be noted that using of DND and DB gradually grows in comparison with fullerenes and NT which were considered as the most perspective for the polymeric nanocomposites forming until recently. First of all the reason of the change is a low price of DNA which is by order of magnitude less then fullerenes one. However the matter is not only the economic question. It is necessary to consider that native particles of DND are initially characterized by crystal structure unlike graphene-like nanocarbons (fullerenes, NT). It is a great advantage for a number of practical applications. On the other hand a native particle of fulleren is a specific single organic molecule and, actually, is not a nanoparticle, the same way as NT. Only aggregates of native particles can be considered as nanoparticles. It is important that DND can be obtained in the course of ammunition with the finished period of storage utilization technology. Respectively the DND production can improve ecology of some regions. Belarus and the Russian Federation have such the enterprises of ammunition utilization.

The unsolved problems of DND effective application are following:

(1) difficulty of obtaining of DND in the form of high-dispersed particles ensemble connecting with self-organization of this dimensional range particles;

(2) difficulty of homogeneous distribution of small and extra-small quantity of DND in a high-viscous polymer matrix;

(3) the presence of impurities in DND as a result of detonation synthesis. It is especially important when DND are used in medicine and biology.

In this project these problems, in part, are solved by functionalization of the DND surface with fluor-radicals of various structures. This approach allows us to reach the effect of self propagation of modified DND (mDND) aggregates in polar polymers matrix.

The main idea of a synthesis of polymer-DND nanocomposites is to do it directly in the process of a polymerization. It allows one to avoid a process of filling through solution or melt. The most promising techniques of controlled radical polymerization – RAFT polymerization – was used for to achieve high quality of nanocomposites via the effective control of polymerization kinetics and molecular mass characteristics. The RAFT polymerization was successfully applied by us for obtaining of poly(methylmethacrylate)-mDND composites with fundamentally reinforced physico-mechanical properties. The nearest future of our investigation is to involve the wide range of polymers and copolymers of various microstructures for polymer-nanocarbon composites formation, assist with RAFT polymerization.

Determination of detonation nanodiamonds concentration in hydrosols by optical methods

Yakovlev R.Yu. [1] , *Kulakova I.I.* [2] , *Golubev O.V.* [2] , *Leonidov N.B.* [1] , *Lisichkin G.V.* [2]

yarules@yandex.ru
[1] Pavlov Ryazan State Medical University
[2] Lomonosov Moscow State University

The use of detonation nanodiamonds (DND) in biomedical applications determines the usage in the form of hydrosols. This creates the problems of standardization, dispergation and determination of DND concentration by independent and easily available methods. The works dedicated to the determination of DND concentration are practically nonexistence [1]. Therefore, the goal of this work was to develop the methods of DND concentration quantification in the hydrosols by optical methods - spectrophotometry and fluorimetry.

The absorption and luminescence spectra of DND hydrosols in the course of their serial dilution were registered by spectrophotometer Shimadzu UV-1800 (Shimadzu, Japan) and fluorimeter Fluorat-02-Panorama (Lumex, Russia), respectively.

The absorption spectra of DND hydrosols don't have any special absorption bands and are represented by smooth exponentially increasing curves when you move to UV extreme. This is characteristic to weakly adsorbing and strongly scattering samples [1]. Therefore, in order to create the calibration function there were no absorption maxima thus for the calibration curves were taken optical densities at λ = 190-700 nm with the step of 50 nm. It is shown that the DND hydrosols absorption spectra correspond to the main spectrophotometric law. This allows to determine the unknown DND concentration with the help of calibration plot. The limit of DND concentration determination is settled as 4 mkg/ml. The DND's concentrations can be measured from 4 to 1000 mkg/ml.

The luminescence of DND hydrosols was excited by the waves with the lengths of 210-690 nm. It is shown that the maximal intensity of photoluminescence of the samples is achieved at λ = 488 nm, which corresponces to the literature data [2]. It was shown that the luminescence of DNDs is directly proportional to their concentrations from 0,3 to 240 ug/ml. It is established that there happens strong self-quenching of luminescence in DND hydrosols, which limits the application of this method to high-concentration hydrosols.

This work was supported by RFBR (grant 14-03-00423).

References

1. Volkov S., Semenyuk P.I. , Korobov M.V., Proskurnin M.A. Quantification of nanodiamonds in aqueous solutions by spectrophotometry and thermal lens spectrometry // J. Anal. Chem. V. 67 (10). P. 842.
2. Mona J., Tu J.-S., Kang T.-Y., Tsai C.-Y., Perevedentseva E., Cheng C.-L. Surface modification of nanodiamond: Photoluminescence and Raman Studies // Diam. Rel. Mat. 2012. V. 24. P. 134.

Poster session 2:
Graphene and related materials.
Analogs of carbon nanostructures in a non-carbon world.
School Presentations of Young Scientists.

Synthesis of high- purity multilayer graphenes using plasma jet

Amirov R.H. [1] , *Iskhakov M.E.* [2] , *Shavelkina M.B.* [1]

mshavelkina@gmail.com

[1] Joint Institute for High Temperatures of Russian Academy of Sciences, Moscow, Russia

[2] Physical Department, Dagestan State University, Mahachkala, Russia

Depending on the method of obtaining graphen is of three different types: namely; single layer graphene (SLG), bi-layer graphene (BLG) and few-layer graphene (n) ≤10 [1]. Many ways have been introduced or employed to produce graphens, such as micromechanical cleavage of highly-oriented pyrolytic graphite (HOPG) , chemical vapor deposition on the surfaces of crystals of metals (e.g., transition metals), arc discharge using graphite electrodes and substrate-free gas-phase synthesis of graphene platelets in a microwave plasma reactor, epitaxial growth of graphene, radio-frequency plasma-enhanced CVD (RF PE-CVD), microwave plasma-enhanced chemical vapor deposition (MW PECVD), and unzipping of CNTs by using an argon plasma etching method [2]. Nevertheless, the quest to improve the high- purity of graphene produced on a large-scale basis is still in progress.

The synthesis of graphene has been investigated used DC plasma torch with power up to 40 kW with an expanding channel of the output electrode and the vortex stabilization of the arc. As the plasma gas helium or argon at pressures of 150 to 730 Torr were used. Carbon source were the most affordable and provide high performance gases – methane, the mixture of propane-butane in the ratio 30:70% and acetylene. It was first investigated the effect of hydrocarbons on the characteristics of the plasma torch to find the limit of their flow rates. Synthesized samples were characterized by means of thermogravimetry, X-ray diffraction, scanning electron microscope. Depending on the synthesis conditions, the morphology of graphene produced varied from crushed lamps to flakes with a transverse dimension up to 600 nm. On the basis of Raman spectroscopy, it was concluded that the number of layers is changed from one to five in synthesized graphene flakes. By variation of hydrocarbon flow rate and gas pressure it was found that the highest yield (95%) of graphene is formed using helium at 710 Torr. Several smaller the yield of graphenes (65%) was in argon, but with the amorphous carbon and the graphitized particles.To evaluate the specific surface area of materials the classic BET method has been used. Specific surface area of sheeted graphene is 300-400 m^2/g. To determine the pore volume, pore radius, and surface area a relatively new method of adsorption "Limited Evaporation" has been used. Synthesized materials composed of polycrystalline graphene flakes having developed porous structure formed mainly of macro- and mesopores of different diameters. In general the experimental data allowing scaling step by step the synthesis of graphene of desirable morphology have been obtained.

Acknowledgements The authors gratefully acknowledge Russian Foundation for Basic Research for the support by grant No 15-08-00165.

References

1. N. R. Rao, A. K. Sood, K. S. Subrahmanyam and A. Govindaraj, Angew. Chem. Int. Ed. (2009) **48,** 7752.
2. H. Kim, E. J. D. Castro, Y. G. Hwang and C. H. Lee, Jouranal of the Korean Phys. Soc. (2011) **58**, 53.

Hole doping of mechanically exfoliated graphene by confined hydration layers

Antipina L.Yu. [1,2,3] , *Sorokin P.B.* [1,3]

lyuantipina@tisnum.ru

[1] Emanuel Institute of Biochemical Physics RAS, Moscow, 119991, Russian Federation
[2] Moscow Institute of Physics and Technology, Dolgoprudny, 141700, Russian Federation
[3] Technological Institute of Superhard and Novel Carbon Materials, Moscow, 142190, Russian Federation

We studied the electronic properties of mechanically exfoliated graphene confining hydration layers (HLs) that result from the preparation under ambient conditions on a prototype insulating hydrophilic substrate namely CaF_2(111), by MD-DFT-PBE methods. We obtained redistribution of charge originating from the interaction between the hydration layers and graphene. Our theoretical results was compared with experimental topography and KPFM measurements for HLs of different thickness. Our observations demonstrate the role of charge transfer between the HLs and graphene in the modification of its electronic properties. The HLs are found to yield hole doping of graphene. By comparing the experimentally determined surface topography with our MD-DFT calculations, we are able to describe HL's electronic contribution to the graphene. The 2 to 3 HLs adjacent to the graphene turn out to be responsible for the hole doping of graphene by forming a net dipole drawing graphene's electrons slightly towards the HLs. HLs beyond this thickness do only marginally contribute to hole doping. Although this investigation has been performed on a specific substrate, namely CaF_2(111), findings can be generalized, as the (hydrophilic) substrate is not involved in the electronic rearrangement. Making use of this doping mechanism in a controlled way by e.g. creating specific hydrophobic/hydrophilic substrate architectures, could be used to tailor graphene's electronic properties for future applications.

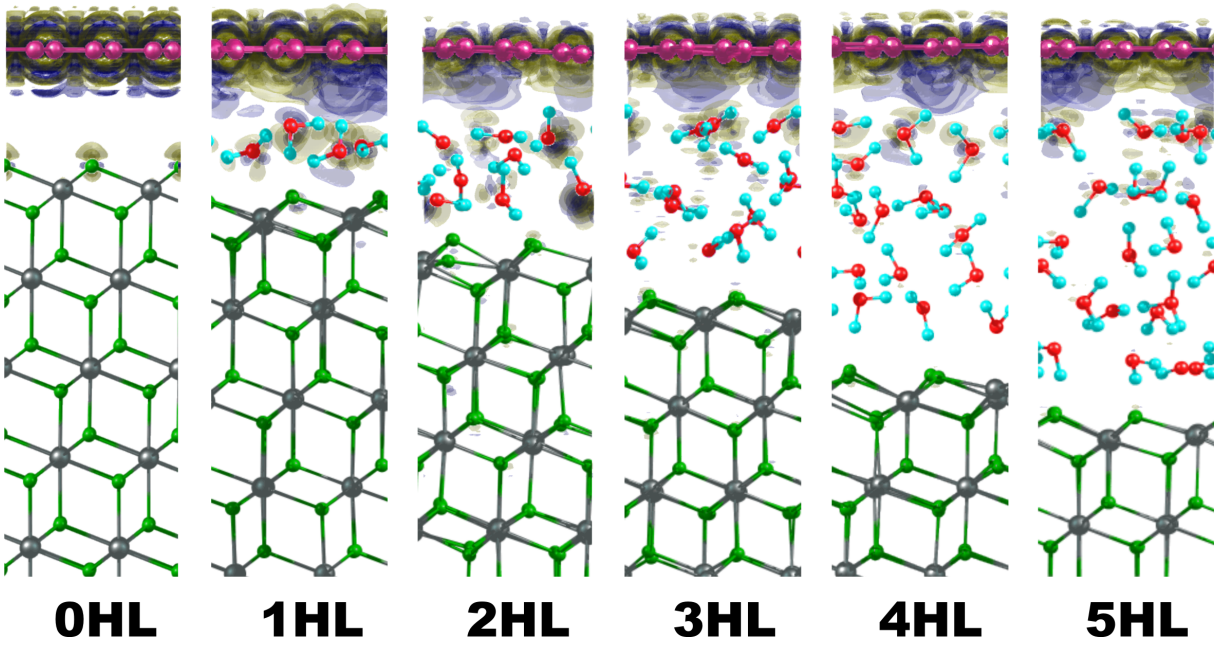

MD snapshots of the atomic positions for n HLs conned by graphene and the CaF_2(111) substrateunderneath (side view) with the electronic in ux and out ux marked by blue and yellow respectively. The calculated electronicredistribution reveals the nett dipole formation of the rst three HLs below the graphene. Carbon (brown), oxygen (red), hydrogen (cyan), calcium (gray) and uorine (green) atoms are marked.

Functionalization of carbon nanoparticles using a Schiff base complex: Application as mediator in electrochemistry

Bezaatpour A. [1] , *Rezapour F.* [1] , *Amiri M.* [1]

a_bezaatpour@yahoo.com
[1] Department of Chemistry, University of Mohaghegh Ardabili, Ardabil, Iran

Recently, carbon nanostructures have been employed in many applications such as sensing. Commercial carbon blacks, Carbon nanoparticles (CNPs), are 1 to 50 nm in diameter with a high surface area accessible for chemical functionalization and ideal for effective interaction with redox active species. CNPs, generally exhibit extremely high surface areas, high conductivity, and a multitude of reactive surface and adsorption sites [1]. CNPs may be considered more economical than other nano-carbons, as they are produced commercially in bulk quantities and also often formed as waste by-products during the formation of other nano-materials such as CNTs [2]. Recently, carbon nanoparticles with sulfonate surface functionality (Emperor 2000™ from Cabot Corp.) have been successfully used as modifier for chemically modified electrode [3]. Various methods for covalent or non-covalent surface attachment to carbon have been developed [4].

Transition-metal complexes have been widely used in catalysis, photonic, medicine and electroanalytical chemistry [5]. The immobilization of these complexes on various inorganic and organic supports has been performed for various purposes [6].

In this research, immobilization of a cobalt Schiff base complex at the surface of carbon nanoparticles (CNPs) has been done. The nanocomposite was characterized by using different techniques such as FTIR, cyclic voltammetry and scanning electron microscopy (SEM). Two redox peaks of cobalt complex were observed in voltammetric determination. The adsorption mechanism of complex at carbon nanoparticles was proposed via π-π interaction and salt linkage. The salt linkage between the positive charge of cobalt complex and the sulfonate group on CNPs surfaces was confirmed. On the basis of our previous works, the Schiff base complexes of cobalt are well-known as effective redox mediators and are capable to catalyze the electrochemical oxidation of various organic and biologically important compounds [7]. On the other hand, CNPs have large surface area and ability to increase the rate of electron transfer [8]. These properties of presented nanocomposite can prepare a novel electron transfer channel for the electrochemical oxidation of some biological and pharmaceutical compounds in future.

References

[1] K. Lawrence, C. L. Baker, . T. D. James, S. D. Bull, R. Lawrence, J. M. Mitchels, M. Opallo, O. A. Arotiba, K. I. Ozoemena, F. Marken, Chemistry – An Asian Journal (2014) **9**, 1226-1241.
[2] J.C. Vinci, I.M. Ferrer, S.J. Seedhouse, A.K. Bourdon, J.M. Reynard, B.A. Foster, F.V. Bright, L.A. Colon, J. Phys. Chem. Lett (2013) **4**, 239-243.
[3] M. Amiri, F. Rezapour, A. Bezaatpour, Journal of Electroanalytical Chemistry (2014) **735** 10–18.
[4] M. Amiri, H. Eynaki, Y. Mansoori, Electrochimica Acta, (2014) **123**, 362– 368
[5] S. Shahrokhian, M. Karimi, Electrochimica Acta (2004) **50**, 77–84.
[6] A. M. Castellani1, J. E. Gonçalves, Y. Gushikem, Journal of New Materials for Electrochemical Systems (2002) **5**, 169-172.
[7] M. Amiri, Z. Pakdel, S. Shahrokhian, A. Bezaatpour, Bioelectrochemistry (2011) **81**, 81–85.
[8] M. Amiri, Sh.Ghaffari, A. Bezaatpour, F. Marken,Sensors and Actuators B (2012) **162**,194– 200.

Adsorption properties of graphene: estimation of adsorption isotherms and heats of adsorption of methane on graphene

Davydov V.Ya. [1]

VYaDavydov@phys.chem.msu.ru
[1] Department of chemistry, M.V. Lomonosov Moscow State University, Moscow, Russia

Porous materials on the base of graphene is of great interest for theirs using in compounds storage. Specific surface area and adsorption capacity of such adsorbents depend on the degree of isolation of graphene sheets. For the characterization of adsorption properties of new adsorbents it is necessary to know adsorption data on graphene. Since at present were are no worked out the methods of preparation of isolated graphene sheets in quantity needed for adsorption investigation so adsorption isotherms of compounds and heats of adsorption on graphene may be estimated by calculation with using adsorption data on graphitized carbon black having uniform surface the same as graphene.

If the isotherms of adsorption on graphitized carbon black can be presented by equation in virial form [1] so the isotherms of adsorption the same compounds at different temperatures and heats of adsorption at different coverage on graphene can be presented by the same virial equation with the correction of virial coefficient responsible for energy interaction with graphene sheets.

For methane adsorption equation on graphitized carbon black only first too virial coefficients and their temperature dependence are known [2]. Using these coefficients and experimental data on adsorption [1] it is possible to estimate next virial coefficients [3] and also virial coefficients responsible for entropy and heat of adsorption. Equation with these virial coefficients fit the experimental data on adsorption of methane on graphitized carbon black well.

Adsorption isotherms of methane at 113, 123, 133, 143 K and the heats of adsorption at different coverage on graphene were calculated by using these equations with the correction of virial coefficient responsible for smaller interaction with graphene sheets. It was assumed that the heat of adsorption of methane at small coverage on graphene is about 90 % of heat of adsorption on graphitized carbon black.

Comparison of estimated adsorption data on graphene with experimental adsorption data on adsorbents on the base of graphene make it is possible to evaluate the degree of isolation of graphene sheets in such adsorbents and to propose their structure.

References

1. N.N. Avgul, A.V. Kiselev, Physical Adsorption of Gases and Vapors on Graphitized Carbon Blacks. Chemistry and Physics of Carbon. Ed. P.L.Walker, Marcel Dekker, New York, 1970, vol. 6, pp. 1-124.
2. N.N. Avgul, A.G. Bezus, E.S. Dobrova , A.V. Kiselev, J. Colloid Interface Sci. (1973) **42**, 486.
3. A.G. Bezus, A.V. Kiselev, Z. Sedlacek, Pham Quang Du, Trans. Faraday Soc. (1971) **67**, 468.

Spin-polarized electronic states at the graphene/Co(0001) interface

Erofeevskaya A.V. [1] , *Usachov D.Yu.* [1]

anna.erofeevskaya@gmail.com

[1] Saint Petersburg State University, St. Petersburg, Russia

In recent years graphene is the subject of numerous researches due to its outstanding electronic properties. In particular dispersion of electrons is conic near the Fermi level, which leads to zero effective mass and extremely high mobility of charge carriers in graphene. Moreover graphene has large spin diffusion length [1], thereby it could be used in spintronics devices [2]. Application of graphene in electronic devices inevitably causes graphene-metal contact and it can strongly influence the electronic properties of graphene [3]. Therefore study of the properties of graphene synthesized on different metal surfaces is an important issue. Graphene/cobalt contact attracts significant attention since cobalt is a ferromagnetic metal and could be used in spintronics devices as a source of spin-polarized currents.

In this work graphene was synthesized on monocrystalline surface of cobalt Co(0001). The structure of this system was investigated using low energy electron diffraction and scanning tunnel microscopy. It was obtained that graphene was strictly oriented on the cobalt surface and also nonequivalence of sublattices in graphene was observed.

Electronic structure of this system was investigated with angle-resolved photoelectron spectroscopy, and as a result dependence of crystalline and electronic structure from synthesis conditions was determined. It was found that there is a spin-polarized Dirac-conelike state near the Fermi level in the electronic structure in the case of strictly oriented graphene [4]. This cone is formed by electronic states with one spin direction, which are localized at the graphene-cobalt interface. It opens up perspectives for using this system for generation and control of spin current, particularly in a spin filter. Moreover the theoretical calculations of the electronic structure were performed and a simple tight-binding model of the spin-polarized interface state was developed. Agreement between experimental and theoretical data confirmed the validity of the proposed model.

The work was supported by the RFBR (Grant 14-02-31150) and Saint Petersburg State University (Grant 11.37.634.2013).

References

1. Wei Han, Pi, W. Bao, K. M. McCreary, Yan Li, W. H. Wang, C. N. Lauand R. K. Kawakami. Appl. Phys. Lett. (2009), **94**, 222109.
2. Cho, Y.; Choi, Y. C.; Kim, K. S.. J. Phys. Chem. C (2011), **115**,
3. A. Rybkina, A.G. Rybkin, V.K. Adamchuk, D. Marchenko, A. Varykhalov, J. Sánchez-Barriga and A.M. Shikin. Nanotechnology (2013), **24,** 295201.
4. Usachov, A. Fedorov, M.M. Otrokov, A. Chikina, O. Vilkov, A. Petukhov, A.G. Rybkin, Yu.M. Koroteev, E.V. Chulkov, V.K. Adamchuk, A. Grüneis, C. Laubschat, and D.V. Vyalikh. Nano Lett. (2015), DOI: 10.1021/nl504693u.

Graphene adsorption on hydrogen passivated MnO polar surface

Ershov I.V. [1] , *Ilyasov V.V.* [1] , *Popova I.G.* [1]

iershov86@gmail.com
[1] Don state technical university, Rostov-on-Don, Russia

Graphene has recently attracted considerable scientific interest due to its unique electronic properties, which makes it a promising candidate for carbon-based electronics. In order to technically exploit these unique features, on the one hand, charge carriers — electrons or holes— are required and, on the other hand, methods to introduce finite band gaps in graphene or, more generally, to manipulate its band structure are required.

In the present work we have performed ab initio simulation of graphene adsorption on hydrogen passivated oxygen terminated MnO polar (111) surface using DFT-D2 approach with Hubbard U correction. It is shown that the band structure of graphene significantly changes due to interaction with hydrogen. The modification of magnetic properties of the interface are also discussed.

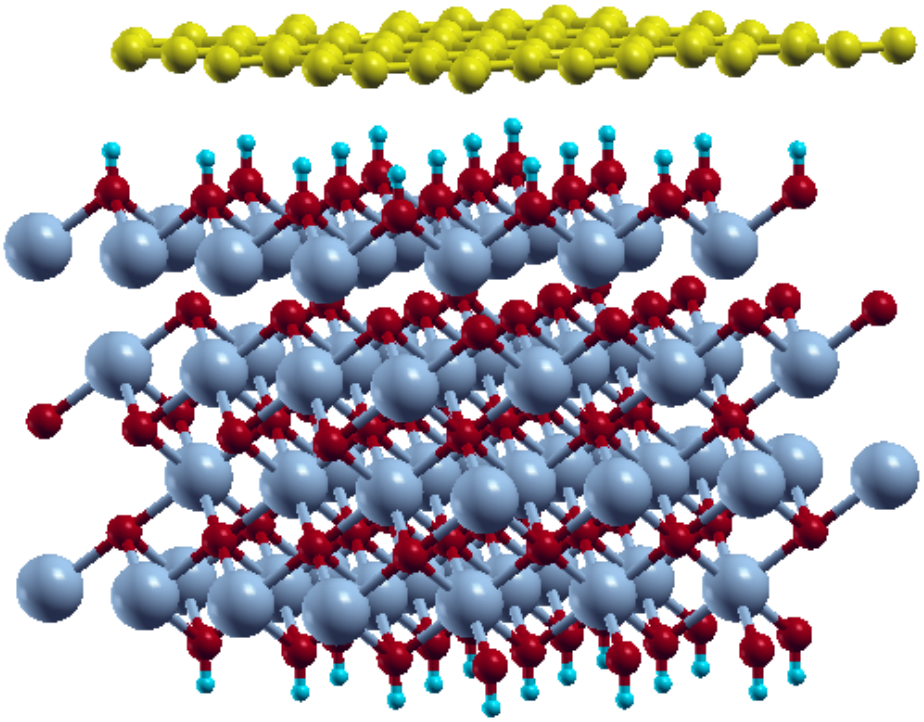

Atomic structure of the graphene - MnO interface

Oxygen-free defective graphene as a support for ultradisperse Pt nanoparticles

Fedorov V.E. [1] , *Grayfer E.D.* [1] , *Kibis L.S.* [2] , *Boronin A.I.* [2] , *Stonkus O.A.* [2] , *Das M.R.* [3]

fed@niic.nsc.ru

[1] Nikolaev Institute of Inorganic Chemistry, Siberian Branch of the Russian Academy of Sciences, 3, Acad. Lavrentiev Prosp., Novosibirsk 630090, Russia

[2] Boreskov Institute of Catalysis, Siberian Branch of the Russian Academy of Sciences, 5, Acad. Lavrentiev Prosp., Novosibirsk 630090, Russia

[3] CSIR-North East Institute of Science and Technology, Jorhat 785006, Assam, India

It is well known that graphenes, when they are functionalized with oxygen groups, may serve as effective supports for dispersed metal nanoparticles (NPs). In this work we show that in addition to this well-reported scenario, other possibilities exist to stabilize NPs on graphene surface. Our experiments have shown that highly disperse Pt NPs (about 2.4 nm on average) may be deposited on defective, but oxygen-free graphene surface.

Few-layer graphene (FLG) used here as a support was prepared by thermal decomposition of a fluorinated graphite intercalation compound ($C_2F{\cdot}0.13ClF_3$) as we described before [1]. Since it is derived from oxygen-free precursor, the target FLG contains only traces of oxygen. On the other hand, the decomposition of intercalation compound in the regime of thermal shock leads to the creation of various defects in the forming FLG. Highly defective nature of FLG is manifested in the high intensity of defect-induced D peak in Raman spectrum and in the high ratio of D and G peaks ($I_D/I_G \sim 1.8$).

Pt nanoparticles were deposited on oxygen-free FLG through the reduction of K_2PtCl_4 with ethylene glycol. TEM and HRTEM images show well-dispersed spherical crystalline Pt nanoparticles relatively uniformly distributed on graphene sheets with somewhat higher content around wrinkled and folded areas (see Figure). The ratio I_D/I_G in the Raman spectrum drops from $I_D/I_G \sim 1.7–1.8$ to $I_D/I_G \sim 1.3–1.4$ for the Pt-containing sample, suggesting the filling of the vacancy-type defects with small metallic formations [2]. The electronic structure of the sample was studied by photoelectron spectroscopy using synchrotron radiation.

Acknowledgements. The work was supported by Russian Scientific Foundation, Project 14-13-00674

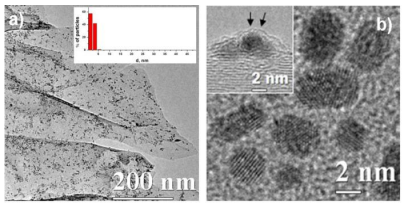

Fig.1. TEM (a) and HRTEM (b) images of the dispersed Pt/FLG and platinum particle size distribution.

References

1. G. Makotchenko, E.D. Grayfer, A.S. Nazarov, S.-J. Kim, V.E. Fedorov. Carbon (2011) **49**, 3233.
2. Y. Koo, H.-J. Lee, Y.-Y. Noh, E.-S. Lee, Y.-H. Kim, W.S. Choi. J Mater Chem. (2012) **22**, 7130.

Reactivity in combustion process for expanded graphites: the influence of the dimensional effect

Logvinenko V.A. [1] , *Makotchenko V.G.* [1] , *Fedorov V.E.* [1]

fed@niic.nsc.ru

[1] Nikolaev Institute of Inorganic Chemistry, Siberian Branch of the Russian Academy of Sciences, 3, Acad. Lavrentiev Prosp., Novosibirsk 630090, Russia

Thermal stability of several expanded graphite phases was studied, and kinetic parameters of the oxidation reaction were calculated. Multilayer graphene (I) was obtained by the thermal decomposition of $C_2F{\cdot}xClF_3$. Several expanded graphite phases were synthesized by thermal decomposition of the hydrolyzed graphite oxide, graphite nitrate and graphite bisulphate; the average numbers of graphene layers were 15 nm (II), 40 nm (III) and 80 nm (IV), respectively. Used natural graphite (V) consists of crystalline particles (200–300 μm).The oxidation of the graphite phases was studied in the standard experimental conditions: argon + oxygen flow, heating rates were from 3 up to 40 K/min. The thermogravimetric data were processed with the computer program Netzsch Thermokinetics [1–2]. Well–known recommendations for performing kinetic computations on thermal analysis data [3] were used.

The thermal stability of the phases under oxidation increases in the series: I < II < III < IV < V (Fig. 1). Oxidation of natural graphite (V) is described by Avrami–Erofeev topochemical equation with the evident diffusion contribution; E = 201 ± 2 kJ/mol, lg A = 7.1 ± 0.1. Multilayer graphene (I) oxidizes with the constant decomposition rate; the reaction zone formes on the grain surface and moves perpendicularly to the graphene layers; E1 = 120 ± 1 kJ mol^{-1}, lg A1 = 4.3 ± 0.1. Different size of sample grains and their different structures result in different thermal stability both in the reaction zone location (i.e. in the topochemical equation forms), and in the values of the kinetic parameters.

Acknowledgements. The work was supported by Russian Scientific Foundation, Project 14-13-00674.

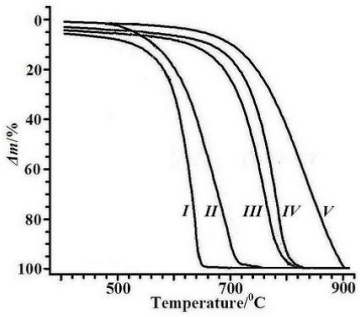

TG curves of the combustion processes for the multilayer graphene (I), the expanded graphite phases (II, III, IV) and the natural graphite (V). Heating rate was 10 K min^{-1}

References

[1] Netzsch Thermokinetics. http://www.netzsch-thermal-analysis.com/us/thermokinetics-workshop
[2] E. Moukhina, J. Therm. Anal. Calorim. (2012) **109**, 1203.
[3] S. Vyazovkin, K. Chrissafis, M.–R. Di Lorenzo, N. Koga, M. Pijolat, B. Roduit, N. Sbirrazzuoli, J.–J. Suñol, Thermochim. Acta. (2014) **590**, 1.

Semiconductor-half-metal transition and magnetism in bilayer zigzag graphene nanoribbons on hexagonal boron nitride

Ilyasov V.V. [1] , *Nguyen V.C.* [1] , *Ershov I.V.* [1]

viily@mail.ru
[1] Don State Technical University, Rostov on Don, Russia

Bilayer zigzag graphene nanoribbons (BZGNRs), alongside with single-layer nanoribbons, represent an essential 1D carbon nanostructure for creation of electronic devices, sensors, solar cells and energy accumulation with their diverse and remarkable physical and chemical properties due to specific edge states and size effects.

The report presents the results of *ab initio* study of electronic structure modulation and edge magnetism in the antiferromagnetic (AF) bilayer zigzag graphene nanoribbons (BZGNR)/hexagonal boron nitride (h-BN(0001)) semiconductor heterostructure induced with transverse external electric field (E_{ext}) and nanomechanical compression (extension), performed within the framework of the density functional theory using Grimme's DFT(PBE)-D2 scheme. For the first time we established critical values of E_{ext} and interlayer distance in bilayer for the AF-BZGNR/h-BN(0001) heterostructure providing for semiconductor-halfmetal-metal phase transition in one of electron spin configurations [1]. We discovered the effect of preserved local magnetic moment (0.3μ*B*) of edge carbon atoms of the lower (buffer) graphene nanoribbon during nanomechanical uniaxial compression (or extension) of the AF-ZGNR/h-BN(0001) semiconductor heterostructure. It has been demonstrated that magnetic properties of the AF-ZGNR/h-BN(0001) semiconductor heterostructure can be controlled using E_{ext} [1]. In particular, the local magnetic moment of edge carbon atoms decreases by 10% at critical value of the positive potential. We have established that local magnetic moments and band gaps can be altered in a wide range using nanomechanical uniaxial compression and E_{ext}, thus making the AF-ZGNR/h-BN(0001) semiconductor heterostructure potentially promising for nanosensors, spin filters, and spintronics applications.

References

1. V.V. Ilyasov, B.C. Meshi, V.C. Ngyen et al. Solid State Com. Vol. 199 (2014) 1-10.

Transport and sensing properties of fluorinated graphene

Katkov M.V. [1,2] , *Sysoev V.I.* [1] , *Guselnikov A.V.* [1] , *Kolesnik-Gray M.* [3] , *Krstic V.* [3,4] , *Bulusheva L.G.* [1,2] , *Okotrub A.V.* [1,2]

katkovmi@gmail.com

[1] Nikolaev Institute of Inorganic Chemistry, Novosibirsk, Russia

[2] Novosibirsk State University, Novosibirsk, Russia

[3] Friedrich-Alexander University, Erlangen-Nuremberg, Germany

[4] Trinity College Dublin, Dublin, Ireland

Graphene is a two-dimensional material considered as a single layer of graphite. Its unique electronic properties, supported by numerous physical measurements, have been of great interest in terms of both fundamental and practical aspects.[1] However, the absence of an energy gap in the pristine graphene band structure and the chemical inertness of its surface can become a significant limitation in its use in electronics. Functionalization is an effective mechanism of changing graphene's electrical properties causing creation of a tunable gap, a barrier at the functionalization site, etc.[2] Moreover, reactive centers on its surface such as defects and functional groups significantly increase the sensing properties of graphene.

In this study, we use fluorination as a way of graphene functionalization. Natural graphite and highly ordered pyrolytic graphite (HOPG) were fluorinated by exposing them to a fluorinating agent, BrF_3. Fluorinated graphene (FG) flakes were separated by mechanical treatment, ultrasonicated in toluene, and sprayed on a SiO_2/Si substrate. A certain fluorine content was achieved by varying the fluorination time and BrF_3 concentration in Br_2. Using Van der Pauw method, we measure FG sample resistivity as a function of fluorine percentage, which shows a minimum at the point of conjugated area discontinuity.

Another way of changing the surface fluorine content is graphite fluoride C_2F reduction.[3] The reduction degree of FG was controlled by measuring the surface resistivity. Chemical interaction of FG surface with molecules in a gas phase produces a change of the electron state. The value of the electrical response revealed upon analyte gas exposure allows us to determine the gas concentration.[4] We showed experimentally that the sensing properties depend on the fluoridation degree and found the correlation of the adsorption energy with the number of fluorine atoms by the use of quantum-chemical calculations.

References

1. A. H. Castro Neto, F. Guinea, N. M. R. Peres, K. S. Novoselov, and A. K. Geim, Rev. Mod. Phys. 81, 109 (2009)

2. F. Withers, M. Dubois, and A. K. Savchenko, Phys. Rev. B 82, 073403 (2010)

3. A.V. Okotrub, I.P. Asanov, N. F. Yudanov, K.S. Babin, A.V. Guselnikov, T.I. Nedoseikina, P.N. Gevko, L.G. Bulusheva, Z. Osvath, and L.P. Biro, Phys. Status Solidi B 246, 2545 (2009)

4. M. V. Katkov, V.I. Sysoev, A.V. Guselnikov, I.P. Asanov, L.G. Bulusheva, and A.V. Okotrub, Phys. Chem. Chem. Phys. 17, 444 (2015)

XPS study of the microwave exfoliated graphite oxide fluorinated with XeF_2

Khavrel P.A. [1] , *Chilingarov N.S.* [1] , *Shulga Yu.M.* [2,3] , *Medvedev A.A.* [1] , *Deyko G.S.* [1] , *Skokan E.V.* [1]

khavrel@thermo.chem.msu.ru

[1] Chemistry Department, Moscow State University, Moscow, Russia

[2] Institute of Problems of Chemical Physics of Russian Academy of Sciences, Chernogolovka, Moscow District, Russia

[3] National University of Science and Technology MISIS, Moscow, Russia

Graphene oxide (GO) and reduced graphene oxide (rGO) have attracted attention due to their unique properties. Chemical functionalization of the GO/rGO platelets provides an effective tool for tuning electrical conductivity, mechanical and optical and other properties. Both of these materials contain appreciable amount of chemically bonded oxygen on basal graphene planes making them hydrophilic. It was discovered recently that fluorination of GO drastically affects its wetting behavior so that amphiphobic material can be obtained. A several methods were elaborated for graphene and GO fluorination.

One of the most widely used tools for elemental composition quantifying and for revealing the character of chemical bonding between constituting atoms is X-ray photoelectron spectroscopy (XPS). It proves to be indispensable for studies of practically unsoluble species.

In present work we suggest novel conditions leading to covalent attaching of fluorine to reduced graphene oxide, namely microwave exfoliated graphene oxide (MEGO). Fluorination of MEGO with xenon difluoride results in rise of the O/C atomic ratio in all the samples of MEGO from 0.087 - 0.115 to 0.128 – 0.261. This observation suggests that fluorination of the MEGO with XeF_2 brings about additional MEGO oxidation to volatile fluorocarbons. The increase in the relative oxygen content indicates that the oxygenated domains of the MEGO are more stable than the fluorinated ones with respect to oxidation. The highest fluorine content (F/C at. ratio 0.467) was achieved for the sample 2h treated with XeF_2 at 70 °C while at longer reaction times the fluorine/carbon ratio decreases. This fact is in agreement with our assumption regarding higher reactivity of the C(-F) carbons towards further fluorination. Furthermore, this implies that fluorination of the double C=C bonds is the limiting stage in the MEGO fluorination.

It was revealed that treatment with water does not affect the oxygen content in fluorinated MEGO, i.e. the C-F bonds do not hydrolyze.

Replacement of the MEGO with graphite results in the increase of the fluorine content in the product. Interestingly, the two substrates are similar in having their oxygen content rising in the course of the fluorination. This corroborates the assumption that the fluorination initially occurs at the C=C double bonds while leaving the oxygenated fragments intact.

XPS data supply evidence of presence of the absorbed XeF_2 in fluorinated graphite despite evacuation of the sample after the fluorination. This is different from the fluorinated MEGO where high defectiveness and larger interlayer spacing facilitates removal of the xenon compounds. In contrast to the fluorinated MEGO, no signatures of the CF_2 and CF_3 groups were found in fluorinated graphite. This difference may be due to the higher defectiveness and smaller size of the carbon crystallites in the MEGO compared to the graphite, which results in an increased number of the edge carbons capable of formation of the CF_2 and CF_3 groups.

Authors are grateful to K.I. Maslakov for acquiring XPS data (SRCCU of Chemistry department of M.V. Lomonosov Moscow State University) and to Panin R.A., Lobach A.S., Baskakov S.A., Shulga N.Y., Ryzhkov A.V. for support in the course of syntheses. The work was supported by grants RFFI 15-03-04987 and 13-03-00311.

Interaction of femtosecond laser radiation with carbon materials: exfoliation of graphene structures and synthesis of low-dimensional carbon structures

Abramov D.V. [1] *, Arakelian S.V.* [1] *, Kochuev D.A.* [1] *, Makov S.A.* [1] *, Prokoshev V.G.* [1] *, Khorkov K.S.* [1]

awraam@mail.ru
[1] Vladimir State University, Vladimir, Russia

Carbon is presented in modern nanomaterials the large variety of modifications. Various methods and technologies are developed to create them. Laser methods take up significant area in this diversity. Action of laser pulses onto graphite may result to the exfoliation of graphene layers. This approach can compete with micromechanical technology of the bundle of graphite [1], which is currently used by the majority of the experimental groups. This report presents the results of the implementation of the method of laser-induced cleavage of graphite in liquid nitrogen with using a femtosecond lasers.

Graphite targets were treated by radiation of femtosecond lasers with Yb:CaF2 and Ti:Sapphire active medium in liquid nitrogen. Samples of the the glassy carbon and highly oriented pyrolytic graphite (HOPG) were used as a source for obtaining the graphene. In the first case, the graphene was obtained in the form of crumpled sheets with characteristic sizes of the structures from 1 to 2 μm and sheet thickness about 20 nm (thickness of structure fold is about 40 nm). In the second case, the sheets with relatively large area of the flat surface are cleaved. Characteristic sizes of the sheets are order 10 μm and sheet thickness is about 14 nm (Fig. 1). Geometric characteristics of the obtained graphene structures are comparable with the parameters of the objects which are most often described in the scientific publications (see review [2]).

The process of obtaining the graphene at laser processing of graphite is accompanied by formation of various types of low-dimensional carbon structures. For example, the arrays of nanorods with a diameter from 30 to 100 nm on the surface of carbon materials were formed.

This study was performed as part of the state task VlSU № 2014/13 to perform state works in the field of scientific activity and also supported under grant of the President of the Russian Federation for state support of the leading scientific schools of the RF № NSh-89.2014.2 and grant of the Russian Foundation for Basic Research № 14-02-97508.

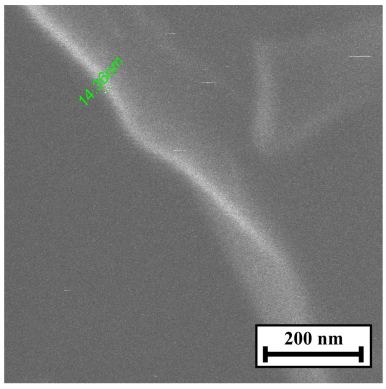

Fig.1. Graphene structures, which were obtained after laser irradiation of a HOPG.

References

1. K.S. Novoselov, D. Jiang, F. Schedin, T.J. Booth, V.V. Khotkevich, S.V. Morozov and A.K. Geim, PNAS (2005) 102, 10451.
2. A.V. Eletskii, I.M. Iskandarova, A.A. Knizhnik and D.N. Krasikov, Phys. Usp. (2011) 54, 227.

Mechanisms and Kinetics of Nanocarbons Growth on Copper Substrates

Koltsova T.S. [1] , *Larionova T.V.* [1] , *Vasilyeva E.S.* [2,1] , *Nasinulin A.G.* [2,1] , *Tolochko O.V.* [1]

annelet@yandex.ru

[1] State Polytechnical University, Saint Petersburg, Russia

[2] Skolkovo Institute of Science and Technology, Moskow, Russia

Carbon nanotubes (CNTs), nanofibers (CNFs) and graphene are promising components for next-generation high-performance structural and functional composite materials. Utilizing copper surfaces with different roughness and varying temperature, pressure and carbon containing gases such as CH_4, CO, C_2H_2 to C_2H_4; we are able to alter the carbon product from nanofibers via few-layered graphene to graphene monolayers. The Chemical Vapor Deposition (CVD) method synthesis is carried out on on the surface of copper foil and micron- and nanosized copper particles.

At the first step, we elaborated an approach to synthesize CNFs directly on the surface of metal micron-sized particles without any additional catalysts. We studied the main regularities of the CNFs synthesis on the copper surface in the temperature range from 700 to 940 °C by using different gas atmospheres. A few-layered graphene was synthesized on the surface of micron-sized copper powder by CVD technique using ethylene as a carbon source. As a result, we synthesized graphene with 8-12 layers on the copper surface.

The study of the nanocarbons growth on the copper foils shows that number of graphene layers are strongly depend on surface roughness, total gas pressure and the gas species. Graphene monolayers were synthesized in methane/hydrogen atmosphere at the total pressure of 2-3 mbar; the increasing of pressure leads to the growth of layers numbers. The increase of surface roughness leads to CNFs “forest” appearance.

Synthesized nanocarbons were studied by high-resolution transmission electron microscopy and Raman spectroscopy, electrical properties of graphene layers and light transmission in the infrared and visible region were also measured. It was shown that the structure of CNFs are strongly depends on temperature and C:H ratio in the gas phase; at the higher carbon concentration there are thicker fibers with the structure of “pile of coins” type, whereas with the decrease of carbon concentration the thickness decreased and fiber showed exact “bamboo”-like structure.

In addition, it was found that independently of experimental conditions the growth of CNFs and graphene layers is controlled by carbon diffusion of the copper surface. The model of formation of the internal angle of the fiber, depending on the ratio of the surface tension of copper and adhesion of the carbon layer had been suggested.

The electron transfer on edges of carbon nanowalls

Komarova N.S. [1] , *Krivenko A.G.* [1] , *Mironovich K.V.* [2] , *Krivchenko V.A.* [2]

komarova@icp.ac.ru

[1] Institute Institute of Problems of Chemical Physics RAS, Chernogolovka, Russia

[2] Department of Microelectronics, D.V. Skobeltsyn Institute of Nuclear Physics, M.V. Lomonosov Moscow State University, Moscow, Russia

The number of publications devoted to the electrochemistry of graphene-like and graphene-containing electrodes has increased dramatically in recent years [1, 2]. Meanwhile, conflicting opinions about the reactivity of the edges of graphene sheets, the defect and defectless regions of the basal planes exist in literature. Some authors' data indicate the considerable increasing of the electron transfer rate for the edge or defective regions as compared to that for the graphene plane [3]. However, some authors take the opposite view [4]. Thus, the presented work is aimed to clarify the features of the electrochemical activity of nanostructured units of carbon materials. We have selected the highly oriented carbon nanowalls (CNWs) obtained by means of non-catalytic plasma-chemical synthesis as an object of investigation. The comparative study of the electrochemical behavior of the pristine and modified electrodes based on CNWs was carried out. The electrochemical modification of CNWs was performed by the application of the anodic potentials corresponding to the oxidation of water. It should be noted that upon modification, the electrochemical capacity of the samples increased by the factor of 30 – 50. In our opinion, the increase of capacity of double layer is affected by the presence of the oxygen-containing functional groups formed during anodic polarization of the electrode. Meanwhile, the Raman- and X-ray spectroscopy data demonstrate that substantial part of these groups (carboxylic mainly) forms on the CNW edges. The rate constants of the electron transfer of $Fe^{+2/+3}$, $[Fe(CN)_6]^{3-/4-}$, $Ru(NH_3)_6]^{3+/2+}$ redox systems for the pristine and modified carbon nanowalls were estimated in order to reveal the effect of these groups on kinetics of the electrode reactions. These data have allowed us to roughly estimate the contribution of the edges and basal planes to the registered current. From the comparative analysis of the cyclic voltammograms of the redox reactions investigated on the pristine and modified CNWs and taking into account the correlation between the growth of the capacity and the redox peak currents it was concluded that the electron transfer reactions proceed mainly on the CNW edges.

This work is supported by the Russian Foundation for Basic Research (project №13-03-00548).

References

1. A. Ambrosi, C.K. Chua, A. Bonanni, M. Pumera, Materials Chem. Rev. (2014), **V. 114**. P. 7150.
2. A.C. Brownson, D.K. Kampouris, C.E. Banks, Chem. Soc. Rev. (2012) **V. 41.** P. 6944.
3. G. Gueell, N. Ebejer, M.E. Snowden, J.V. Macpherson, P.R. Unwin, J. Am. Chem. Soc. (2012) **V. 134**. P. 7258.
4. A.N. Patel, M.G. Collignon, M.A. O'Connell, W.O.Y. Hung, K. McKelvey, J.V. Macpherson, P.R. Unwin, J. Am. Chem. Soc. (2012) **V. 134**. P. 20117.

Room-temperature positive magnetoresistance in graphene grown by CVD on Fe films

Matveev V.N. [1] *, Levashov V.I.* [1] *, Kononenko O.V.* [1] *, Khodos I.I.* [1] *, Volkov V.T.* [1]

oleg@iptm.ru
[1] Institute of Microelectronics Technology and High Purity Materials, Chernogolovka, Russia

Recently magnetoresistance (MR) in graphene has attracted a lot of attention both theoretically and experimentally [1, 2]. Under a perpendicular magnetic field the electron trajectories in a two-dimensional (2D) electron gas system (such as graphene) will be a set of circles. These electron orbits can be expressed by cyclotron frequency $\omega_c = eB/m_c$, where m_c is the effective mass of the electrons. For the semi-classical theory, the curving of electron trajectories usually results in a positive MR (defined as MR = $[R(B)-R(0)]/R(0)$) with a quadratic magnetic-field (B) dependence to protect the rotational symmetry. In this work we investigated the magnetoresistance of graphene grown by CVD.

Fe films were deposited on oxidized silicon substrates by laser ablation through a mask to obtain 0.5 mm wide stripes. Graphene was grown by the CVD method with a short-time acetylene inflow [3]. After Fe deposition, substrates were placed in a quartz tube reactor, which was pumped down to a pressure about 10^{-6} torr and then inserted into a furnace preheated to 900°C. When the samples were heated to the reaction temperature, acetylene was admitted into the quartz tube up to a pressure of 0.5 torr for 5 s and then pumped out and the quartz tube reactor was extracted from the furnace. After graphene growth, Platinum electrodes were deposited on the ends of graphene/Fe stripes. A distance between Pt electrodes was approximately 5 mm. After that samples were etched with $Fe(NO_3)_3 \cdot 9\ H_2O$ aqueous solution to dissolve the Fe stripes. Etching was carried out up to 6 days, and then samples were washed and dried.

The structure of the graphene was studied with high resolution transmission electron microscope at the accelerating voltage 200kV. Micro Raman spectra of graphene were obtained with a SENTERRA BRUKER Raman microscope using 488 nm (2.54 eV) excitation wavelength. The spectral resolution was ≃3 cm^{-1}. The Si peak at 520 cm^{-1} was used as a reference for wavenumber calibration.

Magnetoresistance (MR) in graphene was experimentally investigated by varying magnetic-field strength from 0 to 0.45 T. Magnetoresistance was defined as $([R(B)-R(0)]/R(0))\times100\%$. A maximum value of observed magnetoresistance was about 60%. Measured magnetoresistance was positive with a quadratic magnetic-field (B) dependence.

References

1. G. Yu. Vasil'eva, P. S. Alekseev, Yu. L. Ivanov, Yu. B. Vasil'ev, D. Smirnov, H. Schmidt, R. J. Haug, F. Gouider, G. Nachtwei, JETP Letters (2012) **96**, 471.
2. Z-M. Liao, Y-B. Zhou, H-C. Wu, B-H. Han, D-P. Yu, EPL (2011) **94**, 57004.
3. O.V. Kononenko, V.N. Matveev, D.P. Field, D.V. Matveev, S.I. Bozhko, D.V. Roshchupkin, E.E. Vdovin, A.N. Baranov, Nanosystems: Physics, Chemistry, Mathematics (2014) **5**, 117.

Graphene field-effect transistors on the chemically modified few-layer-graphene substrate

Kotin I.A. [1] , *Antonova I.V.* [1] , *Prinz V.Ya.* [1]

kotin@isp.nsc.ru

[1] Rzhanov Institute of Semiconductor Physics Siberian Branch of Russian Academy of Science, Novosibirsk, Russia

Graphene is well known to have highest carrier mobility (theoretical limit is 200 000 $cm^2V^{-1}s^{-1}$ at room temperature [1]). However, it requires special substrates to provide such high carrier mobility. These substrates have to be prepared from highly resistive material or insulator which does not interact with graphene. Really, substrates strongly influence on graphene properties leading to degradation of carrier mobility. For example, carrier mobility in graphene on SiO_2 which is a commonly used substrate for graphene is about 10 000 $cm^2V^{-1}s^{-1}$ [2]. Suspended graphene demonstrates the highest carrier mobility about 230 000 $cm^2V^{-1}s^{-1}$ at low temperature [3]. However, this technique is unsuitable for device fabrication on wafer scale. Nowadays hexagonal BN (h-BN) is considered more favorable substrate for graphene. Mobility in graphene on h-BN is about 60 000 $cm^2V^{-1}s^{-1}$ at room temperature [4] but h-BN crystals and exfoliated layers has small size (few tens of micrometers). Therefore, alternative substrates search has not still finished. It is necessary to realize high carrier mobility in graphene and ability of wafer scale device production.

Previously, a new approach to create a special high resistive hybrid substrate based on few-layer-graphene (FLG) which provide high carrier mobility in graphene (16 000 – 42 000 $cm^2V^{-1}s^{-1}$) and strong current modulation 3-4 order of magnitude induced by gate voltage [5] has been developed. This technology is to base on intercalation of organic solvent N-methylpyrrolidone (NMP) into FLG with subsequent annealing at temperature range 100-180°C. Due to chemical reaction between graphene and NMP hybrid structure resistivity increases by 6-7 orders of magnitude. Further, top layer of hybrid structure is cleaned and their conductivity is recovered.

In this report, we demonstrate creation of graphene field-effect transistors (GFETs) array with use of our approach mentioned above. Photolithography of CVD grown FLG transferred on SiO_2/Si with subsequent intercalation and annealing was used to fabricate a wafer scaled number of devices. Combination of high carrier mobility, strong current modulation induced by gate voltage, and wafer scale fabrication is obtained. This technique is very promising for modern nanoelectronics.

References

[1] J.H. Chen, C. Jang, S. Xiao, M. Ishigami, and M. S. Fuhrer, Nature Nanotech. 2008, Vol. 3, P. 206

[2] K. Nagashio, T. Yamashita, T. Nishimura, K. Kita, and A. Toriumi, J. Appl. Phys. 2011, Vol. 110, 024513

[3] K.I. Bolotin, K.J. Sikes, Z. Jiang, M. Klima, G. Fudenberg, J. Hone, P. Kim, and H.L. Stormer, Solid State Commun. 2008, Vol. 146, p. 351

[4] C. R. Dean, A.F. Young, I. Meric, C. Lee, L. Wang, S. Sorgenfrei, K. Watanabe, T. Taniguchi, P. Kim, K.L. Shepard, and J. Hone, Nature Nanotech. 2010, Vol. 5, p. 722

[5] I.A. Kotin, I.V. Antonova, A.I. Komonov, V.A. Seleznev, R.A. Soots, and V.Ya. Prinz, J. Phys. D: Appl. Phys. 2013, Vol. 46, 285303

Graphite oxide electron-beam induced reduction

Mikoushkin V.M. [1] , *Kriukov A.S.* [1]

Emreu30@gmail.com
[1] Ioffe Institute, St.Petersburg, Russia

Thermal reduction of graphite oxide (GO) is used to modify its physical properties, e.g., to enhance the conductivity of GO films to be utilized in flexible displays [1]. Recently, GO reduction by electron beams has attracted a certain interest due to possibility of local reduction with lateral resolution [2,3]. Reduction of GO under intensive electron beams used in published studies occurred due to heating the irradiated area in accordance with thermal mechanism characterized by low spatial resolution. A question has arisen whether it is possible to reduce GO by a low-intensive electron beam without heating.

GO film on a silicon substrate fabricated at Ioffe Institute (the A.Ya. Vul' lab) and studied in our earlier research (this book, [4]) was irradiated by a 1500 eV electron beam. The current density (< 0.1 μA/0.5 mm) was too low to heat the irradiated area. Elemental concentration was controlled *in situ* by Auger electron spectroscopy (AES) directly in the modified area. Fig. 1 shows the dependence of the oxygen O*KLL* Auger line intensity measured in the irradiated area on the dose of electron-beam irradiation. Peak-to-peak amplitude of the numerically differentiated spectrum was used as a measure of the line intensity and oxygen concentration. Release of about 40 % of oxygen atoms is observed in the studied range of dozes. The dependence shows a near exponential character. Detachment of the oxygen groups was assumed to occur due to local excitation of valence electrons of the oxygen group into a repulsive state. On the contrary, the corresponding carbon C*KLL* line intensity proved to be approximately constant in the course of GO modification. It means that carbon atoms do not create free molecular complexes with oxygen atoms and that the carbon cage mainly remains undamaged. Thus nonthermal reduction of GO by low intensive electron-beams has been shown to be possible.

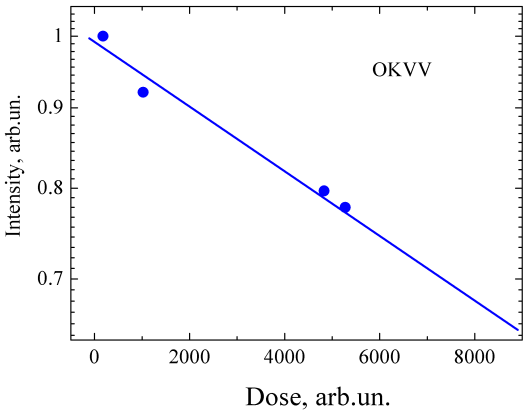

Fig.1. Dependence of the oxygen content in the irradiated GO film on the electron beam irradiation dose.

References

1. S. Pei, H-M. Cheng, Carbon 50 (2012) 3210.
2. P. Kumar, K.S. Subrahmanyam, C.N.R. Rao, Mater. Express 1 (2011) 252.
3. L. Chen, Z. Xu, J. Li, C. Min, L. Liu, X. Song, G. Chen, X. Meng, Mat. Lett. 65 (2011) 1229.
4. V.M. Mikoushkin, A.S. Kriukov, V.V. Shnitov, A.P. Solonitsyna, V.Yu. Fedorov, A. T. Dideykin, D.A. Sakseev, O.Yu. Vilkov, V.M. Lavchiev, J. Electron. Spectrosc. Relat. Phenom. 199 (2015) 51.

Graphite oxide bandgap versus oxygen content

Mikoushkin V.M. [1] , *Kriukov A.S.* [1] , *Shnitov V.V.* [1] , *Nikonov S.Yu.* [1] , *Vul A.Ya.* [1] , *Dideikin A.T.* [1] , *Sakseev D.A.* [1] , *Vilkov O.Yu.* [2]

Emreu30@gmail.com
[1] Ioffe Institute, St.Petersburg, Russia
[2] St. Petersburg State University, St. Petersburg, Russia

Graphite oxide (GO) is known to be a peculiar material whose physical properties and the bandgap width strongly depend on the elemental and chemical compositions which are determined by the fabrication technology features or by the reduction extent [1]. Therefore determination of the GO bandgap width dependence on the oxygen content is of particular interest. Some information on this dependence was obtained in Ref. [2] where the valence band (VB) photoemission spectra of few-layer GO films were studied with using using synchrotron radiation of the BESSY-II electron storage ring. The major part of the valence band, namely, the energy distance between the VB edge and Fermi level, and its dependence on the temperature of the GO thermal reduction were measured. In this research, we studied in parallel the few-layer GO elemental and chemical compositions, the VB spectra and the work function as a function of the GO reduction temperature. The large energy distance between the VB edge and Fermi level (2.9 eV) means that the GO studied is an n-type wide bandgap semiconductor. This result is in agreement with the data of Ref. [3] which show that the donor level almost coincides with the GO conductor valence band bottom: the difference does not exceed 0.1 eV. Unusually large bandgap observed in this research is a result of complete oxidation of natural graphite by the technology used [2]. The C:O ratio was 1:1. The work function was revealed to be almost constant (4.55 – 4.40 eV) throughout the reduction process when the GO bandgap width was continuously vanishing and the GO film completely reduced to few-layer graphite. The work function invariability pointed out that GO remained an n-type semiconductor in all the range of the film transformation in the reduction process. These facts allowed us to obtain the dependence of the few-layer GO bandgap width on the oxygen content represented in Fig. 1. Knowing the oxygen content enables now estimation of the GO bandgap.

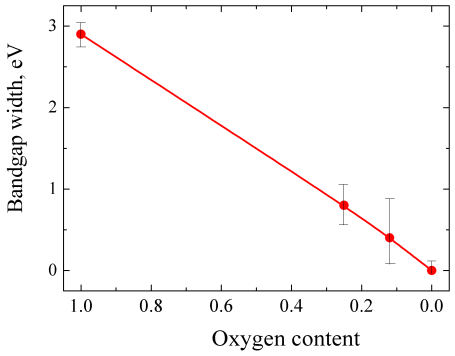

Fig.1. Dependence of the few-layer graphite on the oxygen content.

References

1. Y. H. Wu, T. Yu, Z.X. Shen. J. Appl. Phys. 108 (2010) 071301.
2. V.M. Mikoushkin, V.V. Shnitov, S.Yu. Nikonov, A.T. Dideykin, S.P. Vul', A.Ya. Vul', D.A. Sakseev, D.V. Vyalikh, O.Yu.Vilkov, Technical Physics Letters 37 (2011) 942.
3. H.K. Jeong, M.H. Jin, K.P. So, S.C. Lim, Y.H., Lee, J. Phys. D: Appl. Phys., 42 (2009) 065418.

Magnetic properties of perforated graphene

Komlev A.A. [1,2] *, Geydt P.* [1] *, Zakharchuk I.* [1] *,* <u>*Makarova T.L.*</u> [3] *, Lahderanta E* [1] *, Tur V.A.* [4] *, Okotrub A.V.* [4] *, Bulusheva L.G.* [4]

tatyana.makarova@lut.fi

[1] Lappeenranta University of Technology, FI-53851 Lappeenranta, Finland

[2] St. Petersburg State Electrotechnical University, St. Petersburg, 197376 Russia

[3] Ioffe Physical Technical Institute, Polytechnicheskaya 26, 194021 St. Petersburg, Russia

[4] Nikolaev Institute Inorganic Chemistry, 630060, Novosibirsk, Russia

Graphene-based materials with polyatomic vacancy defects are interesting due to the unique physical and chemical properties defined by the edge states. Whereas single vacancies demonstrate only spin-half paramagnetism, polyatomic vacancies are expected to result in spin polarization and band gap opening. We have investigated magnetic properties on different stages of perforated graphene synthesis.

Graphite oxide (GO) is being prepared from purified natural graphite using strong oxidizing agents to yield graphene oxide (GO), a nonconductive hydrophilic carbon material. Its structure is described as an aromatic lattice of graphene interrupted by epoxides, alcohols, ketone carbonyls, and carboxylic groups

Heating of GO in concentrated sulphuric acid results in partial removal of oxygen and formation of graphene layers with of a significant amount of polyatomic vacancy defects: perforated graphene (PG).

PG can be further annealed (APG) or chemically modified (MPG). Whereas carbon atoms constituting basal graphene plane interact readily with oxygen and fluorine only, the edge atoms are more reactive and can form covalent bonds with other atoms. In this work we consider fluorinated MPG.

We have found that GO is diamagnetic at room temperature and becomes paramagnetic at lower temperatures. Spin concentration is of the order 1×10^{20} spin/g. At low temperatures the M(H) dependence is non-linear, and we fitted the hysteresis loop of sample with Brillouin function demonstrating the existence of superparamagnetic small clusters with the number of coupled spins about ten. PG has similar spin concentration and similar number of coupled spins at low temperature, but its magnetic behaviour is quite different: it shows distinct antiferromagnetic transition at 120 K. The only possible explanation is a formation of zigzag edge states, which form antiferromagnetically interacting collective spins.

Both annealing and chemical modification kill antiferromagnetism. Magnetic behaviour of both APG and MPG is similar: the difference in the measurements made using the zero field cooled (ZFC) and field cooled (FC) protocols starts from room temperature showing that superparamagnetic behaviour is preserved but the clusters represent thousands of atoms. The magnetization values at room temperature correspond to 5×10^{-4} Bohr magneton per carbon atoms.

Supported with the FP7 MCA IRSES project 295180 MagNonMag.

References

1. R. Nair et al., Nature Physics 8,199–202 (2012)
2. Golor, S. Wessel*, and* M. J. Schmidt, Phys. Rev. Lett. 112, 046601 *(*2014)

Mechanical properties of graphene: empirical many-body potentials study

Knizhnik A.A. [1,2] , *Minkin A.S.* [1] , *Popov A.M.* [3]

amink@mail.ru

[1] National Research Center "Kurchatov Institute", Moscow, Russia

[2] Kintech Lab Ltd, Moscow, Russia

[3] Institute for Spectroscopy, Russian Academy of Science, Moscow, Russia

Graphene is an unique two-dimensional material with extraordinary mechanical, transport, electrical and optical properties. For adequate simulation of graphene-based systems consisting of $10^3 - 10^6$ atoms by classical molecular dynamics or Monte Carlo methods the choice of an appropriate interatomic potential is necessary. Here we compare mechanical properties of perfect graphene layer calculated by various covalent potentials. The equilibrium bond length, Young modulus and Poisson ratio are calculated by the variation of energy with the variation of strain for graphene layer with periodic boundary conditions. The bending rigidity a of graphene is obtained using the relationship $U = ar^{-2} + b$ between the energy U and radius r of single walled carbon nanotubes.The calculated characteristics of graphene, literature data for the same potentials [1,2,6,7], experimental data [8] and results of DFT calculations [9] are listed in Table.

Table 1. Calculated characteristics of graphene

	Equilibrium bond length, Å	Poisson ratio	Young modulus, TPa	Bending rigidity, эВ·Å^2/atom
Tersoff potential [1]	1.461	–0.184 –0.158 [2]	1.119 1.2 [2]	1.41 1.34 [1]
Maruyama potential [3]	1.419	0.097	0.535	0.90
Brenner I potential [4]	1.45 [6]	0.412 [6]	0.694 [6]	2.2 [6]
Brenner II potential [5]	1.398 1.42 [6]	0.117 0.397 [6]	1.084 0.715 [6]	1.98 1.8 [6]
PPBE-G potential [7]	1.447	0.284 0.28 [7]	0.865 0.95 [7]	5.20 2.05 [7]
Experiment [8]	1.420	0.249	1.06	1.95
DFT calculations [9]	-	0.149	1.02	-

We found that Tersoff and Maruyama potentials don’t reproduce correctly some elastic constants. Better results are obtained by PPBE-G potential [7] specially designed for graphene and Brenner II potential [5,6]. However additional fitting of the parameters of the potentials are necessary for precise representation of mechanical properties of graphene. Different methods of calculation of elastic constants of graphene using classical potentials are also compared.

References

1. Tersoff, Energies of fullerenes, Phys. Rev. B (1992) **46**, 15546.
2. E. Berinskii and A. M. Krivtsov, Mechanics of Solids (2010) **45**, 815.
3. Yamaguchi and S. Maruyama, Chem. Phys. Lett. (1998) **286**, 336.
4. W. Brenner, Phys. Rev. B (1990) **42**, 9458.
5. W. Brenner, O.A. Shenderova, J.A. Harrison, S.J. Stuart, B. Ni, S.B. Sinnott, J. Phys. Condens. Matter. (2002) **14**, 783.
6. Arroyo and T. Belytschko, Phys. Rev. B (2004) **69**, 115415.
7. Wei, Y. Song, F. Wang, J. Chem. Phys. (2011) **134**, 184704.
8. C. Bowman and J. A. Krumhansl, J. Phys. Chem. Solids (1958) **6**, 367.
9. N. Kudin, G.E. Scuseria, and B.I. Yakobson, Phys. Rev. B (2001) **64**, 235406.

Phenomenology of ripples in graphene

Ktitorov S.A. [1,2] , *Mukhamadiarov R.I.* [1]

ktitorov@mail.ioffe.ru
[1] Ioffe Institute, St.Petersburg, Russia
[2] St. Petersburg Electrotechnical University LETI, St. Petersburg, Russia

Graphene can be viewed as a crystalline membrane. An ideal flat 2D-crystal could not exist at a finite temperature [1], and the long range order in the graphene takes place because of ripples and topological defects. Both of these factors facilitate to achieve thermodynamical stability in graphene [2] and they could be induced to relief the strain of the membrane.

As far as we know, no widely accepted model of ripples in monolayer graphene exists. Crumpled membrane theory does not work for graphene at actual temperatures. Some authors try to obtain a ripple-like solution from the renormalization group approach, but the only result is appearance of some characteristic length of a correct magnitude. The phenomenon under consideration looks too simple to be described with a use of the sophisticated fluctuation theory: we guess that the ripple theory has to be the meanfield one. Rather similar problem of the undulations in biological membranes is solved by taking account of the internal degrees of freedom [3]. One of such fluctuating degrees of freedom was the membrane thickness. In the case of graphene a natural candidate on this position is the in-plane transverse optical phonon. The ripples are considered as an incommensurate superstructure in the two-dimensional crystal, appearing as a result of forming of periodic solutions in the in-plane optical phonon subsystem. The spatial period of the ripple is determined by the ratio of the coefficients in the thermodynamic potential derivative expansion. Out-plane subsystem acquires the periodicity due to the interaction between the subsystems. Two interaction mechanisms: bilinear and biquadratic were considered. Only solutions with vanishing Gaussian curvature are admissible. The suggested phenomenological description needs to be justified by the future microscopic theory.

References

1. N. D. Mermin, H. Wagner, Phys. Rev. Lett. (1966) **17**, 1133.
2. A. H. Castro Neto, F. Guinea, N. M. Peres, K. S. Novoselov and A. K. Geim, Rev. of Modern Phys. (2009) **81**, 109.
3. D. Nelson, T. Piran, S. Weinberg, Statistical Mechanics of Membranes and Surfaces (World Scientific Publishing, Singapore, 2004), p. 49.

On the spillover effect when the solid H_2 intercalation into GNFs

Nechaev Yu.S. [1] , *Filippova V.P.* [1] , *Tomchuk A.A.* [1] , *Yurum A.* [2] , *Yurum Yu.* [2] , *Veziroglu T.N.* [3]

yuri1939@inbox.ru

[1] Bardin Institute for Ferrous Metallurgy, Moscow, Russia

[2] Sabanci University, Istanbul, Turkey

[3] International Association for Hydrogen Energy, Miami, USA

The spillover effect manifestation in hydrogenated carbon-based nanomaterialas has been not enough studied up to nowadays, particularly, relevance for solving the current problem of the hydrogen on-board efficient and safety storage.

In this connection, the thermodynamic analysis [1, 2] (the “open access” Journals) of the related experimental data, including the extraordinary unproduced data {Gupta et al. (2001, 2004)} (Fig. 1) and {Park et al. (1999)}, has been done.

The reported study has been supported by the RFBR (Project #14-08-91376_CT) and the TUBITAK (Project #213M523).

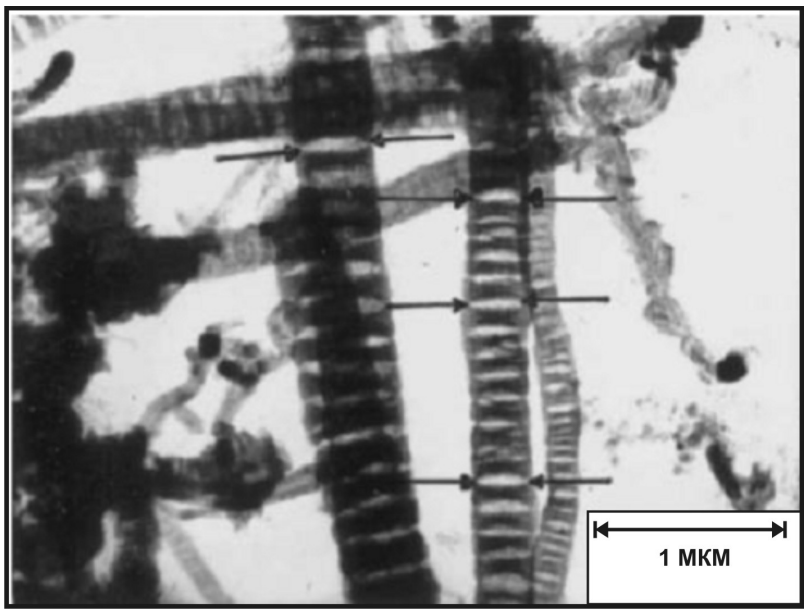

Fig.1. Micrograph {Gupta et al. (2004)} of graphite nanofibers with Pd-catalyst (GNFs), hydrogenated at T = 300 K and initial P_{H2} = 8 MPa, after release from them (at 300 K, for 10 min { Park et al. (1999)}) of the intercalated solid H_2 nanophase (17 mass. %) of a high density of about 0.5 g/cm^3 (analysis [1, 2]). The arrows in the picture indicate some of the slit-like closed nanopores of the lens shape, where the solid H_2 nanophase (under pressure of about 50 GPa, according to data {Trunin et al. (2010)}) was localized [1, 2]. Such a pressure level can be also evaluated [1, 2] by the consideration of the material deformation process and the necessary stresses for forming the lens shape nanopores (at the expense of energy of association of hydrogen atoms to molecules “captured” inside the nanopores). Obviously, it is a manifestation of the spillover effect, relevance to providing the necessary partial pressure of atomic gaseous hydrogen (when the material hydrogenation at initial P_{H2} = 8 MPa).

References

1. S. Nechaev and T.N. Vezirogu, International J. of Physical Sciences (2014) **Vol. 10**, Iss. 2.
2. S. Nechaev, V.P. Filippova, A. Yurum, Yu. Yurum, and T.N. Vezirogu, Journal of Chemical Engineering and Chemical Research (2015) **Vol. 2**, Iss. 1, P. 421.

On the physics of the gaseous H_2 phase intercalation into surface nanoblisters in HOPG and epitaxial graphene

Nechaev Yu.S. [1] , *Filippova V.P.* [1] , *Tomchuk A.A.* [1] , *Yurum A.* [2] , *Yurum Yu.* [2] , *Veziroglu T.N.* [3]

yuri1939@inbox.ru

[1] Bardin Institute for Ferrous Metallurgy, Moscow, Russia

[2] Sabanci University, Istanbul, Turkey

[3] International Association for Hydrogen Energy, Miami, USA

There is a number of recent data on the surface nanoblister formation in highly oriented pyrolytic graphite (HOPG) and epitaxial graphene under hydrogenation in atomic gaseous hydrogen (at low $P_{(Hgas)}$). The process physics has been yet not enough studied. In this connection, the thermodynamic analysis [1,2] of some recent experimental data, particularly, {Waqar (2007)} STM and AFM data for HOPG (Fig. 1), has been done. Similar STM, AFM and other data of different researchers for HOPG and epitaxial graphene have been also analyzed in [1,2]. The process physics has been revealed, allowing the quantitative description of the Waqar data.

The study has been supported by the RFBR (Project #14-08-91376_CT) and the TUBITAK (Project #213M523).

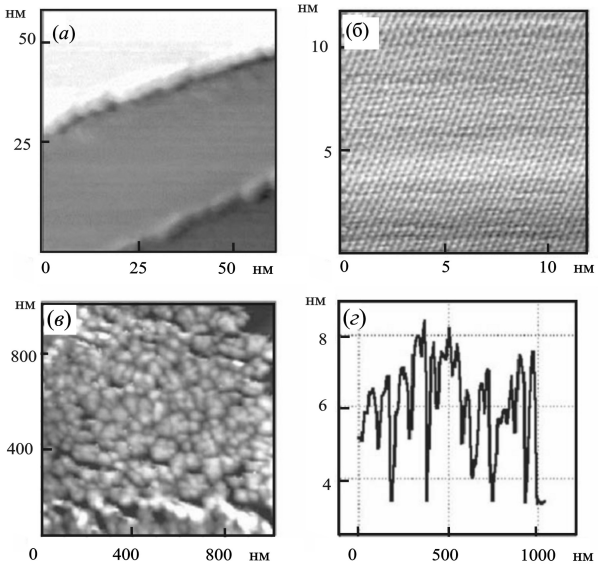

Fig. 1. Model {Waqar (2007), from STM and AFM data} showing the hydrogen accumulation (intercalation) in HOPG, with forming the blister-like surface nanostructures; hydrogenation was done at 300 K and $P_{(Hgas)}$ about 0.1 mPa. (a) Pre-atomic hydrogen penetration step. (b) Molecular gaseous hydrogen, "captured" inside the nanoblisters (at $P_{(H2gas)}$ about 100 MPa), after the intercalation step. The compression effect is of 12 orders (from 0.1 mPa to 100 MPa). According to analysis [1,2], it is at the expense of the energy of association of hydrogen atoms to molecules.

References

1. S. Nechaev and T.N. Vezirogu, International J. of Physical Sciences (2014) **Vol. 10**, Iss. 2.
2. S. Nechaev, V.P. Filippova, A. Yurum, Yu. Yurum, and T.N. Vezirogu, Journal of Chemical Engineering and Chemical Research (2015) **Vol. 2**, Iss. 1, P. 421.

Disclination-structural unit modeling of symmetrical grain boundaries in graphene

Romanov A.E. [1,2] *, Kolesnikova A.L.* [1,3] *, Orlova T.S.* [1,2] *, Hussainova I.* [4] *, Valiev R.Z.* [1,5]

orlova.t@mail.ioffe.ru

[1] ITMO University, St. Petersburg, Russia

[2] Ioffe Institute, St. Petersburg, Russia

[3] Institute of Problems of Mechanical Engineering, St. Petersburg, Russia

[4] Tallinn University of Technology, Tallinn, Estonia

[5] Ufa State Aviation Technical University, Ufa, Russia

In the present work, we propose mesoscopic model for grain boundary (GB) structure in graphene on the base of disclination-structural unit (DSU) approach originally developed for 3D polycrystals [1, 2]. This model allows us to find the dependence of GB energy on misorientation angle, and to study the equilibrium of symmetrical GBs in graphene.

Analyzing the variety of GBs simulated in [3] we have distinguished structural units *A*, *B* (*B'*), and *C* from which all favored and any arbitrary symmetrical GBs in graphene have been constructed. Favored GBs composed of only one type of units *A*, *B* (*B'*), or *C* have misorientation angles θ_1=0º, θ_2=21.8º, and θ_3=60º, respectively [3]. An arbitrary non-favored GB is constructed with the help of two structural units *A* and *B*, or *B'* and *C* belonging to two nearest favored GBs. The structural units permit us to build all known GB structures found by MD method [3].

According to DSU technique [1, 2], the junctions of structural elements with different misorientations θ represent wedge disclinations, and structure of the GB is described as a disclination dipole wall (DDW). The arm of the dipoles depends on GB misorientation θ, and it is multiples to the lengths of structural elements composing DDW. The non-equlibrium GB structures are introduced as non-uniform distribution of structural units, which can be described at mesoscale as disordered network of disclination dipoles. For given θ the equilibrium GB possesses the minimal energy.

In our work the elastic fields and total energy of DDW, in the other words GB, were calculated in the framework of linear elasticity in the whole interval of GB misorientation angles 0º<θ<60º

The obtained dependence for equilibrium GBs is in good agreement with similar dependences found by direct simulation methods for the misorientation angle range of 0º< θ<32.2º. It has been demonstrated that the energy of non-equilibrium GB in graphene can substantially exceed the energy of equilibrium GB with the same misorientation angle.

The proposed DSU model of non-equilibrium GBs in graphene can serve a key structural basis for the description of physical and mechanical properties of graphene GBs, including unique misorientation angle-independent electronic properties of GBs in CVD grown graphene.

Acknowledgements: This study was partly supported by the Russian Foundation for Basic Research (grant no. 14_03_00496_a) and (grant 15-01-05903_a).

References

1. 1. V. Gertsman, A.A. Nazarov, A.E. Romanov, R.Z. Valiev, and V.I. Vladimirov, Phil. Mag. A (1989) **59**, 1113.
2. 2. A. Nazarov, A.E. Romanov, and R.Z. Valiev, Acta Metal. Mater. (1993) **41**, 1033.
3. J. Zhang and J. Zhao, Carbon (2013) **55**, 151.

Atomic and electronic structure of boron-doped graphene on Ni(111) and Co(0001) substrates

Petukhov A.E. [1] , *Usachov D.Yu.* [1] , *Rybkin A.G.* [1] , *Shikin A.M.* [1]

anatolyptkhv@gmail.com
[1] Saint Petersburg State University, St. Petersburg, Russia

Graphene, a two-dimensional monolayer of carbon atoms with a honeycomb lattice, combines unique properties: high mechanical strength, electrical and thermal conductivity and many others. The doping of graphene with various chemical elements like nitrogen [1,2] and boron [3,4] is a very promising way to tune its electronic structure for the further use in carbon based electronic devices.

The present work is devoted to the study of the atomic and electronic structure of the boron-doped graphene synthesized by chemical vapour deposition (CVD) from the boron-containing precursor carborane on top of Ni(111) and Co(0001) films. The research was carried out by scanning tunneling microscopy and spectroscopy (STM and STS) at room temperature in ultra-high vacuum conditions.

It was found that for small concentrations of boron (less than 5 at.%) atom-resolved STM images of doped graphene on both substrates are almost identical to those for the pristine graphene at small bias voltages. There was no contrast in images between carbon and boron atoms. Current imaging tunneling spectroscopic measurements (CITS) revealed features in the local density of electronic states at certain bias voltages. These features were absent in the pristine graphene and could be associated with the presence of boron atoms, which were embedded in the structure of graphene. STM and CITS data analysis showed that boron atoms were located in the lattice site of doped graphene above the hollow cites of the Ni(111) surface. Large concentrations (more than 15 at.%) of boron led to considerable distortions of the system lattice and made it almost impossible to determine the impurity locations relative to the substrate lattice. The system on the nickel substrate exhibited stronger disordering with increasing boron concentration compared with the system based on cobalt.

STM and CITS measurements were performed using Omicron VT SPM at the Resource Center “Physical Methods of Surface Investigation” (RC PMSI) of Research park of Saint Petersburg State University. The work was supported by RFBR (Grant 14-02-31150) and Saint-Petersburg State University (Grants 11.37.634.2013 and 11.50.202.2015).

References

1. J. Koch, M. Weser, W. Zhao, F. Viñes, K. Gotterbarm, S. M. Kozlov, O. Höfert, M. Ostler, C. Papp, J. Gebhardt, H.-P. Steinrück, A. Görling, T. Seyller, Phys. Rev. B (2012) **86**, 075401.
2. D. Usachov, A. Fedorov, O. Vilkov, B. Senkovskiy, V. Adamchuk, L. Yashina, A. Volykhov, M. Farjam, N. Verbitskiy, A. Grüneis, C. Laubschat, D. Vyalikh, Nano Lett. (2014) **14**, 4982.
3. J. Gebhardt, R. J. Koch, W. Zhao, O. Höfert, K. Gotterbarm, S. Mammadov, C. Papp, A. Görling, H.-P. Steinrück, and Th. Seyller, Phys. Rev. B (2013) **87**, 155437.
4. W. Zhao, J. Gebhardt, K. Gotterbarm, O. Höfert, C. Gleichweit, C. Papp, A. Görling, H.-P. Steinrück, J. Phys. Condens. Matter (2013) **25**, 445002.

Synthesis and electronic structure of graphene on a nickel film adsorbed on graphite

Pudikov D.A. [1,2] , *Zhizhin E.V.* [1,2]

gelbry@mail.ru
[1] Saint Petersburg State University, Saint Petersburg, Russia
[2] Research resourse center, Saint Petersburg State University, Saint Petersburg, Russia

The development of graphene synthesis methods and the study of its electronic structure are the main objects of numerous works owing to its amazing physical and chemical properties. Unique transport properties (the highest electron mobility of all known materials) make graphene a perspective material for various applications, for example as a future basis of nanoelectronics and the possible replacement for silicon in integrated circuits.

Commercial use of graphene implies the development of highly effective and cost-effective graphene synthesis methods. Such techniques as mechanical exfoliation from graphite monocrystal, thermal graphitization of silicon carbide and cracking of carbonaceous gases (or CVD) on the surface of transition metals are widely used at present. The cracking of propylene (C_3H_6) on the surface of Ni (111) monocrystalline film is very common now, owing to a very small mismatch between the lattice parameters of this surface and graphene, and leads to the formation of epitaxial well-ordered wafer-scale graphene. Moreover it is well-known that this synthesis reaction is self-limited and a monolayer graphene is fabricated on the surface. This fact favourably distinguishes this method from others, where the probability of multilayer graphene is much higher.

There is a wide discussion in literature about the details of the graphene growth mechanism via the cracking of carbonaceous gases, especially on the Ni (111) surface. One possible way of the graphene monolayer synthesis is through the catalytic decomposition of carbonaceous molecules on the surface of Ni (111) at substrate temperatures 400-600°C with simultaneous dissolving of carbon atoms in the film. The following cooling to room temperature leads to segregation and accumulation of carbon atoms on the surface of Ni (111) film due to the limited solubility of carbon in the bulk Ni. Another supposed mechanism of the graphene synthesis on the surface of Ni (111) is the formation of the nickel carbide Ni_2C in the surface layer with the following transformation at certain temperatures to a monolayer graphene.

This work is devoted to the study of the graphene monolayer synthesis on the Ni (111) film via the segregation and accumulation of carbon atoms on the surface. It should be noted here that these atoms come through to the Ni (111) surface “from underneath” from the carbon-containing wafer, in contrast to the CVD method, where carbon atoms are adsorbed “from above” from gas phase. A highly-oriented pyrolytic graphite (HOPG) was used as a substrate. It will be shown that the segregation process goes along with the formation of nickel film carbidization with the following transformation into the monolayer and multilayer graphene. This process was studied by the analysis of the fine structure, intensities and chemical shifts of C1s core-level line by means of X-ray photoelectron spectroscopy (XPS). Also the research can be viewed as the study of the potential of new graphene synthesis method – the method of “solid-state” interior carbon source, which allows decreasing the temperature required for graphene layer synthesis and increasing the efficiency of this method as compared with others.

Fine reduction of graphene oxide to graphene films

Aleksenskii A.E. [1] *, Baidakova M.V.* [1] *, Dideikin A.T.* [1] *, Rabchinskii M. K.* [1] *, Shestakov M.S.* [1] *, Shvidchenko A.V.* [1] *, Shnitov V.V.* [1] *, Sakseev D.A.* [1] *, Vul A.Ya.* [1]

maxraer@mail.ru
[1] Ioffe Institute, St.Petersburg, Russia

The great variety of technological applications, predicted for graphene-based materials, such as field-effect transistors, passively mode-locked lasers, energy storage and biomedical systems [1], demands production of high-quality large-scale and cheap graphene films. Among the technologies of graphene production chemical oxidation of graphite with subsequent reduction [2] has important advantages: low cost, high yield and due that graphene oxide (GO), the intermediate phase of the process, is hydrophilic, one can make films by simple drop-casting method of aqueous suspensions.

We produced aqueous suspension of graphene oxide flakes of size in the range of 50-100 μm [3] using the new method of graphite oxide production based on the natural crystalline graphite as starting material. Size distribution was determined by optical diffraction (OD) and SEM techniques. Accordingly to the results of analysis of XPS data and FTIR measurements, the new produced graphene oxide contains mostly hydroxyl groups on basal plane, unlike the results of studies of the conventional GO where the epoxy groups are dominating. The former gives the reason for common regarding GO to be unsuitable for making the graphene of high electrical quality [4].

The results of study of UV-Vis spectra demonstrate the reduction to graphene merely by adding of solution of the prepared graphene oxide to alkaline solution together with silicon plates and subsequent heating at 80 C for 24 hours. We observed the formation of 50-100 μm black flakes, distributed in water. Obtained material was characterized by UV-Vis, FTIR and electrical conductivity measurements demonstrated the formation the reduced graphene oxide (rGO). Accordingly to the results of UV-Vis, FTIR the chemical composition of the obtained material is similar to rGO, produced by treatment in hydrazine or annealing in vacuum [4, 5].

As a result we have demonstrated the reduction of GO by simple and soft chemical process without applying high temperatures or strong chemical treatment. This process could be used for preparation thin graphene films by deposition of graphene oxide from its aqueous solution of on the required substrate and subsequent reduction process.

The study was partly supported by the Russian Foundation for Basic Research (project 15-02-005153).

References

1. S. Novoselov, V. I. Falko, L. Colombo, P. R. Gellert, M. G. Schwab & K. Kim. A roadmap for graphene. Nature, 490, 192 (2012)
2. Daniel R. Dreyer, Sungjin Park, Christopher W. Bielawski and Rodney S. Ruoff. The chemistry of graphene oxide. Chem. Soc. Rev., 39, 228 (2010).
3. E. Aleksenskii, P.N. Brunkov, A.T. Dideikin, D.A. Kirilenko, Y.V. Kudashova, D.A. Sakseev, V.A. Sevryuk, M.S. Shestakov., Single-layer graphene oxide films on a silicon surface. Tech. Phys., 58 1618 (2013).
4. Sungjin Park, Jinho An, Jeffrey R. Potts, Aruna Velamakanni, Shanthi Murali, Rodney S. Ruoff. Hydrazine-reduction of graphite- and graphene oxide. Carbon 49, 3019 (2011)
5. Muge Acik, Geunsik Lee, Cecilia Mattevi, Adam Pirkle, Robert M. Wallace, Manish Chhowalla, Keyongjae Cho, Yves Chabal. The role of oxygen during thermal reduction of graphene oxide studied by infrared absorption spectroscopy. J. Phys. Chem. C, 115, 19761 (2011).

Fluorinated reduced graphene oxide as an electrode material for supercapacitors

Rybalchenko A.V. [1] , *Skokan E.V.* [1] , *Goryunkov A.A.* [1] , *Khavrel P.A.* [1] , *Shulga Yu.M.* [2] , *Sidorov L.N.* [1]

alexry@gmail.com

[1] Chemistry Department, Lomonosov Moscow State University, Moscow, Russia

[2] National University of Science and Technology MISIS, Moscow, Russia

High specific surface and electronic conductivity of graphene and its composites allow one to consider these materials as promising components for the production of supercapacitors [1-4]. However, no data are available on application of partially fluorinated graphene in this field. Here we have reported the results of our investigation of specific capacitance of nanostructured composites based on reduced graphene oxide (RGO) and fluorinated RGO (FRGO).

RGO was prepared by microwave treatment of graphite oxide obtained from graphite [5]. Fluorination of RGO carried out with xenon difluoride at 70 °C. X-ray photoelectron spectroscopy (XPS) was used to determine the elemental composition of the products. The fluorine content (F/C at. ratio) in the samples was found to vary within the range of 0.25 – 0.35. The specific capacitance of composites of RGO and FRGO with PEDOT:PSS as conductive polymeric binder were measured by using cyclic voltammetry according to recently described procedure [6]. Significant increase of specific capacitance of FRGO-based composite compared to RGO-based one was observed. Specific capacitances were 26 and 44 F/g for RGO-based and FRGO-based composites, respectively (0.15 M Bu_4NBF_4/1,2-dichlorobenzene as an electrolyte). Influence of electrode mass loading, number of cycles, and potential range on specific capacitance values are discussed.

This work was partially supported by the Russian Foundation for Basic Research (grant no. 15-03-04987 and 13-03-00311a).

References

1. Hao L., Li X., Zhi L. Carbonaceous electrode materials for supercapacitors. // Adv. Mater. 2013. Vol. 25, № 28. P. 3899–3904.
2. Islam M.M. et al. Liquid Crystalline Graphene Oxide/PEDOT:PSS Self-Assembled 3D Architecture for Binder-Free Supercapacitor Electrodes // Front. Energy Res. 2014. Vol. 2, № August. P. 1–11.
3. Antiohos D. et al. Compositional effects of PEDOT-PSS/single walled carbon nanotube films on supercapacitor device performance // J. Mater. Chem. 2011. Vol. 21, № 40. P. 15987.
4. Weng Y.-T., Wu N.-L. High-performance poly(3,4-ethylene-dioxythiophene):polystyrenesulfonate conducting-polymer supercapacitor containing hetero-dimensional carbon additives // J. Power Sources. Elsevier B.V, 2013. Vol. 238. P. 69–73.
5. Y.M. Shulga, S.A. Baskakov, E.I. Knerelman, G.I. Davidova, E.R. Badamshina, N.Yu. Shulga, E.A. Skryleva, A.L. Agapov, D.N. Voylov, A.P. Sokolov and V.M. Martynenko, RSC Adv. (2014) **4**, 587.
6. Stoller M.D., Ruoff R.S. Best practice methods for determining an electrode material's performance for ultracapacitors // Energy Environ. Sci. 2010. Vol. 3, № 9. P. 1294.

Magnetic states at the interface between graphene and iron ultrathin layers

Tadano W. [1] *, Sawada M.* [2] *, Namatame H.* [2] *, Taniguchi M.* [2]

sawa@hiroshima-u.ac.jp

[1] Graduate School of Science, Hiroshima University, Higashi-Hiroshima, Japan

[2] Hiroshima Synchrotron Radiation Center, Hiroshima University, Higashi-Hiroshima, Japan

Ballistic electronic transport realized in graphene is one of important properties for development of spintronics devices, and spin injection into the graphene layer is a key technology to open a new road in the applications of graphene to the spintronics devices. It is essential to clarify the magnetic properties and magnetic states at the interface between graphene and ferromagnetic layers in layered device structure. In this study, we have investigated on the magnetism in Graphene/Fe/Ni(111) films by means of soft X-ray magnetic circular dichronism (XMCD) spectroscopy.

High-quality graphene can be grown on the clean Ni(111) by cracking of propylene gas (C_3H_6) [1]. Post-annealing procedure after an iron deposition onto Graphene/Ni(111) promotes intercalation of Fe underneath the graphene layer, leading to an inert effect of Fe by the graphene layer as passivation layer [2]. We fabricated Graphene/Fe/Ni(111) films for the thickness dependence measurements of XMCD spectra, where the Fe ultrathin films had wedge-type structures up to 10 ML. All the sample preparations and the XMCD experiments were performed *in situ* at HiSOR-BL14 in Hiroshima Synchrotron Radiation Center.

In Fig. 1, we show soft X-ray absorption spectra (XAS) of the Graphene/Fe/Ni(111) sample. In the XAS spectra, thick and thin spectral curves correspond to measurements in parallel and anti-parallel alignment of the saturated magnetization to the helicity vector of the incident X-ray, respectively. Remarkable thickness dependence is found in the XMCD spectra obtained from the difference of the XAS spectra. In the ultrathin limit, the spin magnetic moment per Fe atom is estimated at 2.3 μ_B from a spectral analysis based on magneto-optical sum rule, whose value is slight larger than that for bulk crystal of bcc-Fe. The spin magnetic moment decreases with the iron layer getting thicker. One-third of the value at 2.5 ML is observed at 5.9 ML. The reduction of the saturated spin magnetic moment implies an existence of magnetically dead layer in the Fe ultrathin film that contacts to the surface graphene layer.

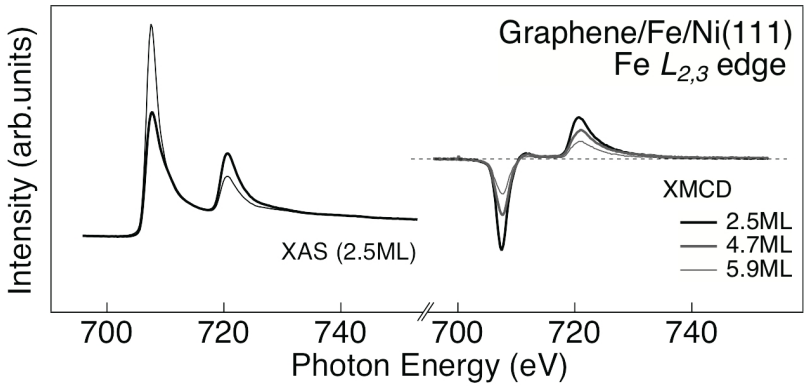

Fig. 1. XAS spectra measured at Fe $L_{2,3}$ edge. The thickness dependence of XMCD spectra is also shown, whose amplitudes are normalized by XAS intensities.

References

1. S. Dedkov, A. M. Shikin, V. K. Adamchuk, S. L. Molodtsov, C. Laubschat, A. Bauer, and G. Kaindl, Phys. Rev. B (2001) **64**, 035405.
2. Y. S. Dedkov, M. Fonin, U. Rüdiger and C. Laubschat, Appl. Phys. Lett. (2008) **93**, 022509.

Study of graphene solid films prepared by Langmuir-Blodgett technology

Seliverstova E.V. [1] , *Ibrayev N.Kh.* [1] , *Alikhaydarova E.Zh.* [1] , *Dzhanabekova R.Kh* [1]

Genia_sv@mail.ru
[1] Institute of Molecular Nanophotonics, Y.A. Buketov Karaganda State University, Karaganda, Kazakhstan

In this paper the method of preparation of graphene films by Langmuir-Blodgett method is presented. The ability of graphene to form stable dispersions in various solvents, and the possibility of obtaining of stable monolayers at the water-air interface are studied. Single laered graphene oxide was use (SLGO) (Cheaptubes, USA). Graphene dispersions were prepared in acetone, chloroform, tetrahydrofuran (THF) and dimethylformamide (DMF) (Sigma-Aldrich). The particle size of graphene in solution was determined by dynamic light scattering analyzer Zetasizer nano (Malvern). The absorption spectra and transmission of the samples were registered by the spectrometer SOLAR CM2203. It was found that after long treatment of graphene solutions with ultrasound the particle size decreases of 2500 nm to 1800 nm for the THF and DMF, and of 1100 nm to 750 nm for acetone and chloroform. In addition, the particle sizes are virtually unchanged after 30 minutes dispersing of solution for both groups of solvent. Measuring the optical density of the solutions at various times is shown that graphene in THF and DMF solution maintains its properties during 48 hours, whereas in acetone SLGO precipitated after 18 hours. Most unstable dispersions were obtained in chloroform - graphene precipitated on the bottom of the cell during of 1 hour after preparation. Solutions of SLGO in THF and acetone were used for the preparation of graphene films. Investigated monolayers were formed on the surface of the subphase by the spreading of the solution in the Langmuir-Blodgett through. Deionized water purified with the water purification system AquaMax was used as subphase. The resistivity of the water was equal to 18.2 MΩ / cm. Surface pressure was equal to 72.8 mN/m at pH 5.6 and a temperature of 22°C. Transfer of monolayers onto solid substrates was carried on by Y-type. The surface morphology of the films was studied by electron microscope Tescan Mira-3. As was shown by the isotherms of compression of monolayers deposited in both solvents, pressures in the range from 0 to 2 mN/mm monolayer is predominantly in a gaseous state. With further compression of the monolayer the nanosheets of graphene approaches and the film becomes a liquid. The broad band with maximum at 230 nm and with the shoulder at 300-310 nm was observed for both films. These values are in good correlation with the data of other authors [1]. The transparency of the films in the wavelength range from 400 nm to 800 nm is equal to 80%. The optical density of the film obtained from the acetone solution is greater than the optical density of the film prepared from THF. Microscopic measurements shows that the films have an island structure. In the images are clearly visible individual graphene sheets. Films prepared from acetone, is more uniform, whereas in films deposited from THF, there are areas with a dense packing of particles of graphene.

References

1. D.S. Sutar, P.K. Narayanam, N. Singh. Thin Solid Films (2012) **520**, 5991.

Graphene and RE metals: formation of graphene by decarbidization of Gd and hybridization of graphene/Gd states

Shevelev V.O. [1] , *Klimovskikh I.I.* [1] , *Rybkin A.G.* [1] , *Vladimirov G.G.* [1] , *Zhizhin E.V.* [1] , *Shikin A.M.* [1]

victorshevelev@yandex.ru
[1] St. Petersburg State University, St. Petersburg, Russia

Graphene, a single layer of carbon atoms, presently attracts much attention due to its unique physical properties [1]. Some of these properties are explained by the behavior of the pi-states near the Fermi level, which have a linear dispersion near the K points of the Brillouin zone. This allows graphene to be the basis of many new generation computing devices [2]. Synthesis of graphene by decarbidization of Me compounds is one of promising methods for industrial production. In this work graphene was synthesized by the decarbidization of Gd compounds, resulting in heating. Atoms of C, appearing as result of decomposition of Gd compounds, segregated on the surface and formed graphene. Any application of graphene in the real electron- or spin-transport devices implies the use of the graphene-metal contacts, which can drastically modify electronic as well magnetic properties of graphene.

In this work we study MG/Gd/HOPG system. Gd is 4f rare-earth metal with magnetic properties. Last two decades RE graphite intercalation compounds [3,4] were in focus because of the interest to the superconductivity of YbC_6 [5]. Also it was calculated [6] that in systems like MG/RE graphene can be strongly n-doped and behavior of its pi-states near the Dirac cone can be strongly influenced by the 4f states of RE metal demonstrating for spin-up electrons a hybridization between valence band states of graphene and RE states. Herewith linear dispersion of the graphene pi-states is conserved for spin-down electrons. Such interaction opens magnetic properties of graphene.

In this work we had studied graphene on Gd and measured dispersion relations of the pi-states near K point of Brillouin zone. Experiments were carried out with use of X-ray photoelectron spectroscopy and angle-resolved photoelectron spectroscopy in ultrahigh vacuum conditions. Behavior of dispersion relations and details of hybridization of the pi-states of graphene with the 4f states of Gd will be studied and analyzed. Interaction of the graphene and 4f RE metals possibly opens new opportunities for applications of graphene in spintronics.

References

1. K. Geim and K. S. Novoselov, Nature Materials 6, 183 (2007).
2. Novoselov, Rev. Mod. Phys. 83, 837 (2011).
3. Shikin, M. Poigin, Y. Dedkov, S. Molodtsov, and V. Adamchuk, Phys. Solid State 42, 1170 (2000).
4. M. Shikin, A. A. Rybkina, A. G. Rybkin, I. I. Klimovskikh, P. N. Skirdkov, K. A. Zvezdin, and A. K. Zvezdin, Appl. Phys. Lett. 105, 042407 (2014)
5. E. Weller, M. Ellerby, S. S. Saxena, R. P. Smith, and N. T. Skipper, Nature Physics 1, 39 (2005).
6. Elena N. Voloshina/ Yuriy S. Dedkov, Volume 69, Issue 7 (Jul 2014).

Kinetic Model of Graphene Nucleation in CVD process

Sinitsa A.S. [1] , *Knizhnik A.A.* [1] , *Potapkin B.V.* [1]

alexsinitsa91@gmail.com
[1] NRC Kurchatov Institute, Moscow, Russia

Chemical vapor deposition (CVD) process of graphene on transition metal surfaces is a promising method for production large-scale graphene films[1]. However, widespread synthesis of graphene and other structures based on it has not been realized yet. For controlling the growth and quality of graphene on the catalyst surface understanding the growth mechanism at atomistic level is necessary. In this study we introduce a theoretical model of graphene nucleation kinetics in CVD process on the Ni(111) surface[2].

Previous theoretical model of the growth rarely took into account different atomistic effects such as, for example, the penetration of carbon atoms in the subsurface layers of metal, dissolution of carbon into the substrate. In the model presented these effects are taken into account. Analytical theory is based on reaction-diffusion model of carbon transport on Ni film. which includes carbon dissolution in Ni film and surface nucleation of grapheme(see figure). The parameters of this model were determined from first-principles calculations. It is shown that the nucleation of graphene depends on the accumulation of carbon in the Ni bulk, which delays the process of nucleation of graphene. Subsurface layer is filled to a certain equilibrium value. When the critical concentration of carbon is reached, carbon starts to form various surface structures. After filling the entire surface further graphene growth is provided by carbon accumulated in the substrate. The results obtained are in good agreement with the results of our atomistic model proposed on the basis of molecular dynamics calculations and qualitatively agree with experiment.

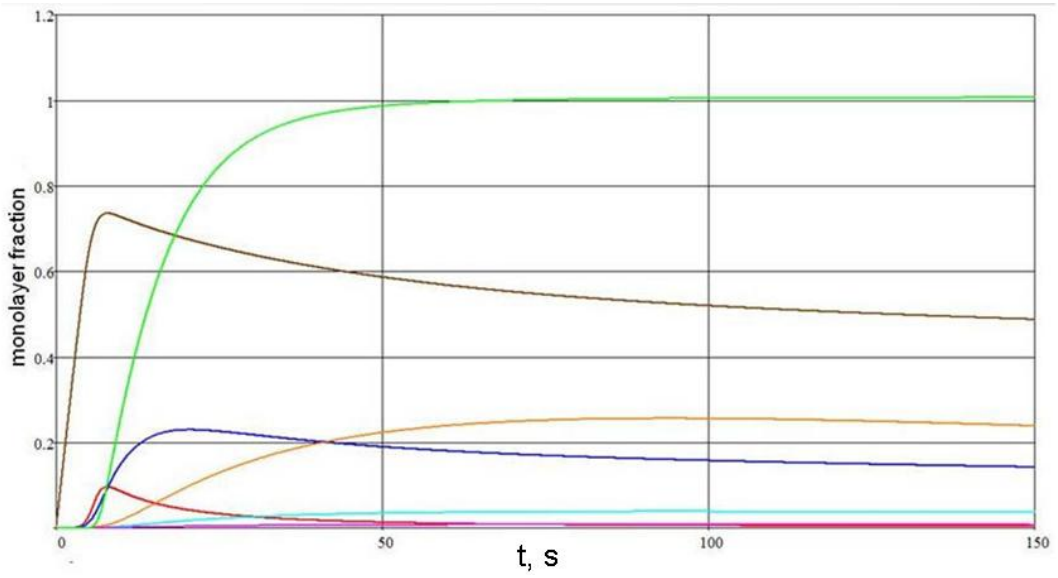

The resulting graph of the model: x axis – total time in seconds, y axis – fraction of carbon atoms. Red line – surface adatoms, green line – surface adatoms, brown, blue, orange, teal and violet lines – first 5 layers of Ni subsurface.

References

1. Loginova, E.,Bartelt, N. C., Feibelman, P. J.,McCarty, K. F., New J. Phys. 2008, 10, pp. 093026.
2. Gomez De Arco, Y. Zhang, A. Kumar, and C. Zhou, TRANSACTIONS ON NANOTECHNOLOGY, VOL. 8, NO. 2, MARCH 2009, pp. 135.

Heat treatment of graphite oxide, exfoliated in a microwave discharge

Chilingarov N.S. [1] *, Havrel P.A.* [1] *, Skokan E.V.* [1] *, Levanov A.V.* [1] *, Isaykina O.Ya.* [1] *, Knotko A.V.* [1] *, Medvedev A.A.* [1] *, Deyko G.S.* [1] *, Shulga Yu.M.* [2]

skokan@mail.ru

[1] Chemistry Department, Moscow State University, Moscow, Russia

[2] National University of Science and Technology MISIS, Moscow, Russia

Exfoliation product of graphite oxide in a microwave discharge (MEGO) finds broad application in electronic devices and uses as starting material for obtaining grapheme derivatives .There are different methods of MEGO functionalization. Some methods are based on chemical reduction of MEGO sample in order to reduce its oxygen content, the heat treatment being the simplest of them. This study was carried out to reveal the influence of vacuum step-annealing of the MEGO sample on its structure and composition, in particular, on the concentration of oxygen in the final product.

The initial MEGO sample was obtained by the method described in [1], and characterized by IR- and Raman spectroscopy. The relative content of oxygen in the sample, states of the carbon atoms were determined using XPS. Annealing was performed in vacuum at mass spectrometric monitoring of the gas phase composition. Two products of MEGO annealed up to 573 K and 1073 K were obtained. According to the mass spectral data, the oxygen was eliminated from MEGO in forms of carbon oxides, CO and CO_2, mainly in the 770 - 1070 K temperature range. Decreasing the oxygen content was confirmed by the IR spectroscopic and XPS data. Annealed products were investigated using electron microscopy, SEM and TEM. The size of graphene regions, the average number of graphene layers and the main types of defects were determined by the X-ray powder diffraction and Raman spectroscopic methods.

The work was supported by grant RFFI 15-03-04987.

References

1. Y.M. Shulga, S.A. Baskakov, E.I. Knerelman, G.I. Davidova, E.R. Badamshina, N.Yu. Shulga, E.A. Skryleva, A.L. Agapov, D.N. Voylov, A.P. Sokolov and V.M. Martynenko, RSC Adv. (2014) **4**, 587.

Field emitter prepared from the contacted ytterbium and carbon nanolayers.

Sominski G.G. [1] , *Sezonov V.E.* [1] , *Zadiranov Yu.M.* [2]

sominski@rphf.spbstu.ru
[1] St. Petersburg State Polytechnical University, Russia
[2] Ioffe Institute, St.Petersburg, Russia

One of the intractable problems of creation of any field emitter is the need to obtain fields of the order or even more than 2×10^7 V/cm near their surface at moderate voltages. We have investigated the possibility of using the fields near the contacts of materials with different work functions eφ [1,2] for this purposes.

It is obvious that for obtaining of an intensive field emission, we have to create a system with a large number of pairs of layers with different work functions and collect current from such layered cathode. Calculations necessary to optimize the layered field emitters were carried out using the program Comsol. The electric fields, the electron trajectories, the current density distribution over the surface of the field emitter and emitter currents collected by the anode were calculated. The calculations were performed for a pair of ytterbium (eφ = 3.1 eV) - carbon (eφ = 4.7 eV). The calculations take into account the existence of a transition zone between the layers of Yb and C, where a mixture of these materials exists.

Optimized in accordance with the results of calculations layered cathode systems, including 10, 20, and 40 pairs of layers of Yb - C were created. Their emission characteristics were experimentally studied. Layers of Yb and C had a thickness of 5 nm and 2 nm respectively. The thickness of the emitter having the 40 pairs of layers was less than 0.3 μm. The width of all emitters was 2 mm. Layered systems were created using magnetron sputtering.

Measurements of the emission characteristics of layered cathodes were conducted in a triode system cathode - gate (grid with transparency 75%) - collector. The gate electrode was set at the distance 1 mm from the cathode. A negative voltage relative to the gate was applied to the cathode to receive the emission current from its surface. A current of electrons transmitted through the grid holes and reached the collector was recorded. The collector was grounded through a measuring equipment. The grid was at a negative potential of 100 V relative to the ground, which minimized of secondary electrons departure from the collector. The measurements were performed in a pulsed mode (2 μs, 200 Hz).

The currents were increased with the number of pairs of layers in the cathode. The average over the cathode surface values of the emission current density of forty pairs of layers was about 10 A/cm^2. The full current from this cathode did not exceed 50 - 70 μA and was limited by the destruction of the emission system at higher currents. Significant increase of the field emission currents from the layered cathodes can be achieved by increasing their width and/or by summing of the currents from the set of identical cathodes.

Technology for creating of the layered cathodes is quite simple. They have a small size and provide extremely high current density field emission. Such cathodes may be promising for use, for example, in miniature microwave devices and in various sensors.

References

1. G.G. Sominski, V.E. Sezonov, Yu.M. Zadiranov, Proc. of 10th Int. Vacuum Electron Sources Conf. and 2nd Int. Conf. on Emission Electronics (St. Petersburg, Russia, June 30 – July 4, 2014) (2014), p.228.
2. G.G. Sominski, V.E. Sezonov, T.A. Tumareva, E.P. Taradaev, Patent of the Russian Federation №118119, 17.02.2012.

Fluorinated graphene films as a gas sensor

Sysoev V.I. [1] , *Katkov M.V.* [1,2] , *Guselnikov A.V.* [1] , *Bulusheva L.G.* [1,2] , *Okotrub A.V.* [1,2]

sysoev@niic.nsc.ru

[1] Nikolaev Institute of Inorganic Chemistry SB RAS, Novosibirsk, Russian Federation

[2] Novosibirsk State University, Novosibirsk, Russian Federation

Graphene is a promising material for a range of applications due to its electronic and mechanical properties. High specific surface area and high sensitivity to adsorbed molecules make graphene an ideal platform for gas sensor. In addition, it has a high signal-to-noise ratio, which is critical for the sensor detection limit. Functionalization of graphene allows creating reactive centers on its surface such as defects and functional groups [1]. Previously, we proposed creating a graphene layer on the surface of fluorinated graphite (GF) by hydrazine vapor exposure [2].

The aim of this work is to study sensing properties of fluorinated graphite to the exposure of ammonia (NH_3) and nitrogen dioxide (NO_2). We created reduced layer on the surface of a fluorinated graphite plate and investigated its sensor properties. Both the sensor response amplitude and time depend on fluorine content. The resistance change as a function of NH_3 concentration follows a general form of the Langmuir isotherm. Comparing the absorption energy extracted from our experimental data with the quantum-chemical analysis, we conclude that carbon atoms chemically bonded with fluorine atoms adsorb analyte molecules.

Also, we report solution-based method allowing uniform deposition of reduced graphene fluoride (rGF) films. GF powder was milled using agate mortar. During continuous mechanical treatment, the powder changed its color caused by reduction. XPS spectra obtained after treatment confirmed decreasing fluorine concentration in the samples. The grained powder was ultrasonicate in toluene and sprayed on SiO_2/Si substrate. The sensor properties of films were tested versus NH_3 and NO_2. The rGF film showed better sensitivity and shorter response and recovery time in comparison with the previous method [3]. The response (resistance increase) of FG was of 25 % to 100 ppm NH_3 and 30 % to 100 ppm NO_2.

References

1. Y.-H. Zhang, Y.-B. Chen, K.-G. Zhou, C.-H. Liu, J. Zeng, H.-L. Zhang, and Y. Peng, Nanotech. (2009) **20**, 185504.
2. A.V. Okotrub, K.S. Babin, A.V. Gusel'nikov, I.P. Asanov, L.G. Bulusheva, Phys. Status Solidi B, (2010) **247**, 3039
3. V. Katkov, V. I. Sysoev, A. V. Gusel’nikov, I. P. Asanov, L.G. Bulusheva, prof. A. V. Okotrub, Phys. Chem. Chem. Phys. (2015) **17**, 444.

RECEPTION AND APPLICATION FOAMING OF GRAPHITE

Moskalyov E.V. [1] *, Ponyaev A.I.* [1] *, Terukov E.I.* [2]

evmosk@gmail.com

[1] SPb Institut of Technology (University),St.Petersburg, Russia

[2] Ioffe Institute, St.Petersburg, Russia

The new material on a basis thermal expanded of graphite by a method of two steps foaming in environment of an organic oxidizer with the help of ultrasound is received. As a result of burning out of organic oxidizers expanded the graphite has no extraneous inclusions and impurity, contains only up to 99,9 % of carbon [1].

By results of researches by methods electronic microscopy and Raman of dispersion is shown, that the new material consists from anisotropic of carbon particles with the sizes about tens of microns and occurrence dispersed of a fraction as a graphene with average thickness about 5 carbon layers. The condition of a material at all stages of experiment was supervised on spectra of combinational dispersion of light. The spectra of various samples were identical each other, that allows to make the conclusion about good practice of technology of reception of a material.

As have shown researches received material, despite of substantial growth in volume (about 1000 times), has low sorbtion capacity on nitrogen. The measured area of a surface on BET to a method makes only 12 - 15 m2/g, that testifies about low openness of its surface. In too time the settlement area of a surface 1 g foaming of graphite with thickness 1,5 nm should make about 800 m2, that allows it to use in quality filler for filters at clearing drinking water.

The study was supported by the Russian Ministry of Education and Science (State task № 1789, Contract 14.574.21.0002, unique identifier RFMEFI57414 X0002) and Russian Foundation for Basic Research (Project 13-08-01425a).

References

1. Kompan M.E., Moskalyov E.V., Terukov E.V etc., Mechanochemical dispersion thermal expanded of graphite // Letter a Magazine of technical physics (journals.ioffe.ru/pjtf.) -2010. -V. 36. - № 13. -p. 81-88.

Studies of graphite and graphene transformation at cold compression

Tikhomirova G.V. [1] , *Petrosyan T.K.* [1] , *Tebenkov A.V.* [1] , *Zharkov A.V.* [1]

galina.tikhomirova@urfu.ru
[1] Ural Federal University, Ekaterinburg, Russia

Conductivity, magnetoresistance and thermal e.m.f. of graphite and graphene have been studied at pressures up to 50 GPa at room temperature. The kinetics of resistivity at changing pressure was also studied. Transport phenomena were used as a tool for finding and interpretation of phase transitions arisen under high pressure. Samples of graphene consisted of flakes with the number of layers from 5 to 20. High pressures have been generated in the high pressure cell with synthetic carbonado-type diamond anvils. The anvils are good conductors and can be used as electric contacts making possible to measure temperature and pressure dependences of resistance. The method used allows us to study the same sample at successive increasing and decreasing pressure and also to keep it loaded during a long time. After pressure treatment, the samples were examined by means of the workstation AURIGA CrossBeam, which is a scanning electron microscope with the possibility of X-ray microanalysis.

The features of the phenomena studied found in graphite at the pressures of 15 to 20 GPa and at 30 GPa were ascribed to phase transitions at these pressures [1-3]. The possibility of formation of new carbon phases from graphite at continuous exposure under pressures up to 50 GPa at room temperature was examined. The exposure time at each fixed value of pressure was twenty four hours. The features in the pressure dependence of resistance as well as its relaxation times were found in the range 27 - 35 GPa. The X-ray image of the sample subjected to the pressure of 45 GPa showed the inclusion of a new phase, which did not disappear after removal of the load. However, the new phase was poorly seen in the pressure dependence of resistivity because of shunting by a large amount of non-transformed graphite. Two different relaxation times were found. The first one was less than 40 s. The second relaxation time appeared only after continuous exposure under pressure in the range of 27 to 35 GPa and was several hours.

The baric dependence of resistance of graphene was of the same character as that for graphite, while the resistance values of graphene were larger by almost one order of magnitude. The first resistivity relaxation time for graphene after changing pressure turned out to be significantly larger than that for graphite. The relaxation times increased in the vicinity of phase transitions (15-20 GPa) up to ~10 min. No new phase were found in the X-ray image.

The transverse magnetic field up to 1 T changed the resistance values and did not change their baric dependences. The negative magnetoresistance was observed for all samples at pressures below 30 GPa for graphite and below 23 GPa for graphene. At higher pressures the magnetic field did not influence on the resistance of both graphite and graphene. The change in magnetoresistance was more pronounced (3-5 %) in the range of 15 to 20 GPa.

The pressure dependences of thermal emf were similar for both graphene and graphite. The features in the thermal emf of graphene were also found in the pressure range of 22 to 34 GPa.

This work was supported by the Government of the Sverdlovsk district and RFBR (grants 13-02-96039-r_ural and 13-02-00633).

References

1. Quan Li, Yanming Ma, A.R. Oganov, Hongbo Wang, Hui Wang, Ying Xu, Tian Cui, Ho-Kwang Mao, Guangtian Zou, Physical Review Letters (2009) **102**, 175506.
2. E. Boulfelfel, A.R. Oganov, S.Leoni. Scientific Reports (2012) **2**, art. 471.
3. Y. Wang, J.E.Panzik, B.Kiefer, K. K. M. Lee, Scientific Reports (2012) **2**, 520.

Synthesis of graphene on cobalt silicide and electron-phonon coupling upon doping with lithium

Vopilov A.S. [1] , *Usachov D.Yu.* [1]

antonvop@mail.ru
[1] Saint Petersburg State University, Saint Petersburg, Russia

Graphene nowadays is one of the most promising materials for use in nanoelectronics. First of all this hopefulness is related to its specific electronic structure which induces amazing properties. At the same time, in the interest of a great financial and intellectual contribution to the development of silicon electronics, there is an intention to introduce graphene into existing technology. Therefore, there is significance in the study of graphene synthesized on the metal silicide surfaces, since they are used for making contacts in silicon devices.

Obtaining of graphene on the surface of the cobalt silicide was controlled by angle-resolved photoemission spectroscopy (ARPES). It turns out that the electronic structure of graphene on cobalt silicide is close to the dispersion of freestanding graphene, and therefore it can be expected that this system can demonstrate many of the unique properties.

Also there is fundamental interest in studying graphene on this substrate. In recent article [1] by A.V. Fedorov it was demonstrated that graphene doping with alkali metals on the gold surface leads to strong electron-phonon coupling which in turn is clue of superconductivity. It was found that critical temperature increases with charge transfer from alkali metal. However, the role of the substrate in the charge transfer mechanism was absolutely unclear. For this reason graphene synthesized on cobalt silicide was doped with lithium. It turns out that the charge transfer is significantly higher than on the other substrates [2]. High electron density allows us to expect a strong increase of the electron-phonon interaction in graphene that makes the investigated system a candidate for the detection and study of superconductivity in graphene

This work was supported by grants of St. Petersburg State University No. 11.37.634.2013 and RFBR No. 14-02-31150.

References

1. V. Fedorov, N. I. Verbitskiy, D. Haberer, C. Struzzi, L. Petaccia, D. Usachov, O. Y. Vilkov, D. V. Vyalikh, J. Fink, M. Knupfer, B. Büchner and A. Grüneis, Nature Commun. (2014) 5, 3257.
2. D. Yu. Usachov, A. V. Fedorov, O. Yu. Vilkov et al., Physics of the Solid State (2015) 57, 1040.

Graphitic C3N4 Nanosheets for Electrochemical Sensing of Hg(II)

Amiri M. [1] *, Salehnia H.* [1] *, Habibi-Yengjeh A.* [1]

mandanaamiri@yahoo.com

[1] Department of Chemistry, University of Mohaghegh Ardabili, Ardabil, Iran

Carbon nitrides can exist in several allotropes that have diverse properties. Particularly, the graphitic phase carbon nitride (g-C_3N_4) with a two-dimensional structure is the most stable under ambient conditions [1]. Owing to their outstanding mechanical, optical, electrical, thermal properties and chemically stable properties, g-C_3N_4 has received a large interest and applied in many areas, such as hydrogen storage [2], lithium-ion battery [3], and fluorescent sensor [4].

Chemically modified carbon-paste electrodes (CMCPEs) have attracted more interest due to their potential applications in various analyses. These electrodes have been widely used in electroanalysis due to their ability to catalyze the redox processes of some molecules of interest. CMCPEs are inexpensive and possess many advantages such as low background current, wide range of potential windows (in both cathodic and anodic region), easy fabrication, rapid surface renewal and modification compatibility with various modifiers [5].

Mercury, as one of the highly toxic heavy metal, is a hazardous pollutant for environment and human health. It can cause serious health problems, like kidney and respiratory failure, damage in the gastrointestinal tract and nervous system [6]. Several detection technologies have been reported for mercury analysis. Among these methods, electrochemical technique as a promising and elegant technique has been widely used for trace analysis of Hg (II) due to the high sensitivity, low cost, inherent simplicity and ease of miniaturization.

In this research, we chose melamine as the precursor for direct synthesis of g-C_3N_4 by pyrolysis approach. These nanosheets possess environmental, economic, non-toxic, biocompatible, electric and thermal behaviour, high mechanical strength and high stability. Morphology, composition and structure of the resultant product were characterized by TEM, FTIR spectroscopy, photoluminescence and XRD techniques. To evaluate the electrochemical sensing ability of the g-C_3N_4 through Hg (II), modification of carbon paste electrode has been performed by casting method. 10 µL of g-C_3N_4 suspension has been casted at the surface of carbon paste electrode; the modified electrode has been used for voltammetric measurements. Experimental results proved the excellent adsorptive properties of g-C_3N_4. Differential pulse voltammetry has been applied for sensitive determination of Hg (II) in real samples.

References

[1] Y. Wang, X.Wang, M. Antonietti, Angew.Chem.Int. (2012) **51**, 68–89.
[2] G. Zhu, K. Lü, Q. Sun, Y.Kawazoe, P. Jena, Computational Materials Science (2014) **81**, 275-279.
[3] Y. Hou, J. Li, Z. Wen, S. Cui, C. Yuan, J. Chen, Nano Energy (2014) **8**, 157-164,
[4] M. Rong, L. Lin, X. Song, Y. Wang, Y.Zhong, J. Yan, Y. Feng, X. Zeng, X. Chen, Biosensors and Bioelectronics (2015) **68,** 210-217,
[5] E. Nossol, A.J.G. Zarbin, Electrochim. Acta (2008) **54**, 582–589.
[6] N.K. Aras, O.Y. Ataman, Trace Element Analysis of Food and Diet, RSC Publ., Cambridge (2006) 252.

The influence of impurities on the electronic properties of single-layer MoS_2: theoretical study.

Antipina L.Yu. [1,2,3] , *Sorokin P.B.* [1,3]

lyuantipina@tisnum.ru

[1] Emanuel Institute of Biochemical Physics RAS, Moscow, 119991, Russian Federation
[2] National University of Science and Technology MISiS, Moscow, 119049, Russian Federation
[3] Technological Institute of Superhard and Novel Carbon Materials, Moscow, 142190, Russian Federation

The investigation of electronic properties of MoS_2-NiS_2 compound on the chemical composition $Mo_xNi_{(1-x)}S_2$ was carried out by DFT-PBE method. It was found that addition of small number of Ni atoms leads to significant changing of electronic structure of the film. Nickel atoms create miniband in a band gap of MoS_2. The width of miniband increases with increasing of concentration of Ni atoms in the film and tends to metallic type of conductivity corresponding to NiS_2 structure. Due to the difference of the electron shells of nickel and molybdenum atoms the introduction of impurities in the system lead to excess of electrons as compared with pure MoS_2. This effect provide the conductivity of the system. Thus, the changing the impurity atoms concentration in the structure of transition-metal dichalcogenides, the last one can change their electronic properties from insulation to metallic.

This work was supported by the Russian Science Foundation (project #14-12-01217).

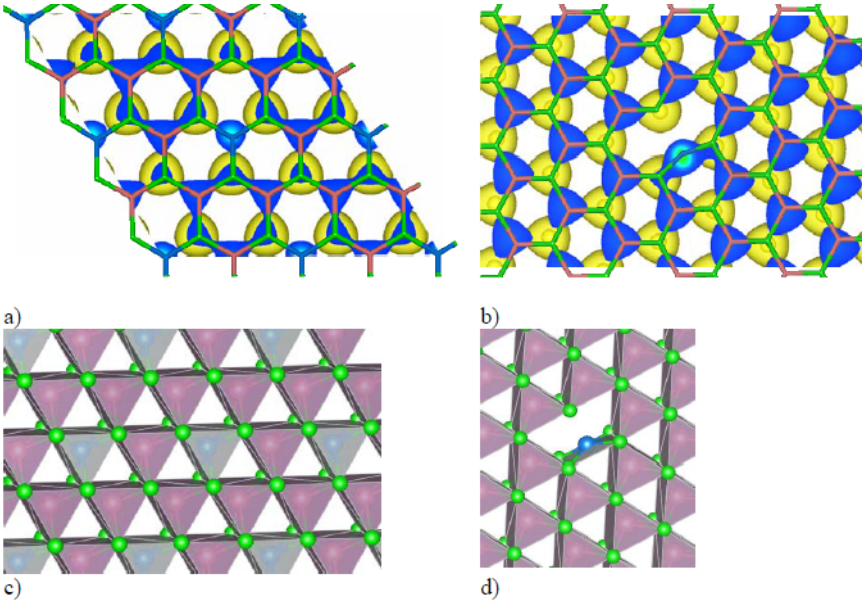

Electron density isosurface of systems $Ni_{0.25}Mo_{0.75}S_2$ (a) and $Ni_{0.04}Mo_{0.96}S_2$ (b) and the corresponding spatial geometry (c and d). Atoms of nickel, molybdenum and sulfur are marked by blue, red and green respectively.

Effect of nano-structure on fluorescence quantum yield of carbon nitride

Ryabova A.V. [1] *, Zinin P.V.* [2] *, Davydov V.A.* [3] *, Khabashesku V.N.* [4] *, Lyapin S.G.* [3] *, Sharma S.K.* [5] *, Pominova D.V.* [1] *, Lyubin E.V.* [6] *, Skryabina M.N.* [6] *, Loshenov V.B.* [1]

vdavydov@hppi.troitsk.ru

[1] Prokhorov General Physics Institute, Russian Academy of Sciences, Moscow, Russia
[2] Scientific-Technological Center of Instrumentation, Russian Academy of Sciences, Moscow, Russia
[3] The Institute for High Pressure Physics, Russian Academy of Sciences, Troitsk, Russia
[4] University of Houston, Houston, Texas, USA
[5] University of Hawaii, Honolulu, Hawaii, USA
[6] Department of Physics, Moscow State University, Moscow, Russia

Fluorescence spectra and quantum yield (QY) of graphitic (*g*-C_3N_4) and spherical (*s*-C_3N_4) modifications of carbon nitride were measured. Both modifications of C_3N_4 were prepared by a high-temperature solid state and solvothermal polycondensation reactions using lithium nitride (Li_3N) as a nitridation and cross-linking agent and cyanuric chloride as a s-triazine building block [1-3]. The fluorescence of powder samples of *g*-C_3N_4 and *s*-C_3N_4 modifications were studied by Carl Zeiss LSM-710-NLO microscope equipped with 32 channel GaAsP detector at room temperature.

The fluorescence spectra of the *s*-C_3N_4 and *g*-C_3N_4 modifications have similar shapes and maxima positions. However, the intensity of the fluorescence at the maximum is five times higher for *s*-C_3N_4 than for *g*-C_3N_4. Our measurements revealed unusually high values of the fluorescence *QY* for *s*-C_3N_4, up to 32% with a 532 nm excitation laser. The high value of the fluorescence *QY* for *s*-C_3N_4 was attributed to the spherical shape of the phase. One interesting feature of the fluorescence excited in *s*-C_3N_4 is high intensity of the anti-Stokes radiation. Using a 633 nm excition laser, the peak at 617 nm (below wavelength of the laser) with the intensity comprising 44% of the intensity of the fluorescence peak with the maximum at 651 nm has been observed. The quantitative measurements of the fluorescence of *s*-C_3N_4 demonstrated that they can be used as effective fluorescent probe.

This work was supported by the Russian Foundation of Basic Research (grant 15-03-04490).

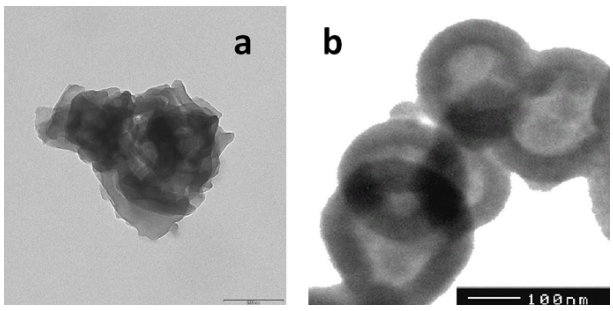

Fig.1. TEM images of the graphitic (a) and spherical (b) modifications of carbon nitride C_3N_4.

References

1. V.N. Khabashesku, J.L. Zimmerman, J.L. Margrave, Chem. Mater. (2000) **12**, 3264.
2. J.L. Zimmerman, R. Williams, V.N. Khabashesku, J.L. Margrave, Nano Lett. (2001) **1,** 731.
3. V.N. Khabashesku, J.L. Margrave, Adv. Eng. Mater. (2002) **4**, 671.

Covalently-bonded heterostructures based on graphene related 2D materials (MoS_2)

Kvashnin D .G. [1] *, Seifert G.* [2] *, Chernozatonskii L.A.* [1]

dgkvashnin@gmail.com
[1] Emanuel Institute of Biochemical Physics RAS
[2] Technische Universitaet Dresden

It is well known that there are two the most developing areas in science and technology. These are: the investigation of graphene which is semimetal with amazing mechanical, electronic and optical properties and MoS_2 which belongs to the family of transition metal dichalcogenides. MoS_2 is a layered material which is a semiconductor with a bulk band gap about 1.6 eV which depends on the thickness. By today technology MoS_2 layers can be easily obtained by nanomechanical cleavage technique. [1]

These two unique materials have complementary physical properties. Therefore, it is natural to investigate the possibility of combining these materials to the purpose of creating heterostructures. Set of separate layers with various compounds (graphene, BN, MoS_2, ect.) allows us to fabricate heterostructures by combining them like LEGO constructor.

Only the drawback of this technique is that obtained heterostructures haven't strong interaction between the layers (non-covalent).

Firstly, we proposed one of the layers decorated by Mo adatoms (self-decoration) and then put the graphene on top of the MoS_2 layer to increase the interaction between the layers in heterostructures.

Impact of adatoms on MoS_2 surface and its electronic properties was observed. Study of electronic properties of heterostructures based on graphene and MoS_2 with Mo adatoms was carried out.

All calculations were carried out using 'Chebishev' and 'Lomonosov' supercomputers of Moscow State University and the Joint Supercomputer Center of the Russian Academy of Sciences. The work was supported by Russian Scientific Foundation №14-12-01217.

References

1. D.M. Tang, D.G. Kvashnin, S. Najmaei, Y. Bando, K. Kimoto, P. Koskinen, P.M. Ajayan, B.I. Yakobson, P.B. Sorokin, J. Lou *et al*.. Nanomechanical Cleavage of Molybdenum Disulphide Atomic Layers // *Nat. Commun.* - 2014. - *V. 5*. - P. 3631-3638.

On the stability of the graphene-like structures

Davydov S. Yu. [1,2] , *Posrednik O. V.* [2]

Sergei_Davydov@mail.ru

[1] Ioffe PhysicalTechnical Institute, St. Petersburg, Russia

[2] St. Petersburg Electrotechnical University, St. Petersburg, Russia

Many unique properties of graphene have awakened interest in the similar 2D graphene-like materials(GLM), such as silicene, germanene, hexagonal boron nitrideand other hypothetical 2D compounds of the A_NB_{8-N} type. However, the problem of the stability of these A_NB_{8-N} structures remains open. This problem has been partly considered in [1] by the Harrison bond-orbital approach. It was shown, that the condition of instability, based on the zero or negative value of the noncentral (shear) force constant, is given by the inequality

$$\Psi \equiv \alpha_p^2 + \alpha_c^2\ (\alpha_c^4 + \alpha_p^2 - \frac{1}{3})\frac{V_1^2}{V_2^2} > \frac{1}{2}, \qquad (1)$$

where $V_1$is the metallic energy; V_2, covalent energy of the σ-bond formed by the sp^2-orbitals of *A* and *B* atoms; α_c, bond covalence; $\alpha_p = (1-\alpha_c^2)^{\frac{1}{2}}$, bond polarity. Since $\frac{V_1}{V_2} < 1$[1], it is clear, that the inequality (1) can be satisfied only for the compound with the appropriately high bond polarity. Here we investigate how the different sets of the atomic energy terms used in the calculations affect the instability problem.

Table 1

Compounds	GaAs	GaP	AlAs	AlP	AlN	GaN	ZnSe	ZnS
α_c	0.90	0.89	0.88	0.87	0.83	0.82	0.73	0.70
α_p	0.44	0.46	0.47	0.49	0.56	0.57	0.68	0.71
Ψ	0.37	0.36	0.38	0.38	0.37	0.39	0.54	0.55

Table 2

Compounds	GaAs	GaP	AlAs	AlP	AlN	GaN	ZnSe	ZnS
α_c	0.92	0.92	0.90	0.90	0.88	0.87	0.78	0.76
α_p	0.39	0.39	0.44	0.44	0.48	0.49	0.62	0.64
Ψ	0.34	0.35	0.36	0.33	0.31	0.31	0.47	0.48

Table 1 demonstrates the results obtained with the Mann's atomic energy terms. It is clear, that the inequality (**1**) is satisfied only for ZnS and ZnSe compounds. Hence, these compounds are unstable or, in other words, the 2D hexagonal structure for ZnS and ZnSe is not implemented. On the other hand, the calculations performed with the Herman–Skillman's terms (Table 2), show that inequality (1) is not satisfied at all, but the Ψvalues for ZnS and ZnSe are on the verge of stability. Note, however, that the present calculations were performed within the harmonic approximation. Taking anharmonicity into account, it is easy to show that the bond's elasticity decreases with temperature, which leads to the increase of the Ψ values and shifts them towards the instability region. Thus, we have to conclude that the existence of the free-standing ZnS and ZnSe 2D hexagonal structures seems to be impossible.

References

Reference

1. S. Yu. Davydov, Semiconductors (2013) **47** (1), 95.

Ballistic electronic transport through functionalized cubane chains

Shostachenko S.A. [1] , *Ryzhuk R.V.* [1] , *Kargin N.I.* [1] , *Katin K.P.* [1] , *Maslov M.M.* [1]

fizik92@inbox.ru

[1] National Research Nuclear University MEPhI, Moscow, Russia

Cubane molecule C_8H_8, firstly synthesized in 1964, has an unusual cubic skeleton, consisted of eight carbon atoms. Despite of non-typical values of valence angles and significant angular deformation energy [1], cubane demonstrates extremely high thermal stability [2] and can participate in chemical reactions without losing its cubic identity [3]. In particular, a number of substituted cubane molecules, in which one or more carbon atoms are replaced by other atoms or chemical groups, are successfully synthesized [4-5]. Moreover, cubanes can attach to each other via covalent bonds and form oligomers and polymers. Theoretical calculations [6-7] predict stability of the family of one-, two- and three-dimensional nanostructures, built from cubane units. They can demonstrate metallic, semiconducting, dielectric and superconducting properties [8-9], related with remarkable electronic structure of cubane molecule. The simplest members of the cubane-based compounds are linear oligomer chains, which are recently identified using X-ray diffraction [10].

Here we present theoretical study of the influence of chemical functionalization on the electronic structure and ballistic transport through the cubane chains. Small radicals N, O, OH, CN, NO, CO, NH, NH_2, NO_2, CH_3, COOH are considered as a functional groups. Optimal chains geometries are defined within the density functional theory with B3LYP/6-311G level of theory as well as the nonorthogonal tight-binding model [11]. The electronic transmission and density of states are calculated in the frame of the non-equilibrium Green's functions method, combined with the extended Hückel approach [12].

We obtained that the cubane-based chains can be functionalized only using single-valence radicals. Functionalization leads to drastic reduction of the semiconducting gap from 4.70 eV for initial chain to 0.38 eV for NO-substituted chain. So, the chemical doping provides the opportunity for synthesis the cubane-based nanostructures with engineering electronic properties.

The work was financially supported by Russian Foundation by Basic Research (grant N. 14-02-31416 mol_a).

References

1. Li and S. L. Anderson, J. Phys. Chem. A (2003) **107**, 1162.
2. M. Maslov, D. A. Lobanov, A. I. Podlivaev, L. A. Openov, Phys. Sol. State (2009) **51**, 645.
3. Y. BENYEI, I. JALSOVSZKY, C. SLUGOVC, G. TRIMMEL, G. PELZL, A. VAJDA, N. EBER and K. FODOR-CSORBA, Liquid Crystals (2005) **32**, 197.
4. E. Eaton, J. Li, S. P. Upadhyaya, J. Org. Chem. (1995) **60**, 966.
5. E. Eaton, K. Pramod, T. Emrick, R. Gilardi, J. Am. Chem. Soc. (1999) **121**, 4111.
6. Valencia, A. H. Romero, M. Kiwi, R. Ramirez, A. Toro-Labbe, J. Chem. Phys. (2004) **121**, 9172.
7. Herrera, F. Valencia, A. H. Romero, M. Kiwi, R. Ramırez, A. Toro-Labbe, J. Mol. Struct.: THEOCHEM (2006) **769**, 183.
8. Valencia, A.H. Romero, M. Kiwi, R. Ramírez, A. Toro-Labbe, Phys. Rev. B (2005) **71**, 033410.
9. http://scitation.aip.org/content/aip/journal/jcp/118/7/10.1063/1.1536637
10. E. Eaton, K. Pramod, T. Emrick, R. Gilardi, J. Am. Chem. Soc. (1999) **121**, 4111.
11. P. Katin, M. M. Maslov, Russ. J. Phys. Chem. B (2011) **5**, 770.
12. Kienle, J. I. Cerda, A. W. Ghosh, J. Appl. Phys. (2006) **100**, 043714.

The production of polymer nanocomposites modified with carbon nanotubes and nonionic surfactants

Bogdanova S.A. [1] , *Gataoullin A.R.* [1] , *Zakirov I.M.* [1] , *Galyametdinov Yu.G.* [1]

polyswet@mail.ru
[1] Kazan National Research Technological University, Kazan, Russia

The creation of new polymer composite materials modified with carbon nanostructures (carbon nanotubes, fullerenes) is an important problem of modern material engineering and polymer science. For efficient polymer nanocomposite reinforcement a homogeneous distribution of nanoparticles in matrix is required. General problem is the tendency of nanotubes to agglomeration due to van der Waals forces, high specific surface energy and hydrophobic interactions. It makes difficult to realize a unique complex of carbon nanostructurs properties in polymer composites. In this regard, the development of technology providing carbon nanotubes dispersing in liquid components used in polymer materials production is of great technical importance.

In this work nonionic surfactants and their mixtures (alkylene oxides block-copolymers and nonylphenol ethoxylates) were used to disperse multilayer carbon nanotubes and to improve their compatibility with polymer matrix . Ultrasonic treatment of carbon nanomodifiers in liquid media (ingredients of composites formulation – solvents, softeners, oligomer systems, appreting and binding mixtures) at presence of the surfactants was used. The intensity of CNT dispersing and the stability of dispersions estimated by means of absorbtion spectrophotometry were shown to depend on the surfactants and CNT concentration, oxyethylating degree and the surfactants mixture content. Malvern Zetasizer Nano analyzer for particle size and zeta potential measurement of CNT was used for the dispersions colloid properties optimization. The structure of dispersions was studied by means of confocal microscopy on an LSM 510 META inverted microscope (Carl Zeiss). The maximum of aggregated nanostructures disintegration in the solutions was found out. CNT noncovalent adsorbtion modifying with the surfactants was confirmed with the help of dispersions surface tension measurement.

Stable concentrated CNT dispersions were used for polymer materials production. Quality_control methods of nanomodifiers distribution in the composite have been developed. The studies of nanomodified polymers were performed on an EVO 50 XVP electronscanning microscope (Carl Zeiss) The analysis of the surface layer of the studied polymer samples was performed using atomicforce microscopy on a Solver BIO Olympus microscope (Nanotekhnologiya MDT).

The optimal conditions of new polymer nanocomposit materials production (epoxy composites, functionalized latexes, polyamide papers, semi-rigid and elastic polyurethane foams) with the improved physical and mechanical properties were worked out.

Acknoledgments

This work was supported by a grant from OPTEK

Asymmetric carbon nanotube network devices as room- temperature detectors of sub-THz radiation.

Gazaliev A.S. [1,2] , *Fedorov G.E.* [1,2,3] , *Gayduchenko I.A.* [1,2] , *Kardakova A.I.* [2] , *Voronov B.M.* [2] , *Finkel M.I.* [2] , *Goltsman G.N.* [2]

gazaliev@fnbic.ru

[1] National Research Center "Kurchatov Institute", Moscow, Russia

[2] Moscow State Pedagogical University, Moscow, Russia

[3] Moscow Institute of Physics and Technology (State University), Dolgoprudny, Russia

Development of sensitive room-temperature detectors of terahertz (THz) radiation is important for different applications ranging from security to medicine. The unique band structure of carbon nanotubes (CNT) makes them good candidates for optoelectronic applications in a wide frequency range. This work reports on the DC voltage response of asymmetric CNT devices to sub-THz radiation in the frequency range of 130 GHz to 400 GHz. Our structures are formed with CNT networks instead of individual CNTs so that effects probed are more generic and not caused by peculiarities of an individual nanoscale object. We conclude that the DC voltage response observed in our structures is mostly diode and thermal in origin.

Two main types of asymmetric devices are considered. The devices of the first type contain CNT's, which are over their length partially suspended and partially Van der Waals bonded to a SiO2 substrate, causing a difference in thermal contact [1]. Devices of the second type have source and drain contacts made of different material. We employ metals such as vanadium and gold or vanadium and palladium that have different work function so as the Schottky barriers at the CNT-metal interface have opposite bending and a p-n junction is formed along the nanotube due to the so called contact doping. The asymmetry incorporated into our devices may result in two effects that in turn may lead to observed DC voltage response to incident radiation at room temperature. One related to the nonlinearity of the IV curve – so called diode type response. Second, the thermal effect is related to the temperature gradient building up across the devices under the action of the radiation. Different heat sinking of CNTs by source and drain gives rise to temperature gradient and consequent thermoelectric power (TEP) as such a device is exposed to the sub-THz radiation. We may conclude that the observed response of our asymmetric devices can be explained by combination of diode and thermal effects. . Sign of the DC signal, its power and gate voltage dependence observed at room temperature are consistent with this scenario.

References

1. Fedorov, A. Kardakova, I. Gayduchenko, I. Charayev, B. M. Voronov, M. Finkel, T. M. Klapwijk, S. Morozov, M. Presniakov, I. Bobrinetskiy, R. Ibragimov and G. Goltsman, Appl. Phys. Lett. (2013), **103**, 181121

Detonation nanodiamonds with surface modified with lanthanide ions

Aleksenskii A.E. [1] *, Zamoryanskaya M.V.* [1] *, Iudina E.B.* [2] *, Vul A.Ya.* [1]

electa@yandex.ru

[1] Ioffe Institute, Saint-Petersburg, Russia

[2] Saint-Petersburg State Institute of Technology (Technical University), Russia

Hybrid nanomaterials with crystalline nanoparticles decorated by various atomic species having specific properties are promising nanostructures for various applications in modern engineering and biotechnology. It was recently shown that detonation nanodiamonds (DND) with surface terminated both by oxygen-containing functional groups and hydrogen atoms can be modified by Cu using the ion exchange in a mixture of water suspension of DND and water solution of copper acetate according to a method proposed at Ioffe Institute [1,2]

In this research we submit results of surface modification of single detonation nanodiamond particles with Eu and Gd ions. The modification were made by evaporation of 4nm DND suspension with negative zeta potential [3] mixed with the metal nitrates solution in rotary evaporator. The main advantage of such method is law-rate of nitrates hydrolysis that prevents the side-effects such as oxysalts formation.

Elemental analysis of DND modified by Eu demonstrate uniform impurity distribution over ND powder. Study of magnetic susceptibility confirmed surface modification of DND by Gd^{3+} ions.

The XRD study revealed that upon modification DND crystal lattice remained unchanged.

The study was partly supported by the Russian Scientific Foundation (project14-13-00795). Special acknowledgments are extended to Kazuyuki Takai (Hosei University, Koganei, Tokyo, Japan) for magnetic susceptibility measurements and to Pavlov S.I. (Ioffe Institute) for SEM measurements.

References

1. A.E. Aleksenskii, M.A. Yagovkina, A.Y. Vul', Phys. Solid State (2004), **V.46**, 685.
2. A.I. Shames, A.M. Panich, V.Yu. Osipov, A. E. Aleksenskiy, A.Ya. Vul', T. Enoki, K. Takai, J. Appl. Phys. (2010), **V.107**, 014318.
3. A.E. Aleksenskii, E.D. Eydelman, A.Ya. Vul', Nanoscience Nanotechnology Lett. (2011), **V.3**, 68.

Field emission from a pointed emitter based on graphene films on SiC

Jityaev I.L. [1] , *Rubashkina M.V.* [1] , *Magomednebiev Z.M.* [1]

jityaev.igor@gmail.com

[1] Institute of Nanotechnologies, Electronics, and Electronic Equipment Engineering, Southern Federal University, Taganrog, Russia

Field-emission cathodes is promising sources of free electrons. You need to create a high electric field strength at the surface for the start of emissions. Application of the tip field emission cathodes with nanometer rounding-off radius of the top allow to achieve high values of the field strength at low voltages [1].

Material of a field emission cathode has great influence on the field emission. Graphene on silicon carbide is applied in our work. Graphene is one of nanocarbon materials, has unique electrical, mechanical and temperature properties. Silicon carbide is a chemical and radiation resistant high-temperature material. As a result cathodes based on silicon carbide with graphene films are promising elements for vacuum electronics.

In this paper we study field emission cathodes cathodes based on silicon carbide with a graphene film on the surface. The samples of silicon carbide doped with nitrogen were prepared to study the electron emission. Then, a point field emission cathodes height of 1 μm and rounding-off radius of 10-40 nm was formed from silicon carbide. Field emission cathodes was formed without lithography method by using a focused ion beams on a pre-designed graphic templates [2]. It is possible to reduce the number of operations in the manufacture of cathodes and reduce the complexity of the process Graphene on the silicon carbide surface was formed by thermal degradation of silicon carbide in a vacuum [3]. This method allows to obtain a graphene on the entire surface of the sample with good adhesive properties to the substrate. Current-voltage characteristics were measured after field emission cathodes manufacturing. The interelectrode gap was 1-5 nm. I-V characteristics showed that the emission from cathodes based on graphene begins at 2 volts. We received currents degree of 10^{-8} A at voltages up to 10 V. I-V characteristics in the Fowler-Nordheim coordinates was built based on the experimental I-V characteristics. The results of theoretical calculations showed that the work function is about 0.75 eV.

Thus, studies have shown that a low work function and low threshold voltage are typical for field emission structures of silicon carbide with graphene films. This confirmed the promising of applications of these materials in micro- and nanoelectronics devices.

This work was supported by The Ministry of Education and Science of Russian Federation, the State Task in the Sphere of Scientific Activities (project no.16.1154.2014/K). The equipment of the Sharing Center and REC “Nanotechnologies” of Southern Federal University was used for this study.

References

1. Svetlichnyi A.M., Ageev O.A., Volkov E.Yu., Jityaev I.L. and Dem'yanenko M.V. Applied Mechanics and Materials (2015) **752-753**, 163.
2. Ageev O.A., Kolomiytsev A.S., Konoplev B.G., Semiconductors (2011) **45**, 1709.
3. Konakova R.V., Kolomys O.F., Okhrimenko O.B., Strelchuk V.V., Volkov E.Yu., Grigoriev M.N., Svetlichnyi A.M., Spiridonov O.B. Semiconductors (2013) **47**, 812.

The research of synthesis parameters in CVD of graphene on copper

Kostogrud I.A. [1,2] , *Smovzh D.V.* [1]

ikostogrud@gmail.com

[1] Institute of Thermophysics SB RAS, Novosibirsk, Russia

[2] Novosibirsk State University Novosibirsk, Russia

The most promising, relatively inexpensive and available method for obtaining a high quality graphene is chemical vapor deposition (CVD) on the surface of transition metals such as Ni, Pd, Ru, Ir, Cu, etc. The advantage of this method is scalability of samples area. The difficulties of this method are associated with a single layer growth control and with the presence of defects in obtained material [1].

In this work the experimental investigation of parameters determining the kinetics of graphene synthesis, obtained using the CVD method on copper, was conducted.

The synthesis of graphene was performed in the thermal reactor represented in Fig.1 under atmospheric pressure on copper substrates. Methane was used as a precursor gas, copper foil AlfaAesar 25 μm thick was used as a substrate. The experiments were performed at different temperatures (860 – 1070 °C), with the different composition of gas mixture (Ar+H2+CH4), with the different exposure times (5 – 40 min.) and at different rates of samples cooling. The analysis of synthesized films was conducted using the optical microscopy, Raman spectroscopy and scanning electron microscopy.

The samples of single-layer and multilayer graphene with the different extent of surface coverage were obtained. It was shown that parameters governing the synthesis are the temperature of the synthesis, the concentration of methane and the dynamics of samples cooling.

Fig.1.Schematic view of a setup for CVD synthesis.

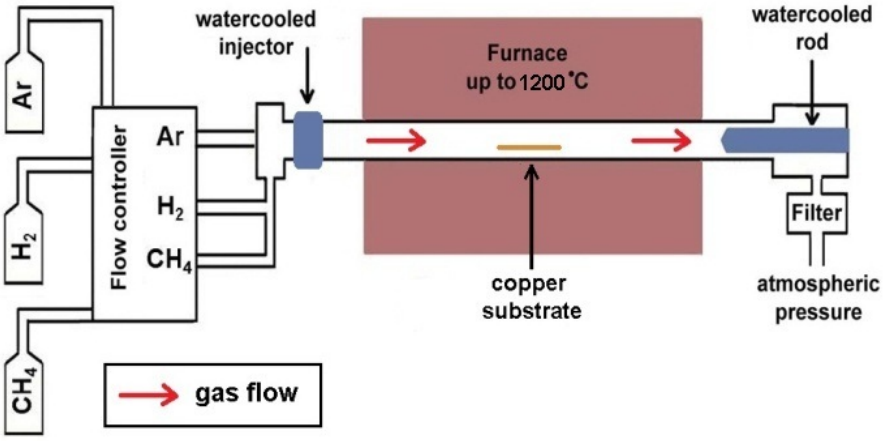

References

1. Mattevi C., Kim H., Chhowalla M. A review of chemical vapour deposition of graphene on copper // J. Mater. Chem. - 2011. – Vol. 21. – P. 3324–3334.

Graphite oxide surface and bulk chemical composition by Auger electron spectroscopy

Mikoushkin V.M. [1] , *Kriukov A.S.* [1] , *Shnitov V.V.* [1] , *Solonitsyna A.P.* [1] , *Fedorov V.Yu.* [1] , *Dideikin A.T.* [1] , *Sakseev D.A.* [1] , *Vilkov O.Yu.* [2] , *Lavchiev V.M.* [3]

Emreu30@gmail.com

[1] Ioffe Institute, St.Petersburg, Russia

[2] St. Petersburg State University, St. Petersburg, Russia

[3] Institute for Microelectronics and Microsensors, Johannes Kepler University, Linz, Austria

Graphite oxide (GO) has attracted a great interest last decades due to its unique properties and important applications [1]. The GO peculiarity is that its electronic and optical properties strongly depend on chemical composition. X-ray photoelectron spectroscopy methods with using both Al/Mg K_α X-ray sources and synchrotron radiation (SR) are considered to be one of the most efficient quantitative methods for GO chemical composition diagnostics. The quanta energies of the X-ray sources (1486.6/1253.6 eV) provide information on several atomic layers and characterize the GO bulk, whereas typical SR quanta energies (< 600 eV) give information mainly on the GO surface. Therefore the problem arises whether the chemical compositions of the surface and bulk GO layers are identical and these methods provide the same information. The result of this research is that GO surface and bulk compositions are completely different.

GO chemical and elemental compositions were studied by Auger techniques (see this book) which is based on the Auger transition energies C*KVV* and O*KVV* of the GO main functional groups obtained in SR experiment [2]. Table 1 presents chemical and elemental compositions of the GO film obtained in the analysis of the carbon and oxygen spectra and the corresponding Auger electron mean free paths λ [3] which characterize the analyzed depth of GO film. These data show that the C*KVV* line characterizes mainly the surface monolayer (1 nm), while O*KVV* line includes large contribution of the bulk. Both lines in Table 1 give similar elemental composition, whereas the chemical content proved to be essentially different, e.g. 25 and 37 at % for the COC group. Taking into account relation $\lambda_O[COC]_O = \lambda_C[COC]_C + (\lambda_O-\lambda_C)*[COC]_X$, obtain the content of COC group in the bulk layer: $[COC]_X$ = 66 at %. Thus the minor phase (COC) of the GO surface (25 at %) appears to be dominating in the bulk (66 at %). Depletion of the epoxide group on the surface can be caused by different efficiency of the GO group formation on the surface and in the bulk or by surface degradation under natural light.

Table 1. GO film chemical and elemental composition.

	C*KVV*	O*KVV*
E_k, eV	270	515
λ, nm	1.7	2.4
[C-OH]:[C-O-C]	75 : 25	63 : 37
[C] : [O] : [H]	42:33:25	46:33:21

References

1. H. Wu, T. Yu, Z.X. Shen. J. Appl. Phys. 108 (2010) 071301.
2. M. Mikoushkin, A.S. Kriukov, V.V. Shnitov, A.P. Solonitsyna, V.Yu. Fedorov, A. T. Dideykin, D.A. Sakseev, O.Yu. Vilkov, V.M. Lavchiev, J. Electron. Spectrosc. Relat. Phenom. (2015) 199, 51.
3. A. Kolmakov, D.A. Dikin, L.J. Cote, J. Huang, M.K. Abyaneh, M. Amati, L. Gregoratti, S. Günther, M. Kiskinova, Nature Nanotechnology 6 (2011)

Modification of EL phosphor surface with shungite carbon

Matveychikova P.V. [1] , *Mjakin S.V.* [1] , *Sychov M.M.* [1] , *Ogurtsov K.A.* [1] , *Rozhkova N.N.* [2] , *Vasina E.S.* [1]

matveychikovapolina@gmail.com

[1] St. Petersburg state institute of technology (technical university), St. Petersburg, Russia

[2] Institute of geology, Karelian scientific center, Petrozavodsk, Russia

The studied electrophosphor of structure of AIIBVI finds broad application as a part of electroluminescent light sources (ELS) used in manufacturing techniques of displays in production of flexible luminescent panels, and also in other industries. For ensuring effective and long-term work of a phosphor activators and the special alloying components are entered into its structure. Along with an alloying apply modifying of a surface.

In [1] it was shown that introduction to structure of phosphors of the shungite carbon (SC) – the natural nanostructured carbon material possessing fuller similar structure and high activity of a surface – allows to regulate the maintenance of the superficial centers, important for an electroluminescence, in particular the Brensted of acid groups with a pKa 2.1 … 2.5.

In this work research of influence of modifying of a surface of an ZnS:Cu electrophosphor was conducted by nanoclusters of the shungite carbon. Modification of surface was carried out by sedimentation of nanoparticles of SC with a size about 50 nanometers from steady water dispersions with various concentration of SC according to the technique described in [2]. Then on the basis of the modified phosphor ELS were made and their spectral and brightness characteristics are measured.

Research showed that sedimentation of SC on a surface of a phosphor leads to change of characteristics of an electrophosphor. About increase in quantity of the entered SC decrease in the general brightness of an electroluminescence of samples that can be caused by opacity of the put layer is observed. However, change of spectral strips of a luminescence that is connected with reduction of the centers with a pKa 2.5 corresponding to CuxS-H groups and increase in the centers with a pKa 2.1 is revealed. - characteristic for SC surface. Change of intensity of a "blue" band of a luminescence with λ = 455 nanometers (corresponding to associates of two Cu atoms one of which is in an interstitial position of a crystal lattice) and 490-510 nanometers (corresponding to Cu atoms substituting zinc in combination with vacancies of sulfur and impurity of chlorine) depending on quantity of the entered SC is observed. It testifies interaction with SC - carbon is fixed on rather more hydrophobic sites of a surface of a ZnS-phosphor (phase CuxS sites). In general the obtained data allow to draw a conclusion on possibility of regulation of the spectral and brightness characteristics of the studied electrophosphor by introduction of microquantities of the available modifying additive that is the promising in terms of modern technology of EL.

This work was supported by Russian fund for basic research, grant 14-07-00277, Ministry of Education of the Russian Federation (Agreement 14.574.21.0002, ID RFMEFI57414X0002) and Program No.7 of the Chemistry and Materials Sciences Division of the Russian Academy of Sciences.

References

1. Volodina O.V. et al. CSYS’2013, St.Petersburg, p.42.
2. N.N.Rozhkova, Shungite Nanocarbon, Karelian Research Center RAS, 2011.100 p.

Structural and electrical properties investigation of “fullerene-quantum dots” composite materials

Pavlov S.I. [1] , *Kirilenko D.A.* [1] , *Nashchekin A.V.* [1] , *Sokolov R.V.* [1]

Pavlov_Sergey87@mail.ru
[1] Ioffe Institute, Saint-Petersburg, Russia

Composites based on colloidal quantum dots (QD) coupled with fullerenes are promising materials for optoelectronic devices. QD have some advantages, such as the tunability of the band gap by controlling the QDs size or composition [1], high extinction coefficient and large intrinsic dipole moment favouring charge separation [2], potential for generating multiple electron–hole pairs with a single photon. At the same time, fullerenes can be used for effective charge separation and transfer because of its high acceptor properties.

It’s known [3] that being dissolved in mixed solvents fullerenes form stable clusters with sizes up to several hundred nanometres. Furthermore, mixing fullerene solution with QD solution lead to forming the composite material.

In this work toluene solution of colloidal QD with known concentration was mixed with C60 toluene solution. The obtained solution was slowly injected in larger amount of acetonitrile to form composite clusters. Clusters were deposited by electrophoretic deposition onto glass substrate with transparent ITO electrode forming films with thickness up to a few microns. SEM images show that clusters size is about 100 nm and different shape for composite and of pure fullerene cluster. TEM study including electron diffraction show that pure fullerene clusters have FCC crystalline structure, but composite clusters are amorphous. TEM and EDS measurements reveal presence of QDs in single cluster (fig. 1, left) [4].

I-V characteristics were measured in “sandwich” configuration. Aluminium contact layer was deposited on composite film by vacuum thermal evaporation. In C_{60}/QD composite value of measured current was an order of magnitude higher, then in pure C_{60} film (fig. 1, right) and increased when affected by visible spectral range of light. This effect can be explained by high extinction coefficient of QDs and effective charge separation and transfer by fullerenes.

Such composites are perspective for optoelectronics in wide spectral range as organic light sensitive material with tuneable absorption depending on QDs composition.

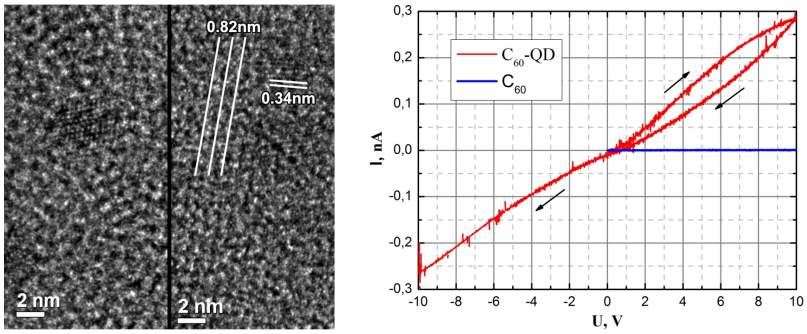

Fig.1. Structure (left) and current-voltage characteristics (right) of composite films

References

1. Kongkanand, K. Tvrdy, K. Takechi, M. Kuno, P.V. Kamat, J. Am. Chem. Soc. (2008),130, 4007.
2. W.W. Yu, L. Qu, W. Guo, X. Peng, Chem Mater. (2003), 15, 2854
3. G. Alargova, S. Deguchi and K. Tsujii, J. Am. Chem. Soc. (2001), 123, 10460.
4. I. Pavlov, D. A. Kirilenko, A. V. Nashchekin, et al. Tech. Phys. Lett. (2015), 41, 4, 33.

Spin- and angle-resolved photoelectron spectroscopy as the method for investigation of the electronic and spin structure of graphene

Rybkina A.A. [1] , *Rybkin A.G.* [1] , *Klimovskikh I.I.* [1] , *Filianina M.V.* [1] , *Pudikov D.A.* [1] , *Zhizhin E.V.* [1] , *Shikin A.M.* [1]

rybkina-anna@bk.ru
[1] Saint Petersburg State University, Saint Petersburg 198504, Russia

Photoelectron spectroscopy (PES) is one of modern methods for investigation of occupied electronic states of solids including additional information about many-electron and quasiparticle effects. Photoeffect is a basis of this method. Electron in an occupied state can be excited to unoccupied state by photon. If the energy of photon $\hbar\omega$ is larger than a work function of solid some electrons can leave a solid and then can be registered. Using of the synchrotron radiation is prevailing last time. Ultrarelativistic charged particle motion in the storage ring leads to the synchrotron radiation which allows to achieve a monochromatic radiation with a high energy resolution and a high intensity during registration of photoelectron energy distribution [1,2].

Angle-resolved photoelectron spectroscopy (ARPES) is widespread method for measurement of dispersion dependences and symmetry of energy bands of solid (see fig. 1). Basically this method has a conservation of parallel to the surface component of quasimomentum of photoelectron when overcoming the potential barrier. We can investigate features of the electronic structure of graphene when measuring dispersion dependences of electronic states in different directions of surface Brillouin zone.

Spin-resolved ARPES experiments allow us to investigate the spin structure of surfaces and solids (see fig. 1). Mott detector is used in this method for detection of spin projections of photoelectrons. In this detector beam of photoelectrons is accelerated to high energies and then scattered on a heavy-element scattering target and electrons are detected by two channeltrons. This allows an effective separation of the spin-polarized electron beam into two channels: spin-up and spin-down electrons [3]. So, we can analyse the spin-polarization and spin-splitting in 2D materials, such as graphene. Rashba spin-orbit splitting of π states in graphene on top of different substrates was demonstrated in our work.

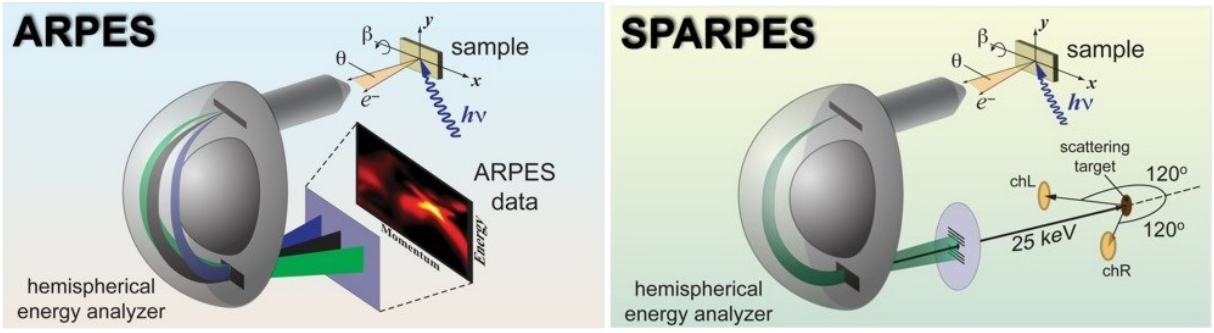

Fig. 1. Sketch of ARPES and spin-resolved ARPES measurements [from http://www.fhi-berlin.mpg.de/pc/horn/photoelectronspecscop.html].

References

1. Hüfner. Photoelectron spectroscopy: principles and applications. — Berlin Heidelberg: Springer-Verlag, 1995.
2. A.M. Shikin. Interaction of photons and electrons with solid. - Saint Petersburg: VVM, 2008.
3. D. Johnson, Rep. Prog. Phys. (1997) **60**, 1217

Definition sterically available groups of detonation nanodiamonds.

Shumilov F.A [1] *, Kalinin A.V.* [1] *, Choreva A.Kh.* [1]

Itachi16@mail.ru

[1] S.V.Lebedev Research Institute for Synthetic Rubber, Saint-Petersburg, Russia

The use of detonation nanodiamonds (DNA) is limited with the possibility of receiving ones with Characteristics set in advance.The main ways to produce DNA with set parameters is detonation synthesis control [1] or, which is more available in practice, modification of the DNA particles' surface. That is why it is clearly necessary to represent a surface character– quantity and the nature of functional groups.

As a rule, functional superficial groups are determined by the liquid- and solid-state NMR methods and the infrared spectroscopy method. From the point of view of practice, the disadvantage of application of these methods is the fact it gives information about all existing functional groups into volume of a sample. However, not all registered functional groups are on THE surface of particles' units. The part of these groups is in a latent state into volume of indestructible units. In addition, it is impossible to define a ratio of latent and interface groups quantitatively. In this work we represent a definition technique of the interface functional groups. It should be noted that from a large number of various functional groups on a surface of the DNA particles only groups with a labile proton are strictly established. As these groups are used for chemical modification of a surface, the technique developed by us is focused on them.

The known reactions offered by Grinyar are the basis for the technique.

$$CH_3MgI + R'OH \rightarrow CH_4\uparrow + R'OMgI$$

These reactions are put in the basis of the Chugayev-Tserevitinov's method of measurement of groups with a labile proton in solutions of organic compounds. This method was modified by us to define groups with a labile proton on the interface surface of nanocarbons powders. Such approach allows to consider the difficult structure of DNA units and to make quantitative modification, i.e. to receive a surface with in advance set characteristics.

References

1. P. Voznyakovskii, V.Yu. Dolmatov and F.A. Shumilov, Detonation synthesis of nanodiamonds. Control problems // Journal of SuperHard Materials, 2014. -**V.36**, - №3 - p.165-170

Carbon nanotube based conductive coating for biomedical use

Stepanova T.S. [1,2] , *Fedorov G.E.* [1,2] , *Gayduchenko I.A.* [2] , *Presnyakov M.* [2] , *Khailov N.A.* [2]

tanja.stepanova36@gmail.com

[1] Moscow Institute of Physics and Technology (State University), Dolgoprudny, Russia

[2] National Research Center "Kurchatov Institute", Moscow, Russia

We report on fabrication and investigation of transparent and conductive structures based on carbon nanotubes (CNT) that may be used as a sensitive element in biosensor devices. CNTs were synthesized by CVD method on silicon and quartz substrates using different catalyst. First the morphology and characteristics of the films were investigated by scanning electron microscopy (SEM), atomic force microscopy (AFM) and Raman spectroscopy. It was found that most of the CNTs forming the synthesized film are a single-wall CNTs having a diameter of 1.0 to 2.5 nm. The resistance of the film depends on the composition of the catalyst mixture; the best result is 500 ohm/square.

Next, we have conducted research work on non-covalent functionalization of our nanotube films with different pairs of antigen / antibody. Non-covalent binding is preferable in terms of film characteristics as compared to the covalent one. Results of enzyme-linked immunosorbent assay (ELISA) showed good levels of antibody binding to CNT films. We found a correlation between the adsorption and conductivity of the films.

Another perspective way of using conductive CNT-based films is creation of the biocompatible multi electrode systems for the investigation the neuronal cell cultures. In this case, the transparency of such coating provides the ability to control the proliferation and differentiation of cells in real time.

Structural features and sorption properties of shungite

Sukhinina N.S. [1] , *Khodos I.I.* [2] , *Zverkova I.I.* [1] , *Turanov A.N.* [1] , *Karandashev V.K.* [2] , *Masalov V.M.* [1] , *Emelchenko G.A.* [1]

suhinina@issp.ac.ru
[1] Institute of Solid State Physics RAS, Chernogolovka, Russia
[2] Institute of Microelectronics Technology and High Purity Materials RAS, Chernogolovka, Russia

Shungite is a natural mined in Karelia material formed by a carbonization of hydrocarbons. In addition to carbon shungites can contain silicates and carbonates [1], which cause different properties and a structure of samples. By its morphology, carbon of shungite has many forms. There are several distinct types of structures: globules, stacks, scales, films [2]. A molecular shungite structure is presented by a wide range of solid carbon from a graphite-like structure to close glass-like carbon [3]. Nanoscale structural elements of shungites include fullerene-like particles, nanotubes, onion-like structures, ultrafine diamond which are differed by a high surface area and a reactivity [4].

In this paper structural features of shungites from two different occurrences (Nigozero, Shunga) and their sorption effectiveness relative to uranium and associated elements have been studied. These shungites comprised a different carbon contain on their composition (~ 20 and ~ 90 wt. %). The first sample has heterogeneous composition: C - 12-30 wt. %, Si - 16-21 wt. %, O - 44-50 wt. %, Al - ~ 5 wt. %, other elements have less than 2 wt. %. According to data of X-ray diffraction phases of chamosite, quartz, albite, et al. are present in shungite. Another sample contains carbon up 98 wt. %. Preliminary experiments on the infiltration promising sorbent tetraoctyldiglycolamide (TODGA) [5] by shungite demonstrated a high sorption efficiency of the latter compared to the previously studied materials. SEM-, HRTEM-images and the electron diffraction pattern of shungite are showed on Fig. 1.

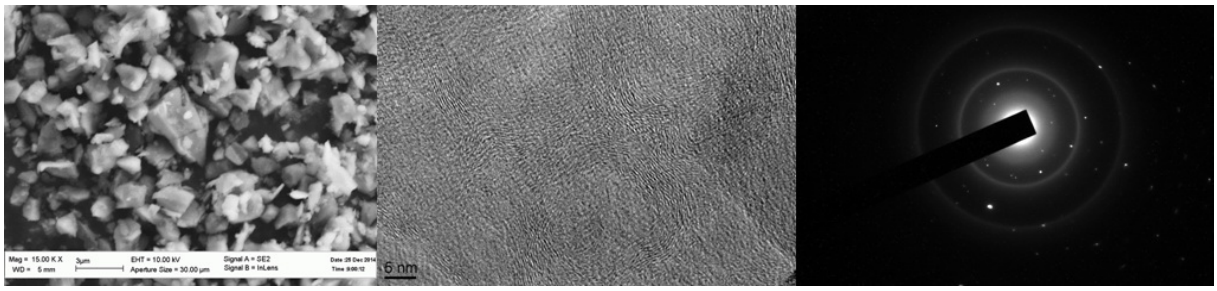

Fig.1. Common view (SEM, left), high resolution TEM image (middle) and the electron diffraction pattern (right) of shungite.

References

1. Yu.K. Kalinin and V.V. Kovalevski, Geology and useful minerals of Karelia (in Russian) (2014), **17**, 94.
2. V.V. Kovalevski, Zhurnal neorganicheskoi khimii (in Russian) (1994), **39**, 31.
3. Yu.K. Kalinin, Uglerodsoderzhaschie shungitovye porody i ih prakticheskoe ispolzovanie (dissertation) (2002) (in Russian).
4. N.N. Rozhkova, Perspectives of fullerene nanotechnology, ed. E. Osawa, Dordrecht (2002), 237.
5. A.N. Turanov, V.K. Karandashev, N.S. Sukhinina, V.M. Masalov, A.A. Zhokhov and G.A. Emelchenko, RSC Advances (2015), **5**, 529.

Optimization of multitip field emitters with fullerene protecting coatings

Taradaev E.P. [1] , *Sominski G.G.* [1] , *Tumareva T.A.* [1]

evgeny_tar@hotmail.com
[1] St. Petersburg State Polytechnical University, Russia

Field emitters are very attractive electron sources that can be used for fabrication of different vacuum electron devices such as high voltage microwave electron devices and X-ray sources. However, they have not found widespread application in these applications because of several major challenges, the most significant of which are low durability at technical vacuum conditions and obtaining high currents. Performed early investigations [1, 2] showed that developed multitip cathodes with protective fullerene coatings can be used in high voltage devices operating at technical vacuum conditions. However, the effect of their surface morphology on field emission current is not fully understood. In the main, the various theoretical calculations of average field emission current density given in some of the literature were made for carbon nanotubes [3,4]. CNT were simulated by long conducting cylinders closed with a hemisphere. In this paper we investigate the effect of surface morphology cathodes with different form of tips on cathode emission current.

Tips were simulated by spherical tip cone. Vertically aligned tips of uniform height H and radius R were placed on a cathode that was separated from the grounded anode by distance 1.5 mm. A negative potential was applied to the cathode. Emission area of all the cathodes were 0.2 cm^2. Calculations were made for different work functions 4.1 eV ≤ eφ ≤ 5.3 eV. Maximum work function 5.3 eV was corresponded to the work function of fullerene coating. Minimum work function 4.1 eV was corresponded to the work function of fullerene coating activated with potassium ions. Radius of the tips was varied from 5 nm to 25 nm. Choice of the radius was corresponded to the original silicon structure and structure with deposited metal-fullerene coating. Our array of tips was simulated for inter-tips separations S ranging from 5 to 720 μm. Calculations were made for height of the tips ranging from 10 to 60 μm. Multitips cathodes were simulated in 3D in COMSOL software. The electric fields, the field emission currents density of the tips, average emission current density on the surface and full currents were calculated.

Calculations showed that maximum emission current can be obtained when the inter-tip separation approaches two times the tip height. Calculation showed that the emission current could be increased if height of tip was increased. Also calculation demonstrated that such multitips field emitters can provide necessary emission current for vacuum electronic devices. Calculation data are in reasonable agreement with the results of the experiment.

References

1. G. Sominski, E.P. Taradaev, T.A. Tumareva, M.V. Mishin, and A.N. Stepanova, Proc. of 39th Int. Conf. Infrared, Millimeter, and THz Waves, September 14-19, 2014), Tucson, USA, W5-P25.7.
2. G. Sominskii, T.A. Tumareva, E.P.Taradaev, M.V. Mishin, A.N. Stepanova, Technical Physics, 2015, 60, No1, 133.
3. M. D. Bel'skii, G. S. Bocharov, A. V. Eletskii, T. J. Sommerer, Technical Physics, 2010, 55, No2, 289.
4. G. S. Bocharov, A. V. Eletskii, T. J. Sommerer, Technical Physics, 2011, 56, No4, 540.

Synthesis and study of «detonation nanodiamond-pyrophosphatase» hybrid systems

Valueva A.V. [1] , *Yakovlev R.Yu.* [1]

anastacia.lithium90@gmail.com
[1] Pavlov Ryazan State Medical University, Ryazan, Russia

Calcium pyrophosphate deposition disease (CPDD) is a metabolic arthropathy caused by the deposition of calcium pyrophosphate dihydrate in and around joints. There has not been yet developed any effective therapy against it. Introduction of inorganic pyrophosphatase enzyme (PPase) to the body can become the promising solution to this problem because PPase hydrolyses the pyrophosphate into phosphate. However PPase is inactivated in the intercellular space. Therefore in order to increase the stability of PPase the development of hybrid system nanodiamond-PPase was suggested. Detonation nanodiamond (DND) is bio-compatible, non-toxic, can easily enter the cell and has high surface area with a lot of functional groups that allows easy chemical modification. This system may become an advanced solution to fight the CPDD.

A lot of factors has been studied that influence the properties of the hybrid system DND-PPase such as DND surface functionalization, aggregate's size, length of the linker chain between PPase and DND and also different immobilization methods (adsorption and covalent ones).

Different kinds of chemically modified DNDs were synthesized and characterized: hydrogenated (DND-H), oxidized (DND-COOH), aminated (DND-NH_2). For sorption immobilization of the PPase DND hydrosols of different particle size (up to 30, 50-70 and 200 nm correspondingly) were obtained. For covalent immobilization of the PPase the DND-NH_2 and DND grafted by hexamethylenediamine linker (DND-$(CH_2)_6NH_2$) hydrosols were used. It was found that the enzyme activity of the adsorbed PPase depends on the DND surface type. The samples of PPase adsorbed on DND-COOH and DND-H demonstrated the highest activity level (85-86% of native enzyme activity), while DND-NH_2 showed the lowest activity level (about 39%). It was found that DND-NH_2 particle size had nearly no influence on the PPase activity, while the optimal particle size for DND-H and DND-COOH was 70 nm. The increasing of particle size led to reduction of enzyme activity down to 24-29%. For the DND hydrosols with particle size of 20 nm it was impossible to determine the adsorbed PPase activity because of protein desorption. The covalent immobilization of PPase on aminated DND was performed by use of glutaraldehyde. It was found that in case of immobilization of PPase on DND-NH_2 up to 65% of enzyme activity remained, and up to 95% in case of DND-$(CH_2)_6NH_2$. Catalytical activity of the grafted PPase was higher in average compared to adsorbed PPase, and PPase activity completely retained with the use of linker. The study of DND-PPase conjugates thermostability at 65 and 75°C show that conjugates are inactivated deeper compared to the native enzyme. At the same time the denaturation kinetic constants for all the samples are comparable and at 75°C they are even lower for the conjugates than for the native PPase.

Therefore optimal particle sizes, surface chemistry and immobilization method to obtain the effective DND-PPase system were determined [1].

The authors thank E.V. Rodina Ph.D. and N.B. Leonidov D.Sc., Prof. for continuous support and helpful study discussion.

The study is maintained by RFBR grants №13-08-00647 and №14-03-00423.

References

1. Jakovlev R.Ju., Rodina E.V., Valueva A.V., Vorob'eva N.N., Lisichkin G.V., Leonidov N.B. RU2542411, 2013.

Fractal cluster formation in PVA cyano ethyl ester – $BaTiO_3$ nanocomposites

Krasovskii A.N. [1] , *Vasina E.S.* [2] , *Matveychikova P.V.* [2] , *Sychov M.M.* [2] , *Rozhkova N.N.* [3]

ledykatrin@mail.ru

[1] Institute for Analytical Instrumentation, Russian Academy of Sciences

[2] St. Petersburg State Institute of Technology, St.Petersburg, Russia

[3] Institute of Geology, Karelian Research Centre of Russian Academy of Sciences

The effect of submicron $BaTiO_3$ particles surface modification by the deposition of shungite carbon (SC) nanoclusters from aqueous suspensions on the structure and properties of dielectric composites obtained earlier [1] by incorporating 40%vol. modified $BaTiO_3$ particles into cyano ethyl ester of polyvinyl alcohol (CEPVA) matrix.

Raman scattering and SEM data show that SC deposition onto the filler surface significantly improves the uniformity of the composites compared with the use of non-modified $BaTiO_3$ probably due to enhanced interfacial interactions in the system.

The introduction of SC leads to the appearance of prominent peaks in the spatial correlation function g(R) for the distribution of filler particles on the composite surface (Fig. 1a) and aggregates of $BaTiO_3$ particles (Fig. 1c) as compared to the composite obtained in the absence of SC (Fig. 1b, 1d). This indicates an ordered distribution of particles with the formation of two spatial sublattices corresponding to the most probable distances $r_1 \approx 0.5$ mm and $r_2 \approx 0.8$ mm. Furthermore, an infinite fractal cluster of the particles with the fractal dimension $D = 1.92 \pm 0.04$ is formed featuring with g(R) decrease in to a minimum followed by its increase approaching the asymptote g (R) = 1 on the scale of the correlation length $\xi \approx 6.5$ m (Fig. 1d).

Moreover, SC incorporation in the optimal amount provides a sharp increase in the permittivity of the obtained composites (up to ~250 relating to ~150 for the non-modified $BaTiO_3$) that correlates with the observed extreme dependencies of the composite surface energy upon SC content. This is due to increased interface interactions during composite formation.

This work was supported by the Ministry of Education of the Russian Federation (Agreement 14.574.21.0002, ID RFMEFI57414X0002) and Program No.7 of the Chemistry and Materials Sciences Division of the Russian Academy of Sciences.

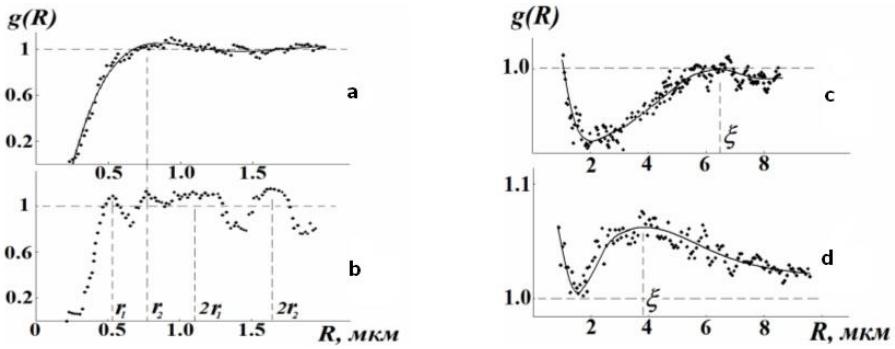

Fig. 1. The functions g (R) for BaTiO3 microparticles in composites without SC (a), with SC (b) and the functions g (R) for aggregates of BaTiO3 in composites without SC (c) and with SC (d)

References

1. Mjakin S.V., Kolovangina E.S., Pack V.G. et al. Advanced Carbon Nanostructures and Methods of Their Diagnostics, July 03, 2013 St.Petersburg, Russia, p.41

Electron-microscopy imaging of carbon nanotubes

Vysochanskiy N.A. [1] , *Fedorov G.E.* [2] , *Domantovskiy A.G.* [3]

n.vysochanskiy@yandex.ru

[1] Moscow Institute of Physics and Technology (State University), Moscow, Russia

[2] Laboratory of physics of nano and bio materials, NRC "Kurchatov Institute", Moscow, Russia

[3] Laboratory of radiation technologies, NRC "Kurchatov Institute", Moscow, Russia

It is known that single-walled carbon nanotubes produce a very bright contrast being scanned at low accelerating voltage (~1kV). Moreover they seem much wider then they really are (their apparent width is about 50nm while the nanotube diameter is about 2-3nm). Both effects are described by many authors, but complete qualitative description of this effect is still missing. Our goal was to summarize all described mechanisms of contrast and widening, to evaluate their contribution and to create a numerical model of the process. We believe that understanding the mechanisms responsible for the nanotube apparent width and brightness and, for example, the oxide thickness, will allow for using a nanotube as a local probe of the underlying dielectric parameters

Both contrast and width depend on many parameters. For our experiments we firstly have chosen two of them: the accelerating voltage and the silicon dioxide thickness as being the most significant and easy-controlled (our nanotubes were grown on a silicon substrate covered with a thermal oxide layer of different thickness varying from 50nm to 560nm). Results of the experiments and their analysis will be presented in this work.

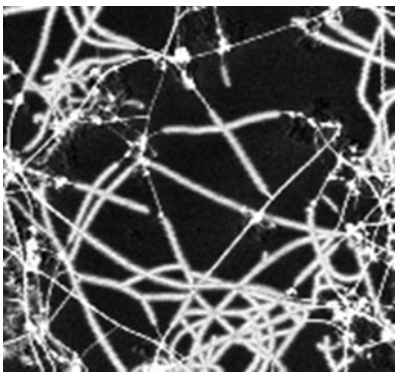

References

1. David C. Joy, Caroline S. Joy, *Micron* (1996), **27**, 247.
2. Homma, S. Suzuki, Y. Kobayashi, M. Nagase, D. Takagi, *Appl. Phys. Lett.* (2004), **84**, 1750
3. Y. Zhang, Y. Wei, L.A. Nagahara, I. Amlani, R.K. Tsui, *Nanotechnol.* (2006), **17**, 272.
4. Nojeh, B. Shan, K. Cho, R.F.W. Pease, *Phys. Rev. Lett.* (2006), **96**, 056802

Poster session 3:
Carbon Nanotubes.
Other nanocarbons.

Aluminum foil reinforced by carbon nanotubes

Alekseev A.V. [1] , *Predtechensky M.R.* [2]

artem.alekseev@ocsial.com

[1] International Science Centre of Thermal physics and Energetics (OCSiAl group), Novosibirsk, Russia
[2] Institute of Thermal physics SB RAS, Novosibirsk, Russia

Additives of carbon nanotubes can greatly improve the strength properties of aluminum and its alloys [1, 2, 3].

At present moment in most studies exactly powder metallurgy methods are used to make aluminum based composites reinforced by carbon nanotubes (CNT). These methods include manufacturing of powder compact followed by its hot deformation [4].

In our research the method of manufacturing Al-CNT composite by hot pressing and cold rolling was tried out.

Addition of one percent of multiwalled carbon nanotubes synthesized by OCSiAl provides significant increase of ultimate tensile strength of aluminum. Composite with a tensile strength as well as tensile strength of medium-strength aluminum alloy was made.

Analysis of fracture surface of aluminum reinforced by carbon nanotubes shows good adhesion between CNT and metal matrix.

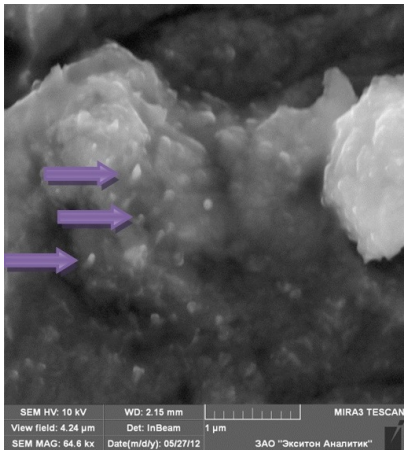

Fig. 1 Photo of fracture surface of composite Al + 1 %wt. CNT

References

1. *Hansang Kwon, Dae Hoon Park, Jean Franзois Silvain, Akira Kawasaki.* Investigation of carbon nanotube reinforced aluminum matrix composite materials, Composites Science and Technology (2010), Vol. 70, Issue 3, Page 546
2. *Srinivasa R. Bakshi, Arvind Agarwal*. An analysis of the factors affecting strengthening in carbon nanotube reinforced aluminum composites, Carbon (2011), Vol. 49, Issue 2, Page 533
3. *H.J. Choi, J.H. Shin, D.H. Bae.* Grain size effect on the strengthening behavior of aluminum-based composites containing multi-walled carbon nanotubes, Composites Science and Technology (2011), Vol. 71, Page 1699
4. *Sie Chin Tjong* Recent progress in development and properties of novel metal matrix nanocomposites reinforced with carbon nanotubes and graphene nanosheets, Materials Science and Engineering (2013) R 74, Page 281

Quantum-chemical researches of the interaction of carbon nanotubes with the harmful impurities combustive-lubricating materials

Zaporotskova I.V. [1] , *Arkharova I.V.* [1]

arkharova_irina@mail.ru
[1] Volgograd State University, Volgograd, Russia

During exploitation the oil changes its physical - chemical and performance properties ("aging") and its quality is become worse. During aging oil has been oxidated, and its acidity increases under the influence of other factors.

This paper presents the results of a research of CNTs interaction with some basic products, named sulfurous acid molecule, a hydroxyl group, oxides of iron and aluminum. These products made the quality of oil worse. So, if they will be interact with CNT it will be significantly better for aged oil. Calculations of the carbon nanotubes type zig - zag (6,0) with these molecules have been carried out using the framework of quantum - chemical method DFT (density functional theory) using the B3LYP functional. To exclude the influence of the edge effects of the boundaries of the clusters confined hydrogen atoms, played role of “pseudoatoms”.

We investigate the adsorption process on the single-walled carbon nanotubes surface of the various molecules (See Fig. 1). The process was simulated by step-by-step approaching (with a step of 0.1 Å) to the surface of carbon tube. The molecules approached to the nanotube surface with the oxygen atom located in the nearest to the tube variant of orientation.

Analysis of the results suggested us that the most active is the process of adsorption of iron oxides. Thus, the number of activity of CNTS on the selected fuel components can be formed as follows: FeO, Fe_2O_3, OH, H_2SO_3, Al_2O_3.

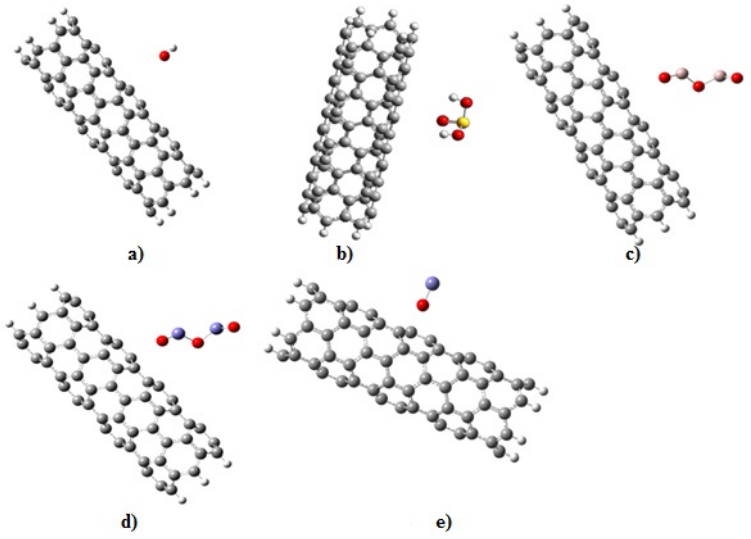

Figure 1. A molecular model of a cluster of single-layer carbon nanotubes (6,0), interacted with: a) OH-group; b) sulfurous acid molecule; c) the elementary fragment aluminum oxide Al_2O_3; d), e) elementary fragments of aliovalent oxides: Fe_2O_3; FeO respectively

Investigation of the sorption properties of carbon nanotubes with different concentration of boron impurities.

Boroznin S.V. [1] , *Zaporotskov P.A.* [1] , *Zaporotskova I.V.* [1] , *Polikarpova N.P.* [1]

sboroznin@mail.ru
[1] Volgograd State University, Volgograd, Russia

The discovery of carbon NTs in the early nineties was followed by intensive investigation into their electronic structure and energy spectrum parameters as well as physical and chemical properties. Due to high surface activity nanotubes can be used as basis for fabricating various types of composites.

However, apart from carbon nanotubes, current research focuses on theoretical and experimental investigation of non-carbon nanotubes, namely recently discovered boron-carbon nanotubes with different concentration of boron in it (25% or 50%).

In this paper we present the results of theoretical research into the properties of two types of boron-carbon nanotubes (BCNTs) within the framework of an ionic-built covalent-cyclic cluster model and an appropriately modified MNDO quantum chemical scheme as well as DFT method. We studied the mechanism of Cl, O and F atoms sorption on the external surface of single-walled arm-chair nanotubes (fig. 1). We defined the optimal geometry of the sorption complexes and obtained the sorption energy values. Further, we considered the possibility of multiple regular adsorption of these atoms on the BCNT surface. We modeled the process of superlattice formation by gas atoms above the nanotube surface. The electron density is located near the surface atoms of the tube.

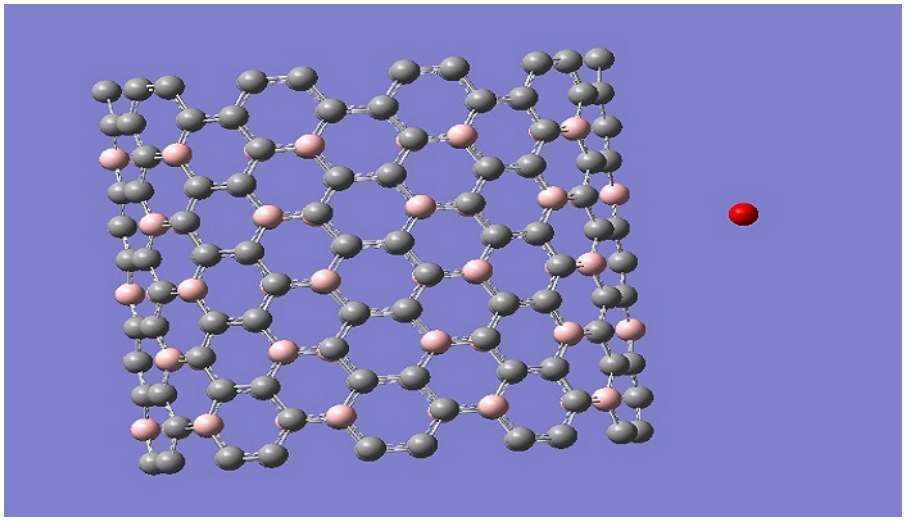

Figure 1.nanotube (10,10) with an absorbed oxygen atom on the nanotube surface

Low-temperature synthesis of CNTs by CVD from carbon monoxide

Mironov A.E. [1] *, Dubkov S.V.* [2] *, Sysa A.V.* [2] *, Gromov D.G.* [2] *, Belov A.N.* [2] *, Shaman Yu.P.* [3]

sv.dubkov@gmail.com

[1] University of Illinois, Urbana-Champaign, USA

[2] National Research University of Electronic Technology, Zelenograd, Russia

[3] Scientific Manufacturing Complex Technological Centre, Zelenograd, Russia

Carbon nanotubes are of great interest in research and development for more than 25 years [1]. Such attention is paid to this carbon material is due to the fact that they possess a number of interesting properties, such as ballistic conductivity, high thermal conductivity, low electron work function value and high strength characteristics. Variety of different properties allows you to find many ways of use for carbon structures, such as heavy-duty construction materials, diodes and transistors based on carbon nanotubes and graphene, emission cathodes [2].

Modern methods of obtaining carbon structure, allow many modifications of carbon with a sufficiently high degree of reproducibility. However, the temperature of such processes is usually about 600-700ºC that in some technologies, such as in integrated circuit technology is unacceptably high. The process temperature depends on the carbon-containing reagent, variety of such reagents is quite wide.

Another problem with the production of carbon nanostructures at low temperatures is the increase of amorphous component in the carbon residue. As it is shown in [3] by adding hydrogen to the carbonaceous reagent - solid-phased carbon yield is increased.

Previously, we have shown that during the thermodynamic simulation of the H_2 and CO gas mixture with increasing of hydrogen content in the gas mixture in dependence with the temperature of the system - has shown that the release of carbon is energetically favorable at temperatures about 100-300°C [4].

In this regard, this work is devoted to the development of the deposition of carbon nanotubes by chemical vapor deposition in the low temperature range of 300-500°C from carbonaceous mixture of CO + H_2 + Ar in order to identify the range of their sustainable form.

References

1. Iijima. Nature (1991) **354**, 56.
2. G. Rinzler, J.H. Hafner, P. Nikolaev, P. Nordlander, D.T. Colbert, R.E. Smalley, D. Tománek. Science (1995) **269**, 1550.
3. Wang, G. Cao. Adv. Mater (2008) **20**, 2251.
4. E. Mironov, D. G. Gromov, S. A. Gavrilov, V. A. Galperin. Russian Journal of Physical Chemistry A (2013) **87**, 63.

Magnesium spinel reinforced by carbon nanotubes

Duong T.T.T. [1] *, Zharikov E.V.* [1] *, Popova N.A.* [1] *, Faikov P.P.* [1]

duongtrannho2012@gmail.com

[1] D. Mendeleev University of Chemical Technology, Moscow, Russia.

Nowadays, there is a need to provide a material with specified properties: low density, thermal stability, sufficient strength, increased fracture toughness. Ceramic composite matrix containing carbon nanotubes (CNT)combines all of these properties [1].

Bringing CNT into ceramics gives significant improvement of characteristics of composite structural material due to special microstructure, chemical inertness and excellent mechanical properties [2].

It was demonstrated [3], that the 8% vol. of CNTs– alumina composite with significantly improved fracture toughness may be obtained by simple vacuum sintering.

Recently, carbon nanotube (up to 16.7 vol.% CNT) –magnesium aluminate spinel nanocomposites were obtained during hot-pressing method [4].

In present study for the first time a composite material based on magnesium aluminate spinel reinforced with a large amounts of nanotubes (by 30 vol. %) was fabricated using hot-pressing method.

The microstructure of composite samples was investigated by SEM — scanning electron microscopy (Jeol JSM-5910LV) and their microhardness was measured by Vickers hardness test.The microstructure of the composite at a magnification of 40,000 times shows that carbon nanotubes forming the frame structure binding the neighbor grains in the matrix of composite (Fig. 1).In addition,the nanotubes are agglomerated in the place of crystal defects and prevent from formingthe closed pores in the magnesium spinel matrix.

The results of characterization and photos of microstructure will be presented on wall poster.

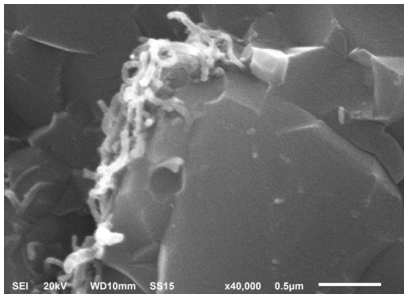

Fig.1. SEM -micrograph of magnesium spinel composite with carbon nanotubes

References

1. Carbon Nanotube Reinforced Composites: Metal and Ceramic Matrices Sie Chin Tjong, 242 p., May 2009
2. G. Yamamoto , K. Shirasu , T. Hashida , T.Takagi , Ji Won Suk , Jinho An, Richard D. Piner , Rodney S. Ruoff, Carbon 2011, P. 3709
3. Duong T.T.T**.,** Zharikov E.V., Popova N.A., Faikov P.P. , International conference «Advanced carbon nanostructures» (July 1-5, St. Petersburg, Russia): Book of abstracts. 2013. P. 214.
4. Peigney , S. Rul, F. Lef`evre-Schlick, C. Laurent . Journal of the European Ceramic Society 2007, vol. 27 (n° 5). P. 2183-2193.

ELECTROPHYSICAL STUDY OF METHYL METHACRYLATE REINFORCED WITH CARBON NANOTUBES

Zaporotskova I.V. [1] *, Belonenko M. B.* [1] *, Krutoyarov A. A.* [1] *, Elbakyan L.S.* [1]

lusniak-e@yandex.ru
[1] Volgograd, Russia

As it is known, carbon nanotubes can be used as additives in polymers to give them special mechanical properties. Formed in the polymer matrix the spatial mesh of the conductive chains of nanotubes can also lead to the emergence of new electrophysical properties of these polymer composites with low volume content of CNT [1]. We have investigated polymer material methyl methacrylate. It is used mainly in the form of plastic sheets, powders for molding and forming, surface coatings, pellicle, etc.. It was prepared a sample of methyl methacrylate, where as a reinforcing agent was taken a mixture containing 80 vol.% carbon nanotubes and 20 vol.% nanodispersed carbon. To the obtained samples were applied potential difference in the range of -1 V to 20 V with a frequency of 200 kHz, 300 kHz and 400 kHz. The potential difference was created by using two metal electrodes, between which was clamped the analyzed sample. It was discovered an unusual nonlinear dependence of the conductivity of the generated sample on the voltage (Fig. 1) and frequency. The theoretical explanation of the obtained regularities is given, which is based on the fact that incorporated in the matrix polymer nanotubes act as additional resistances that are connected in parallel to the existing grid resistance in the environment of the polymer.

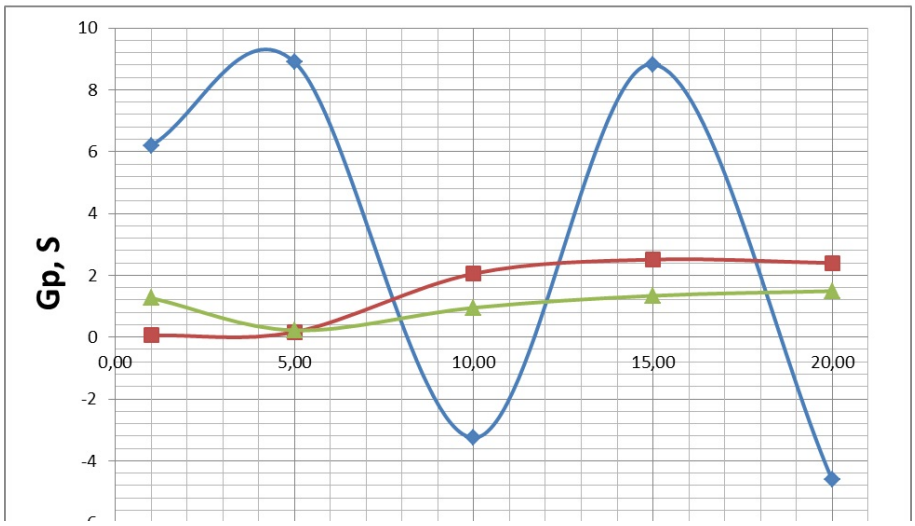

Fig. 1. The conductivity of the material at different values of a potential difference for frequencies above 200 kHz schedule blue color, 300 kHz schedule red color and 400 kHz schedule green color.

References

1. N. A. Drokin, Century A. Fedotov, D. A. Glushchenko, G. N. Churilov. Impedance spectroscopy of high molecular weight polyethylene with carbon nanotubes // solid state Physics, 2010, vol 52, ISS. 3, S. 607-611.

Spark plasma sintering simulation of alumina composite modified with carbon nanotubes

Fedosova N. A. [1] , *Koltsova E. M.* [1]

kolts@muctr.ru
[1] D. Mendeleyev University of Chemical Technology of Russia

Spark plasma sintering method is increasingly used for the production of composite ceramic materials. This sintering technique uses pulsed (on-off) directed electric current under low atmospheric pressure to perform high speed consolidation of the powder particles. Spark plasma sintering allows in a short time period obtain porous-free small-grained samples. High reproducibility of results is achieved by the complete controllability of sintering process parameters.

We obtained a high-density ceramic composite based alumina matrix reinforced with carbon nanotubes (20-50 %vol.) sintered by spark plasma sintering. The structure of the resulting material is tightly sintered alumina grains surrounded with carbon nanotubes. Nanotubes are homogeneously distributed in the bulk of composite. The fracture toughness of samples with 50% vol. nanotubes is approximately 3.3 times higher than samples of pure alumina, and the elastic modulus is 2.8 times higher. However, not all temperature conditions yielded nonporous material with improved strength characteristics. In order to determine the optimum parameters for the process of spark plasma sintering method a numerical simulation of the sintering process was carried out. To simulate a change in the porosity of the spark plasma sintering process the balance equation of the pore size (type Liouville equation) was used. The rate of change in pore size depends on the heating rate (for the pulse impact step) and on the maximum holding temperature (for holding step). Kinetic parameters of the rate of change in pore size depends on the amount of carbon nanotubes in the composite.

The sintering process was divided into two independent stages: stage with impact of pulsed electric current and holding stage at the maximum temperature. For each of these stages we made a mathematical description including the factors influencing the process. For the first stage of sintering process such parameter is the heating rate of the compact powder, for the second stage it is the holding temperature. The amount of carbon nanotubes is considered in both stages of the process.

For the numerical solution of the problem two approximation schemes were examined: the scheme "CABARET" and "Z-scheme". These schemes are used in solving problems of continuum mechanics. After investigating these schemes, it was found that "Z-scheme" is advantageous since it is absolutely stable and the scheme "CABARET" conditionally stable at a ratio of $\Delta t / h \leq 1$. Based on this we used "Z-scheme" as the most suitable scheme.

While developing the mathematical model we have introduced additional constants (12 constants). These new parameters are responsible for the specificity of the sintering process in more detail. The numerical values of the constants were found after analytical assessment. It is allowed us to describe a mathematical model more accurately at every stage of the sintering. The relative error on the output characteristic (final porosity) is 5%. Thus the developed mathematical model can be used to calculate the optimal parameters of the sintering process for the ceramic composite to improve its desired characteristics.

This work was supported by a grant RSF 14-19-00522.

Heterostructures of carbon nanotubes and few-layer molybdenum disulfide sheets

Golub A.S. [1] , *Zaikovskii V.I.* [2,3] , *Lenenko N.D.* [1]

golub@ineos.ac.ru
[1] Institute of Organoelement Compounds RAS, Moscow, Russia
[2] Institute of Catalysis SB RAS, Novosibirsk, Russia
[3] Novosibirsk State University, Novosibirsk, Russia

A novel convenient room-temperature method for surface covering of carbon nanotubes (CNTs) with few-layer MoS_2 shell is reported and discussed basing on TEM and XRD results. To obtain the target heterostructures, liquid-phase single-layer dispersions of molybdenum disulfide produced by chemical exfoliation of its lithium intercalate, $LiMoS_2$, were applied. After being brought in contact with CNTs, the dispersed MoS_2 particles tend to attach to the CNT surface. Upon the interaction of the components, MoS_2 layers evidently adjust their morphology to the shape of nanotubes, thus enveloping them so as the most of deposited sulfide particles make close contact with the outer layers of CNTs [1]. Measuring the interlayer distances in the vicinity of the MoS_2-CNT interface showed that deposited particles typically contain 1-3 MoS_2 layers (Fig.1).

The presence of cationic polymers containing polydiallyldimethylammonium units upon interaction of CNTs with MoS_2 single-layer dispersions was found to lead to the incorporation of polymer molecules in the shell in the form of 0.5 nm thick organic interlayers between the monolayers of MoS_2. This incorporation was found to occur due to ability of MoS_2 dispersions to interact with these polymers giving the structures with alternating sulfide and polymer layers [2].

The presented method has a great potential for designing other nanohybrid structures with participation of CNTs and layered metal sulfides.

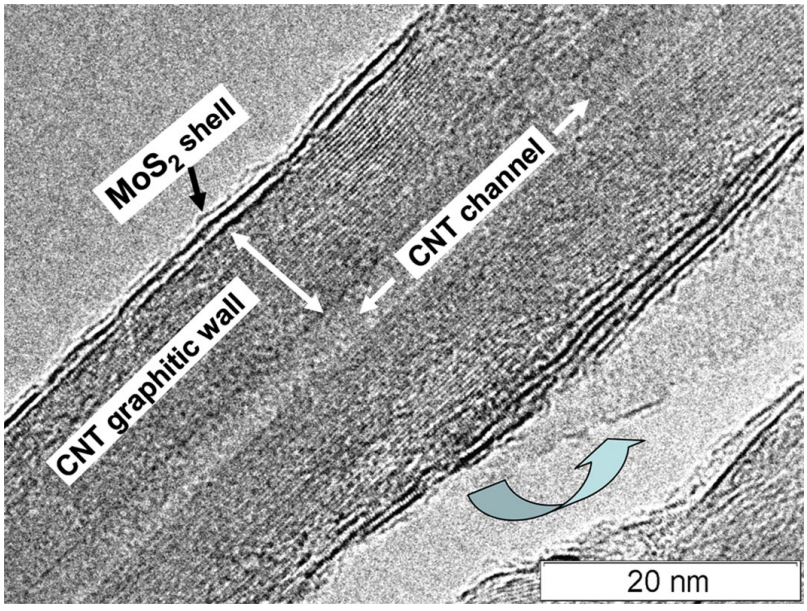

Fig. 1. HRTEM image of MoS_2-CNT heterostructure.

References

1. N.D. Lenenko, V.I. Zaikovskii, A.S. Golub. Superlatt. Microstruct. (2014) **76**, 26.
2. A. S. Golub, N. D. Lenenko, V. I. Zaikovskii, M. Yu. Antipin. Russ. Chem. Bull. (2012) **61**, 1950.

Paramagnetic centers and conductivity evolution in the process of thermal reduction of graphite oxide

Gudkov M.V. [1] , *Melnikov V.P.* [1]

gudkovmv@gmail.com
[1] Semenov Institute of Chemical Physics, Moscow, Russia

The interest in graphite oxide (GO) which was first synthesized in 1859 year has grown in recent ten years after discovery of unique properties of graphene. Process of synthesis, reduction methods, properties and structure of oxidizing and reduction forms of GO was studied by many groups of researchers. However, the mechanism of chemical reactions and restructuring in the process of chemical and thermal treatment on graphite oxide are still discussed [1, 2].

Paramagnetic centers (PMC) and conductivity evolution in the course of thermal reduction of GO at 150 and 165°C was studied by electron paramagnetic resonance method. Graphite oxide was obtained by Hummer's method [3] with varied quantity of $KMnO_4$ at range 1.5-3 g per 1 g of graphite.

Concentration of PMC was shown to increase at the initial stage of heat treatment, after that it reaches a maximum value during further heat treatment and then decreases (fig. 1). Moreover, increase of PMC concentration correlates with intense evolution of gaseous products decomposition of oxygen containing groups of GO. PMC concentration decrease is described by the kinetic equation of the first order with an effective constant k_e and the activation energy of 32 kcal/mol. Values of k_e are decrease with increasing of $KMnO_4$ quantity used for oxidation of graphite (from 1.5 to 3 g per 1g). Conductivity change of graphite oxide samples was determined by measurement of microwave power absorption in the resonator of electron paramagnetic resonance spectrometer. It has been shown, that this change correlates with death of radicals and begins after the termination of oxygen containing groups decomposition.

These results indicate that PMC are involved in GO thermal reduction process. Slow restructuring stage follows after fast destruction of oxygen containing groups. It leads to death of localized PMC, forming conjugated bonds between *sp-2* hybridized clusters and increasing conductivity. These processes indicate the important role of the PMC formation and destruction in the thermal decomposition chemical reactions and restructuring of GO.

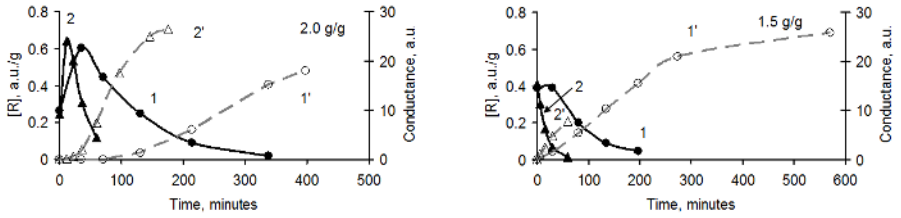

Fig.1. PMC concentration (1, 2) and relative conductance (1', 2') of GO samples versus time of annealing at temperatures 150 (1) and 165 °C (2).

References

1. K. Chua, M. Pumera, Chem. Soc. Rev. (2014) 43, 291
2. G. L. Acik, C. Mattevi, Y. Chabal, J. Phys. Chem. C (2011) 115, 19761
3. S. Hummers, R.E. Offeman, J. Am. Chem. Soc. (1958) 80, 1339

Structures of the carbon nanotubes as photosensitive element

Ichkitidze L.P. [1] , *Gerasimenko A.Y.* [1] , *Polohin A.A.* [1] , *Blagov E.V.* [2] , *Pavlov A.A.* [2] , *Kitsuk E.P* [3] , *Shaman Yu.P.* [3]

leo852@inbox.ru

[1] National Research University of Electronic Technology "MIET", Zelenograd, Russia

[2] Institute of nanotechnology of microelectronics of the RAS, INME, Moscow, Russia

[3] Scientific-Manufacturing Complex "Technological Centre", MIET, Zelenograd, Russia

Photodetectors based on the films of single-walled carbon nanotubes is actively developed [1]. However, there are big technological problems in their practical implementation, referring to a large spread their functional parameters. Therefore, it seems more simple photodetectors based on structures of multi-walled nanotubes (MWCNTs).We investigate the characteristics of test samples of the structures of the MWCNTs as photosensitive element to create a matrix photodetector operating in the wavelength range 0.5–8 μm.

To fabricate photosensitive structures with MWCNTs, we developed a technique for forming experimental samples, which is totally compatible with the standard microelectronic technologies. The important features of the structure formation are deepening in a silicon substrate for ensuring a reliable contact between MWCANTs and silicon and selection of a catalytic material for synthesizing MWCNTs. The short-time oxygen annealing of the structures enhances the IR response and leads to an increase in the efficiency of sensitive elements. The techniques that have been developed for studying characteristics of test samples of the sensitive elements based on the MWCNT structures, including spectral sensitivity, response time, and geometric size, as well as the effect of thermal treatment on these parameters.

It has been established that the samples based on the MWCNT structures are photosensitive in the radiation wavelength range 0.5–8 μm and their mean ampere-watt sensitivity is about 7 mA/W, i.e., the volt-watt sensitivity is 1 mV/W. The maximum attained photoresponse exceeds manifold the relative mean value and is comparable with the maximum photoresponse (~10 mV/W) observed in a bolometer of the similar type at modulation frequencies below 1 kHz [2].

The experimentally determined response time was 70 μs. The depth and diameter of the MWCNT-based photosensitive elements were about 2.5 μm. These values were repeated upon multiple cyclic measurements.

The results obtained will be useful for fabricating an MWCNT-based photodetector with a matrix density of no less than 10^6 elements/cm^2.

This work was supported by Russian Ministry of Education (Contract No.14.430.11.0006).

References

1. Jiangbo Zhang, Ning Xi, and King Lai. SPIE Newsroom, No. 10.1117/2.1200701.0514 (3 p).
2. M.E. Kozlov. *J. Appl. Phys.* 2013. Vol. **113.** 164307 (7 p). http://dx.doi.org/10.1063/1.4802582

Composite with carbon nanotubes for compound biological tissue

Ichkitidze L.P. [1] , *Gerasimenko A.Y.* [1] , *Podgaetsky V.M.* [1] , *Selishchev S.V.* [1]

leo852@inbox.ru

[1] National Research University of Electronic Technology "MIET", Zelenograd, Russia

Laser welding of biological tissues has a number of advantages as compared with conventional surgical techniques, namely, non-contact removal of biological tissues, minimal level of injuries, prevention of cicatrization after healing of scar biotissues etc. Various solders based on composite including such a protein as albumin have been used to improve mechanical properties of laser welds. However, laser welds are less strong than the joints made using surgical suture materials (thread, metal staple etc.). In this respect, the study aims at the laser solder (LS) based on the composite biomaterial for compound biological tissues. LS consist the bovine serum albumin (BSA, matrix) and carbon nanotubes (CNT, filler).

In our experiments we used LS based on the aqueous dispersion: 25 wt.% BSA+0.2 wt.% single-walled CNT (SWCNT) and 25 wt.% BSA+0.2 wt.% multi-walled CNT (MWCNT). SWCNT had the external diameter ~1 nm, the length <1 μm and the high purification rate of SWCNT-99A [1], while MWCNT had the external diameter ~30-80 nm, the length >20 μm, being of Taunite-MD type and manufactured by "Taunite" company [2].

Laser welding tests were carried out on dissected pig skin and bovine cartilage. The thin layer of LS was placed on the surface of the biological tissues to be joined and then the junction was exposed to laser irradiation with the following parameters of continuous irradiation mode: power ~1 W/cm^2, wavelength 970 nm. Laser welding process lasted for 5-20 s. After that we measured the tensile strength of the welded joint, s, and the tensile strength of the uncut region of the tissues, s_s. As a result, welded joints obtained using LS based on the aqueous dispersion 25 wt.% BSA+0.2 wt.% SWCNT were characterized by s_s »15 ± 5 MPa, s/s_s » 10 % for pig skin and s_s »6±2 MPa, s/s_s » 20 % for bovine cartilage. In case of MWCNT dispersion-based LS the values of s/s_s were lower by 20-30 % compared with SWCNT-based LS.

In many cases the welded joints are not strong enough at the early periods after the operation. To avoid it the surgical mesh of polypropylene of the PROLENE type manufactured by Ethicon was used in addition to LS. The surgical mesh overlaped the junction of tissues by 2-3 mm leading to the value s/s_s~25-35 % for both types of alloys containing either SWCNT or MWCNT.

Thus, the laser solders based on CNT (SWCNT or MWCNT) allow to increase the level of laser weld strength (s ~ 2–4 MPa , s/s_s » 20–35 %) by 1-2 orders of magnitude compared with LS based on pure BSA. These results demonstrate the potential of laser solders based on composite materials with carbon nanotubes for welding of biological tissues.

This work has been supported by Russian Federation Ministry of Education (No. 14.575.21.0044)

References

1. A.V.Krestinin, A.P. Kharitonov, Yu.M. Shul'ga, and et al. *Nanotechnologies in Russia,* 2009, vol. 4(1-2), p. 60.
2. www.nanotam@yandex.ru

Carbon nanotube transformations under microwave irradiation of fixed and variable frequency

Karaeva A.R. [1,2] *, Kazennov N.V.* [1] *, Mitberg E.B.* [1,2] *, Mordkovich V.Z.* [1,2]

karaeva@infratechnology.ru
[1] Technological Institute for Superhard and Novel Carbon Materials, Moscow, Russia
[2] INFRA Technology LLC, Moscow, Russia

It is known that microwave frequency impact on catalysts, sorbents and construction materials may lead to transformations, which are not equal to the effect of thermal treatment.

This work is devoted to investigation of transformations, which occur with multiwalled carbon nanotubes (CNT) under microwave irradiation of fixed or variable frequency. The variable frequency irradiation is especially interesting because it is characterized by homogeneous energy distribution throughout the sample volume and also by no electric arc appearance between the sample components [1, 2].

The variable frequency treatment was done at the MicroCure 3100 (Lambda Technologies Group.) equipment in air or in nitrogen atmosphere in the frequency range 5.85-7.0 GHz with irradiation power below 1.6 kW and treatment duration from 9 to 240 s. The CNT samples were synthesized by CVD method as described elsewhere [3]. The CNT synthesized were characterized by substantial occurrence of residual Fe catalyst and non-CNT structures.

The fixed frequency treatment was done at the equipment manufactured in-house. The equipment included a CVD reactor (the same method after [3] and a microwave treatment zone. The CNT in as-synthesized form were transported by the hydrogen gas into the microwave zone, where they were subjected to 2.45 GHz microwave treatment.

The samples before and after treatment were characterized by scanning and transmission electron microscopy (SEM and TEM). It was shown that both ways of microwave treatment result in effective removal of both non-CNT carbon particles and the residual Fe catalyst. Some of the outer walls of CNT are also removed provided they have many defects.

Thus it was shown that both fixed frequency and variable frequency microwave treatment of CNT may lead to effective CNT purification.

References

1. Lin W., Moon K.-S., Zhang Sh., Ding Y., Shang J., Chen M., Wong Ch.-P. // Microwave Makes CNTs Less Defective. // ACS Nano, 2010, 4 (3), pp. 1716–1722.
2.http://www.microcure.com/pdf/MICROWAVE%20FUNDAMENTALS,VFM&MATERIALSHEATING.pdf
3. Karaeva A.R., Khaskov M.A., Mordkovich V.Z. et al. // Fuller. Nanotub. Car. N. 2012. V. 20. N. 4-7. P. 411-418.

Decoration of carbon nanotubes with metal nanoparticles

Kharissova O [1] , Ortega B [1] , Rasika Dias H [2] , Kharisov B [1]

bkhariss@hotmail.com

[1] University Autonomus of Nuevo Leon, Mexico

[2] University of Texas at Arlington, Tx, USA.

Carbon nanotubes (CNTs) can be decorated by indirect or direct physico-chemical and physical methods mainly with noble and transition metals. The fabricated nanocomposites possess a series of useful applications in the fields of fuel cells, chemo/biosensors, solar cells, drug delivery, catalysis and hydrogen storage. The first principal calculations and other related theoretical studies on these metal-CNTs nanohybrids are discussed. As a result of 20 years' intensive investigations in a hottest topic in the nanotechnology – study of structure and properties of pristine and functionalized carbon nanotubes, a series of CNTs applications have been offered, in particular those related with fuel cells, chemo/biosensors, solar cells, drug delivery, catalysis and hydrogen storage. In this respect, the CNTs, functionalized with elemental metal nanoparticles (NPs), have revealed an extraordinary or elevated activity in these and other uses of CNTs. A significant challenge is how to deposit metal nanoparticles uniformly on the surface of carbon nanotubes due to the inherent inertness of carbon nanotube walls. In this work, the application of ultrasound for external decoration of CNTs with elemental metal nanoparticles is studied. The samples were characterization by TEM, Raman and IR spectroscopy. The MWCNTs with Fe and Ag nanoparticles of 20-30 nm were obtained and characterized.

Variations of Interlayer Spacing in Carbon Nanotubes

Kharissova O [1] *, Ortega B* [1] *, Rasika Dias H* [2]

okhariss@mail.ru

[1] University Autonomus of Nuevo Leon, Monterrey, Mexico

[2] University of Texas at Arlington, Arlington, Tx, USA

Carbon nanotubes (CNTs), among other carbon allotropes in nanotechnology, are intensively studied after publication of thousands of experimental articles, reviews, books and chapters. Interlayer distance/spacing, an important property of multi-wall CNTs, was determined much earlier, in particular by Dresselhaus,[1] who observed that the interlayer distance ranges from 0.342 to 0.375 nm, and that it is a function of curvature and the number of layers/shells comprising the tube. However, in the last 15 years several reports, sometimes contradicting, have appeared periodically on slight variations between interlayer distances. We believe that this topic has not yet lost its importance, since the carbon nanotubes possess enormous applications, where properties of their nanocomposites and nanomaterials could depend on interspacing distances. In this work, we studed of data and analysis on the interlayer distances in MWCNTs. Simulations on interlayer spacing, analysis of TEM images, applications of Raman spectroscopy, X-ray and neutron diffraction methods, influence of synthesis methods, heat and radiation (gamma-rays, electron and ion beams) treatments are discussed, as well as the polygonization and intercalation of CNTs. It is shown that the spacing values of DWCNTs and MWCNTs vary from 0.27 up to 0.61 nm. The synthesis method, raw materials, diameter of CNTs and the symmetry of layers influence on the inter wall spacing (Fig.1).

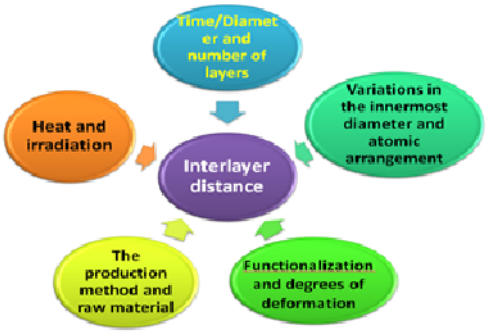

Fig.1 The influence on the variations of interlayer spacing in carbon Nanotubes.

Tunable hydrophylicity/hydrophobicity of fluorinated carbon nanotubes via gas-phase grafting of monomers

Kharitonov A.P. [1,2] , *Zha J.* [3,4] , *Dubois M.* [3,4]

khariton@binep.ac.ru

[1] Branch of the Talrose Institute for Energy Problems of Chemical Physics of the Russian Academy of Sciences, Chernogolovka, Moscow region, 142432, Russia

[2] Tambov State Technical University, Sovetskaya street, 106, Tambov, 392000, Russia

[3] Clermont Universite, Universite Blaise Pascal, Institut de Chimie de Clermont-Ferrand, BP 10448, F-63000 Clermont-Ferrand, France

[4] CNRS, UMR 6296, Institut de Chimie de Clermont-Ferrand, F-63171 Aubiere, France

Carbon nanotubes have unique properties and can be applied in polymeric composites, electronic devices, field emission display, hydrogen storage, etc. Unfortunately pristine CNTs exist in a form of bundles so their dispersion in liquids is highly restricted and further functionalization by ordinary methods of “wet” chemistry is made difficult. To improve their solubility CNTs must be functionalized. One of the most promising and frequently applied methods of the CNTs surface functionalization is the direct fluorination which makes the CNTs surface more polar and reduces nanotubes agglomeration in solutions. Solubility of fluorinated CNTs in alcohols and water is increased as compared with pristine CNTs but nevertheless remarkable amount of CNTs are still combined in bundles. So an additional modification, namely CNTs covalent functionalization is needed to improve their solubility. Majority of known from literature methods include multistep procedures, need too large time (sometimes – up to several days) and protocols are not always clear. All the proposed functionalization methods are used at elevated temperature and also highly toxic and volatile liquids such as DMF, THF, HNO_3, HCl, etc. are used. We propose method of “dry” chemistry which does not use highly toxic and volatile chemicals, process duration is not too large (4-5 hours), samples should not be filtered, washed or centrifuged after treatment. CNTs are placed into a closed reaction vessel, evacuated to a low vacuum (~0.1 mbar) and heated up to 100-300^{o}C. Then gaseous fluorine at a pressure below ambient is inserted into the vessel. Treatment duration is around 1-2 hours. Then fluorine is removed from the vessel and fluorinated CNTs are moved into another closed vessel which is evacuated and filled with monomer vapours (acrylic acid of styrene) at room temperature to provide graft polymerization. In 0.5-2 hours the reaction vessel is evacuated and grafted CNTs are ready for use. The total treatment duration does not exceed 4-5 hours. Formation of radicals was confirmed by ESR spectroscopy. The amount of radicals was decreased by a factor of 2 in 30 minutes after the end of fluorination and reached a steady-state level without change during 1 month. Styrene and acrylic acid grafting was confirmed by FTIR and ^{19}F NMR spectroscopy. For virgin and fluorinated only SWCNTs strong precipitation was observed just in 5 minutes after sonication in water, ethanol, toluene and chloroform. SWCNTs with grafted poly (acrylic acid) can be well solved (dispersed) in ethanol and no precipitation was observed even in 65 hours after sonication. Small precipitation was observed in 195 hours. SWCNTs with grafted polystyrene can be solved (dispersed) in toluene and chloroform. No precipitation was observed even in 33 hours after sonication. Small precipitation was observed only in 128 hours.

The research has been supported by the grant of the Russian Foundation of Basic Research 13-03-12086-OFI-M and State Contract #16.711.2014/K from the Ministry of Education and Sciences of Russian Federation.

The information system for simulation of the electronic structure of carbon nanotubes with substitutional impurities

Khoroshavin L. O. [1] *, Dyachkov P. N.* [2] *, Koltsova E. M.* [1]

freem.trg@gmail.com
[1] Mendeleev University of Chemical Technology of Russia, Moscow, Russia
[2] Kurnakov Institute of General and Inorganic Chemistry, Russian Academy of Sciences, Moscow, Russia

A method for simulation of the electronic structure of the point and complex substitutional impurities in the single-walled carbon nanotubes (SWNTs) based on a Green's function technique is developed [1]. The Green's function of a defect nanotube is calculated using the Dyson matrix equation. The host SWNTs electron Green's function is calculated using a linear augmented cylindrical wave (LACW) method [2]. The consideration is carried out in terms of the local density functional theory and the muffin-tin approximation for the electronic potential. During the simulation takes into account the helical and the rotational symmetries. Due to the account of these symmetry properties the method applicable to any tubule including the chiral SWNTs with defects independent of the number of atoms in translational unit cell of the host system.

On the basis of the developed method computing module was created. Using the information about the structure of nanotube it can be used to simulate the band structure and density of states. Modeling of the electronic structure of nanotubes with impurities requires much more time and computational resources than modeling of nanotubes without defects. Therefore the optimization of computing module has been made taking into account the supercomputer architecture. As a result the computation time was reduced up to 8 times.

To provide quick and convenient access to the computing module the information system was developed [3]. After logging into the system users get access to create computing tasks and manage their computations via the web-interface. After computational task created the information system automatically add it in the general queue of tasks of the supercomputer. The system also provides a convenient interface for processing the results of calculations.

This work was financially supported by RFBR (project №14-07-00960)

References

1. D. Z. Kutlubaev, D. V. Makaev, P. N. D'yachkov. Electronic structure of carbon nanotubes with an impurity point defect. Russian Journal of Inorganic Chemistry, vol. 56, pp. 1301-1305, (2011).
2. P. N. D'yachkov, O. M. Kepp, A. V. Nikolaev. Linearized Augmented-Cylindrical-Wave Method in the Electronic Structure Theory of Nanowires. Doklady Chemistry, vol. 365, pp. 67-72, (1999).
3. L. O. Khoroshavin, E. M. Kol'tsova. Architecture of the high performance client-server application for quantum mechanical calculations of single walled carbon nanotubes with atomic-scale defects. Achievements in chemistry and chemical engineering, vol. 28, pp. 26-29, (2014).

New composite materials based on multiwall carbon nanotubes coated with titanium carbide

Kremlev K.V. [1] *, Obiedkov A.M.* [1] *, Ketkov S.Yu.* [1] *, Kaverin B.S.* [1] *, Semenov N.M.* [1] *, Gusev S.A.* [2] *, Tatarsky D.A.* [2] *, Yunin P.A.* [2]

kkremlev@mail.ru

[1] G.A. Razuvaev Institute of Organometallic Chemistry of RAS, Nizhniy Novgorod, Russia

[2] Institute for Physics of Microstructures RAS, Nizhniy Novgorod, Russia

Hybrid materials based on multiwall carbon nanotubes (MWCNTs) with various metal-containing nanoparticles or coatings deposited on their surface are promising sources for new reinforced composites with polymer or metal matrices as well as for construction of new chemical and mechanical devices [1]. Titanium carbide nanoparticles show a good chemical inertness and a good conductivity, so they are widely used as for abrasion-resistant surface coatings on metal parts, as a heat shield coating, in optics and energy-related applications [2]. It is mainly motivate to obtain MWCNTs coated with titanium carbide nanocoatings on the surface, which, in particular, can be used with polymer or metal matrices as catalytic systems, additives in various alloys, additives in acrylate adhesive compositions and as gas sensors.

We synthesized multiwall carbon nanotubes arrays with the 80 nm average outer diameter of nanotubes by metalorganic chemical vapor deposition (MOCVD) at 825 °C. Ferrocene and toluene were used as precursors [3]. Deposition of titanium carbide nanocoating on the surface of MWCNTs was performed by MOCVD with an organotitanium compound as precursor. Titanium carbide nanocoatings with various morphology and structure depending on the synthesis parameters were prepared. We obtained titanium carbide thin films with the thickness of 2 - 15 nm on the surface of MWCNTs. The composition and structure of hybrid material TiC/MWCNTs were investigated. The data of the structures and properties of the samples were collected with the XRD, TGA, SEM and HRTEM methods.

This work was supported by the RSF (Project 14-13-00832).

References

1. D. Eder, Chemical Reviews (2010), V. 110, N. 3, P. 1348.
2. D. Ranjan, C. John, Y. Gleb, G. Yury, L. Giovanna, S. Jonathan, Carbon (2006), V. 44. P. 2489.
3. A.M. Obiedkov, B.S. Kaverin, V.A. Egorov, N.M. Semenov, S.Yu. Ketkov, G.A. Domrachev, K.V. Kremlev, S.A. Gusev, V.N. Perevezentsev, A.N. Moskvichev, A.A. Moskvichev, A.S. Rodionov. Letters on Materials (2012), V. 2, P. 152.

NEXAFS studies of the composite $MoC_{0.7}$/MWCNTs by synchrotron radiation

Kremlev K.V. [1] , *Obiedkov A.M.* [1] , *Kaverin B.S.* [1] , *Ketkov S.Yu.* [1] , *Sivkov V.N.* [2] , *Petrova O.V.* [2] , *Nekipelov S.V.* [2] , *Vyalikh D.V.* [3]

svn@dm.komisc.ru

[1] G.A. Razuvaev Institute of Organometallic Chemistry of RAS, Nizhniy Novgorod, Russia

[2] Komi Science Center Ural Division RAS, Syktyvkar, Russia

[3] Technische Universitat Dresden, Dresden, Germany

Multiwall carbon nanotubes (MWCNTs) are novel carbon materials, which show very promising properties for nanotechnology applications. The most fascinating aspect of these composites is related to the modifications that occur in their physicochemical properties when they are coated by metals, metal carbides or metal oxides. At present research the composite $MoC_{0.7}$/MWCNTs was studied. New composite material - multiwall carbon nanotubes coated with thin molybdenum carbide layers have been prepared by MOCVD (metalorganic chemical vapor deposition) growth technique using $Mo(CO)_6$ as the precursor. It is very important to investigate the electron structure of $MoC_{0.7}$ – MWCNTs interface and $MoC_{0.7}$ coating using techniques that are sensitive to changes in both electronic properties, as well as to the presence of metal carbides, and to the kind of interaction between thin layer of $MoC_{0.7}$ coating and nanotubes. The NEXAFS (near edge x-ray absorption fine structure) spectroscopy is the available tool for the investigation of the MWCNTs based composites, because the NEXAFS-spectroscopy methods are characterized by atomic selectivity, dipole selection rules, fast response atomic composition and spatial conformation [1]. Various data about structures and properties of the samples were obtained by XRD, TGA, SEM, TEM and HRTEM methods.

The NEXAFS C1s-, Mo3p- and O1s- absorption edges of the MWCNTs based composites were studied by total electron yield (TEY) mode with using synchrotron radiation of Russian-German beamline at BESSY-II [2]. The atomic structure and chemical composition of the coatings and interfaces $MoC_{0.7}$/MWCNTs composite were obtained.

The NEXAFS studies have shown that top layers of the MWCNTs in composite do not have essential destruction, covering coat of MWCNTs-surface is $MoC_{0.7}$ and covering coat is continuous. Studies have shown that the surface layer of the composite $MoC_{0.7}$/MWCNTs comprises a layer of molybdenum oxide. The metal oxide adhesion is carried out by chemical binding between the carbon atoms of the MWCNTs top layer and the oxygen atoms of the coat.

The synthesis of $MoC_{0.7}$/MWCNTs composite was supported by the RSF (Project 14-13-00832). Investigations by NEXAFS-spectroscopy methods were supported by grants RFBR 13-02-00272-a, Program BR of UD RAS and by the Bilateral Program of the Russian-German Laboratory at BESSY II.

References

1. J. Stohr, NEXAFS Spectroscopy (Springer, Berlin, 1992).
2. S.A. Gorovikov, S.L. Molodtsov, R. Follath, Nucl. Meth. A. (1998), V. 411, P. 506.

Electrical properties of Carbon Nanotubes/WS_2 Nanotubes Hybrid Films

Ksenevich V.K. [1] , *Gorbachuk N.I.* [1] , *Ho V.* [1] , *Shuba M.V.* [2] , *Kuzhir P.P.* [2] , *Maksimenko S.A.* [2] , *Paddubskaya A.G.* [3] , *Valusis G.* [3] , *Wieck A.D.* [4] , *Zak A.* [5] , *Tenne R.* [6]

ksenevich@bsu.by

[1] Department of Physics, Belarusian State University, Minsk, Belarus

[2] Research Institute for Nuclear Problems, Belarusian State University, Minsk, Belarus

[3] Center for Physical Sciences and Technology, Vilnius, Lithuania

[4] Department of Physics and Astronomy, Bochum Ruhr-University, Bochum, Germany

[5] Department of Sciences, Holon Institute of Technology, Holon, Israel

[6] Department of Materials and Interfaces, Weizmann Institute of Science, Rehovot, Israel

Interest to investigation of hybrid materials based on organic and inorganic nanostructures is induced by their unique electrical, mechanical, optical and thermal properties [1]. Multifunctionality of hybrid films provides possibility for number of applications, including elements for energy transfer and conversion [2]. In this paper we focused our efforts on studying of AC- and DC electrical properties of hybrid films consisting from organic and inorganic components (carbon nanotubes (CNT) and WS_2 nanotubes (NT), respectively).

Both single-wall carbon nanotubes (SWCNT) and multi-wall carbon nanotubes (MWCNT) were used as organic components. SWCNT/WS_2-NT and MWCNT/WS_2-NT hybrid films were produced on cellulose acetate membrane filter (Millipore, 0.22 μm pore size) via filtration process. WS_2-NT were grown in the large-scale fluidized-bed reactor. Detailed description of the growth mechanism was described in [3]. Measurements of the temperature dependences of resistance *R(T)* were carried out in the frequency range 2-300 K. Characterization of AC electrical properties was done by means of impedance spectroscopy in the frequency range 20 Hz - 1 MHz at temperatures 4.2, 77 and 300 K and in the range of applied bias voltage 0−5 V.

SWCNT/WS_2-NT and MWCNT/WS_2-NT hybrid films were characterized by higher values of temperature coefficient of resistance in comparison with SWCNT films and MWCNT films, respectively. We assume that the role of the low-conductive WS_2 nanotubes in hybrid films is mainly related to the increase of the influence of potential barriers between CNT. Equivalent circuits for modeling of the impedance for both types of the hybrid films's were proposed.

References

1. M. Naffakh, A. Diez-Pascual and M.A. Gomez-Fatou, J. Mater. Chem., (2011) **21**, 7425.
2. Eder. Chem. Rev. (2010) **110**, 1348.
3. Zak, L. Sallakan-Ecker, A. Margolin, M. Genut and R. Tenne, NANO (2009) **04**, 91.

ADSORPTION OF BIOLOGICALLY ACTIVE NITRILES CONTAINING THE DIPHENYLOXIDE FRAGMENT ON THE EXTERNAL SURFACE OF CARBON NANOTUBES

Kulbasova A.K [1] *, Ermakova T. A* [1] *, Zaporotskova I.V.* [1] *, Davletova O.A* [1] *, Korchagina T.K.* [2] *, Popov U.V* [2]

k_a_k_1301@mail.ru
[1] Volgograd State University, Institute of Priority Technologies, Volgograd, Russia
[2] Volgograd State Technical University, Volgograd, Russia

The closed superficial structures of carbon (fullerenes and nanotubes) show a number of the specific properties allowing to use them as special materials and to consider as interesting physical objects and chemical systems. Remarkable feature of carbon nanotubes (UNT) is connected with their unique sorption characteristics: strongly bent surface of the nanotube which is completely consisting of superficial atoms (in case of one-wall UNT), allows to adsorb on its surface organic molecules – the substances containing a diphenyloxide fragment which are new structures, the similarity which are characterized by high rates to known medicinal substances and absence at connections of the expressed toxic properties, and also showing a wide range of pharmacological properties [1, 2]. In this regard the combination of opportunities of transport of UNT modified by biologically active molecules can lead to creation of new nanomaterials for purposeful delivery of medicinal substances in live organisms [3].

In work quantum and chemical researches of the adsorptive interaction of carbon nanotubes with biologically active agents are presented - 1,2-di-(phenoxyphenyl) - 2-cyanoethylene and 1-(3-phenoxyphenyl) - 2-cyanoethylene , by means of the semi-empirical scheme PM6 in a software package of Gaussian. For calculations models of carbon nanotubes like armchair (3.5), (8.0), (6.0) and (6.6) were used. As a result of the executed calculations optimization of geometry of nuclear systems was performed and features of a spatial configuration of molecules were revealed. For the adsorbed biologically active nitriles options of one-center accession to UNT surface through various adsorptive centers as which atoms of oxygen and nitrogen acted were considered. The executed calculations allowed to construct a profile of a surface of potential energy for adsorption process. The analysis of power curves established that molecules of nitriles is adsorbed on UNT surface that is confirmed by existence of a minimum on power curves.

The analysis of the obtained data showed that adsorption of biologically active agents containing a diphenyloxide fragment is possible on an external surface of carbon nanotubes. Thus the interatomic distance varies from 3 to 3,6 Å, energy of the adsorptive interaction of biologically active nitriles makes 1,2-1,4 эВ in case of accession of molecules to UNT atom of nitrogen, and energy of adsorption of these molecules attached to UNT by atom of oxygen - 2,6 - 3,4 эВ.

References

1. V. Popov. Synthesis 2-(3-fenoksibenzoil) cyclohexanone / Yu. V. Popov and [other]//the Magazine of the general chemistry. - 2012. - T. 82, вып. 7. - Page 1220-1221.
2. A. Kravchenko. The semiempirical research the adsorption of biologically active molecules on the quter surface of carbon nanotubes/A. A. Kravchenko, T.A. Ermakova, O. A. Davletova, I.V. Zaporotskova, T. K. Korchagina, U.V. Popov, G. A. Kalmikova//NANOSYSTEMS: PHYSICS, CHEMISTRY, MATHEMATICS, 2014, 5 (1), P. 98–100
3. Piotrovsky of L. B. Fullerena in Biology / Piotrovsky L. B., Kiselyov O. I. — SPb.: Rostock publishing house, 2006 — Page 246-251.

Chemistry model of synthesis of carbon nanotubes from metals carbonyls

Leshchev D.V. [1]

dimvovich@narod.ru
[1] CAS of SPbPU, Saint-Petersburg, Russia

In recent decades, novel carbon materials such as fullerene, carbon nanotubes and nanopearls have been intensively investigated because of their great potential applications. A wide array of techniques have been developed for the synthesis of those novel carbon materials, among them chemical vapor deposition (CVD), and this technique has been proven to be a very versatile and convenient tool [1]. Laser chemical vapor deposition (LCVD) is a derivative of CVD whereby the global heat source for the furnace is replaced with a localized spot heated by a laser [2, 3].

The base of chemistry for nanotube synthesis is to use the floating catalyst method, whereby a mixture of metals carbonyls, hydrocarbons, and inert gas reagents was used. At that high hydrocarbons concentrations increase not only the number of tubes formed in region but also decreases their size [2]. Generally metals carbonyls are convenient precursor for metal catalyst particles. They can serve as a catalyst and a carbon source for nanoparticles growth. Using two or more metals carbonyls makes possible changing metals concentrations in reagents mixture to control ratio of the size and the number of nanotubes.

Constructed chemistry model bases on the results of quantum chemical calculations and includes the following types of reactions (M is metal atom):

$M_x(CO)_y \rightarrow M_x(CO)_{y-1}+CO$ — initial dissociation of carbonyl and CO evaporation;

$M_x(CO)_y + M_z(CO)_u \rightarrow M_{x+z}(CO)_{y+u}$ — carbonyl association in cluster;

$MCO(s)+CO \rightarrow C(b)+M(s)+CO_2$ — disproportionation of CO on cluster surface and formation carbon bulk;

$M(s)+CO \rightarrow MCO(s)$ — formation of reaction sites;

$M_x(CO)_y \rightarrow C(b)+ M_x(CO)_{y-1}+CO_2$ — disproportionation of CO in cluster;

$M(s)+C_xH_{2y} \rightarrow xC(b)+M(s)+yH_2$ — formation carbon bulk from hydrocarbons.

The proposed chemistry model allows to describe basic chemical processes in CVD synthesis and can be used in gas-dynamic calculations.

References

1. Chow, D. Zhou, A. Hussain, S. Kleckley, K. Zollinger, A. Schulte, H. Wang, Thin Solid Films (2000) **368**, 193.
2. N. Bondi, W.J. Lackey, R.W. Johnson, X. Wang, Z.L. Wang, Carbon (2006) **44**, 1393.
3. Rohmund, R.-E. Morjan, G. Ledoux, F. Huisken and R. Alexandrescu, J. Vac. Sci. Technol. B (2002) **20**, 802.

Modelling of catalyst metal particles formation processes in CVD of carbonyls

Leshchev D.V. [1]

dimvovich@narod.ru
[1] CAS of SPbPU, Saint-Petersburg, Russia

Modelling of gas-dynamic processes plays important role in modern technology. It allows to optimize synthesis conditions. We used gas-dynamic methods for testing chemistry model of formation particles of metal from different metal carbonyls. These metal particles can be used as catalyst in chemical synthesis and centres of carbon nanoclusters growth (for example, fullerene, carbon nanotubes, and nanopearls) in chemical vapor deposition (CVD) technique. We used different initial concentration and condishions, and different mixtures of reagents to identify dependences of process to mixture composition. Mixture of reagents can include metal carbonyls ($Co(CO)_8$, $Fe(CO)_5$, $Ni(CO)_4$), hydrocarbons (as C_2H_2) and inert gas (Ar).

We describe forming nanocluster processes in terms of equations of the quasi-chemical condensation model [1]. In this model, it is assumed that clusters grow via association reactions of carbonyls. Through obtained cluster size distribution function we can get the solution for nanoclusters growth from CO and hydrocarbons.

As an example for the simulation we used CVD of carbon nanotubes [2]. The performed simulation shows different size distributions of metal-carbon clusters and different growth rate of nanoclusters.

References

1. Yu.E. Gorbachev, Technical Physics (2003) **48**, 5, 655.
2. S.N. Bondi, W.J. Lackey, R.W. Johnson, X. Wang, Z.L. Wang, Carbon (2006) **44**, 1393.

CCVD synthesis of nitrogen-doped carbon nanotubes using Ni, Co and Fe polyoxomolybdates

Lobiak E.V. [1] , *Bulusheva L.G.* [1,2] , *Shlyakhova E.V.* [1,2] , *Lonchambon P.* [3] , *Flahaut E.* [3] , *Okotrub A.V.* [1,2]

lobiakev@niic.sbras.ru

[1] Nikolaev Institute of Inorganic Chemistry SB RAS, Novosibirsk, Russia

[2] Novosibirsk State University, Novosibirsk, Russia

[3] Paul Sabatier University-CNRS (CIRIMAT), Toulouse, France

There is a possibility to control properties of carbon nanomaterials using replacement of carbon by an heteroatom. Nitrogen is the most applicable for this purpose due to the similarity of nitrogen and carbon atoms in size. Nitrogen inserted into a carbon nanomaterial structure is able to change its electronic structure. These changes influence both the electroconductivity and reactivity of carbon nanomaterials. Hence, nitrogen doped carbon nanomaterials are very promising for investigation both electrode materials and field emission cathode.

Nitrogen-doped carbon nanotubes (N-CNT) are synthesized using both nitrogen precursor during carbon nanotube (CNT) synthesis procedure and post-treatment of CNTs by nitrogen containing molecules at high temperature. Some species of nitrogen are formed during N-CNTs synthesis. Thus, there are three main forms of nitrogen inserted into CNTs structure such as graphitic, pyridinic and pyrrolic. Temperature is a key parameter for control of nitrogen content and the nature of nitrogen species.

In the present work, we use ε-Keggin-type polyoxomolybdates $Mo_{12}O_{28}(\mu_2\text{-}OH)_{12}\{Ni(H_2O)_3\}_4$, $Mo_{12}O_{28}(\mu_2\text{-}OH)_{12}\{Co(H_2O)_3\}_4$ and $[H_4Mo_{72}Fe_{30}O_{254}(CH_3COO)_{10}\ \{Mo_2O_7(H_2O)\}\{H_2Mo_2O_8(H_2O)\}_3(H_2O)_{87}]\bullet 80H_2O$ as catalyst precursors for catalytic chemical vapour deposition (CCVD) synthesis of N-CNTs. Cluster molecules were uniformly distributed on MgO support to prevent agglomeration. We had shown that bimetallic alloys Ni/Mo, Co/Mo and Fe/Mo catalyze growth of CNTs. Acetonitrile was used as a nitrogen-carbon source and delivered in furnace by hydrogen. TEM investigation indicated that the CCVD products contained individual CNTs with mesoporous carbon, which were not contaminated by amorphous carbon species. Raman investigations showed that defectiveness of obtained carbon material increased in a line of Co-Fe-Ni in agreement with an increase in mesoporous carbon according to TEM. According to statistical analysis of TEM images, average diameter of N-CNTs was 5 nm, 10 nm and 15 nm, respectively in a line of Ni-Co-Fe. It was found how the catalyst composition influences the concentration and the nature of species of inserted nitrogen according to XPS data. It was shown that N-CNTs obtained using Co/Mo and Ni/Mo catalysts had more pyrrolic nitrogen than Fe/Mo catalyst. The obtained carbon materials are expected to demonstrate improved properties as electrode materials.

This work was supported by the Russian Foundation of Basic Research (grant 14-03-32089).

Optimization of surface abrasive treatment in processes of MWNT layers synthesis on bulk nickel

Kukovitsky [1] , *Lvov S.G.* [1] , *Shustov V.A.* [1] , *Lyadov N.M.* [1]

lvov@kfti.knc.ru
[1] Zavoisky Physical-Technical Institute, Kazan, Russia

As known, carbon nanotube layers obtained directly on the surface of catalytic metal have a number of advantages for many practical applications, for example, for manufacturing electron field emitters. The growth of carbon nanotubes is substantially accelerated on surfaces subjected to intensive plastic deformation. Such deformation can be achieved by different treatment techniques in that number surface mechanical attrition treatment [1]. Carbon material was shown to deposit on nanostructured surfaces in chemical vapor deposition (CVD) process but no product was found on the untreated samples at the same conditions [2].

To clarify surface features promoting formation of homogeneous MWNT layers on bulk nickel, carbon chemical vapor deposition on surfaces generated by abrasive treatment was experimentally studied. Two main phenomena, complicating graphite-like carbon deposition on rough nickel surface in comparison with the perfect one, were revealed due to study of earlier stages of carbon deposition. The first phenomenon is the rate increase of carbon formation at surface defects including small confined spaces with large surface-to-volume ratio (pits, gaps, cracks, etc.). Small cavities in subsurface layer are also places of enhanced carbon formation. The cause of this increase is the specific chemistry of hydrocarbon pyrolysis in the conditions of prolonged residence time realized in confined space. The high rate of carbon formation leads to fast growth of highly disordered (coke-like) graphite carbon inside such defects. This conclusion is based also on previous observations of increasing carbon deposition in confined geometry of catalytic surfaces [3]. The second phenomenon is the fast metal dusting of micron-sized surface asperities formed by plastically deformed metal and generated by abrasive treatment. Numerous micro-cracks created on surface in course of metal dusting promote the first phenomenon becomes operative. It was proposed that the roughness of catalytically active surface can be the cause of pyrolysis surface chemistry change comparing with smooth surface.

These observations have permitted to optimize procedure of abrasive surface pretreatment and obtain uniform MWNT layers on nickel foil. As expected, presenting results will allow producing MWNT cold cathodes with improved emission characteristics.

References

1. Lu K and Lu J., Mater. Sci. Eng. A (2004) **375-377**, 38.
2. Xu J.Y., Lei X.C., Yang R., Fan Z.Z., Nanomaterials (2014) Article ID 690630.
3. E.F. Kukovitsky and S. G. Lvov, J. Solid State Sci. & Tech. (2013) **2**, M1.

Modification of magnetic, electroconductive and mechanical properties of zirconium oxide ceramics by means of multiwalled carbon nanotubes

Lyapunova E.A. [1,2] , *Uvarov S.V.* [1,2] , *Grigoriev M.V.* [3] , *Kulkov S.N.* [3] , *Naimark O.B.* [1]

lyapunova@icmm.ru

[1] Institute of continuous media mechanics, Ural branch of Russian Academy of Sciences, Perm, Russia

[2] Perm State University, Perm, Russia

[3] Institute of strength physics and materials science, Siberian branch of Russian Academy of Sciences, Tomsk, Russia

Production of ceramic composites reinforced by carbon nanotubes (CNTs) is one of intensively developed direction in modern material science because of intriguing electromagnetic, mechanical and others properties of CNTs [1]. Their ability to change ceramic structure, intensify sintering processes and decrease crystallite size was found earlier [2, 3]. Nowadays vast amount of research is concentrated on increasing the effectiveness of such modification of convenient ceramics by optimizing CNTs arrangement in ceramic matrix and reducing crystallite size. Besides, it is important to observe all the spectra of ceramic composite properties: mechanical, electromagnetic and heat conductive in order to make correct estimates of the CNTs effect on the material. The current work is an attempt in this direction, namely, it is devoted to estimation of mechanical, magnetic and electroconductive properties of nanocomposite produced on the basis of zirconium oxide and CNTs.

Preparation of composite includes [4]: hydrothermal synthesis of dense hydrogel from suspension of zirconium salt and CNTs; critical point drying of hydrogel; thermal treatment of obtained zirconium oxide/CNTs aerogel; consolidation of aerogel fragments by hot pressing for getting bulk samples.

Ferromagnetic properties of sintered aerogel fragments were investigated by means of original experimental setup and magnetic field frequency-dependence of composite susceptibility was determined [4]. Electroconductive properties of bulk composite are also discussed.

Mechanical properties of composite were investigated by nanoindentation system NanoTest. Series of indentations with different applied load as well as multiple loading with increasing value of maximum applied load were carried out. It was found that composite exhibits huge fraction of energy dissipated into material which increases with increasing load (indentation depth). Moreover, for all investigated values of maximum applied loads there were no cracks in the edges of indentation trace. The obtained results have shown that synthesized composite is highly effective in suppressing the cracks growth.

This work is supported by Russian Found of Basic Research (grant 14-01-96015-ural-a).

References

1. Z. Xia, L. Riester, W.A. Curtin, H. Li, B.W. Sheldon, J. Liang, B. Chang, J.M. Xu. Acta Mater. (2004). **Vol. 52.** p. 931
2. E. Lyapunova, O. Naimark, S. Kulkov, E. Dedova, I. Sobolev. Inorg. Mater. (2015) **Vol. 51.** No. 1, p. 20
3. A.L. Vasiliev, R. Poyato, N.P. Padture. Scripta Mater. (2007) **Vol. 56.** p. 461
4. E. Lyapunova, I. Lunegov, S. Uvarov, O. Naimark. Actual problems of condensed media physics. (ICMM UB of RAS, Perm, 2015) p. 83

Topochemical transformations in carbon nanotubes: fracture-induced defect, and ad-dimer welding

Moliver S.S. [1]

moliver@sv.uven.ru
[1] Ulyanovsk State University, Ulyanovsk, Russia

Native point defects of graphene and carbon nanotubes are related to C—C dimer. The first type is a topochemical turn of a single honeycomb C—C bond around its centre (SW defect, introduced in 1986 by A.J. Stone & D.J. Wales). The second one is incorporation of adsorpted dimer molecule (ad-dimer) into honeycomb carbon net (grafted ad-dimer, or di-interstitial).

1) Recently we have solved the problem of generation of SW in small-diameter tubes under mechanical fracture-type deformation, when mechanical stress is concentrated in a small area of the tube [1]. Fracture of zigzag (8,0) and armchair (5,5) tubes was considered by means of quantum chemistry. The SW on the compressed side of the tube is energetically favourable in comparison with the stretched side. At a fracture angle above critical value –

yield point: 1.7 degrees for (8,0), and 2.7 degrees for (5,5),

– the formation of SW decreases total energy of deformed defectless tube. Thus, fracturing deformation of the tube «turns on a plasticity channel» in the form of mechanical generation of the Stone–Wales defect. Deformations above yield point were experimentally studied only with large-diameter multiwalled tubes [2]. Kink of such a sample obeys continuous-media mechanics, perhaps the honeycomb structure of the tube is preserved in the kink area. Thus, a topochemical phenomenon of SW generation in small-radii tubes waits for experimental support.

2) Covalent chemical bonding between a pair of kriss-kross nanotubes should be achieved, if we could align tubes carefully, in order to make two parallel C—C bonds, one of each tube, come into [2+2] cyclo-addition. A reliable bonding – welding – can be achieved with the help of ad-dimer, that shifts and rotates adjusting to neighbour chemical bonds. Versatile chemical behaviour of ad-dimer (di-interstitial) in graphite has been analyzed theoretically [3]. Experiments [4] with acetylene intercalation in fullerite[60] give one more route to prepare nanotubes for welding across the chemically bonded HCCH.

References

1. S. Moliver. Fullerenes, Nanotubes, and Carbon Nanostructures (2012) **20**, 531.
2. Jensen, W. Mickelson, A. Kis, and A. Zettl. Phys. Rev. B (2007) **76**, 195436.
3. Teobaldi, K. Tanimura, and A.L. Shluger. Phys. Rev. B (2010) **82**, 174104.
4. M. Shulga, V.M. Martynenko, S.A. Baskakov, A.N. Trukhanenok, E.M. Anokhin, A.V. Maksimychev, S.S. Khasanov, K.G. Belay, C.A. Weatherford, and G.L. Gutsev. Chem. Phys. Lett. (2009) **483**, 115.

Nanocomposites with antibacterial properties using CNT with magnetic properties

Ortega B [1] , *Kharissova O* [1] , *Rasika Dias H* [2]

beatriz.ortega24@gmail.com
[1] University Autonomus of Nuevo Leon, Monterrey, Mexico
[2] University of Texas at Arlington, Arlington, TX, USA.

It is well-known that diverse polymers possess antibacterial properties, as well as several nanoparticles (for example Ag NPs) or carbon nanotubes (CNTs). The CNTs can be slightly magnetic, if they contain iron nanoparticles inside as a result of use of Fe-containing catalysts during their production. Incorporating the nanoparticles into a polymer matrix, it is expected that all NPs properties are transferred to the polymer, resulting in its antibacterial and magnetic properties. There are many applications reported for polymer-NPs nanocomposites with antibacterial properties; in case of possessing additionally magnetic sensibility, an alternative for drug delivery or biosensor applications could be found.

A natural polymer chitosan belongs to the group of antibacterial polymers ; it is compatible with tissues and utilized in biomedicine. In this work, the dopation of CNTs with Ag and Fe and their further uniform dispersion in chitosan polymeric matrix is studied. Distinct NPs concentrations and two methods (Fig. 1) were applied for NPs incorporation. The formed nanocomposites were analyzed via IR, X-ray diffraction, SEM and TEM, antibacterial analysis and magnetic measurements.

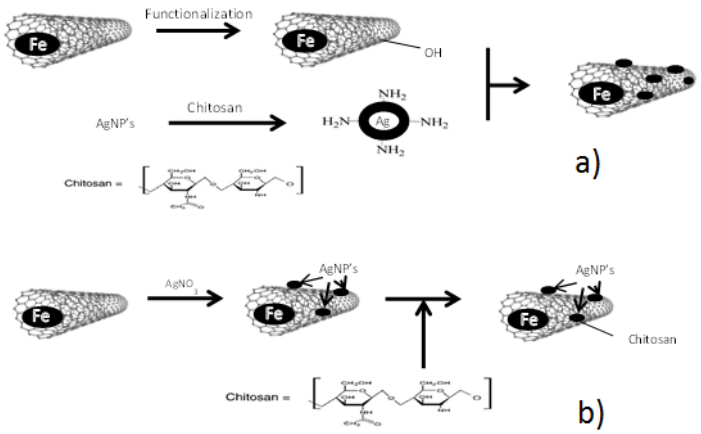

Fig. 1 a) First method for incorporation of NPS into the polymeric matrix; b) Second method for incorporation of NPS into the polymeric matrix.

Sensor activity of the nitro group modified carbon nanotube for some metal atoms

Polikarpova N.P. [1] *, Zaporotskova I.V.* [1] *, Vil'keeva D.E.* [1] *, Boroznin S.V.* [1] *, Zaporotskov P.A.* [1]

n.z.1103@mail.ru
[1] Volgograd State University, Volgograd, Russia

To date, nanometer scale objects are being widely applied in various fields of science and technology. The discovery of carbon nanotubes (CNTs) is among the most significant achievements of modern science. CNTs possess unique electronic properties, high sorption activity and are effective adsorbents of different particles. There exist a great number of studies on the wide range of gas sensors, the basic principle of which is the adsorption of gas molecules in which the molecule gives or takes away an electron in a nanotube, which leads to changes in the electrical properties of CNTs that can be detected and registered. Devices with boundary-modified carbon nanotubes can perform as sensors.

In previous research we studied interaction between carbon nanotube modified with a carboxyl group and alkali metal atoms [1]. In this study we investigated the mechanism of boundary modification in single-walled carbon nanotube with a nitro functional NO2 and calculated the interaction of this boundary-modified system with atoms and ions of alkali metals: lithium, sodium and potassium. The calculations were performed using the MNDO method and DFT. The process was simulated as incremental movement of the selected atoms or metal ions to the atom O of the functional group. The energy curves of the nanosystems "CNT - NO2» with selected atoms or ions enabled to determine the basic characteristics of the interaction (the distance and energy). Analysis of the results allowed to conclude the following: since the interaction distance corresponding to the minimum on the energy curves is rather large, it can be assumed that interaction between the boundary-modified nanotubes and selected metals is characterized as a weak van der Waals interaction. This fact shows that the sensor probe could be used repeatedly and would not be subject to destruction, which would have happened in case a chemical reaction in the system had occured.

References

1. Sensor Activity of Carbon Nanotubes with a Boundary Functional Group. I.V. Zaporotskova, N.P. Polikarpova, D.E. Vil'keeva. Nanoscience and Nanotechnology Letters. V 5. № p. 1169-1173.

Stone-Wales rearrangements in fluorinated SWCNTs – a theoretical study

Pykhova A.D. [1] , *Ioffe I.N.* [1]

a.d.pykhova@gmail.com
[1] Moscow State University, Chemistry department, 119991, Moscow, Russia

The Stone-Wales defects constitute one of the most common types of imperfections in carbon nanostructures such as fullerenes, carbon nanotubes (CNTs), and graphene. They formally consist in rotation of a C-C bond by 90°, which, in the case of CNTs or graphene, results in formation of a substructure of two adjacent 7-membered rings and two 5-membered rings.

Such defects can significantly alter the electronic properties such as bandgap, thus having an obvious effect on the possible practical applications. In addition, introduction of Stone-Wales defects in the nanotubes can make possible regioselective sidewall functionalization, whereas the lack of preferable reaction centers in the defectless nanotubes prevents their controllable derivatization, which is disadvantageous for potential practical use. Note that functionalization of CNTs is also regarded as an approach to solve some important problems like low solubility and aggregation of pristine nanotubes.

The present study is addressed to the interplay of the Stone-Wales defects and the sidewall functionalization of SWCNTs, e.g. fluorination. It has been motivated by the recent observations of Stone-Wales transformations in chlorinated fullerenes at unexpectedly moderate temperatures compared to the pristine fullerene molecules [2]. We present a DFT study of consecutive fluorination of the finite length segments of the (5,5)CNT with and without the Stone-Wales defects. It is demonstrated that in the defective regions the binding energy of the exohedral substituents becomes noticeably increased, which provides stabilization of the defects. Furthermore, fluorination enables alternative defect formation pathways, similar to those observed in chlorinated fullerenes, characterized by remarkably low activation barriers.

Worth to mention are certain methodological complications associated with the treatment of a finite substructure rather than a periodic system. It was observed that the calculated energies and electronic levels can pronouncedly depend on i) the distance of the functionalization sites to the edges of the nanotube segment and ii) whether the selected segment obeys or violates Clar's sextet rule [2]. Therefore, even though the approaches of the molecular quantum chemistry may generally be more convenient and reliable in calculating the energetic effects, particular care should be taken to relate their results to a real quasi-infinite nanotube structure.

The present work was supported by the RFBR grant 15-03-05083. We thank the Supercomputer Center of the Moscow State University for computational support.

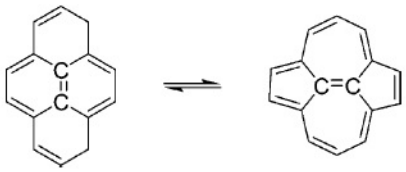

Fig.1. Stone-Wales defect formation scheme.

References

1. Ioffe I.N., Goryunkov A.A., Tamm N.B., Sidorov L.N., Kemnitz E., Troyanov S.I., Angew. Chem. Int. Ed. (2009) **48**, 5904.
2. Clar E., Polycyclic Hydrocarbons, Academic Press: New York, 1964.

Large-scale direct synthesis of carbon nanostructures using thermal plasma jet at low pressure

Amirov R.H. [1] , *Shavelkina M.B.* [1] , *Tyuftyaev A.S.* [1]

mshavelkina@gmail.com
[1] Joint Institute for High Temperatures of Russian Academy of Sciences, Moscow, Russia

Today, plasma technologies are in demand in the field of nanotechnology. It is important to solve the problem of large scale production of nanomaterials. From this point of view very interesting application of thermal plasma when plasma torches are used [1-2]. For the synthesis of carbon nanostructures thermal plasma generator was used which is a high current divergent anode-channel DC plasma torch. In the experiment the carbon sources with the working gas (helium, argon) has been introduced into the plasma torch, wherein heating and decompositions of components occurred in the plasma jet and in the region of the arc discharge followed by condensation of the synthesis product on metallic surfaces. In the experiments, the plasma torch electric power reached 40 kW. The main parameters were: varying pressure in the range from 350 to 730 torr and gas flow rate.

Synthesis of carbon nanotubes and nanofibers was produced by pyrolysis of soot in the presence of catalysts (dispersed metal powders Ni, Co, Y_2O_3) and decomposition of hydrocarbons (propane, butane, methane, acetylene) without catalytic additives. The methods of x-ray diffraction and of electronic microscopy were applied to investigate the structure of final products. The thermogravimetric analysis was used to determine the phase structure of carbon nanomaterials.

Experiments on the synthesis of carbon nanostructures in a plasma jet demonstrated the ability to control the morphological and structural properties of nanotubes and nanofibers. Figure 1 presents SEM images of typical carbon nanostructures. In general, the method developed allows you to scale production of carbon nanostructures desired morphology.

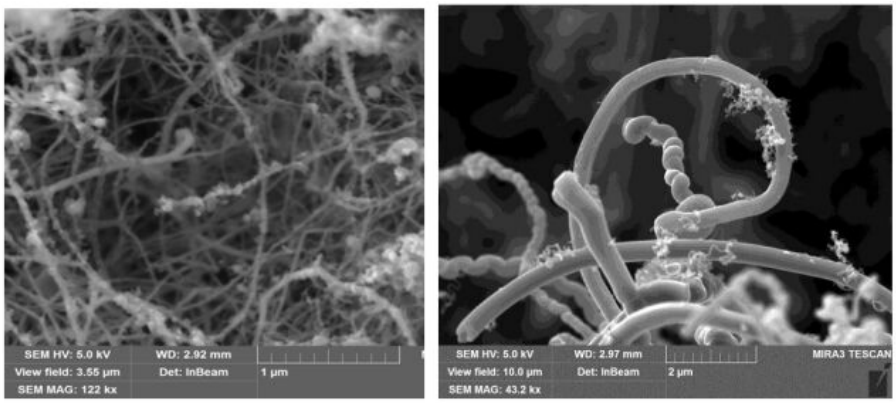

Fig.1. Carbon nanotubes and nanofibers.

References

1. L. Fulcheri, G. Flamant, T. Gruenberger, J. Gonzalez-Aguilar, F. Fabry, N. Probst and E. Grivei, Abstract Amer. Chem. Soc. (2004) **227,** 808.
2. K.S. Kim, G. Cota-Sanchez, C.T. Kingston C T, M. Imris, B. Simard and G. Soucy, J. Phys. D: Appl. (2007) **40,** 2375

Computational modeling of hexaprismane and octaprismane thermokinetic stability

Shostachenko S.A. [1] , *Katin K.P.* [1] , *Maslov M.M.* [1] , *Ryzhuk R.V.* [1] , *Kargin N.I.* [1]

fizik92@inbox.ru
[1] National Research Nuclear University MEPhI, Moscow, Russia

Carbon [*n*,*m*]prismanes (polyprismanes) can be regarded as stacked layers of dehydrogenated cycloalkane molecules, where *m* is the number of vertices of a closed carbon ring, and *n* is the number of layers [1]. For large *n* polyprismanes represent single-walled carbon nanotube analogs with an extremely small cross-section as a regular polygon. Although the [*n*,*m*]prismanes are of considerable fundamental and practical interest, the efficient methods of their synthesis are not developed. The main trends in their study are the analysis of tubular inorganic metal-carbon sandwich molecules based on prismanes [2] and their electronic characteristics investigation for possible further application in nanoelectronics as nanoscale conductors [3]. However, despite some obvious achievements in physical chemistry of polyprismanes, the question of their thermal stability is still open. Detailed study of the decay channels and decomposition products of [*n*,*m*]prismanes and their derivatives modified by various functional groups could suggest the possible ways for their synthesis.

The main aim of our work was to simulate numerically thermal stability of [2,6]- and [2,8]prismanes. Their dynamics was studied in a wide temperature range, their activation energies and frequency factors in the Arrhenius equation were determined, their lifetimes at different temperatures were estimated. Moreover the mechanisms of their isomerization were studied in detail and the minimum heights of the energy barriers preventing the decomposition were calculated. The geometries of hexa-, octaprismane and their isomers were optimized using the GAMESS program package [4]. Density functional theory within B3LYP/6-311G level of theory [5,6] was used to optimize the geometries and obtain the structural and energy characteristics of the prismanes, as well as originally developed nonorthogonal tight-binding total energy model for hydrocarbon compounds [7].

It is shown that the increase of vertices in prismanes' layers reduces their thermal stability. So the lifetimes of hexa- and octaprismane at room temperature (300 K) are equal to 100 ms and 1 ns, respectively. The initial stage of decay, which initiates the further destabilization of the framework is the rupture of one of the C–C bonds. The main products of the decomposition are the two independent rings – benzene C_6H_6 and cyclooctatetraene C_8H_8 for hexa- and octaprismane, respectively.

References

1. G. Lewars. Modeling Marvels: Computational Anticipation of Novel Molecules. (Springer, Dordrecht, 2008), P. 185.
2. Kuzmin, W.W. Duley, Phys. Rev. A (2011) **83**, 507.
3. Kuzmin, W.W. Duley, Ann. Phys. (Berlin) (2013) **297**, 525.
4. W. Schmidt, K.K. Baldridge, J.A. Boatz, S.T. Elbert, M.S. Gordon, J.H. Jensen, S. Koseki, N. Matsunaga, K.A. Nguyen, S.J. Su, T.L. Windus, M. Dupuis, J.A. Montgomery, J. Comput. Chem. (1993) **14**, 1347.
5. Lee, W. Yang, R.G. Parr, Phys. Rev. B (1988) **37**, 785.
6. D. Becke, J. Chem. Phys. (1993) **98**, 5648.
7. M. Maslov, A.I. Podlivaev, L.A. Openov. Phys. Lett. A (2009) **373**, 1653.

The formation of the structured film of single-walled carbon nanotubes using a self-organized silica template

Voronin A.S. [1,2,3] , *Simunin M.M.* [3,4] , *Ivanchenko F.S.* [1,3] , *Fadeev Y.V.* [3] , *Khartov S.V.* [2,3]

a.voronin1988@mail.ru

[1] Siberian Federal University, Krasnoyarsk, Russia

[2] Krasnoyarsk Scientific Centre SB RAS, Krasnoyarsk, Russia

[3] Ltd. "FunNano", Krasnoyarsk, Russia

[4] Moscow Institute of Electronic Technology, Zelenograd, Russia

One of the possible fields, where single-walled carbon nanotubes (SWCNT) can reveal their potential, is the production of optically transparent conductive films. However, the non-optimum transparency:surface resistance ratio prevents from their application. An attempt has been suggested to improve the transparency:surface resistance ratio by using nanotexturing [1], however, this method is not scalable for the samples with an appropriate area (over 100 cm^2).

A method has been suggested for improving the transparency of SWCNT films by structuring a film using a self-organized silica template. The template is formed as a result of quasi-ordered fracturing of a thick film of polysilicic acid sol. The fracturing occurs in the process of sol-gel transition. The evolution of fractures in the gel film is due to the evolution of mechanical deformations resulting from the film compression when dried. The fracturing parameters can be controlled by varying pH and the film thickness of the initial sol. Here, the sol pH was equal to 1, the film thickness was 50.3 μm, and alkali glass was used as a substrate. The average cluster size of the obtained template (Fig.1 a) was 72.8±21.9 μm, with the average fracture width being 15.5±5.7 μm.

An aqueous colloid of SWCNT (10^{-3} g/l), stabilized by cetyl trimethyl ammonium bromide (CTAB) (10^{-4} g/l), was deposited on the template using the ultrasonic deposition method. After the dry removal of the silica clusters, there remained a structured SWCNT film (Fig.1b-1c) on the glass substrate. The film was further annealed in the air at 400°C for 1 minute and doped with nitric acid vapors to improve the film conductivity; this process in general allows one to increase the film conductivity 7-9 times. Among the obtained samples of the structured SWCNT films, the film with the surface resistance 510 Ohm/square at 86% transparency has the most appropriate parameters. The transparency of the structured SWCNT films is 5-6% higher than that of continuous SWCNT films at the same surface resistance. It is also worth noting that the suggested method allows one to make coatings on large areas using the roll-to-roll technique.

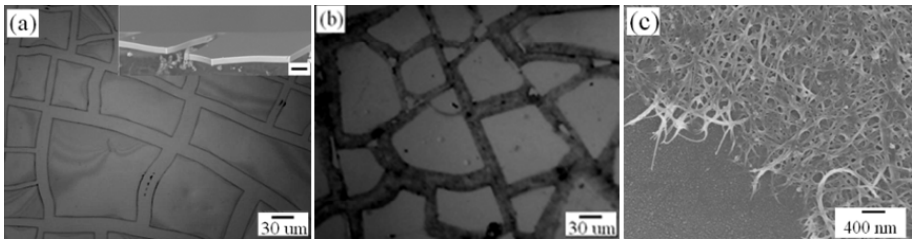

Fig.1. a- micrograph of the silica template; b- micrograph of the structured SWCNT film; c- path boundary of SWCNT

References

[1] M.H. Kim, J.-Y. Choi, H. K. Choi, S.-M. Yoon, O. O. Park, D. K.Yi, S. J. Choi and H.-J. Shin //Adv. Mater. 2008.V.20.P.457.

Peculiarities of the p-electron conjugation in single-wall carbon nanotube

Tomilin O.B. [1] , *Muryumin E.E.* [1] , *Rodionova E.V.* [1]

tomilinob@mail.ru
[1] Mordovian Ogarev State University, Saransk, Russia

This work comprises an investigation of regularities of p-electron carbon atom conjugation in cylindrical carbon systems, in particular in fragments of single-wall carbon nanotubes (SWCNT) with chiralities of (n, 0) and (n, n). A model of conjugation estimation in SWCNT based on of energy gap value ΔE as the characteristics of conjugated system is suggested. It is shown that the conjugation in the examined model molecules is determined by interaction of π- conjugation (the longitudinal factor) and ρ-conjugation (the cross-section factor) of p-electrons dependent on chirality type of SWCNT [1]. The results obtained describe qualitatively the cause of occurence of different quantitative dependences of ΔE on chirality index n in (n,0) and (n,n) SWCNTs and can be a theoretical base for targeted modification of electronic properties of single-wall carbon nanotubes. Calculation of model systems was carried out by the Hartee-Fock method within a 3-21G basis set [2].

This work was supported by the Ministry of Education and Science of Russian Federation (Project No. 1384).

References

1. O. B. Tomilin, I. V. Stankevich, E. E. Muryumin, and E. V. Rodionova, Carbon (2012) **50**, 5217.
2. M. W. Schmidt, K. K. Baldridge, J. A. Boatz, S. T. Elbert, M. S. Gordon, J. J. Jensen, S. Koseki, N. Matsunaga, K. A. Nguyen, S. Su, T. L. Windus, M. Dupuis, and J. A. Montgomery, J. Comput. Chem. (1993) **14**,1347.

The mechanism of amino group boundary functionalization of carbon nanotubes as method of design sensory device

Vil'keeva D.E. [1] , *Zaporotskova I.V.* [1] , *Polikarpova N.P.* [1] , *Boroznin S.V.* [1] , *Sokolova S.S.* [1] , *Elbakyan L.S.* [1]

vidinara@mail.ru
[1] Volgograd State University, Volgograd, Russia

The ability of carbon nanotubes to adsorb particles of various origin and conductivity enables them to be used as chemical and biological sensors. Sensors can be designed on the base of devices modified by carbon nanotubes. The atomic force microscope with the tip of the cantelever modified by carbon nanotube with a specific boundary functional group can serve as a sample of this device.

To investigate the possibility of the probe formation the binding process of amino group $–NH_2$ to an open boundary of semi-infinite carbon nanotubes (6, 0) and (6, 6) was studied.

Calculations showed that the amino group binds to the nanotube (6,6) at an angle of 114˚. The length of the C-N was equal to 1,35 Å, N-H -1 Å. For the binding process of nanotube (6.0) the following parameters were revealed: angle = 122 ˚; bond lengths: C-N = 1,33 Å; N-H = 1 Å.

The binding process between the amino group $–NH_2$ and the selected carbon atom at the open boundary of nanotubes (6.6) and (6.0) was simulated in increments of 0,1 Å perpendicularly to the edge of the tube and with orientation to the C atom. As a result, the energy curves were constructed for the systems "nanotube - $–NH_2$." The energy minimum on the curves indicates chemical bond formation between the tube and the functional group. It is found that the moment - NH_2 binds to the tubulene electron density is transferred from the C-atom to the nitrogen atom of the amino group. As a result, change in the number of carriers enables conductivity in the system and the nanotubular system acts as the probe sensor.

The investigation proved the possibility to modify carbon nanotubes by amino groups to design sensors based on them.

Carbon Nanotube: Synthesis and Applications in Solar Cell

Utkarsh K. [1] , *Yadav B. C.* [1]

balchandra_yadav@rediffmail.com

[1] Nanomaterials and Sensor Research Laboratory, Department of Applied Physics, School for Physical Sciences, Babasaheb Bhimrao Ambedkar University, Lucknow-226025, U.P., India

Carbon Nanotubes are unusually structured molecules with robust mechanical and electronic properties [1]. Their versatility is astounding; envisioned application range from field emission displays in vacuum electronics to impregnated metal composites, battery storage media, nano-electronic devices, functional AFM tips, building block for next generation of VLSI, nano lithography, energy storage as lithium batteries, hydrogen storage and biological as bio-sensors and DNA sequencing.

The combination of simple constituency, diverse behavior, and ease of fabrication makes these materials a cornerstone topic in current research. They have also very wide applications in electronic devices and also identifying the potential application which occurred due to low bias ballistic transport at few nanometers. Since valance and conduction bands are symmetric so they have direct band gap and due to this it can be used in optical emission. CNT's can be synthesized [2] via three major techniques which named as arc discharge, laser ablation and chemical vapor deposition but the CVD process is mainly used for synthesis because yield of CNT in such case will be more than 98% pure. Sometimes some extra purification process are used for forming 100% pure CNT's by using such type of MWCNT have multiple chirality then the optical property increases and it also enhanced the property of solar cell by implementing CNT's in the cell [3]. The dye sensitized solar cells are fabricated by using CNT composite and functionalized nanotubes.

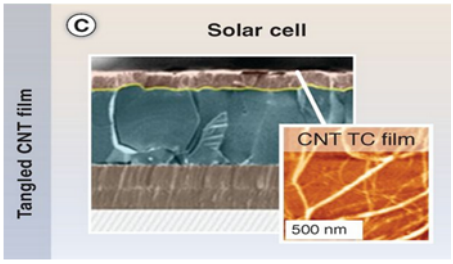

Use of CNT in a Solar Cell

References

1. Introduction to the important and exciting aspects of Carbon Nanotubes Science and Technology, D. Tomanek, A. Jorio, M.S. Dresselaus and G Dressehaus, Carbon Nanotubes: Advanced Topics in the Synthesis, Structure, Properties and Applications, Springer, Heidelberg, 2008, 1-12.
2. Structure, properties and applications of fullerenes, B.C. Yadav and Ritesh Kumar, International Journal of Nanotechnology and Applications (2008) **2**, **1**, 15-24.
3. Potential Applications of Carbon Nanotubes, M. Endo, M. Strano and PM Ajayan Carbon Nanotubes: Advanced Topics in the Synthesis, Structure, Properties and Applications, Springer, Heidelberg, 2008, 13-61.

Composites on the basis of the bitumen reinforced by carbon nanotubes for road constrruction

Zaporotskova I.V. [1] , *Arkharova I.V.* [1] , *Zadorozhnyi A.V.* [1] , *Zaporotskov P.A.* [1]

irinazaporotskova@gmail.com
[1] Volgograd State University, Volgograd, Russia

It is assumed that carbon nanotubes can be used as an additive, which will improve the properties and functional characteristics of asphalt concrete coverings. The basic principles of creation of the new road material received by bitumen reinforcing by carbon nanotubes are presented.

The plan's analysis for development in the road and transport sphere suggested, that there are need of application of the new technologies. In this paper we suggested the new technology of road asphalt qualities improving using carbon nanotubes. For this reason studying of some properties of the received composite mixes is important.

The asphalt brand BND 90/130 has been used for the preparation of asphalt concrete. The carbon nanomaterials (CNM) «Taunit» produced by «Nano tech Center» (Tambov, Russia) have been applied as a bitumen modifier. The amount of the carbon nanomaterial was 0.001 – 0,1% by weight of bitumen. We investigated the behavior of the mechanical characteristics of the sample. Receiving modified bitumen was carried out as follows. The bitumen is heated to a temperature of 100°C, then it was added the required amount of carbon nanomaterial and stirred in an ultrasonic stirrer for 6 hours to obtain a homogeneous mechanical mixture with uniform distribution of the nanomaterial. After that, the bitumen was cooled for 10 hours until the end of crystallization. Then some tests on the mechanical compressive strength and flexural strength have been carried out.

The results of the experiment showed that the strength and elasticity of the resulting asphalt pavement have been increased, as well as increased water resistance, heat resistance and cold resistance and extended temperature range of its installation in the region of negative temperatures. This method is economical, effective and aimed at obtaining highly durable material having improved physical and mechanical properties and performance.

Sensor activity of the amino group boundary-modified CNT to some metal atoms

Zaporotskova I.V. [1] , *Vil'keeva D.E.* [1] , *Polikarpova N.P.* [1] , *Boroznin S.V.* [1] , *Zaporotskov P.A.* [1]

n.z.1103@mail.ru

[1] Volgograd State University, Volgograd, Russia

It is known that gas sensors can be based on pure single and multi-walled carbon nanotubes and nanotubes modified with functional groups. We assume that modified carbon nanotubes that are applied as elements in sensor devices (probes) are not limited to the detection of gases. Boundary-modified nanotubes can be used to identify other chemical elements, for example metals and ions that make up salts and alkalis.

We investigated sensory properties of the probe based on the amino group modified CNT with respect to atoms and ions of sodium, potassium, lithium, magnesium. We studied the process of random surface scanning to detect an atom (or ion) under investigation and calculated the activity of the selected nanotubes modified with the boundary functional group in relation to the selected element. The process of a metal atom (ion) approach to the functional group was modeled in increments parallel to the border of the modified nanotubes at a distance of 2,0 Å. (Fig. 1). Analysis of the interaction energy curves found that tubules with the selected functional group become sensitive to the selected metal atoms (ions).The curves show characteristic minimum indicating the interaction between a metal atom and the modified system "CNT - amino group." The results indicate the possibility of using modified carbon nanotubes as sensors for certain elements and radicals whose presence can be experimentally detected by change in the potential of the probe system based on nanotubes modified with the functional group.

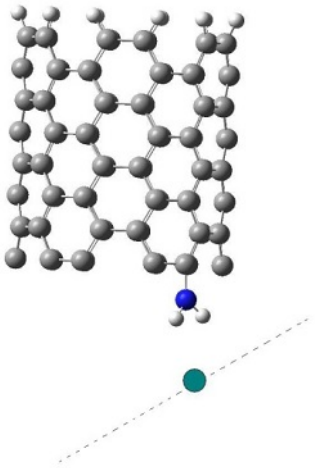

Fig. 1. The model of the surface containing a metal atom scanning process

Diffraction-based characterization of amorphous sp^2 carbon: sensitivity to domain-like packing of nanostructures

Neverov V.S. [1] , *Borisova P.A.* [1] , *Kukushkin A.B.* [1,2] , *Voloshinov V.V.* [3]

Kukushkin_AB@nrcki.ru

[1] National Research Center "Kurchatov Institute", Moscow, Russia

[2] National Research Nuclear University "MEPhI", Moscow, Russia

[3] Institute for Information Transmission Problems (Kharkevich Institute) of Russian Academy of Science, Moscow, Russia

We extend the method [1] suggested for estimation of structural properties of amorphous sp^2 carbon and applied to amorphous fullerene and its derivatives produced by vacuum annealing. The main features of the method [1] are as follows: (i) we consider fitting of the neutron or x-ray powder diffraction patterns for scattering wave vector's modulus q in the range from few units to several tens of inverse nanometers (the inverse problems is formulated similar to that suggested in [2]); (ii) a structured component of a sample is described with a limited number, N_{str}, of structural blocks of a limited number of atoms, N_{atom} ; (iii) the above structural blocks in a sample are packed heterogeneously, in the domains of a linear size exceeding 10 nm (for q in the above-mentioned range, the interference of scattering by such separate domains may be neglected), with various average atomic density and various degree of spatial ordering of structural blocks; (iv) packing of structural blocks in a domain is modeled using the Rigid Body Molecular Dynamics (RBMD) with variable parameter of pair interaction of atoms in the neighboring rigid-body structural blocks. The degree of spatial ordering of domains is defined by the total potential energy of the ensemble of blocks on the various stages of the RBMD modeling. The simulation starts with a random distribution of blocks and the highest total potential energy of the ensemble and ends with an ordered steady state and the lowest total potential energy. The method was applied in [1] to interpreting the data of neutron diffraction by an amorphous C_{60} fullerene annealed at various temperatures (600, 800, 850, 900 and 1000 ^{o}C). The set of candidate structural blocks included the C_{60} fullerene molecules and the sp^2 carbon flakes with graphene-like atom arrangement of various curvature and size. The results for N_{str}=36 and N_{atom}=14÷285 enabled us to quantify structural properties of the samples in terms of the average size and curvature of the sp^2 carbon structures. The sensitivity of results to the mutual positions of these structures was analyzed in [1] in the two limiting cases: (A) domains (taken as ensembles of nanostructures from a few dozens to several thousands in number) which contain only identical structural blocks and (B) domains of a mixture of different structural blocks within domains with the structural content of blocks taken from the solution of inverse problem in the case "A". Here we extend this analysis to the intermediate cases which correspond to domains of type "B" with the sub-domains of type "A". For the amorphous fullerene samples analyzed in [1], such a domain-like structuring allows to analyze the difference of inverse problem solutions in the cases "A" and "B" at low annealing temperatures (600 and 800^{o}C).

References

1. S. Neverov, P.A. Borisova, A.B. Kukushkin, V.V. Voloshinov, Preprint arXiv:1412.7494 [cond-mat.mtrl-sci] (paper in press).
2. A.B. Kukushkin, V.S. Neverov, N.L. Marusov, I.B. Semenov, B.N. Kolbasov, V.V. Voloshinov, A.P. Afanasiev, A.S. Tarasov, V.G. Stankevich, N.Yu. Svechnikov, A.A. Veligzhanin, Ya.V. Zubavichus and L.A. Chernozatonskii, Chem. Phys. Lett. (2011) **506**, 265.

Research of the vacancy migration process dependence on the substitution of boron in carbon nanolayers

Boroznin S.V. [1] , *Polikarpova N.P.* [1] , *Polikarpova N.* [1] , *Zaporotskova I.V.* [1]

sboroznin@mail.ru
[1] Volgograd State University, Volgograd, Russia

Research of the novel structures with the ionic conductivity is very important for the development of modern batteries. These novel materials with developed properties will allow users to avoid such demerits as little time of life, small energy, and possibility of leak from battery.

In this paper we present the results of ionic conductivity process investigation on the surface of pure carbon nanolayers and with different concentration of substituted boron atoms in them from 0 % from 100 %. For this aim, we have modeled five types of nanolayers with different concentration of boron in them (0%, 25%, 50%, 75%, 100%). The calculations of the migration process have been carried out using the MNDO method within the framework of a molecular cluster model and DFT method using B3LYP functional and 6-31G basis. For investigation of ionic conductivity processes the vacancy formation on the each type of nanolayer has been modeled. Energetic and electronic characteristics of these processes have been carried out. It has been proved that the 25 % boron substitution in the carbon nanolayer is the most energetically favorable to the vacancy formation process. So, our further research has been carried out only for the type of boron substitution in carbon nanolayer for 25 %. We considered two types of boron and carbon location in the nanolayer. The vacancy migration process has been modeled. The dependence of conductivity coefficient from the temperature has been found.

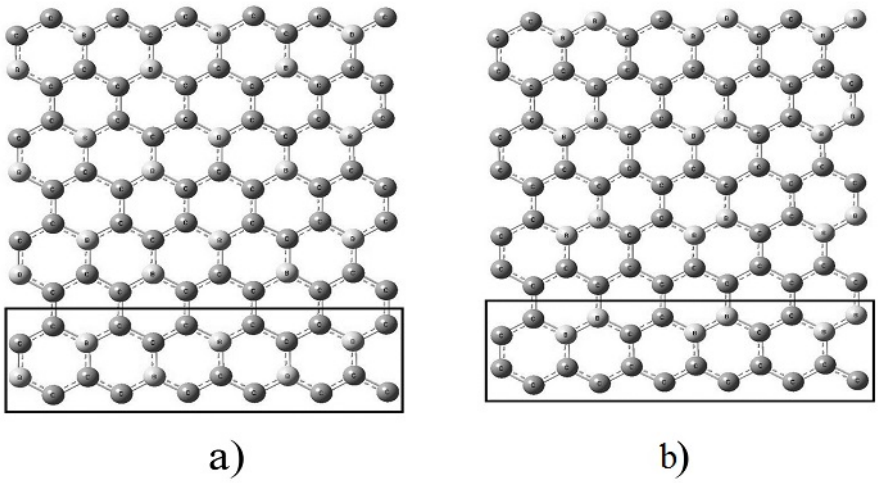

Fig. 1 Two types of boron and carbon location in the BC_3-nanolayer. Rectangle marks the elementary cell of the structure

Power-like corrections to the conductivity of Mo-C nanocomposites

Bozhko A.D. [1]

bozhko@lt.gpi.ru

[1] A.M. Prokhorov General Physiscs Institute of RAS, Moscow, Russia

The metal-carbon nanocomposites, which combine the outstanding mechanical properties inherent to the hard forms of amorphous carbon and functional flexibility of the granular systems [1], are the materials of special interest. Their hierarchically multi-scaled disordered amorphous carbon phase structure can help to enhance the current understanding of the charge transport nature in strongly disordered granular matter. The aim of this work is to study the peculiarities of the electron transport in the Mo-C nanocomposites over the wide range of temperature and metal concentration.

The films of amorphous Mo-C nanocomposites were grown on dielectric substrates in a hybrid deposition setup [2]. The carbon phase was deposited using PECVD of siloxanes vapors in DC discharge. The metal phase was introduced into the growing films by simultaneous co-sputtering of the metal target. After deposition the films were patterned in Ar RF discharge through mechanical mask for the conductivity measurements in routine 4-terminal configuration.

It was shown that conductivity of the nanocomposite films decreases with temperature in the range 4.2 – 400 K over the entire Mo concentration range 0.15 – 0.4. The derivative of the conductivity on temperature allows to reveal the fine structure of *s(T)* dependences which appears as two temperature intervals with typical power-like temperature behavior of the conductivity in each one. The fitting parameters of *s(T)* power dependences of the Mo-C nanocomposite films are sufficiently dependent on metal concentration. The power exponent in both temperature intervals varies by the non-monotonic way in the range 0.25 - 1.1 with a minimum at 0.2 – 0.26 of molybdenum content. Such behavior of the power exponent contradicts to the modern theories of the charge transport in granular materials [1]. The identity of the temperature-independent conductivity terms results in assumption that temperature corrections to the conductivity of Mo-C films are formed in both temperature intervals by the analogous way in the tunneling current paths shunting the parts of the same infinite conducting cluster in agreement with the tunneling-percolation model of the charge transport in granular metal-insulator mixtures [3]. The experimental data are simulated in the framework of the model of inelastic tunneling of the electrons in amorphous dielectrics [4] within effective medium approximation. In this model the infinite conducting cluster with conductivity weakly varying with temperature consists of the conducting grains connected by the tunnel junctions with not more than one localized state inside the intergrain potential barriers. The conducting channels with more than two localized states in the barriers partly shunt some sections of the cluster giving the major contribution to the temperature corrections of the conductivity.

This approach leads to a reasonable agreement with experimental conductivity-temperature dependences of Mo-C nanocomposites. The correlation between the concentration evolution of the model parameters and experimental ones is discussed.

References

- S. Beloborodov, A.V. Lopatin, V.M. Vinokur, K.B. Efetov, Rev. Mod. Phys. (2007) 79, 469
- Dorfman, Thin Solid Films (1992) **212**, 267
- Ambrosetti, I. Balberg, and C. Grimaldi, Phys. Rev. (2010) **B82,** 134201
- I. Glazman, and K.A. Matveev, Sov. Phys. JETP (1988) **67**, 1276

Production and properties of anodic oxide-diamond coating of aluminium

Burkat G.K. [1] *, Safronova I.V.* [2] *, Aleksandrova G.S.* [1] *, Dolmatov V.Yu.* [2] *, Myllymaki V.* [3]

DiamondCentre@mail.ru

[1] St.Petersburg State Technological Institute (technical university), Saint-Petersburg, Russia

[2] FGUP "SKTB "Technolog", Saint-Petersburg, Russia

[3] Carbodeon Ltd. Oy, Vantaa, Finland

Electrochemical anodic oxidation of details of aluminium and its alloys is a basic method of corrosion protection, increase in wear-resistance and giving dielectric properties to the surface of machine parts, mechanisms and devices. Inorganic oxide coating of aluminium obtained by means of etching method represents a nonmetallic porous film of Al_2O_3.

Detonation nanodiamonds (DND) having a negative charge in the electrolyte move to the anode (Al) at electromotive force application and penetrate into the pores generated during the oxidation, keeping there not only mechanically but also by Van der Waals and other physical- chemical forces.

In the present work the process of anodic oxidation of aluminium (sort Aludrill AO) in the sulfuric electrolyte (200 g/l H_2SO_4) with additives of DND (sort DND-TAN – detonation nanodiamonds modidied with ammonia at high temperature and pressure) in number of 0,5-10,0 g/l or standard diamond-containing blend (DB, a semi-product of production of DND) in number of 1 – 5 g/lat temperature of 11±1°C (with DB) and at 16±1°C (with DND) was studied. Conditions and results of obtaining of the anodic oxide-diamond coatings of aluminium are presented in Table.

All the obtained samples were passed a test on breakdown of 1,5 kV.

Table. Characteristics of the obtained anodic oxide-diamond coatings of aluminium

Process parameters and characteristics of the obtained coatings		**Diamond**	**Additive**
		DB	DND
1. Optimum current density, A/dm^2		2	3
2. Optimum concentration of an additive in the electrolyte, g/l		3	7
3. Film thickness, mm	no additive	18,85	15,4
	with additive	22,34 (↑by 20%)	16,3 (↑by 6%)
4. Percentage of film weight of samples mass, %	no additive	7,5	9,0
	with additive	10,0 of	10,7
5. Pores volume, ml/cm^2	no additive	0,035	-
	with additive	0,011	-

The work has been accomplished under the support provided by the Ministry of Education and Science of the Russian Federation within Federal Target Program “R&D along Priority Directions of Development of the Scientific and Technological Complex of Russia for Years 2014–2020” (Agreement on Grants No. 14.579.21.0001, RFMEF157914X0001)”.

Physicochemical properties of silver coatings obtained in the presence of diamond-containing additives

Safronova I.V. [1] *, Burkat G.K.* [2] *, Dolmatov V.Yu.* [1] *, Vehanen A.* [3] *, Myllymaki V.* [3]

DiamondCentre@mail.ru

[1] FGUP "SKTB "Technolog", Saint-Petersburg, Russia

[2] Saint-Petersburg State technological institute (Technical University), Saint-Petersburg, Russia

[3] "Carbodeon Ltd., Oy", Vantaa, Finland

Silver coatings are used in many industries for giving high electroconductivity, antifriction properties, fine appearance to products. At the same time silver coatings have a number of disadvantages such as: small hardness and wear-resistance, high porosity and low corrosion resistance.

In order to improve physicochemical properties of silver coatings detonation nanodiamonds treated with ammonia water (DND-TAN) and diamond-containing blend (DB, a semi-product of synthesis of DND) were added into dicyanargentaterhodanate (without cyanide) electrolyte of silver-plating. The used additives practically 2-fold increase the throwing power of the electrolyte (coating uniformity) and display surface-active properties.

Study of the microstructure of silver coatings in the presence of the additives has demonstrated that the grain size of coatings decreases 4 times – to 40 nm, coating density is increased. The content of carbon in the coating symbatically increases as the concentration of the additives in the electrolyte is increased. The silver-DND coating contains 2 times more carbon than the silver-DB-coating at equal contents of the additives in the electrolyte. The dependence of an effect of DND on the microhardness of silver coatings has two strongly marked maxima: at the content of DND in the electrolyte of 0,5 and 2 g/l. The first maximum can be explained by the presence of individual DND-particles in the double layer behaving as a surface-active substance. The second maximum relates to the action of this additive as a compositional one which is mechanically introduced into the coating and overgrown with the deposited silver.

The DND-additive has an impact on wear-resistance of silver coatings. At the concentration of DND in the electrolyte of 1,5 g/l the wear-resistance is increased 30 times as compared with those of a pure silver coating. Porosity of silver coatings is decreased practically 9 times when adding the DND into the electrolyte (even at the coating thickness of 3 mm), corrosion resistance is symbatically increased. The DB-additive improves physicochemical properties of silver coatings less effectively than DND. Use of the above additives is ecologically safe.

The work has been accomplished under the support provided by the Ministry of Education and Science of the Russian Federation within Federal Target Program “R&D along Priority Directions of Development of the Scientific and Technological Complex of Russia for Years 2014–2020” (Agreement on Grants No. 14.579.21.0001, RFMEF157914X0001)”.

Methods of diagnostics of nanocomposites based on silica-reinforced carbon nanotubes

Eseev M.K. [1] , *Goshev A.A.* [1] , *Horodek P.* [2,3] , *Kapustin S.N.* [1] , *Kobets A.G.* [2,4] , *Osokin K.S.* [1]

m.eseev@narfu.ru

[1] Northern Arctic Federal University, Arkhangelsk, Russia

[2] Joint Institute for Nuclear Research, Dubna, Moscow Region, Russia

[3] PAS, Institute of Nuclear Physics, Krakow, Poland

[4] NAS, Institute of Electrophysics and Radiation Technologies, Kharkov, Ukraine

This paper presents the results of experimental studies of the properties of nanocomposites based on silica filler in the form of carbon nanotubes by dielectric relaxation and positron annihilation spectroscopy. On the basis of these results proposed the technique of diagnosis and control of the investigated materials.

There are currently actively developed and applied research methods of mechanical, thermal and electrical properties of nanocomposites with the addition of carbon nanotubes [1]. In the studied nanocomposites matrix of SiO_2 reinforced multiwall carbon nanotubes manufactured CVD-method. Mass fraction of impurities from the nanotubes have ranged 0.01-1%. Control of the surface state of the composite was performed by SEM and AFM. The state of the inner layers of the composite are determined by other methods. Using the method of dielectric relaxation spectroscopy of the obtained materials were determined characteristics such as conductivity, real and imaginary part of the dielectric constant. This allowed us to obtain the concentration dependence of the electrical properties of the mass fraction of carbon nanotubes in the material. Also for the analysis of the inner layers of materials can be used positron annihilation spectroscopy is sensitive to the concentration of inhomogeneities and defects [2]. Facility the LEPTA [3] allows the study stratified by measuring the Doppler broadening of the annihilation gamma line at different energy positrons in materials [4].

Our studies allow us to offer a method for determining the concentration of carbon nanotubes in nanocomposites.

This work was supported by the project the Ministry of Education of the Russian Federation №3635 "Investigation of the properties nanocomposites with controlled modification of the structure reinforced with carbon nanotubes".

References

1. A. V. Eletskii, A. A. Knizhnik, B. V. Potapkin, J. M. Kenny, Phys. Usp. (2015) **58**, in print (3).
2. V. I. Grafutin, E. P. Prokop'ev, Phys. Usp. (2002) **45** 59.
3. A. V. Akhmanova, M. K. Eseev, , A. G. Kobets, I. N.Meshkov, A. Y. Rudakov, A. A. Sidorin, , S. L. Yakovenko, Phys. Part. Nucl. Lett. (2012) **9**, 373.
4. A. A. Sidorin, I. Meshkov, E. Ahmanova, M. Eseev, A. Kobets, V. Lokhmatov, V. Pavlov, A. Rudakov and S. Yakovenko, Mater. Sci. Forum (2013) **733**, 322.

Phase transformations of polyacrylonitrile and carbon fiber in the process of heat treatment

Fazlitdinova A.G. [1] , *Tyumentsev V.A.* [1]

fazlitdinovaag@mail.ru
[1] Chelyabinsk State University, Chelyabinsk, Russia

High performance characteristics of carbon fibers (CF) obtained on the basis of polyacrylonitrile (PAN), determines the final structure that begins to form in the process of thermomechanical treatment on the stage of thermal stabilization. A new nanostructure of thermally stabilized fiber formed in the volume of the original PAN filaments at temperatures ~250°C. In further recrystallization of nanostructured material at a high temperature treatment (~1500 - 3000°C) there is a change in the dispersion composition, the interlayer distance d_{002} and texture.

For working off the optimal modes of thermomechanical effects on fiber precursor at temperatures from ~200 to ~3000°C in order to form the desired final structure of the carbon fiber is necessary to establish the relationship between the modes of production and structural changes of the material. X-ray analysis is one of the most common methods of controlling the parameters of the structure of materials. However, when using a standard method of the experiment a large penetration depth of X-rays causes that the diffraction peak mainly formed layers of material lying below the plane of the self-focusing of X-rays by Bragg-Brentano. For these layers is not realized the condition of self-focusing, which leads to a change of the FWHM and 2Theta. In addition, the experimentally observed diffraction peak 010 PAN and 002 CF is not described by a standard function, there is a significant asymmetry of the maximum that may be due to the simultaneous presence in the material component, markedly different in coherent-scattering region (CSR) sizes and interplanar distance.

We have eliminated the instrumental distortion of the diffraction peaks due to high penetration depth of X-rays, and analysis of the profiles 010 PAN at different stages of transition in thermally stabilized condition is made using the software package Origin, as well as 002, 004 and 006 CF obtained at substantially different conditions.

It was shown that carbon fiber material is heterogeneous, component composition of CSR differ interplanar distance and size is determined by the conditions of production and depends on the angle of orientation relative to the axis of the thread. The average sizes of CSR as we move to the components corresponding to smaller values d_{002}, increase and thus depend on the angle of orientation relative to the axis of the thread [1].

Crystalline component structure of the precursor PAN fiber is represented by two kinds of PAN CSR, differing by an order of magnitude in their average sizes. At the initial stage of isothermal stabilization is observed to improve the structure of PAN filaments - increasing the size of large CSR and improving the texture of the material. Phase transition PAN into structure of thermally stabilized fiber develops by forming new highly dispersed phase in a local micro-volumes by the size of the order of one nanometer [2, 3].

References

1. A. Tyumentsev, A.G. Fazlitdinova. Russian J App Chem (2013). V.86(5), 760.
2. Fazlitdinova A.G., Tyumentsev V.A., Podkopayev A., Shveikin G.P. J Mater Sci (2010). V.45. 3998
3. Fazlitdinova A.G., Tyumentsev V.A. Technical Physics. Russian J App Phys (2011). V.56(12), 1768.

Interactions of shungite nanocarbon, a graphene family nanomaterial, with biomacromolecules

Goryunov A.S. [1] , *Rozhkov S.P.* [1] , *Borisova A.G.* [1] , *Rozhkova N.N.* [2]

goryunov@krc.karelia.ru
[1] Institute of Biology, Karelian Research Centre RAS, Petrozavodsk, Russia
[2] Institute of Geology, Karelian Research Centre RAS, Petrozavodsk, Russia

The solubility of graphene oxide (GO), which, unlike graphite, is soluble in water and polar solvents, and less soluble reduced graphene oxide (r-GO) has been studied intensively in the past few years. On this basis water nanodispersion of shungirte carbon (ShC), a natural source of nanocarbon, has been proven to present a dispersion of 20-100 nm aggregates of globules formed by ~1.5 nm stacks consisting of 5-6 layers of r-GO nanosheets, the basic structural element of ShC [1,2]. The role of nanocarbon released from shungite rocks upon its interaction with water in the mechanism of ShC biological activity is of specific interest. Shungite nanocarbon-induced effects on vertebrate blood proteins and erythrocyte membranes have been studied and compared with those of fullerenes and nanodiamonds with the aim to elucidate the effects of nanocarbon dispersions on the structural dynamic, thermodynamic, hydrodynamic, and redox properties of the biomacromolecules and cell membranes which are expected to underlie shungite nanocarbon biological activity.

Fe(II) induced reduction of the stable spin-probe to hydroxylamine in water solution and in erythrocyte membrane lipid bilayer as well as subsequent hydroxylamine oxidation has been shown to accelerate with increasing ShC concentration in nanodispersion. Adsorption of serum albumins (SA), and not hemoglobins (Hb), that reach its maximum values for the majority of carbon nanoparticles (NP) within few minutes, leads to the complexation with the formation of a ShC NP-protein corona formed by the layers of hard and soft corona differing in the intensity of bio-nano interaction. The study of the oxidative effect of ShC nanodispersions on proteins using the spontaneous oxidation of Hb has shown a significant acceleration of Hb molecule Fe(II) oxidation indicating the prooxidant effect of shungite nanocarbon on protein in solution. Heme proteins autooxidation pathways consideration suggests that the most probable mechanism of the effect is determined by ShC electron-acceptor capacity and involves a pH-independent transfer of an electron from a deoxyheme to an O_2 molecule [3].

Differential scanning calorimetry (DSC) and electron spin resonance (ESR) spin-probing data demonstrate that SA molecules are expanded somewhat in water dispersion of nanocarbon particles as compared to the protein water solution. ShC NPs have been shown to interact with protein via the fatty acids binding sites on SA predominantly, leading to the occupation of some protein ligand binding sites. ESR spin-labeling and DSC data have shown the increased thermal stability of the proteins of erythrocytes cytoskeleton complex, whereas their membrane proteins have not been affected. The overall cell membrane integrity has been decreased at the same time. The effects revealed can potentially lead to subsequent adverse biological responses.

This work is supported by RFBI grant №13-03-00422

References

1. B.S. Razbirin, N.N. Rozhkova, E.F. Sheka, D.K. Nelson, and A. N. Starukhin, J. Exp. Theor. Phys. (2014) **118**, 735.
2. B.S. Razbirin, N.N. Rozhkova, E.F. Sheka, D.K. Nelson, A. N. Starukhin, and A.S. Goryunov, Nanosystems (2014) **5**, 217.
3. S.P. Rozhkov, and A.S. Goryunov, Rus. J. Gen. Chem. (2013) **83**, 2585.

Structure of graphene layers in shungite carbon

Kovalevski V.V. [1] , *Moshnikov I.A.* [1]

kovalevs@krc.karelia.ru

[1] Institute of Geology, Karelian Research Center, RAS, Petrozavodsk, Russia

One of the more intriguing types of non-crystalline carbon occurs in the shungite rocks of Karelia (Russia), from which the first natural occurrence of fullerenes was reported [1] and hollow nanospheres and fibers were described [2]. Carbon from shungite rocks is of the non-graphitizable variety and is characterized by turbostratic stacking of graphene layers. All high-resolution transmission electron microscopy (HRTEM) images of shungites contain well-defined fringes, and these occur in packets of 5 to 14 sheets. Those suggest that some 3-dimensional closed shells occur but, more commonly, there are fractions of such shells or regions of graphene structure that are highly disordered into short bent stacks and enveloped nano-sized pores. Some graphene layers form irregular closed shells similar to those in carbon nanotubes.

Two types of carbon layers have been revealed in shungites by HRTEM. The first type, graphite-like carbon layers are characterized by strongly marked hexagonal symmetry, but are corrugated layers. The layers consist of domains about 1 nm in diameter, some of those are elevated and form hillocks and others are down and form hollows. The distance between hillocks and hollows is about 2 nm. Imperfections of the latter type of carbon layers on the molecular level connected with irregularities of 100 fringes that suggest a disorder of the graphene layers from HRTEM images. Some of those are connected with essential disorder of fringes that can be resulted from the presence of impurity atoms or clusters in the stack of graphene layers. Other imperfections connected with insignificant disorder in the direction of fringes and the distance between them, and can be due to point defects or the four-, five-, eight-membered or other carbon rings that are signs of fullerene-like structures [3]. But those are also corrugated layers with the similar features.

This work was supported in part by the RFBR grant 13-05-98811.

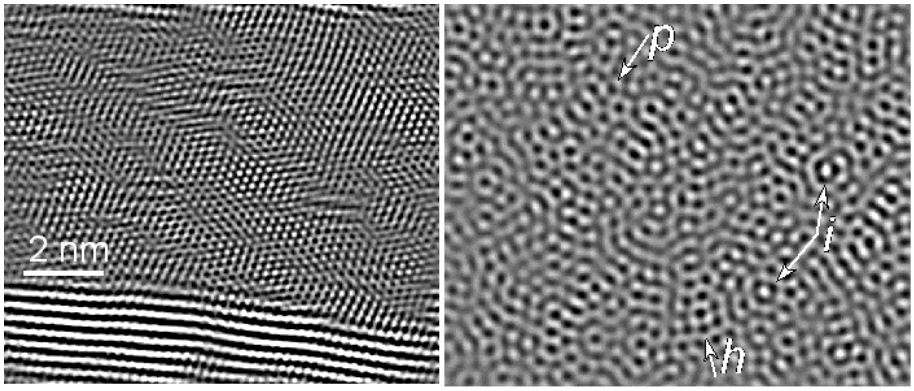

Fig.1. HRTEM images of graphite-like and fullerene-like carbon layers (p- pentagonal, h- heptagonal carbon rings, i- noncarbon inclusions) in shungites.

References

1. P.R. Buseck, S.J. Tsipursky, R. Hettich. Fullerenes from the geological environment. Science (1992) **257**, 215.
2. V.V. Kovalevski, A.N. Safronov, Ju.A. Markovski. Hollow carbon microspheres and fibres produced by catalytic pyrolysis and observed in shungite rocks. Mol Mater. (1996) **8**, 21.
3. F. Cataldo. The impact of a fullerene-like concept in carbon black science. Carbon (2002) **40(2),** 157.

New prospective composite nanostructures based on graphene, C_{60} and TMDs.

Kvashnin A.G. [1,2,3] , *Sorokin P.B.* [1,2,3] , *Chernozatonskii L.A.* [1]

agkvashnin@gmail.com
[1] Emanuel Institute of Biochemical Physics RAS, Moscow, Russian Federation
[2] Mocsow Institute of Physics and Technology, Dolgoprudny, Russian Federation
[3] Technological Institute for Superhard and Novel Carbon Materials, Troitsk, Russian Federation

Recently a great interest of the scientists around the world directed to composite materials with new physical properties which differs from the properties of their components. The most widespread composite materials are C_{60} fullerenes inside the carbon nanotube (C_{60}@CNT) [1] or C_{60} between graphene layers [2,3]. Fullerenes C_{60} with CNTs functionalized by carboxyl groups were studied as well [4]. The importance of both experimental fabrication and theoretical studies of known materials (e.g. CNTs of MoS_2 materials) modified by C_{60} fullerenes dictates by the broad perspective of its applications in photovoltaic. It is well known fact that C60 fullerenes are acceptors for electrons and they are well excited by light [5]. Even if there is no chemical bonding between C_{60} and MoS_2 nanotube (MoS_2NT) than photoelectrons caught by fullerenes can be easily transferred to the nanotube which increases the energetics of light to electricity conversion [5].

In this work we considered new quasi-two-dimensional structure based on graphene, fullerene C_{60} and MoS_2 monolayers. Through the conductive properties and wide electronic spectra due to the interaction with fullerene tube such composite materials can be used in photogalvanic devices. We also carried out the investigation of composite graphene/MoS_2/C_{60}/graphene structures which potentially can be used in photovoltaic as element for solar cells due to the presence of two conductive surfaces (graphene) and composite fullerene based structure inside which can easily catch photoelectrons and transfer them through the graphene surfaces.

This work is supported by Russian Scientific Foundation project № 14-12-01217.

References

1. *Carbon Nanotubes: Properties and Application*. FL, USA: 2006.
2. Ishikawa, M.; Kamiya, S.; Yoshimoto, S.; Suzuki, M.; Kuwahara, D.; Sasaki, N.; Miura, K. *J. Nanomat.* (2010) **2010**, 891517
3. Saito, S.; Oshiyama, A. *Phys. Rev. B* (1994) **49**, 17413
4. Li, C.; Chen, Y.; Wang, Y.; Iqbal, Z.; Chhowalla, M.; Mitra, S. *J. Mat. Chem.* (2007) **17**, 2406
5. Sariciftci, N. S.; Braun, D.; Zhang, C.; Srdanov, V. I.; Heeger, A. J.; Stucky, G.; Wudl, F. *Appl. Phys. Lett.* (1993) **62**, 585

Alignment of carbon nanotubes in polystyrene matrix determined by atomic force microscopy and magnetometry

Geydt P. [1] *, Zakharchuk I.* [1] *, Makarova T.L* [2] *, Lahderanta E* [1] *, Kanygin M.A.* [3] *, Sedelnikova O.V.* [3] *, Kurenya A.G.* [3] *, Bulusheva L.G.* [3] *, Okotrub A.V.* [3]

tatyana.makarova@lut.fi

[1] Lappeenranta University of Technology, FI-53851 Lappeenranta, Finland

[2] Ioffe Physical Technical Institute, Polytechnicheskaya 26, 194021 St. Petersburg, Russia

[3] Nikolaev Institute Inorganic Chemistry, 630060, Novosibirsk, Russia

Nanotube-polymer composites is a large arena of studies, which shows that the remarkable properties indigenous to the nanotubes could be transferred to the polymer matrix. Particular attention is paid to the composites with aligned nanotubes, as they can be used as elastomers, membranes, polymer electrodes. The alignment can also affect the effective conductive pathway for electrons and phonons, profoundly improving the electrical and thermal properties of the composite. In the development of contemporary approaches in the directional alignment of carbon nanotubes in polymer matrices, it is important to elaborate the methods for control the degree of alignment. Standard characterization methods have limited applicability, as the samples are not crystalline, both matrix and nanotubes have similar chemical composition and optical refractive indices. We made an assessment of nanotubes alignment using two methods: atomic force microscopy and magnetization measurements with magnetic field parallel to the tubes and in perpendicular direction.

Polystyrene plates with 5 wt% CNT loading were prepared using forge-rolling and stretching methods. A required amount of CNTs separated from the silicon substrate was put into a toluene solution of polystyrene and the mixture was mechanically stirred until complete polymer dissolving. The sonicated solution was dried to a viscous state. In the first method, a composite plate was repeatedly forge-rolled along a certain direction. In the second method, soft composite plate was uniaxially stretched at a heating, which was provided by a hot air gun.

AFM measurements showed that both forge-rolled and stretched composites contained aligned nanotubes. Quantitative information was obtained from magnetic measurements. The samples comprised a three-component system: polystyrene matrix, carbon nanotubes and iron catalyst. Iron particles were responsible for typical ferromagnetic loops, which did not show any directional dependence. Total magnetic moment of the nanotubes can be viewed as the sum of several components: atomic core diamagnetism, orbital diamagnetism coming from itinerant π-electrons in band structure of a semimetal, van Vleck paramagnetism originating from virtual magnetic dipole transitions between the valence and conduction bands, ferromagnetic term from magnetic impurities, Landau diamagnetic and Pauli paramagnetic contributions from conduction electrons. Ferromagnetic contribution subtracted, the observed magnetic response is diamagnetic and anisotropic with the component along the nanotubes less diamagnetic than that of the perpendicular. The anisotropy is consistent with theoretical predictions. We estimate that 80% of nanotubes in stretched matrix and 70% nanotubes in forge-rolled matrix are directionally aligned.

Supported with the FP7 MCA IRSES project 295180 MagNonMag.

Dependence of properties of aqueous electrolyte-based supercapacitors on micro- and nanoporous carbons structure

Maltsev A. A. [1] , *Bibikov S. B.* [1] , *Razumovskiy S. D.* [1] , *Podmasteryev V. V.* [1] , *Kalinichenko V. N.* [2]

alex.a.maltsev@gmail.com

[1] N.M. Emanuel Institute of Biochemical Physics of RAS, Moscow, Russia

[2] N. N. Semenov Institute of Chemical Physics

One of the most important problems of modern electrochemistry is providing both high energy density and power density in one device. Supercapacitors, also called electric double-layer capacitors (EDLC), are most likely to provide these properties. As the carbon electrodes are the most variable parts of supercapacitors, criteria of choosing carbon electrode materials may be helpful for carbon electrodes research.

In this paper, some properties of porous carbons derived from pyrolised rice strains were investigated. Specific surface area measured with BET method and method of methylene blue adsorption [1] were compared between each other. The linear correlation of specific surface area and capacity was proved. However, method of methylene blue adsorption is slightly more informative for design of carbon electrodes for non-aqueous-electrolyte based supercapacitors in comparison with BET method because the molecule of methylene blue is more alike organic electrolyte molecule than molecule of nitrogen.

In addition, scanning electron microscopy (SEM) micrographs were used for characterizing microstructure of some materials to explain different values of equivalent serial resistance (ESR) of supercapacitors.

All the electric properties of material (such as capacitance, resistance and others) were measured in 0.5 M Na_2SO_4 aqueous solution. All being investigated materials were formed into symmetrical supercapacitors electrodes by covering surface of pyrolytic carbon tissue or stainless steel gauze with binding of colloidal graphite solution or poly(tetrafluorethylene) respectively.

The results of measuring equivalent serial resistance (ESR) of experimental supercapacitors were compared with the particles scanning electron micrographs (SEM). The particles with lower BET-surface area was found to have less ESR than particles with higher one. The method of defining specific surface area with methylene blue absorbtion was proved to characterize electrolyte-available surface of electrode as well as BET method. Method of methylene blue adsorption gives a C/S parameter value (average capacity/surface ratio) alike the one of graphene [2].

References

1. GOST 13144-79. Graphite. Methods for the determination of specific surface. Cited by: http://gostexpert.ru/gost/gost-13144-79
2. NATURE COMMUNICATIONS | 5:3317 | DOI: 10.1038/ncomms4317

Optical properties of diamond-like carbon films modified with silver and platinum

Prikhodko O.Yu. [1] *, Manabaev N.K.* [1] *, Mikhailova.S.L.* [1] *, Guseynov N.R.* [1] *, Daineko E.A.* [1] *, Maksimova S.Ya.* [1] *, Mukhametkarimov Ye.S.* [1]

skysvetik91@mail.ru
[1] al-Farabi Kazakh National University, Almaty, Kazakhstan

In this work comparative results of amorphous diamond-like carbon films with silver (a-C:H<Ag> films) and platinum (a-C:H<Pt> films) clusters structure and optical properties study are presented. The films were fabricated by ion-plasma magnetron sputtering of combined polycrystalline graphite-metal target. The sputtering process was carried out in hydrogen and argon gas mixture. The films were deposited on quartz and silicon substrates. The content of platinum and silver impurity in the films was changed from 0 to 9 at. % and from 0 to 20 at. %, respectively. Concentrations of metal in the films were changed by alteration metal and graphite area relation in the combined target.

Presence of isolated clusters in the films was found by transmission electron microscopy (TEM). The diameter of Pt clusters weakly changed with a rise of a metal content and was ~5 nm. On the contrary, the average size of the Ag clusters grows from 2 nm at 2 at. % to 8 nm with a metal content increase to 20 at. %.

An important feature of a-C:H<Pt> and a-C:H<Ag> films optical properties was the presence of absorption peak in the visible range of the optical absorption spectra. The absorption peaks in spectra of the a-C:H<Pt> films situated in the range from 495 to 498 nm and for the a-C:H<Ag> films lied at 420 nm. The intensity of the peaks rose with increase of metals concentration in the films. Besides, the peaks were more intensive in a-C:H<Ag> films in comparison to the a-C:H<Pt> films at the same metal concentration. It is supposed that the absorption peaks in both cases are the result of surface plasmon resonance on metal clusters in the films. Size of clusters was determined from resonance absorption spectra and it was in good agreement with TEM results.

Modeling of the resonance absorption process with a usage of Mie theory for the isolated metal clusters imbedded in the dielectric matrix provides good coincidence with our experiment.

Thus, a-C:H<Pt> and a-C:H<Ag> films are nanostructure heterophased material characterized by presence of absorption peak in the visible range of optical absorption spectrum.

A part of the research was carried out in framework 4608/GF4 grant of Ministry of Education and Science of Kazakhstan Republic.

Electrophysical properties of shungite at low temperatures.

Moshnikov I.A [1] , *Kovalevski V.V.* [1]

igorm@krc.karelia.ru

[1] Institute of Geology, Karelian Research Center, RAS, Petrozavodsk, Russia

Shungite rocks are carbonaceous volcanic and sedimentary rocks of Karelia. Carbon of those can be described as natural fulleren-like nanostructured matter with a number of unique physical and chemical properties [1,2]. One of the most informative and practically demanded properties of carbon materials are electromagnetic properties, which are closely related to the band and the atomic structure of the material and directly determined by the degree of ordering of carbonaceous matter (the size of the crystallites, the length of graphene layers, and so on). The effect of temperature on the electromagnetic properties allows to select shungite rocks from a number of carbonaceous materials. Magnetic susceptibility of shungites characterized by different structural parameters differ significantly at temperatures from 90 to 150 K. Diamagnetic effect is the greatest for samples with preferred orientation of graphene layers, and is not observed for shungite with chaotic orientation of the layers [3].

Our measurements of temperature dependences of electrical conductivity and shielding effectiveness of shungite rocks in the range of 77-300 K revealed particular features of shungite rocks. Most shungite samples has a nonlinear dependence of the conductivity on temperature (fig.1) similar to that described for semiconductors, in which the charge carrier can be a small radius polaron [4]. The conductivity decreases with increasing temperature due to scattering of electrons by phonons as a function of $(T)^{-1/2}$ in the temperature range from 180 to 250 K.

Correlation value of the energy of the π+σ plasmon with the changing of the frequency dependence of the shielding effectiveness of temperature was revealed. The higher the energy, the slower is the growth of the shielding effectiveness with frequency at the temperature close to 77 K. The samples with the energies of 24.9, 25.3 and 26 eV show the decrease of the growth rate with frequency in 55, 70 and 95% accordingly in relation to room temperature. Comparison with other carbon materials showed that the observed effects are associated with the structure of shungite rocks, namely orientation of graphene layers and energy of the π+σ plasmon.

This work was supported in part by the RFBR grant 13-05-98811.

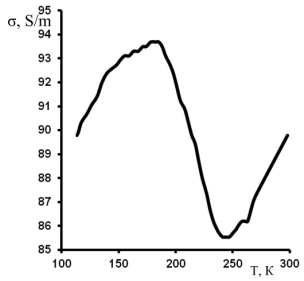

Fig.1. The dependence of the conductivity of shungite from temperature.

References

1. V.V. Kovalevski. Zapiski RMO (2009) **5**, 97.
2. M.A. Augustyaniak-Jablokow, Y.V. Yablokov, B. Andrzejewski, W. Kempinski, S. Los, K. Tadyszak, M.Y. Yablokov, V.A. Zvikharev. Physics and chemistry of minerals (2010) **37(4)**, 237.
3. V.V. Kovalevski, A.V. Prikhodko, P.R. Buseck. Carbon (2005) **43**, 401.
4. N.F. Mott, E.A. Davis. Electron processes in non-crystalline materials. Mir, M.(1982). P.108.

Fine microstructure and thermal conductivity of wood-derived biomorphic carbon

Orlova T.S. [1] , *Kartenko N.F.* [1] , *Parfeneva L.S.* [1] , *Smirnov B.I.* [1] , *Smirnov I.A.* [1]

orlova.t@mail.ioffe.ru
[1] Ioffe Institute, St. Petersburg, Russia

Biomorphic high-porous carbon materials processed by carbonization of natural wood are promising materials for processing carbon-based composites and electrodes in supercapacitors. In the present paper the results on correlation between fine microstructure and thermal conductivity of biocarbons carbonized from beech wood at different temperature T_{carb} in the interval 600–2400°C are presented.

Biocarbons obtained at different T_{carb} (600–2400°C) present natural nanocomposites consisting of an amorphous matrix and nanocrystallites of graphite- and graphene-types [1]. The sizes of graphite and graphene nanocrystallites increase from 10 to 24 Å and from 27 to 60 Å, respectively, when T_{carb} increases from 1000 to 2400°C. The volume fractions of the amorphous and nanocrystalline phases as well as of graphite and graphene nanocrystallites separately have been determined as functions of T_{carb} for the first time (Fig. 1). Temperature dependences of the phonon thermal conductivity κ(T) of the biocarbons with T_{carb}=1000 and 2400°C have been analyzed for the range of 5–300 K. It has been shown that κ(T) of the biocarbon with T_{carb} = 1000°C is controlled by the amorphous phase in the range of 5–50 K and by the nanocrystalline phase in the range of 100–300 K. For biocarbon with T_{carb} = 2400°C the character of κ(T) is determined by the heat scattering in the nanocrystalline phase over the entire temperature range of 5 - 300 K. The quantitative estimations have showed that the thermal conductivity of the nanocrystalline phase κ_{nano} at 300 K is almost three times higher for T_{carb} = 2400°C than for T_{carb} = 1000°C. Analysis of thermal conductivity in correlation with fine microstructure features shows that such difference is mostly due to the increase in dimensions of the nanocrystallites with increasing T_{carb}. The role of strongly disordered grain boundaries between nanocrystallites in thermal conductivity of biocarbons is discussed.

Acknowledgements: This study was partly supported by the Russian Foundation for Basic Research (project no. 14_03_00496_a) and the Presidium of the Russian Academy of Sciences (program P_20).

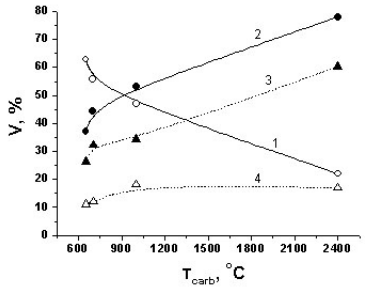

Fig.1. Volume fractions (%) of amorphous (1) and nanocrystalline (2) phases in beech-derived biocarbon as a function of T_{carb}. (3) and (4) are volume fractions of nanocrystallites of graphite- and graphene- types, respectively.

References

1. L.S. Parfeneva, T.S. Orlova, N.F. Kartenko, N.V. Sharenkova, B.I. Smirnov, I.A. Smirnov, H. Misiorek, A. Jezowski, T.E. Wilkes, K.T. Faber. Phys. Solid State (2010), **52**, 1115.

Raman characterisation of large area 2D materials

Ponkratov K. [1] , *Milikofu O.* [2] , *Tim B.* [3]

kirill.ponkratov@renishaw.com
[1] OOO Renishaw, Moscow, Russia
[2] Renishaw KK, Tokyo, Japan
[3] Renishaw plc, Wotton-under-Edge, UK

Raman spectroscopy was used to examine large areas of 2D materials and their 3D precursors, by analysing uniformity, strain/stress and defects. This work demonstrates the usefulness of Raman spectroscopy, and especially StreamLine Slalom Raman fast imaging, for the fast surveying of large regions of 2D materials.

Graphene, h-BN, MoS_2, and other 2D materials, have immense potential in a very wide range of application areas. However, for this potential to be achieved, production processes need to be improved, so that large areas of high quality material can be grown. Chemical vapour deposition (CVD) is a promising technique for graphene growth, with some groups growing material over regions larger than a square metre. Unfortunately on these length scales the quality of the graphene can become compromised, with the film comprising many layers of graphene instead of the required single or double layer. Here we report on Raman measurements of industrial scale graphene samples. These results demonstrate the variation in material quality on large length scales, and highlight the need for improvements in growth recipes.

Whilst graphene manufacturing is moving towards mass production, other 2D materials, for example h-BN, are firmly in the research stage. It is possible to use mechanical exfoliation to obtain single layers of h-BN in the same way that graphene can be exfoliated from graphite. However, large h-BN crystals are not readily available, making it a challenge to get high quality single layers of h-BN for test structures. Here we use 3D Raman mapping to examine large h-BN crystals produced using a temperature gradient method. With Raman spectroscopy the magnitude and distribution of the local strain field can be gauged in three dimensions. This is important information that can be used to help understand the growth mechanism and ultimately improve the growth recipe, enabling better single layer h-NB to be obtained.

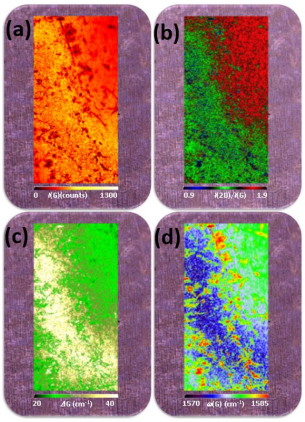

Figure 1. Raman images of CVD graphene grown on a Cu foil. The area mapped was 500 µm × 1000 µm. These images illustrate: (a) Intensity of graphene G band. (b) I_{2d}/I_g ratio. A value greater than 2 (red) is indicative of single layer graphene and 1 to 2 bilayer graphene. (c) G band width. Often used to assess material uniformity. (d) Peak position of the G band. This is an indicator of strain and electronic properties. These images all highlight significant variations over what is described as a uniform graphene film.

The high non-linearity of the electromagnetic waves absorption for Astralenes at the THz frequency region

Ponomarev A.N. [1] , *Melnikov L.A.* [2] , *Kolodiajny G.U.* [1]

9293522@gmail.com
[1] SPbSPU, St.Petersburg, Rusia
[2] SGTU, Saratov, Russia

We have researched of the peculiarities the electromagnetic waves absorption by different kinds of nanocarbon particles in THz frequency range. The fullerenes (C-60 and C-70), two types of multiwall carbon nanotubes (arc and gas phase technology made), colloidal graphite, astralenes [1], sulfo-adducts of the two or three-layer graphenes and carbon nanoporous microfiber (NPMF) [2] have been studied. As it was found, for the wide range of the wave lengths (75μ-6000μ) and for the wide diapason of the most famous type nanocarbon particles concentration (1%-15% mass.) the relations between the absorption coefficients and the concentrations of these particles in the transparent samples are rather goodly conformed with the Lambert-Beer low. However, it is not so for the astralenes and NPMF. This case the relations between the absorption coefficients and concentrations of these kind of the nanocarbon particles became highly non-linear from a not so big concentrations (3%-5% mass.).

Authors suppose, that the main reason for this phenomena is the giant resonance Van-der- Vaals forces between the astralenes (tor-like particles) [3] if there is enough amount of the astralenes in the nearest neighbourhood, so the high intensively agglomeration processes are taking place. The high level of the agglomeration lead to increasing the mass of big oscillators, especially for relatively low frequency interval the absorption spectra. The model the phenomena of the non-linear optical sorption have been suggested may be illustrated by the photos of the astralenes after 0,0025 THz microwave treatment – it became like a small sphere aggregates.

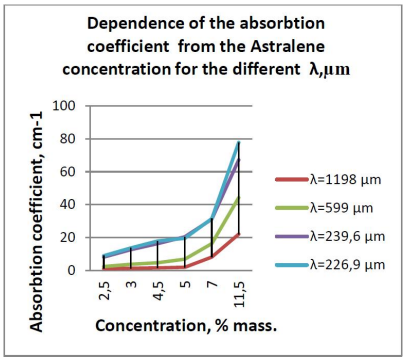

Fig. 1. The dependence of the absorption coefficient from the Astralenes concentration

References

. 1.A.I.Shames, E.A.Katz, A.M.Panich, D.Mogilyansky, E Mogilko, J.Grinblat, V.P.Belousov, I.M.Belousova, A.N.Ponomarev, Diamond & Related Materials, 2009, v.18, p.505.
2. Ponomarev A.N. Carbon Nanoporus MicroFiber/**RU** Patent Claim № 2014151923/, 2014, December 23.
3. A.N.Ponomarev, M.E.Yudovitch, M.V.Gruzdev, V.M.Yudovitch, J. Scientific Israel – Technological Advantages, 2009, V. 11, № 3, P. 20 – 26.

Synthesis, identification and physical-chemical properties of adduct of light fullerene C_{60} and argenine$C_{60}(C_6H_{12}NaN_4O_2)_8H_8$

Semenov K.N. [1,2] , *Charykov N.A.* [1,3] , *Ivanova K.A.* [2] , *Letenko D.G.* [4] , *Nikitin V.A.* [5] , *Klepikov V.V.* [3] , *Cherepkova I.A.* [3] , *Matuzenko M.Yu.* [3] , *Tyurin D.P.* [3] , *Shestopalova A.A.* [3] , *Manyakina O.S.* [3] , *Ivanova K.V.* [6]

semenov1986@yandex.ru

[1] Public Joint Stock Company "Scientific and Production Association "TECHNOLOGIES", Saint-Petersburg, Russia

[2] Saint-Petersburg State University, Saint-Petersburg, Russia

[3] Saint-Petersburg State Technological Institute (Technical University), Saint-Petersburg, Russia

[4] Saint-Petersburg State University of Architecture and Civil Engineering, Saint-Petersburg, Russia

[5] Saint-Petersburg State Polytechnical University, Saint-Petersburg, Russia

[6] Saint-Petersburg State Electro-Technical University (LETI), Saint-Petersburg, Russia

Water soluble fullerenes may be used in wide ranges of applications: machinery, building, medicine, pharmacology (as the result of compatibility with water, physiological solutions, blood, lymph, liquor, gastric juice), cosmetics. The synthesis of water soluble adduct of light fullerene and argenine$C_{60}(C_6H_{12}NaN_4O_2)_8H_8$was provided by the method represented in the original work [1]. The adduct of light fullerene C_{60} with L-arginine was formed – $C_{60}(C_6H_{13}N_4O_2)_8H_8$ with the yield ≈ 80 % from the theoretically possible.

Identification of $C_{60}(C_6H_{12}NaN_4O_2)_8H_8$ was provided by the methods of: element analysis, infrared and electronic spectroscopy, complex thermal analysis.

In $C_{60}(C_6H_{12}NaN_4O_2)_8H_8$-water binary system at 25°C concentration dependencies of density, average and partial molar volumes of water and $C_{60}(C_6H_{12}NaN_4O_2)_8H_8$, refraction indexes were measured. Molar and specific $C_{60}(C_6H_{12}NaN_4O_2)_8H_8$ refractions was determined and calculated according to additive refraction rule.

In $C_{60}(C_6H_{12}NaN_4O_2)_8H_8$-water binary system at 25°C concentration dependencies of electrical conductivity,seeming dissociation degrees and concentration dissociation constants of $C_{60}(C_6H_{12}NaN_4O_2)_8H_8$ in water solutions were investigated.

Solubility of $C_{60}(C_6H_{12}NaN_4O_2)_8H_8$ in water in temperature range 20-60°C was determined. Diagrams consist of single branch of the crystallizationof non-hydrated $C_{60}(C_6H_{12}NaN_4O_2)_8H_8$and have no invariant point.Thermal gravimetrical analysis of $C_{60}(C_6H_{12}NaN_4O_2)_8H_8$ was provided.

The investigation of concentration dependence of the dimension of the associates $C_{60}(C_6H_{12}NaN_4O_2)_8H_8$ in water solutions at 25°C we have provided by the method of the dynamic light scattering in visible wavelength region. Different typesassociates (monomers form I-type, I-type form II-type, II-type form III-Type, III-type form IV-type) were discovered. For the description association processes in these systems the model of consequent hierarchical association model was used.

Investigations were supported by Russian Found of Fundamental Investigations – RFFI (Project N 15-08-08438) and with the help of the equipment of Resource Center of S-Petersburg State University GEOMODEL.

References

1. Liang Bing GAN, Chu Ping LUO. Water-soluble fullerene derivatives, synthesis and characterization of ß-alanine C60 adducts. Chinese Chemical letters. 1994.Vol.5, No.4, p 275-278.

The morphology of arc discharge carbon soot formed in presence Si or Al vapours.

Smovzh D.V. [1] , *Zaikovskii A.V.* [1] , *Novopashin S.A.* [1]

smovzh@itp.nsc.ru
[1] Kutateladze Institute of Thermophysics SB RAS, Novosibirsk, Russia

It is known that the presence of metal vapours at condensation of the sprayed products in the electric arc discharge affects significantly the composition of the products, such as carbon nanotubes, nanofiber, and fullerene structures [1]. We studied the morphology of the metal-carbon nanostructures formed at the joint electric-arc evaporation of metal-carbon vapours.

Plasma-arc synthesis was carried out in helium at the pressures of 25-200 Torr, at the voltage of 20 V and current of 100 A. The sprayed electrode consisted of a graphite rod with the diameter of 7 mm, with a hole along its axis, where the mixture of metal and carbon powder was pressed; the range of metal concentration was 1-15 mass %. Al and Si were used as the working metals. The synthesized material was collected from the cooled walls of the reactor. The materials were analyzed by means of X-ray diffraction and transmission electron microscopy.

The material synthesized by spraying the aluminum-carbon electrode was a composite of soot formations of a spherical shape with the diameter of 10-30 nm. The contrast in the TEM images is insufficient to determine the parameters of structures containing Al, and this indicates a small particle size; the XRD method has registered a weak reflex of AlC_4. Various hollow structures (spheres, nanotubes) are formed at calcination of obtained Al:C composite.

When spraying the silicon-carbon electrodes, the presence of metal leads to formation of grapheme planes with incapsulated Si particles of Si 5-10 nm.

Thus, it is experimentally shown that the presence of Al and Si vapours at condensation in the arc discharge affects significantly the morphology of the formed soot particles. In the presence of Al the spherical and cylindrical structures are formed, which serve as a framework for carbide deposition; in the case of silicon the graphene planes are formed predominantly at vapour condensation (Fig.1). The optimal concentration of metal in the sprayed electrode is 10-15% for all the cases.

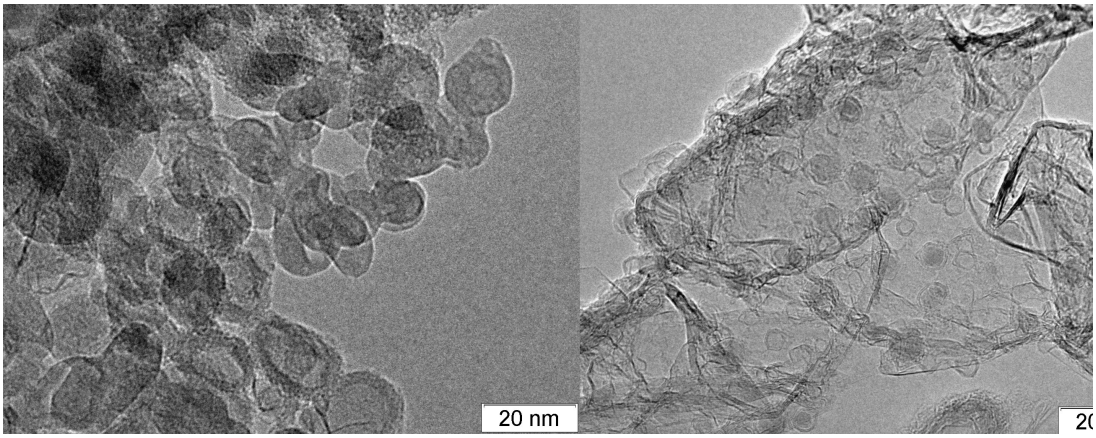

Fig.1. TEM of synthesized carbon material with Al-left and Si-right.

References

[1] N. I. Alekseev. On the mechanism of carbon nanotube formation: II. The kinetics of explosive condensation of carbon molten drops in a metallic catalyst. Technical Physics, 2004, Vol. 49, Is. 8, P. 1004-1011.

Playing with the nanodiamond surfaces to modulate up-take and therapeutic activity of plant secondary metabolites

Reina G. [1] *, Orlanducci S.* [1] *, Gismondi A.* [2] *, Gay S.* [1] *, Lavecchia T.* [1] *, Angjellari M.* [1] *, Tamburri E.* [1] *, Terranova M.- L.* [1]

terranova@roma2.infn.it

[1] Dep. Chemical Sciences and Tecnologies, Tor Vergata University, Rome, Italy

[2] Dep. Biology, Tor Vergata University, Rome, Italy

Our researches on bio-related applications of detonation nanodiamond (DND) are presently addressed at the development of strategies to conjugate such nanomaterial to natural bioactive molecules. To produce DND-based adducts, the plant secondary metabolites ciproten and quercetin have been firstly chosen. Preliminary investigations carried out by using Rhodamine B as model molecule [1], already evidenced that the features of DND up-take and release of active moieties are strongly conditioned by the chemical state of the nanodiamond surfaces. In view of this, various protocols to control the surface chemistry of DND by oxidation or reduction processes (wet chemistry, plasma etching) have been settled.

The chemical state of the DND surfaces before conjugation with the natural bioactive molecules has been fully characterized by surface enhanced Raman spectroscopy (SERS), using an innovative substrate obtained by coupling DND with Au nanoparticles [2]. We prepared and tested a series of different coumarin- and quercitin-DND adducts, obtained avoiding in any case the use of potentially toxic solvents. Taking advantages of the SERS technique, it has been possible to correlate for the first time the amounts of DND drug-loading to the binding sites identified at the surfaces of the differently treated nanodiamonds [3]. It has been also demonstrated that chemical and structural modifications of nanodiamond surfaces influence the bioactivity of the conjugated molecules. The nanodiamond loaded with plant molecules behaves as a perfect intracellular carrier, able not only to penetrate in cell cytoplasm but and also to remain embedded in the nuclear membrane , avoiding degradation of the bioactive compounds. After nanodiamond conjugation, the ciproten and quercetin antiproliferative effects on human (HeLa) and murine (B16F10) tumor cells were found improved. On the other hand, when associated with nanodiamonds, such molecules highly reduce their in vitro pro-oxidant, cytotoxic and pro-apoptotic activity.

These findings suggest that natural drug-nanodiamond adducts act at cellular level by molecular mechanisms different with respect to the pure plant metabolites.

The results obtained in our labs suggest the feasibility to use bioactive plants molecules conjugated with DND for cancer therapy applications.

References

[1] Reina, G., et al. “Rhodamine/Nanodiamond as a System Model for Drug Carrier”. Journal of Nanoscience and Nanotechnology 15.2 (2015): 1022-1029.

[2] Orlanducci, S., et al. “Gold nanoparticles on nanodiamond for nanophotonic applications” MRS Proceedings. Vol. 1452. Cambridge University Press, 2012.

[3] Gismondi, Angelo, et al. “Nanodiamonds coupled with plant bioactive metabolites: A nanotech approach for cancer therapy”. Biomaterials 38 (2015): 22-35.

Selective formation of color-centers in diamond and nanodiamond by catalytic CVD methodologies

Orlanducci S. [1] *, Gay S.* [1] *, Reina G.* [1] *, Tamburri E.* [1] *, Angjellari M.* [1] *, Cianchetta I.* [1] *, Terranova M.-L.* [1]

silvia.orlanducci@uniroma2.it

[1] Dept. Science and Chemical Technology, University Tor Vergata of Rome, Rome, Italy

Absorption and fluorescence bands can arise from localized electronic states around impurities, vacancies, charge carriers and their combinations, inside a crystalline lattice. The electronic wavefunctions of these emitters, often called *color centers*, are opening new scenarios in research and technology and the creation of emitting centers in crystalline materials is nowadays a key point to be pursued. The research on the NVs defects (neutral NV and negatively charged NV^-) has leaded the field until now, either on centers found in natural diamond, or on those artificially produced by CVD synthesis or ion implantation [1]. Recently other color centers, such as those related to Si, Cr and Ni [2-4], are gaining more and more attention, particularly for the possibility of exploiting their near-IR emission for telecommunication and biological applications.

We report here on the chemical methodologies that are being settled in our labs for the insertion in diamond of foreign atoms and consequent creation of fluorescent defects. The inclusion of Si, Cr, Ge, able to produce color centers, is directly obtained during the process of diamond synthesis by means of a CVD technique. In particular we illustrate the methodologies employed to introduce Si and, Cr fluorescent centers inside the diamond by the aid of a catalytic process based on nanoparticles modification of the substrate. Moreover the photoluminescence emission from a series of diamond samples grown on different substrates (Si, Ge and Ti) has been investigated and is discussed with reference to the morphological/structural features of the diamond phase and to the experimental procedures adopted for substrate preparation.

References

1. Beha, K., Batalov, A., Manson, N. B., Bratschitsch, R., & Leitenstorfer, A. (2012). Optimum photoluminescence excitation and recharging cycle of single nitrogen-vacancy centers in ultrapure diamond. *Physical review letters*, *109*(9), 097404
2. Neu, E., Steinmetz, D., Riedrich-Möller, J., Gsell, S., Fischer, M., Schreck, M., & Becher, C. (2011). Single photon emission from silicon-vacancy colour centres in chemical vapour deposition nano-diamonds on iridium. *New Journal of Physics*, *13*(2), 025012.
3. Aharonovich, I., Castelletto, S., Simpson, D. A., Stacey, A., McCallum, J., Greentree, A. D., & Prawer, S. (2009). Two-level ultrabright single photon emission from diamond nanocrystals. *Nano letters*, *9*(9), 3191-3195.
4. Cianchetta, I., Tomellini, M., Tamburri, E., Gay, S., Porchetta, D., Terranova, M. L., & Orlanducci, S. (2014). Can a metal nanoparticle based catalyst drive the selective growth of bright SiV color centers in CVD diamonds?. *Journal of Materials Chemistry C*, *2*(45), 9666-9673.

Carbon nanomaterials in Catalysis. The role of surface chemistry and carbon matrix structure in 1,2-dichloroethane dechlorination and aliphatic alcohols conversion

Tveritinova E.A. [1] , *Zhitnev Yu.N.* [1] , *Kulakova I.I.* [1]

kulakova-inna@yandex.ru
[1] Lomonosov Moscow State University

A combination of unique physical and chemical properties attracts researcher's attention to carbon materials such as detonation nanodiamond, carbon nanotubes, graphene and others. In particular, regular structure, electronic properties and easily modifiable surface allows of application in catalysis. Still in the vast majority of cases, carbon materials are used as a support for metal nanoparticles. However, carbon materials can be catalytically active without the addition of metal particles in some reactions, that opens a promising way of decreasing the consumption of expensive and usually toxic metals in catalysis.

We have studied own catalytic activity of the following carbon nanomaterials: detonation nanodiamond (ND), carbon nanoflakes (UNFs), including doped with nitrogen (UNFs-N), carbon nanotubes (CNTs), These materials are formed by carbon atoms in state sp^3-, sp^2 -, and curved sp^2 - hybridization, respectively. The composition of the surface functional groups of these materials was due to the conditions of cleaning after synthesis. The surface and structure of the carbon materials were characterized using different methods: BET, DTA, SEM, TEM, XPS, XRD, TPR, diffuse reflectance IR spectroscopy. As test reactions were selected - conversion of all alcohols C2-C4 and dechlorination of 1,2-dichlorethane.

Catalytic activity in the conversion of 1,2-dichloroethane was shown only in the case of ND. Three main reactions were observed: (i) dehydrochlorination, the removal of 2 HCl molecules with acetylene forming, (ii) dechlorination resulting in ethylene, and (iii) hydrodechlorination or reductive dechlorination, which takes place in the presence of hydrogen and leads to the formation of ethylene. In all reactions studied, selectivity to ethylene was always above 99%, selectivity to acetylene below 1 % and no other products were observed. The surface of nanodiamonds, as it is known, contains a large quantity of highactive groups that are associated with sp^3-hybridized surface carbon atoms. These groups potentially may be active in DCE reactions.

In the conversion of aliphatic C2-C4 alcohols CNTs and ND showed catalytic activity in various degrees, while UNFs were inactived. The conversion of secondary alcohols (2-propanol and 2-butanol) on CNTs occurs with predominant formation of the dehydration products (propene,1- butene and 2-butene) with a selectivity of ~90%, whereas the main products of conversion on ND are dehydrogenation products (acetone and butanone). This allowed us to conclude that the Lewis acid centers play a key role in the catalysis on the surface of the CNTs, while the basic oxygen-containing centers on the ND surface responsible for the catalysis on it. Experimental data confirm participation in the conversion of aliphatic alcohols on the CNTs surface oxygen-containing Lewis sites and unsaturated surface C=C bonds. Catalytic centers in the conversion of aliphatic alcohols on ND are only oxygen-containing surface groups (e.g., carbonyl, carboxyl, etc.). UNFs-N, containing 10% nitrogen, exhibit catalytic activity only in the conversion of primary alcohols, and products dehydrogenization are mainly formed. This nanocarbon material was inert in the conversion of 2-propanol and 2-butanol, that allows to judge about the participation only of nucleophilic nitrogen-containing groups in the conversion of alcohols.

This work was supported by RFBR (grant 13-08-00647).

High pressure sintering of Si_3N_4-C(nano) nanocomposites and their properties

Urbanovich V.S. [1] , *Krivulets A.I.* [1] , *Pavlovskaya D.G.* [1] , *Sudnik L.V.* [2] , *Niss V.S.* [3] , *Grigoriev S.V.* [3] , *Oychenko V.M.* [4]

urban@physics.by

[1] Scientific and Practical Materials Research Centre of NAS of Belarus, Minsk, Belarus
[2] Research Institute of Impulse Processes with Pilot Factory, Minsk, Belarus
[3] Belarusian National Technical University, Minsk, Belarus
[4] Ioffe Institute, Saint Petersburg, Russia

Ceramics based on silicon nitride is a very advanced structural material for bearing parts, since it has high physical and mechanical properties. Addition of nanostructured carbon can enhance its physical-mechanical and tribological properties due to the formation of carbonitride or silicon carbide during activating sintering under high pressure, since the presence of nonconjugated atomic bonds in the fullerene black and fullerene soot can lead to active interaction with silicon nitride. The free carbon can reduce the friction coefficient too.

The density and microhardness of Si_3N_4-C (black, soot) nanocomposites with contents of 0.5, 1, 5 and 10 wt. % of fullerene black and 0.5 wt. % fullerene soot, sintered at a pressure of 4 GPa and temperatures of 1100-1800 ^{o} C are studied (fig.1). XRD and SEM analysis were also used for study of the phase composition and a microstructure of composites. Submicron α-Si_3N_4 powder (E-10, Industries Inc., Japan) with the particle size of 150-200 nm and nanocarbon powders (Ioffe Institute, Russia) with the particle size of 40-50 nm were used as initial.

It is found that dependence of microhardness on sintering temperature is nonmonotonic. With increasing of sintering temperature up to 1700 ^{o} C the density and microhardness of nanocomposites grow up to maximal value if the content of fullerene black is of 0.5-5 wt.%. Microhardness of composite is higher than of Si_3N_4 without additives, if the content of fullerene black reaches of 0.5-1 wt. %.

It is found that during sintering of composites with different content of fullerene black the activation of their densification due to α→β transformation in silicon nitride does not occur. With an increase in the content of black from 1 to 10 wt. % in nanocomposite its hardness decreases and ductility increases. The addition of fullerene soot allows increasing hardness up to 34 GPa.

The obtained results are discussed in comparison with the literature data.

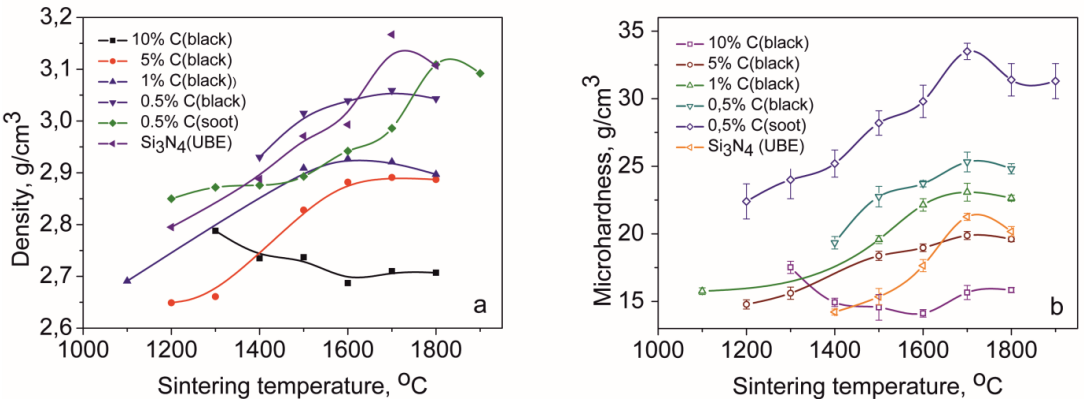

Fig.1. Dependence of density (a) and microhardness (b) of Si_3N_4-C(nano) composites on sintering temperature.

Magnet-induced behavior of Iron Carbide Fe7C3@C Nanoparticles in the Cytoplasm of Living Cells.

Alieva I. [1] *, Kireev I.* [1] *, Rakhmanina A.* [2] *, Garanina A.* [1] *, Strelkova O.* [1] *, Zhironkina O.* [1] *, Cherepaninets V.* [1] *, Davydov V.A.* [2] *, Khabashesku V.N.* [3] *, Agafonov V.* [4] *, Uzbekov R.* [5,6]

rustem.uzbekov@univ-tours.fr

[1] A.N.Belozersky Institute of Physico-Chemical Biology, Moscow State University, 119992 Moscow, Russia.

[2] Institute of High Pressure Physics RAS, 142190 Troitsk, Moscow region, Russia.

[3] Center for Technology Innovation, Baker Hughes Inc., Houston, TX, 77040, USA.

[4] GREMAN, UMR CNRS 7347, Universite Francois Rabelais, 37200 Tours, France.

[5] Laboratoire Biologie Cellulaire et Microscopie Electronique, Faculte de Medecine, Universite Francois Rabelais, 37032 Tours, France.

[6] Faculty of Bioengineering and Bioinformatics, 119992, Moscow State University, Moscow, Russia.

Intracellular events and details of nano-magnetic particles (NMP) interactions with living cells were investigated on the models of normal untransformed (PK line) and cancer cell (HT1080 line). It was shown that PK and HT1080 cells were capable to capture NMP appeared on the upper cell membrane, as well as on the surface of substrate. Captured NMP were dislocated within the cell cytoplasm to the cell nucleus region. Immunofluorescence studies with intracellular endosomal membrane marker showed that NMP aggregates can be located in endosomes or can be settled in the cytoplasm without any membrane-structures connection. NMP accumulation in cell cytoplasm had no apparent effect on cytophysiological characteristics of the cells. When attached cells were magnetic field exposed, we observed incorporated NMP displacement to the direction of magnet. At the same time slightly attached or non-attached cells, like mitotic cells or cells after cytoskeleton drugs treatment, moved towards the magnet direction. We took notice that under the action of magnetic field NMP-containing cells gradually lost NMP as the result of removing exocytosis-discarded NMP from cell surface. Our data allow us to conclude that NMP magnetic properties are sufficient for successful NMP -manipulation at the intracellular level, as well as for whole cell handling.The structure of NMP outer shell allows firmly associate with different types of biological molecules, which creates prospects to use these complexes for targeted delivery and selective removal of chosen biological molecules from living cells.

References

1. Uzbekov R.E., Kireev I.I., Alieva I.B., Davydov V. A., Rakhmanina A.V., Agafonov V. (2013) Interaction of Iron Carbide Nanoparticles protected by Carbon Shell Onion- like Structure with living Cells. Joint International conference "Advanced Carbon Nanostructures" (ACNS' 2013). St.Petersburg, Russia.

2. Davydov V., Rakhmanina A., Kireev I., Alieva I., Zhironkina O., Strelkova O., Dianova V., Samani T. D., Mireles K., Yahia L.H., Uzbekov R., Agafonov V., Khabashesku V. (2014) Solid state synthesis of carbon-encapsulated iron carbide nanoparticles and their interaction with living cells. Mater. Chem. B, Volume **2**, 4250.

The effect of detonation nanodiamonds on the isomers distribution of mononitrotoluene during toluene nitration with mixed acids

Veretennikov E.A. [1,2] , *Tsekinskiy I.V.* [1] , *Dolmatov V.Yu.* [3]

eaveret@gmail.com

[1] Saint-Petersburg State Technological Institute (technical university), Saint-Petersburg, Russia

[2] LLC "Chemical-Pharmaceutical technologies", Saint-Petersburg, Russia

[3] FGUP "SKTB "Technolog", Saint-Petersburg, Russia

At the industrial nitration of toluene with mixed acids of different concentration the isomeric composition of mononitrotoluene (MNT) is determined by contributions of the reactions taking place in (1) the kinetic regime in the bulk acid phase, (2) the diffusion film and (3) the boundary absorption monolayer into the overall nitration rate. The increased content of p-MNT denotes the increase of a role of diffusion processes and, particularly, the increase of contribution of the reactions taking place in the boundary monolayer, whereas the increase in yield of o-MNT denotes the increase of contribution of the reactions taking place in the kinetic regime.

To shift the reaction zone to either area the different additives are used besides the variation of the stirring rate of the reaction mass, reaction temperature and composition of mixed acids.

The presence of certain functional groups at the surface of detonation nanodiamonds (DND) can promote the fixation of a nitronium-ion as a nitrating particle due to donor-acceptor interaction or the formation of a covalent bond. Such interaction will lead to the increase the volume of a nitrating agent that will result in the complication of an attack of o-position of toluene, the increase in p-isomer content, and as a result, the shifting the reaction zone to the diffusion area.

We have studied the change the MNT-isomers-ratio at nitration of toluene with mixed acids with an initial concentration of sulphuric acid of 35.70 mol %, 4% excess (mol) of nitric acid (a toluene sample - 0,015M) at temperature of 30 and 50^{o}C depending on the stirring rate from 300 to 5000 rpm.

As an additive affecting the MNT-isomers-ratio, DND with the stated specific surface of (S_{sp}) 284±1 $m^2 \cdot g^{-1}$ were used.

Among the chemical functional groups being at the DND surface carboxylic acids, their esters, anhydrides, lactones are of the great interest. It is possible to increase the specific content of such groups by chemical modification of the diamond surface carrying out the liquid-phase oxidation with full-strength mixed acids.

Addition of 50 mg of the oxidized DND into the reaction results to the great decrease in o-/p-MNT-ratio from 1,91 to 1,25 in the mononitration product at 30^{o}C as the stirring rate is increased as compared with the initial nitration. At the reaction temperature of 50^{o}C there is the most complicated isomers ratio-stirring rate dependence. So, the decrease in o-/p-ratio from 1,12 to 1,00 is observed from 300 to 2000 rpm, after then the rise to 1,16 and 1,26 at 3000 and 5000 rpm, respectively, takes place.

At the initial toluene nitration without DND the o-/p-MNT-ratio decreases from 2,70 to 2,37 at the reaction temperature of 50^{o}C as the stirring rate is increased at the range of 300 ÷ 5000 rpm.

The obtained experiment data on the o-/p-MNT-ratio well conform to the above stated theoretical proposition.

Thermophysical properties of polyurethane nanoclusters composites

Vozniakovskii A.A. [1]

alexey_inform@mail.ru
[1] Ioffe Institute, St.Petersburg, Russia

Modern polymer materials can no longer meet the requirements of current industry, both strength properties and parameters for insulation. It should be noted that demand of increasing or decreasing of heat-insulating parameters is defined, depending on a specific target of a material's application. At present, composite materials (CM) are commonly used for solution of such task. One may assert that the final properties of composite depend on polymer matrix and filling agent in equal parts. Generally, one focus attention on carbon's influencing on a complex of polymer strain parameters.

In our study, polyurethane was used as a polymer matrix and detonation diamonds, nanotubes and fullerenes were used as a fillers. We investigate the effect of different carbon materials on the properties of the composite modifying additives nature impact on the complex on thermos-physical parameters of polyurethane matrix

Fillers were introduced in polymeric matrix while a process of synthesis. This technique allowed us to disperse filler particle in bulk of polymer matrix uniformly. Thermal conductivity was measured by flash method. This method couple thermal diffusivity (α, sm^2/s), specific heat (C_p, J/(kg*K)) and thermal conductivity (λ**,** W/(m*K)), see Eq. 1.

$$\lambda = \alpha * C_p * \rho \quad (1)$$

where ρ - density of material, g/sm^3. Specific heat of CM was measured with differential scanning calorimetry method. Results are collect in table 1.

Table 1 Thermophysical properties of nanocomposites

Properties	Sample, polyurethane			
Carbon type	-	DND	fullerene C60	nanotube
Carbon content, %	0	0,1	0.2	0,05
vitrification temperature, ºC	-36,12	-35,92	-37,32	-36,62
specific heat, J/(kg*ºK)	240	215	183	168
heat diffusivity,	0,0012	0,0012	0,0012	0,0012
density,	1,2	1,2	1,2	1,2
heat conductivity, W/(m*K)	0,033	0,025	0,026	0,023

The surprising results were revealed in the course of our work. We have showed drastic decreasing of thermal conductivity. Vitrification temperature constancy with nature of nanocarbon particles give us an evidence that there is no of components chemical interaction on the interphase boundary. We match the decreasing of the specific heat, with the distribution of modifying particles on the elements of local tension. In this case, additive decrease system energy. Nanoparticles can play role of center at witch phonon scattering is occurred. This hypothesis can explain the decreasing of the thermal conductivity.

This work was supported by the Russian Foundation for Basic Research, grant 14-23-01015 "Development of methods of combined neutron-synchrotron diagnostics for the analysis of a structure of composite materials on the basis of nanocarbon and polymeric structures".

The influence of nanocarbon cluster additive on polyurethane supramolecular structure. SAXS method.

Voznyakovskii A.P. [1] , *Smirnov A.V.* [2] , *Fedorov V.A.* [2] , *Khoreva A.Kh.* [1]

voznap@mail.ru

[1] 1S.V.lebedev Research Institute for Synthetic Rubber, Saint-Petersburg, Russia

[2] National Research University of Information Technologies, Mechanics and Optics Saint-Petersburg, Russia)

Polyurethanes (PUs) are an important class of polymers that have wide application in a number of different industrial sectors. Nowadays requirements to structural material becomes considerably more rigid and expanded. In other words, modern materials technology needs for materials of new generation.

The addition of nanoscale inorganic particles into bulk polymers in order to generate nanocomposites with reinforced properties relative to the parent materials is a rapidly expanding field. In addition, the first stage of such investigation is the investigation of nanocarbon clusters impact nanocomposites molecular organization. In present work, comparative analysis of all kinds of nanocarbon clasters impact on supramolecular organization of PUs have been carrying out with the method of SAXS.

It was obtained, that intensities of X-rays scattered at low angles (wave-length λ=0,1542) follows Guinier' s law as for PU, so for nanocomposites on their base (see fig). Based on sample scattering curves analysis of the native PU one may conclude that its bulk structure include random distributed imperfections diameter ~50 nm, as show the Guinier's method (curve 1). In turn, these imperfections include some fine nanocarbon clusters with mean diameter~2 nm (curve 2-4). In spite of minor amounts of nanocarbon additives, the figure show dramatic change of the SAXS profiles in initial domain of the intensities of X-rays scattered

It may be supposed, that the modification of the PU matrix with nanocarbon clusters result in changing of imperfection's dimension and form. On the other hand the structure of fine nanocarbon clusters evidently stay invariable, as we can conclude from coincidence of SAXS profiles in angle range of scattering more than 20 mrad.

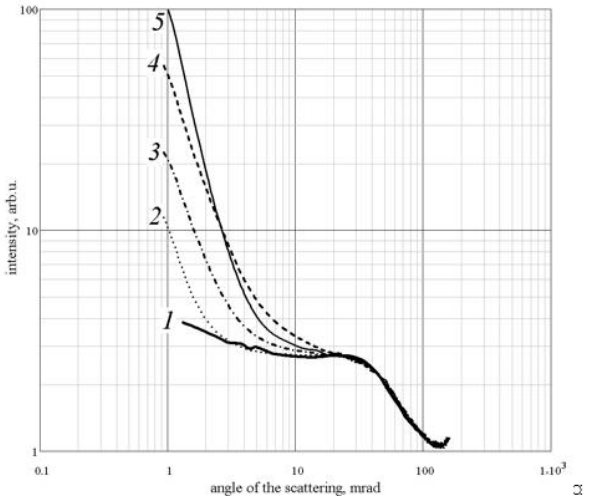

Figure 1. SAXS profiles obtained for the (1) native PU, (2) - + fullerene C_{60} (0,5% mas; (3) fullerene soot (0,1% mas); (4) - nanotubes (0,1% mas); (5) – carbonized lignin (0.5 % mas)

Full Contents

Author Index

Author Index

Author Index

Author Index

Author Index

Author Index

T

Author Index

Fund for Infrastructure and Educational Programs (part of RUSNANO Group)

- A non-profit organization that promotes the creation of infrastructure for the Russian nanotechnology industry and is part of the "innovation lift" system of Russian development institutions. The Fund is financed by the Russian federal budget.

The Fund works in seven main areas:

(1) Development of technology infrastructure.
(2) Building human resources for the nanoindustry:
(3) Development of the market for innovative products.
(4) Standardization, certification and safety assessment of nanotechnology products.
(5) Metrological support for the nanoindustry.
(6) Improvement of legislation in the innovation sphere.
(7) Popularization of nanotechnologies.

(1) Development of technology infrastructure

- **Network of nanotechnology centers** – platforms for conveyor-belt generation of technology start-ups in Russian regions:

- ✓ Projects for the creation of nanocenters are selected through open competitive procedures and a private co-investor is always involved in their financing;
- ✓ Each center specializes in specific technology areas, which are chosen depending on scientific competences and market demand in the respective region;
- ✓ Residents have access to the complete cycle of business development services, which is at the disposal of the nanocenter network (from financing to lease of unique equipment);
- ✓ Average time needed to implement a start-up is 5 years and average investments are RUB 10 million.

- **Engineering companies:**
  - ✓ Projects for the creation of engineering companies are selected through open competitive procedures and a private co-investor is always involved in their financing;
  - ✓ The mission of engineering companies is to use their own know-how to develop technologies, equipment and products to order for third parties.

- Other infrastructure projects (Sarov Technopark, Penza Center for Commercialization of Technology, Russian Academy of Sciences and RUSNANO Technology Transfer Center, which select projects with commercial potential at RAS institution, Startbase communication portal).
- Russian-Israeli industrial R&D projects.

(2) Building human resources for the nanoindustry

- Development of specialized educational programs (including digital programs) to order for nanotechnology companies. The Foundation acts as a mediator between business and universities, organizing their cooperation in the retraining of enterprise staff.
- Establishment of professional standards for the nanoindustry with involvement of leading nanotechnology companies and technical institutes.
- Implementation of the RUSNANO School League program to update school curricula in biology, chemistry and physics, with a focus on training of specialists for the nanotechnology industry.

(3) Developing markets for innovative production

- Regional programs to stimulate demand in key Russian regions. Several regions (Belgorod, Krasnoyarsk, City of Moscow, Tatarstan, Tomsk, Ulyanovsk, Chuvashia) have instituted a mandatory share of innovative products (5-10%) in the structure of public procurement.
- Sector programs to stimulate demand from public-sector companies, including Gazprom, Russian Railways, Avtodor (the Russian highways agency) and Rosreserve (the state goods and inventory manager).
- Introduction of nanotechnology solutions in the agricultural sector, in association with the Ministry of Agriculture.
- Maintaining a register of innovative products, technologies and services that are recommended for use in the Russian Federation.

(4) Standardization, certification and safety assessment of nanotechnology products

- Design of standards (both standards designed to harmonize with international requirements and preliminary national standards).
- Updating existing regulations (sanitary and hygiene norms, other state standards) to ensure free circulation of nano-products in the market.
- Quality and safety assurance of nanotechnology products through the Nanocertification system of voluntary certification.
- Classification of products and technologies by potential hazards according to methodology approved by Rospotrebnadzor (the Russian consumer rights watchdog).

(5) Metrological support for the nanoindustry (in association with the RUSNANO metrology center)

- Development and validation of measurement techniques for use in the nanotechnology industry.
- Establishment of benchmarks for composition and properties of materials, reference measures and standard tests for use in the nanoindustry and nanotechnology.
- Measurement of a wide range of functional and physico-chemical parameters of nanotechnology products, including nano-powders, suspensions, aerosols, porous materials, coatings, film structures, and bulk materials.
- Metrological study of investment projects, diagnosis and optimization of metrological support for nanoindustry companies.

(6) Improvements to legislation in the innovation sphere

Preparing proposals for the improvement of legislation governing innovation in the following spheres:

- Public procurement;
- Support for small and medium-sized enterprises;
- Intellectual property;
- Taxation (simplification of the tax regime);
- Corporate law, including establishment and improvement of the legal and contractual basis for innovation projects.

(7) Popularization of nanotechnologies

- The exhibition "This is NANO", which makes the world of nanotechnology interesting and accessible, and a series of master classes and other activities and projects to develop and maintain public interest in nanotechnology;
- Displays and presentations at trade exhibitions.
- Special projects in the media and social media.

The Foundation Strategy in the period up to 2020:

- *16 nanocenters, 450 small innovation companies;*
- *12 engineering companies.*
- *150 educational programs for the training of at least 10,000 professionals;*
- *Helping to achieve a sales target of RUB 1.3 trillion for Russian nanotechnology products and high-tech materials;*
- *Design and submission to Rosstandart of 250 national standards and 600 documents (certificates, expert opinions) on quality and safety compliance of nanoindustry products;*
- *220 developed and certified methods of measurement and standard samples of nanomaterials.*

10a Prospect of the 60th Anniversary of October,Moscow, 117036, Russia,

Telephone: +7 (495)988 53 88

E-mail: info@rusnano.com

www.rusnano.com

Chemical Abstracts Service, CAS (www.cas.org), a division of the American Chemical Society, is the world's authority for chemical information. CAS is the only organization in the world whose objective is to find, collect and organize all publicly disclosed chemical substance information. A team of scientists worldwide curates and controls the quality of the databases, which are recognized as the most comprehensive and authoritative by organizations around the world.

SciFinder® is a research discovery application tool developed and maintained by CAS and provides unlimited access to the world's most comprehensive and authoritative source of references, substances and reactions in chemistry and related sciences. SciFinder is an easy end-user search tool to explore references, structures and reactions covering all chemistry. You can explore references from 10,000+ scientific journals from 185 countries and patents from 63 authorities, chemical substances i.e. by name, structure and molecular formulae. Researchers using SciFinder have access to the most timely and comprehensive chemical databases, including CAS REGISTRY^{SM}, the "gold standard" for substance information.

SciFinder gives you access to the following databases:

CAplus	– 41+ million patent and journal references since 1907
REGISTRY	– 96+ million substances and 65+ million bio sequences
CASREACT	– 78+ million reactions since 1840
CHEMLIST	– 343,000 inventoried or regulated chemicals
CHEMCATS	– 100+ million chemical substances (28 million unique CAS numbers)
MARPAT	– 1+ million Markush structures from 410,000 patents
MEDLINE	– 24+ million biomedical references

For Notes

Издательство ФТИ им. А.Ф. Иоффе РАН
194021 С.-Петербург, Политехническая ул., д. 26
Лицензия ЛР №040971 от 16.06.99
Тир. 260 экз., 25.06.15
Отпечатано с готового оригинал-макета, подготовленного ЗАО “Интеллект”